



**Differential responsiveness of
Tumour Necrosis Factor Receptors (TNFR)
type 1 and 2 - the critical role of the TNFR stalk region**

Dipl. biol. Christine Richter

Thesis submitted in partial fulfilment of the requirements
of the regulations for the degree of Doctor of Philosophy
Newcastle University
Faculty of Medical Sciences
Institute of Cellular Medicine
July 2011

Declaration

The work reported in this thesis was performed from February 2008 to January 2011. The work in this thesis was carried out in the Musculoskeletal Research Group, Institute of Cellular Medicine, Newcastle University. Except for commonly held concepts, and where specific reference is made to other work, the content of the thesis is original. All experiments were carried out by myself under the guidance of my supervisors, Dr Anja Krippner-Heidenreich and Prof. Derek A. Mann.

No part of this thesis has been submitted for the award of any other degree.

Abstract

The pro-inflammatory cytokine tumour necrosis factor (TNF) exerts its bioactivity via two plasma membrane receptors, TNF receptor (TNFR)1 and TNFR2. Both receptors are fully activated by membrane-bound TNF, while soluble TNF (sTNF) activates only TNFR1 efficiently. Preliminary data from our group suggest that the membrane proximal extracellular region (stalk region) and/or the transmembrane region of the TNFR control the differential responsiveness to sTNF. The aims of this project were to ascertain the region determining sTNF responsiveness and to investigate the underlying molecular mechanism(s).

Fibroblasts from *tnfr1^{-/-}/tnfr2^{-/-}* double knockout mice were stably transfected with chimaeras consisting of the extracellular and transmembrane domain of TNFR and the intracellular portion of Fas (TNFR-Fas). Using this cellular system, I could show that 42 amino acids within the TNFR2 stalk region control responsiveness to sTNF. Replacement of the stalk regions of TNFR1-Fas and TNFR2-Fas with artificial linkers proved that stalk region length does not determine differential responsiveness. Furthermore, responsiveness to sTNF was not affected when either conserved proline residues or O-glycosylation sites in the TNFR2 stalk region were mutated. Moreover, partial replacement of the TNFR2 stalk region with overlapping artificial linkers also left sTNF responsiveness unaltered. Therefore, the underlying molecular mechanism controlling responsiveness to sTNF appears to be more complex and remains to be elucidated.

Importantly, the critical role of the TNFR stalk region in sTNF responsiveness could also be confirmed for wild type TNFR2 at the level of signalling complex formation. Data from chemical crosslinking and confocal microscopy studies revealed that the stalk region controls ligand-independent receptor pre-assembly and formation of larger receptor clusters.

Taken together, data obtained in this PhD thesis indicate that the TNFR2 stalk region is a major determinant of differential sTNF responsiveness and ligand-independent receptor-receptor interactions, the latter being a potential prerequisite for the formation of larger ligand/receptor clusters and signal initiation.

Table of contents

Declaration	ii
Abstract	iii
Table of contents	iv
List of figures	x
List of tables	xiv
Acknowledgements	xv
Abbreviations	xvi
<u>CHAPTER 1: General Introduction</u>	1
1.1 Tumour Necrosis Factor	1
1.2 The TNF ligand and TNF receptor superfamilies	1
1.3 The type 1 and type 2 TNF receptors	5
1.3.1 The cysteine-rich extracellular domains of TNFR1 and TNFR2	5
1.3.2 Transmembrane domain and stalk region	8
1.3.3 Intracellular domains of TNFR1 and TNFR2	10
1.4 TNF/TNFR-mediated signalling	11
1.4.1 Anti-apoptotic TNFR1 signalling through NF- κ B activation	12
1.4.2 Pro-apoptotic signalling of TNFR1	16
1.4.2.1 Mitogen-activated protein kinase cascade	16
1.4.2.2 Caspase-dependent pathways	17
1.5 TNFR2-mediated signalling and crosstalk between TNFR1 and TNFR2	20
1.6 TNF and TNFR in health and disease	21
1.6.1 Physiological implications for sTNF and membrane-bound TNF	21
1.6.2 Divergent roles of TNFR1 and TNFR2 in health and disease	22
1.6.2.1 Modulation of immune tolerance by TNFR2	22
1.6.2.2 Involvement of TNFR1 and TNFR2 in host defence	23
1.6.3 TNFR1 and TNFR2 in the central nervous system	24
1.6.4 Anti-TNF treatment in autoimmune diseases.....	26
1.7 Scope of this thesis	30

<u>CHAPTER 2: Materials and methods</u>	33
2.1 Materials.....	33
2.1.1 Chemicals and reagents.....	33
2.1.2 Cell culture media and reagents.....	34
2.1.3 Molecular biology enzymes.....	36
2.1.4 Antibodies.....	36
2.1.5 Ligands.....	37
2.1.6 Plasmids.....	38
2.1.7 Oligonucleotides.....	38
2.1.8 Competent cells.....	38
2.1.9 Small interfering RNA.....	39
2.1.10 Software.....	40
2.2 Molecular biology methods.....	41
2.2.1 Determination of DNA concentrations.....	41
2.2.2 Agarose gel electrophoresis.....	41
2.2.3 Agarose gel extraction.....	42
2.2.4 Enzymatic modifications of DNA.....	42
2.2.4.1 Restriction digests and dephosphorylation of vector DNA.....	40
2.2.4.2 Ligation of vector and insert DNA.....	41
2.2.5 Heat shock transformation of chemically competent <i>E. coli</i> DH5 α cells.....	43
2.2.6 Preparation of plasmid DNA from <i>E. coli</i> DH5 α cells.....	45
2.2.6.1 Mini plasmid preparation.....	45
2.2.6.2 Midi plasmid preparation.....	46
2.2.7 Replacement of the complete stalk region with glycine-serine-linkers.....	47
2.2.7.1 Subcloning of linker sequences.....	50
2.2.7.2 Cloning of S _{GSL} sequences into pBS SK (+) TNFR-BamHI-Fas.....	53
2.2.7.3 Cloning of S _{GSL} sequences into pEF PGKpuro polyA TNFR-Fas.....	54
2.2.8 Partial replacement of the TNFR2 stalk region with glycine-serine-linkers.....	55
2.2.9 Mutagenesis of conserved proline residues in the TNFR2 stalk region.....	60
2.2.10 Generation of TNFR2-(S/TM) _{R1} -R2 and TNFR2-(S _{Δ42} /TM) _{R2} -R2 constructs ...	63
2.2.11 Generation of vectors for inducible HEK 293 Flp-IN T-Rex cells.....	65
2.3 Cell culture.....	66
2.4 Transfection of mammalian cells.....	67

2.4.1	Transfection of mammalian cells with mammalian expression plasmids.....	67
2.4.2	Transfection of HeLa cells with siRNA.....	69
2.5	Cell sorting and flow cytometry.....	70
2.5.1	Cell sorting.....	70
2.5.2	Flow cytometry.....	71
2.6	Cell viability assay using crystal violet staining.....	72
2.7	Bradford protein assay.....	73
2.8	SDS-polyacrylamide gel electrophoresis.....	73
2.9	Western Blot analysis.....	75
2.10	Protein crosslinking with bis[sulfosuccinimidyl]suberate.....	77
2.11	Inhibition of core 1 and core 2 O-glycosylation in MF TNFR-Fas cells.....	78
2.12	TNFR2/TRAF2 co-immunoprecipitation from HeLa cell lysates.....	80
2.13	Analysis of p65 translocation in MF via immunofluorescence.....	81
2.14	Confocal microscopy of HEK FlpIN T-Rex cells over-expressing TNFR2 and TNFR2 variants.....	82
<u>CHAPTER 3: Results I: Control of sTNF responsiveness by the TNFR1 and</u>		
	TNFR2 stalk regions.....	84
3.1	Introduction.....	84
3.2	The TNFR2 stalk region inhibits sTNF responsiveness in TNFR2-Fas chimaeras	88
3.3	Influence of the stalk region on sTNF-mediated TNFR2 complex formation....	94
3.3.1	The TNFR2 stalk region inhibits sTNF-mediated TRAF2 recruitment.....	94
3.3.2	Suitability of soluble and oligomerised TNFR2-selective TNF to study differential responsiveness of TNFR.....	104
3.3.3	TNFR1 activation does not affect TNF-mediated TRAF2 recruitment to TNFR2	107
3.4	Preliminary experiments on the role of the TNFR2 stalk region in sTNF- mediated p65 translocation.....	118
3.5	Discussion.....	125

3.5.1	The TNFR2 stalk region determines sTNF responsiveness in TNFR2-Fas chimaeras.....	125
3.5.2	The stalk region determines sTNF responsiveness of wild type TNFR2.....	127
3.5.3	sTNF-mediated downstream signalling of TNFR2 variants	130
3.6	Conclusion.....	131

CHAPTER 4: Results II: Investigations into molecular mechanisms by which the TNFR2 stalk region controls sTNF responsiveness **132**

4.1	Introduction	132
4.2	Length of the stalk region does not control TNFR2 responsiveness towards sTNF.....	134
4.3	Mutagenesis of individual conserved proline residues in the TNFR2 stalk region does not alter responsiveness to sTNF	141
4.4	Influence of the O-glycosylation status of the TNFR2 stalk region on responsiveness towards sTNF	147
4.4.1	sTNF responsiveness of TNFR2-Fas chimaeras after site-directed mutagenesis of predicted O-glycosylation sites.....	147
4.4.2	sTNF responsiveness of TNFR-Fas chimaeras upon inhibition of core 1/core 2 O-glycosylation	152
4.5	Effect of partial replacement of the TNFR2 stalk region on sTNF responsiveness	156
4.6	Discussion	162
4.6.1	Stalk region length does not determine responsiveness towards sTNF	162
4.6.2	The influence of conserved proline residues in the TNFR2 stalk region on sTNF responsiveness	163
4.6.3	O-glycosylation of the TNFR2 stalk region does not determine responsiveness to sTNF.....	165
4.6.4	Partial replacement of the TNFR2 stalk region suggests a more complex regulation of sTNF responsiveness by the stalk region.....	167
4.7	Conclusion.....	168

CHAPTER 5: Results III: Influence of the TNF receptor stalk regions on ligand-independent receptor homodimerisation and formation of larger receptor clusters..... **169**

5.1	Introduction	169
5.2	The stalk region of TNF receptor type 2 counteracts ligand-independent receptor homo-dimerisation	171
5.3	The stalk region of TNFR2 abrogates efficient cluster formation of TNFR2-Fas and wild-type TNFR2.....	177
5.3.1	The TNFR2 stalk region inhibits formation of larger TNFR2-Fas clusters	179
5.3.2	Cluster formation of wild type TNFR2 is abrogated by the TNFR2 stalk region	185
5.4	Discussion	193
5.4.1	Control of TNFR2-Fas homo-dimerisation by the TNFR2 stalk region	193
5.4.2	Inhibition of TNFR2 and TNFR2-Fas cluster formation by the TNFR2 stalk region.....	196
5.5	Conclusion.....	199
<u>CHAPTER 6: General Discussion</u>		200
6.1	General perspective	200
6.2	The TNFR stalk region and its prominent molecular features in the control of receptor responsiveness to sTNF.....	202
6.2.1	The role of stalk region O-glycosylation in sTNF responsiveness of TNFR2..	203
6.2.2	Control of sTNF responsiveness by proline residues in the TNFR2 stalk region	206
6.3	Inhibition of ligand-independent TNFR interactions and cluster formation by the TNFR2 stalk region	207
6.3.1	The TNFR2 stalk region abrogates ligand-independent TNFR interactions.....	207
6.3.2	The TNFR2 stalk region counteracts TNFR2 cluster formation	209
6.4	Future work	213
6.5	Summary	215
References		216
Appendix		243
I	Mammalian expression plasmids for wild-type TNFR2 variants.....	244
II	Mammalian expression plasmid for TNFR2-(S _{Δ42} /TM) _{R2} -Fas.....	245
III	Subcloning plasmids for the introduction of S _{GSL} into TNFR-Fas.....	246

IV	Mammalian expression plasmids for TNFR-S _{GSL} -TM-Fas chimaeras.....	252
V	Mammalian expression plasmids for partial stalk exchange mutants.....	254
VI	Plasmids for the generation of inducible HEK 293 FlpIN T-Rex cells.....	256

List of figures

Figure 1. Schematic representation of the members of the TNF ligand and receptor superfamilies.....	3
Figure 2. Schematic representation of the human TNF receptors TNFR1 and TNFR2....	6
Figure 3. Overview of TNFR superfamily member stalk regions.....	9
Figure 4. Schematical representation of TNFR1-mediated anti-apoptotic NF- κ B and pro-apoptotic JNK signalling crosstalk.....	14
Figure 5. DISC formation and caspase-dependent signalling of TNFR1.....	19
Figure 6. Construction of the 15 aa glycine-serine-linker for TNFR.....	48
Figure 7. Subsequent cloning of glycine-serine-linker sequences for TNFR.....	49
Figure 8. Schematic representation of the partial replacement of the TNFR2 stalk region with an artificial glycine-serine linker (Ex _{aa 202-219}).....	59
Figure 9. Chemical Structure of Benzyl-2-acetamido-2-deoxy- α -D-galactopyranoside.....	79
Figure 10. Schematic representation of TNFR-Fas chimaeras.....	86
Figure 11. Preliminary data suggest a role for stalk and/or TM regions of TNFR in sTNF responsiveness.....	87
Figure 12. The aa sequences of the TNFR1, TNFR2 and TNFR2-(S _{Δ42/TM}) _{R2} -Fas stalk regions.....	89
Figure 13. Characterisation of TNFR2-Fas chimaeras with a shortened stalk region....	90
Figure 14. MF TNFR2-(S _{Δ42/TM}) _{R2} -Fas are responsive to sTNF.....	92
Figure 15. Partial responsiveness of MF TNFR2-(S _{Δ42/TM}) _{R2} -Fas to sTNF is an intrinsically regulated phenomenon.....	93
Figure 16. Characterisation of HeLa cells stably expressing TNFR2, TNFR2-(S/TM) _{R1-R2} and TNFR2-(S _{Δ42/TM}) _{R2-R2}	97
Figure 17. Endogenous TRAF2 levels in HeLa cells expressing different TNFR2 variants.....	98
Figure 18. The TNFR2 stalk region counteracts sTNF-mediated recruitment of endogenous TRAF2 to TNFR2 in HeLa cells.....	101
Figure 19. Quantitative analysis of TNF-mediated TRAF2 recruitment to TNFR2, TNFR2-(S/TM) _{R1-R2} and TNFR2-(S _{Δ42/TM}) _{R2-R2}	102
Figure 20. Evaluation of the activity of the TNFR2-selective ligands FLAG-sTNF(143N/145R) and FLAG-TNC-scTNF(143N/145R).....	106

Figure 21. Optimisation for the reduction of TNFR1 cell surface expression by RNA interference.....	109
Figure 22. Reduction of TNFR1 levels by RNA interference does not alter TNFR2 cell surface expression of HeLa cells.....	111
Figure 23. TNFR1 cell surface expression in HeLa cells overexpressing TNFR2 constructs after treatment with TNFR1-specific siRNA.....	112
Figure 24. sTNF-mediated recruitment of TRAF2 to TNFR2 constructs is independent of TNFR1 signalling.....	114
Figure 25. TNF-mediated TRAF2 recruitment to TNFR2 constructs in HeLa cells after treatment with TNFR1-specific siRNA.....	116
Figure 26. Characterisation of MF stably expressing TNFR2, TNFR2-(S/TM) _{R1} -R2 and TNFR2-(S _{Δ42} /TM) _{R2} -R2.....	120
Figure 27. TNF-mediated nuclear translocation of p65 in MF TNFR2-(S/TM) _{R1} -R2 (preliminary data).....	123
Figure 28. TNF-mediated nuclear translocation of p65 in MF TNFR2-(S _{Δ42} /TM) _{R2} -R2 (preliminary data).....	124
Figure 29. Shortening of the TNFR2 stalk region leads to the loss of conserved proline residues and potential O-glycosylation sites.....	133
Figure 30. Composition of artificial stalk regions for TNFR-Fas chimaeras.....	136
Figure 31. Western Blot analysis of TNFR-Fas chimaeras containing 15 aa and 56 aa long artificial stalk regions.....	137
Figure 32. Characterisation of cell surface expression and TNF responsiveness of MF overexpressing TNFR1-Fas chimaeras with artificial stalk regions.....	139
Figure 33. Characterisation of cell surface expression and TNF responsiveness of MF overexpressing TNFR2-Fas chimaeras with artificial stalk regions.....	140
Figure 34. Western Blot analysis of TNFR2-Fas chimaeras in which conserved proline residues of the stalk region had been mutated.	143
Figure 35. Replacement of the conserved proline residues P205, P211 and P219 in the TNFR2 stalk region does not alter TNF responsiveness.	145
Figure 36. Replacement of the conserved proline residues P231, P233, P237 and P249 in the TNFR2 stalk region does not alter TNF responsiveness.....	146
Figure 37. Characterisation of putative O-glycosylation sites within the TNFR2 stalk region.....	149

Figure 38. Characterisation of cell surface expression and TNF responsiveness of MF TNFR2-Fas with reduced O-glycosylation.....	151
Figure 39. O-glycosylation in the TNFR2-Fas stalk region can be inhibited by Benzyl-2-acetamido-2-deoxy- α -D-galactopyranoside.....	153
Figure 40. Inhibition of core 1/2 O-glycosylation does not alter sTNF responsiveness in MF TNFR1-Fas.....	154
Figure 41. Inhibition of core 1/2 O-glycosylation does not alter TNF responsiveness in MF TNFR2-Fas.....	155
Figure 42. Western Blot analysis of TNFR2-Fas chimaeras with partially substituted stalk regions.....	157
Figure 43. Partial replacement of the TNFR2 stalk region does not alter TNF responsiveness.	160
Figure 44. Schematic representation of chemical crosslinking of primary amino groups with bis-(sulfosuccinimidyl)-suberate.....	172
Figure 45. Shortening of the TNFR2 stalk region increases ligand-independent receptor-receptor interactions in TNFR2-Fas chimaeras.....	175
Figure 46. Ligand-independent receptor-receptor interactions of TNFR1-Fas chimaeras containing the TM and shortened stalk region of TNFR2.....	176
Figure 47. Dose-dependent doxycycline-induced expression of TNFR2 in HEK 293 FlpIN T-Rex cells.....	178
Figure 48. Kinetics of doxycycline induced expression of TNFR2-(S _{Δ42} /TM) _{R2} -Fas in HEK 293 Flp-IN T-Rex cells.....	180
Figure 49. Control of receptor cluster formation by the TNFR2 stalk region in TNFR2-Fas chimaeras.....	183
Figure 50. Ligand-independent receptor cluster formation of TNFR2-Fas and TNFR2-(S _{Δ42} /TM) _{R2} -Fas chimaeras.....	184
Figure 51. Time-course of doxycycline-induced expression of TNFR2 and variants thereof.....	186
Figure 52. Cell surface expression of TNFR2 in HEK 293 Flp-IN T-Rex cells upon induction with doxycycline.....	187
Figure 53. Cell surface expression of TNFR2-(S/TM) _{R1} -R2 in HEK 293 Flp-IN T-Rex cells upon induction with doxycycline.....	188
Figure 54. Cell surface expression of TNFR2-(S _{Δ42} /TM) _{R2} -R2 in HEK 293 Flp-IN T-Rex cells upon induction with doxycycline.....	189

Figure 55. The stalk region prevents cluster formation of wild type TNFR2.....	191
Figure 56. Ligand-independent receptor cluster formation of wild type TNFR2 and variants thereof.....	192

List of tables

Table 1. Chemicals and reagents.....	33
Table 2. Cell culture reagents and media	35
Table 3. Antibodies	36
Table 4. Sequencing primers.....	38
Table 5: ON-TARGETplus SMARTpool TNFRSF1A siRNA strands	39
Table 6. Amino acid composition of S _{GSL} for TNFR1 and TNFR2.....	50
Table 7. Oligonucleotides for the replacement of the complete stalk region with S _{GSL} ..	51
Table 8. Oligonucleotide annealing temperatures for complete stalk region replacement with S _{GSL}	52
Table 9. Subcloning plasmids generated for S _{GSL} introduction into TNFR1 and TNFR2..	53
Table 10. pBS SK(+) TNFR-S _{GSL} -Fas plasmids.....	54
Table 11. Amino acid sequences of the wild type and partially replaced TNFR2 stalk regions	55
Table 12. Oligonucleotides for partial stalk replacements in TNFR2-Fas	56
Table 13. Oligonucleotide combinations and annealing temperatures for partial stalk replacements.....	57
Table 14. Mammalian expression vectors encoding for partial stalk exchange mutants of TNFR2-Fas	58
Table 15. Oligonucleotides for proline mutants of TNFR2-Fas	60
Table 16. Two step site directed mutagenesis of conserved proline residues in the TNFR2 stalk region - oligonucleotide combinations and annealing temperatures	61
Table 17. Mammalian expression vectors encoding for proline mutants of TNFR2-Fas	62
Table 18. Oligonucleotides for the generation of TNFR2-(S/TM) _{R1} -R2.....	64
Table 19. pcDNA5/FRT/TO vectors for the generation of HEK 293 Flp-IN T-Rex cells	65
Table 20. Colour codes and abbreviations for plasmid maps	243

Acknowledgements

I would like to thank my supervisors, Dr Anja Krippner-Heidenreich and Professor Derek A. Mann, for supervising my PhD project and their advice over the past three years. I would also like to thank Dr Jelena Mann and Dr Fiona Oakley for their help and support with my cloning and translocation experiments. Special thanks to Dr Michele Sweney for being so patient and helpful when teaching me how to do confocal microscopy. In addition, I would like to thank all of the technical staff for their great help.

Thank you to all the members of the department, especially the ones in the Tunnel, for their friendship and for making the time in the lab a very enjoyable one. I would especially like to thank Nadine Binai, Jeroen Stoop, Patricia Garrido-Castro and Henrike Knizia for being so supportive and for the great times we had together. Special thanks to Amit Patel for supporting me all throughout my PhD and tolerating my bad mood when things did not go according to plan with my project.

I would also like to thank my family for their immense understanding and support and for encouraging me to give the Northeast of England a go. I thank the German Research Council (DFG project grant reference number KR3307/1-1) and the Institute of Cellular Medicine for funding this PhD.

Abbreviations

aa	Amino acid
ADAM17	A disintegrin and metalloproteinase 17
AP-1	Activator protein 1
Apaf-1	Apoptotic protease activating factor 1
APS	Ammonium peroxodisulphate
APRIL	A proliferation-inducing ligand
ASK1	Apoptosis-signal regulating kinase 1
ATF	Activating transcription factor
ATP	Adenosine-5'-triphosphate
BAFF	B-cell-activating factor
BAFFR	B-cell-activating factor receptor
BCG	<i>Bacillus Calmette-Guérin</i>
Bcl-2	B-cell lymphoma protein-2
Bcl-x _L	B-cell lymphoma-extra large protein
BCMA	B-cell maturation antigen
Benzyl- α -GalNAc	Benzyl-2-acetamido-2-deoxy- α -D-galactopyranoside
Bid	BH3 interacting domain death agonist
BS ³	“bis[sulfosuccinimidyl]suberate” (1-[8-(2,5-dioxo-3-sulfo-pyrrolidin-1-yl)oxy-8-oxooctanoyl]oxy-2,5-dioxopyrrolidine-3-sulfonic acid)
BSA	Bovine serum albumin
CD	Cluster of differentiation
CD27L	CD27 ligand
CD30L	CD30 ligand
CD40L	CD40 ligand
cFLIP	Cellular Fas-associated protein with death domain-like IL-1 β -converting enzyme inhibitory protein
cIAP	Cellular inhibitor of apoptosis protein
CNS	Central nervous system
Co-IP	Co-immunoprecipitation
CRD	Cysteine-rich domain

CysTNF	Cysteine-TNF (a mimic of membrane-bound TNF)
DCR	Decoy receptor
DD	Death domain
ddH ₂ O	Double-distilled water
DISC	Death-inducing signalling complex
dNTP mix	Deoxynucleotide mix
DMEM	Dulbecco's Modified Eagle Medium
DMSO	Dimethyl sulfoxide
DNA	Deoxyribonucleic acid
DN-TNF	Dominant-negative TNF
DPBS	Dulbeccos's phosphate buffered saline
DR	Death receptor
dsDNA	Double-stranded DNA
<i>E. coli</i>	<i>Escherichia coli</i>
EDA	Ectodermal dysplasin
EDAR	Ectodermal dysplasin receptor
ED ₅₀	Half-maximal effective dose
EDTA	2,2',2'',2'''-(ethane-1,2-diyldinitrilo)tetracetic acid
ELISA	Enzyme-linked immunosorbent assay
ERK	Extracellular signal-regulated kinase
Etk	Endothelial/epithelial tyrosine kinase
Fab	Fragment antigen binding
FACS	Fluorescence-activated cell sorting
FADD	Fas-associated death domain
FasL	Fas ligand
FCS	Foetal calf serum
FHC	Ferritin heavy chain
FITC	Fluorescein isothiocyanate
FoxP3	Forkhead box P3
FRET	Fluorescence energy transfer
Gadd45 β	Growth arrest and DNA damage protein 45 β
GITR	Glucocorticoid-induced TNF receptor
GITRL	Glucocorticoid-induced TNF receptor ligand
GSL	Glycine-serine-linker

HEK	Human embryonic kidney
HOIL-1	Haem-oxidised IRP2 ubiquitin ligase-1
HOIP	HOIL-1-interacting protein
HRP	Horseradish peroxidase
HSA	Human serum albumin
HVEM	Herpes-virus entry mediator
IBD	Inflammatory bowel disease
IgG	Immunoglobulin G
IgM	Immunoglobulin M
I κ B	Inhibitor of NF- κ B
IKK	I κ B kinase
JNK	c-Jun N-terminal kinase
KAc	Potassium acetate
K _d	Dissociation constant
LPS	Lipopolysaccharide
LT α	Lymphotoxin alpha
LT β	Lymphotoxin beta
LT β R	Lymphotoxin beta receptor
LUBAC	Linear ubiquitin chain assembly complex
MAPK	Mitogen-activated protein kinase
MAPKKK	MAPK kinase kinase
MEKK	MAP/ERK kinase kinase
MF	Murine embryonic fibroblast from <i>tnfr1</i> ^{-/-} / <i>tnfr2</i> ^{-/-} double knockout mice
MgCl ₂	Magnesium chloride
MKK	MAP kinase kinase
Mn-SOD	Manganese superoxide dismutase
MS	Multiple sclerosis
MW	Molecular weight
NaCl	Sodium chloride
NaN ₃	Sodium azide
NaOH	Sodium hydroxide
NEMO	NF- κ B essential modulator
NF- κ B	Nuclear factor-kappa B

NGF	Nerve growth factor
NGFR	Nerve growth factor receptor
NIK	NF- κ B-inducing kinase
OD	Optical density
OPG	Osteoprotegerin
OX40L	OX40 ligand
PAGE	Polyacrylamide gel electrophoresis
PBA	Phosphate buffered saline containing bovine serum albumin and sodium azide
PBS	Phosphate buffered saline
PBS-T	Phosphate buffered saline-Tween 20
pBS SK (+)	pBluescript SK (+) plasmid
PCR	Polymerase chain reaction
pEF PGKpuro	Mammalian expression plasmid encoding the elongation factor
polyA	1a promoter sequence, a puromycin resistance gene under the control of a phosphoglycerate kinase promoter and a poly A sequence
PEST sequence	Proline, glutamic acid, serine and threonine sequence
PKB	Protein kinase B
PLAD	Pre-ligand binding assembly domain
PMA	Phorbol-12-myristate-13-acetate
pmol	Picomole
PMSF	Phenylmethanesulfonyl fluoride
PVDF	Poly-1,1-difluoroethene
RA	Rheumatoid arthritis
RANK	Receptor activator of NF- κ B
RANKL	Receptor activator of NF- κ B ligand
RELT	Receptor expressed in lymphoid tissue
RGB	Resolving gel buffer
RIP1	Receptor-interacting protein 1
RNA	Ribonucleic acid
ROS	Reactive oxygen species
scTNF	Single-chain TNF
SDS	Sodium dodecyl sulphate

SDS-PA	SDS-polyacrylamide
SGB	Stacking gel buffer
S _{GSL}	Artificial stalk region consisting of glycine and serine residues
siRNA	Small interfering RNA
SLE	Systemic lupus erythematosus
Smac	Second mitochondrial activator of caspases
sTNF	Soluble TNF
TAB	TAK1 binding protein
TACE	TNF alpha converting enzyme
TACI	Transmembrane activator and cyclophilin ligand interactor
TAE	Tris-acetate-EDTA buffer
TAK1	Transforming growth factor- β activated kinase 1
<i>Taq</i>	<i>Thermus aquaticus</i>
TBE	Tris-boric acid-EDTA buffer
t-Bid	Truncated Bid
T _{conv}	Conventional T-cell
TE	Tris-HCl/EDTA
TEMED	N,N,N',N'-tetramethyl-ethane-1,2-diamine
TIMP-1	Tissue inhibitor of matrix metalloproteinase-1
TM	Transmembrane domain
TNC	Tenascin C
TNF	Tumour necrosis factor
TNFR	TNF receptor
TRADD	TNFR-associated death domain
TNFR-Fas	Chimaeric receptors consisting of the extracellular part of the TNFR and the cytoplasmic part of Fas
TRAF	TNF receptor associated factor
TRAIL	TNF-related apoptosis-inducing ligand
TRAILR	TRAIL receptor
T _{reg}	Regulatory T-cell
TRID	TNFR1 internalisation domain
Tris	2-amino-2-hydroxymethyl-propane-1,3-diol
TWEAK	TNF-like weak inducer of apoptosis
U	Unit

UV	Ultra-violet
V	Volt
v/v	Volume/volume
VEGI	Vascular endothelial cell-growth inhibitor
WGA	Wheat germ agglutinin
w/v	Weight/volume
wt	Wild type
XEDAR	X-linked EDA receptor
XIAP	X-chromosome linked inhibitor of apoptosis protein
zVADfmk	z-Val-Ala-DL-Asp-fluoromethylketone

CHAPTER 1

General Introduction

1.1 Tumour Necrosis Factor

Cytokines are soluble or membrane-bound signalling molecules involved in autocrine, juxtacrine and paracrine cell-cell communication. They mediate their action via specific receptors and influence various biological processes including cell differentiation, cell migration and inflammation (reviewed in Foster, 2001, Ozaki and Leonard, 2002, Feldmann, 2008).

A cytokine, which has been found to be involved in e.g. inflammation, immune responses, regulation of cell proliferation and differentiation as well as various autoimmune diseases, is tumour necrosis factor (TNF). TNF was first described in 1975 as a serum-factor from lipopolysaccharide (LPS)-challenged mice, which was found to cause necrosis of transplantable sarcomata (Carswell *et al.*, 1975). TNF was then cloned successfully and characterised biochemically in the 1980s (Pennica *et al.*, 1985, Aggarwal *et al.*, 1985). It is expressed as a 26 kDa type II transmembrane protein that exists as homotrimers in the plasma membrane (Tang *et al.*, 1996). Proteolytical cleavage of these homotrimers from the plasma membrane by the metalloprotease TNF alpha converting enzyme (TACE/ADAM17; Black *et al.*, 1997) results in a soluble form of TNF (sTNF). The bioactivity of membrane-bound and sTNF is exerted through two plasma membrane receptors, the type 1 (TNFR1; CD120a/p55/p60) and the type 2 TNF receptor (TNFR2; CD120b/p75/p80).

1.2 The TNF ligand and TNF receptor superfamilies

TNF is the name giving member of a large family of ligands, the TNF ligand superfamily, which is complemented by a family of corresponding receptors, the TNF receptor (TNFR) protein superfamily (reviewed in Locksley *et al.*, 2001, Aggarwal, 2003). In the years following the discovery of TNF, more and more members of the TNF ligand superfamily, such as receptor activator of NF- κ B ligand (RANKL), TNF-related apoptosis-inducing ligand (TRAIL/APO2L) and Fas ligand (FasL), were

discovered. The members of this superfamily are type II transmembrane proteins and are characterised by a C-terminal 150 aa long “TNF homology domain” (reviewed in Bodmer *et al.*, 2002). To date, the TNF ligand superfamily comprises 19 members and 29 members have been described for the TNFR superfamily (Locksley *et al.*, 2001, Aggarwal, 2003). Members of both superfamilies are schematically depicted in Figure 1.

While for receptor expressed in lymphoid tissue (RELT) the ligand has yet to be determined, for several of the ligands interaction with more than one member of the TNFR superfamily has been described. Lymphotoxin α (LT α), for example, has been found to be able to bind to TNFR1, TNFR2 (Brockhaus *et al.*, 1990, Schall *et al.*, 1990), the cellular herpes-virus entry mediator (HVEM; Mauri *et al.*, 1998) and, in a heterotrimer with LT β (LT α 1 β 2), to the lymphotoxin β receptor (Crowe *et al.*, 1994), while TNF can interact with TNFR1 and TNFR2 (Hohmann *et al.*, 1989, Brockhaus *et al.*, 1990). Furthermore, recent evidence emerged that the growth factor progranulin can compete with TNF and LT α in binding both, TNFR1 and TNFR2 and can inhibit TNF-mediated signalling (Tang *et al.*, 2011), further highlighting the complexity of TNF ligand superfamily signalling.

Most of the members of the TNF ligand superfamily can exist either in their membrane-bound form or can be shed from the plasma membrane, resulting in their soluble variants (Aggarwal, 2003). For several of these ligands differences in their signalling potential and biological function have been described. The pro-apoptotic activity of FasL, for example, was found to be strongly reduced for the soluble form of the ligand (Suda *et al.*, 1997, Schneider *et al.*, 1998). In contrast to its membrane-bound form, soluble FasL was found to promote autoimmunity in FasL transgenic mice and was proposed to trigger non-apoptotic, pro-inflammatory signalling pathways (O'Reilly *et al.*, 2009). Differences in receptor activation potential between the soluble and membrane-bound forms of several other members of the TNF ligand superfamily including TRAIL (Wajant *et al.*, 2001), a proliferation-inducing ligand (APRIL; Bossen *et al.*, 2008), OX40 ligand (Müller *et al.*, 2008) and TNF-like weak inducer of apoptosis (TWEAK; Roos *et al.*, 2010) have been described. Ligand trimer stabilisation and/or oligomerisation have been identified as important parameters for the efficient activation of some of the TNFR superfamily members including TNFR2 (Müller *et al.*, 2008, Wyzgol *et al.*, 2009, Rauert *et al.*, 2010).

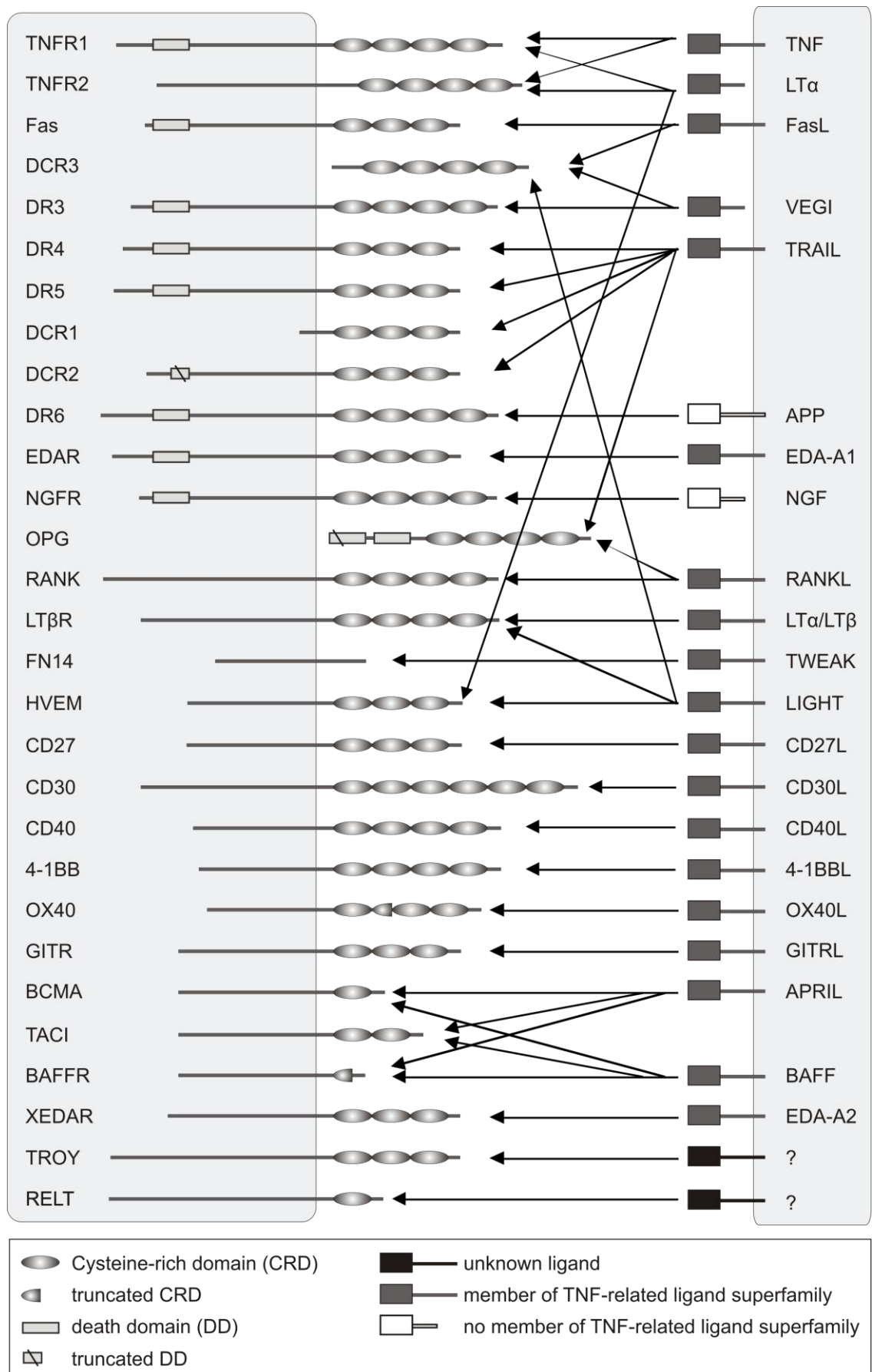


Figure 1. Schematic representation of the members of the TNF ligand and receptor superfamilies.

Shown are the members of the TNF ligand superfamily and the TNFR superfamily. The latter are characterised by presence of cysteine-rich domains (CRD) in the extracellular portions of the receptors. Some of the TNFR superfamily members contain a so-called death domain (DD) and are hence referred to as death receptors. Due to their pleiotropic nature some of the ligands can bind to more than one receptor superfamily member.

The ligand superfamily comprises TNF, lymphotoxin alpha and beta (LT α and LT β), Fas ligand (FasL), vascular endothelial cell-growth inhibitor (VEGI), TNF-related apoptosis-inducing ligand (TRAIL), ectodermal dysplasin (EDA), receptor activator of nuclear factor κ B ligand (RANKL), TNF-like weak inducer of apoptosis (TWEAK), a proliferation-inducing ligand (APRIL), LIGHT, CD27 ligand (CD27L), CD30 ligand (CD30L), CD40 ligand (CD40L), 4-1BB ligand (4-1BBL), OX40 ligand (OX40L), glucocorticoid-induced TNF receptor ligand (GITRL) and B-cell-activating factor (BAFF).

Members of the receptor superfamily are TNFR1 and TNFR2, Fas, decoy receptors 1, 2 and 3 (DCR1, DCR2 and DCR3), death receptors 3, 4, 5 and 6 (DR3, DR4, DR5 and DR6), EDA receptor (EDAR), X-linked EDAR (XEDAR), nerve growth factor receptor (NGFR), Osteoprotegerin (OPG), receptor of nuclear factor κ B (RANK), transmembrane activator and cyclophilin ligand interactor (TACI), BAFF receptor (BAFFR), LT β receptor (LT β R), FN14, CD27, CD30, CD40, 4-1BB, OX40, glucocorticoid-induced TNF receptor (GITR), B-cell maturation antigen (BCMA), herpes-virus entry mediator (HVEM), TROY and receptor expressed in lymphoid tissue (RELT). Data on LT α binding to TROY are conflicting (Bossen *et al.*, 2006, Hashimoto *et al.*, 2008) and for RELT the ligand is yet to be determined.

Nerve growth factor (NGF) and beta-amyloid precursor protein (APP) are no TNF ligand superfamily members but act as ligands for NGFR and DR6 (Nikolaev *et al.*, 2009), respectively. (Graphic was adopted from Aggarwal, 2003, and modified).

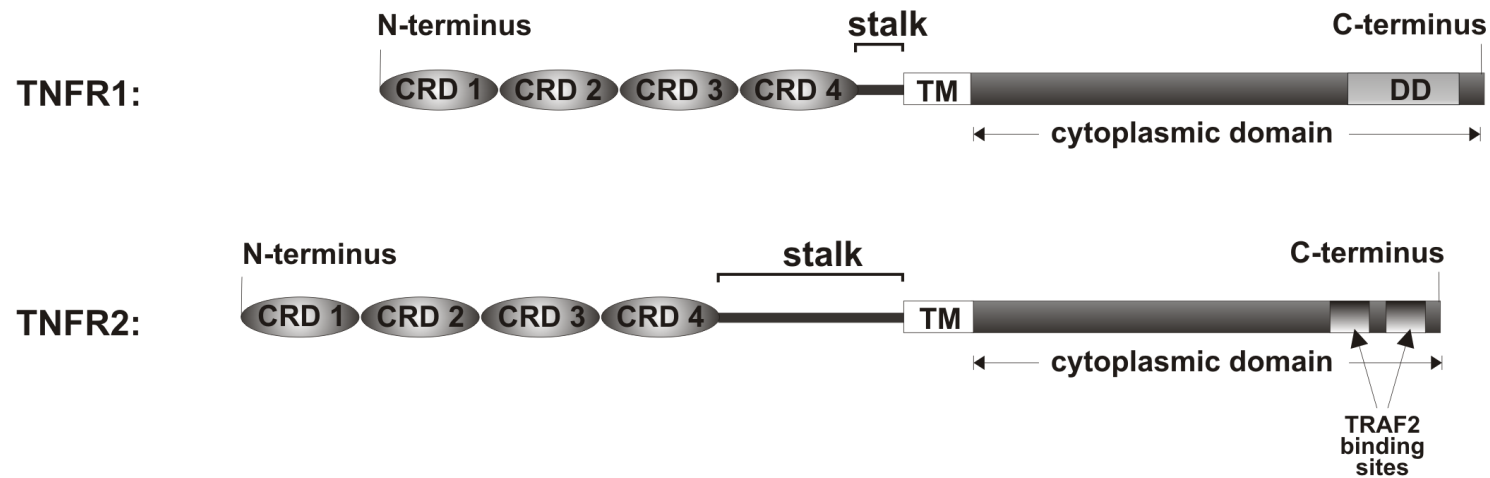
1.3 The type 1 and type 2 TNF receptors

As mentioned above, TNF exerts its bioactivity through the two receptors TNFR1 and TNFR2. In contrast to TNFR1, which is ubiquitously expressed in all tissues, TNFR2 is strongly regulated in its expression and mainly expressed on cells of the immune system, neuronal tissues, cardiac myocytes, mesenchymal stem cells and endothelial cells (reviewed in Faustman and Davis, 2010). With $K_d = 1.9 \times 10^{-11}$ M for TNFR1 and $K_d = 4.2 \times 10^{-10}$ M for TNFR2, both receptors are capable of binding homotrimeric sTNF with high affinity at 37 °C (Grell *et al.*, 1998b). However, sTNF was shown to lead to an efficient activation of only TNFR1, whereas membrane-bound TNF is capable of activating both TNFR1 and TNFR2 (Grell *et al.*, 1995). The molecular basis of this differential responsiveness is not yet understood.

TNFR1 and TNFR2 have been characterised biochemically. O-glycosylation has only been described for TNFR2 while N-glycosylation has been reported for both, TNFR1 and TNFR2 (Hohmann *et al.*, 1989), with the two asparagines N149 and N171 as potential sites of N-glycosylation in TNFR2 (Pennica *et al.*, 1993). Furthermore, O-glycosylation in the membrane proximal region of the extracellular portion of TNFR2 has been described (Pennica *et al.*, 1993) and TNFR2 has been found to be predominantly phosphorylated at serine residues (Pennica *et al.*, 1992). To date, several crystal structures of the extracellular domain of TNFR1 have been published (Banner *et al.*, 1993, Naismith *et al.*, 1995, Naismith *et al.*, 1996a, Naismith *et al.*, 1996b) and recently the extracellular domain of TNFR2 was crystallised and its structure solved (Mukai *et al.*, 2009, Mukai *et al.*, 2010). Further biochemical characterisation in combination with molecular modelling revealed specific functions for the different domains of the TNFR.

1.3.1 The cysteine-rich extracellular domains of TNFR1 and TNFR2

The extracellular domains of members of the TNFR superfamily are relatively diverse in their primary structure. However, in their tertiary structure, there are cysteine-rich sub-domains (CRD) which adopt similar folds. Typically, the TNFR superfamily proteins contain one to six of these sub-domains (Naismith and Sprang, 1998) with TNFR1 and TNFR2 each containing four CRD (see Figure 1 and Figure 2).



9

Figure 2. Schematic representation of the human TNF receptors TNFR1 and TNFR2.

TNFR1 (UniProtKB accession number P19438) and TNFR2 (UniProtKB accession number P20333) each consist of four cysteine-rich domains (CRD), which are connected to the transmembrane domains (TM; aa 212-234 of TNFR1, aa 258-287 of TNFR2) by a stalk region, and a cytoplasmic domain. The intracellular part of TNFR1 is 221 aa long and contains a death domain (DD, aa 356-441), whereas the intracellular part of TNFR2 is 174 aa long and contains two TNF receptor associated factor 2 (TRAF2) binding domains (aa 420-428 and aa 448-459 (Grech *et al.*, 2005)).

The CRD of TNFR1 and TNFR2 have been described to be composed of different modules. The nomenclature of these modules is based upon aa composition and length (module type A, B or C) and the number of disulphide bonds occurring within the module (one or two; Naismith and Sprang, 1998). CRD1, CRD2 and CRD3 of TNFR1 and CRD1 and CRD2 of TNFR2 are composed of A1 and B2 modules. A1 modules have the consensus sequence Cys1-X₂-Gly-X-Tyr/Phe-X-X_{4,9}-Cys2, whereas B2 modules have the consensus sequence Cys1-X₂-Cys2-X_{3,6}-X₅-Cys3-Thr-X_{2,5}-Asn-Thr-Val-Cys4 (X is any aa; Naismith and Sprang, 1998). CRD3 of TNFR2 consists of an A2 and a B1 module (Naismith and Sprang, 1998, Mukai *et al.*, 2010). The resulting module compositions are A1-B2-A1-B2-A2-B1-A1-B1 for TNFR2 and A1-B2-A1-B2-A1-B2-A1-C2 for TNFR1. The C2 module is unique to TNFR1.

A crystal structure of the extracellular domain of TNFR1 in complex with the homotrimeric ligand LT α has been solved (Banner *et al.*, 1993), in which the receptors bind to the grooves between the individual LT α monomers of the trimer. All receptor-LT α contacts are mediated by CRD2 and to a lesser extent by CRD3 of TNFR1 (Banner *et al.*, 1993). Homology modelling data by Fu *et al.* (1995) suggested similar interactions for TNFR1 and TNFR2 with TNF. This is in agreement with recent crystallography data of a TNF-TNFR2 complex, which indicated interactions of TNF with the A1 and B2 modules of CRD2 and the A2 module of CRD3 of TNFR2 (Mukai *et al.*, 2010).

Furthermore, ligand-independent oligomerisation of TNFR can occur (Chan *et al.*, 2000, Branschädel *et al.*, 2010). TNFR1 and TNFR2 are thought to self-associate prior to ligand binding via their pre-ligand binding assembly domains (PLAD). These PLAD are located in CRD1, which has been shown to be not directly involved in ligand binding (Chan *et al.*, 2000). Fluorescence energy transfer (FRET) data suggest that upon ligand binding a conformational change in the pre-assembled receptor complex takes place, which might affect downstream signalling (Chan *et al.*, 2001). Deletion of CRD1 was found to abrogate TNF binding to both TNFR1 and TNFR2 (Chan *et al.*, 2000, Mukai *et al.*, 2010). Molecular modelling data suggest that in case of TNFR1 the loss in TNF binding may be caused by a destabilisation of the A1 module of CRD2, which results from the deletion of CRD1 (Branschädel *et al.*, 2010). For receptor activation TNFR pre-assembly on the cell surface alone is not sufficient but presence of the ligand is also required for signalling initiation. However, data from arthritis and systemic lupus erythematosus (SLE) mouse models highlight the importance of TNFR pre-assembly

for receptor activation as the use of soluble PLAD proteins interfered with both TNFR1- and TNFR2-mediated signalling (Deng *et al.*, 2005, Deng *et al.*, 2010). In addition, microscopical and biochemical data indicate that efficient signalling requires the formation of large TNF/TNFR aggregates (Krippner-Heidenreich *et al.*, 2002, Schneider-Brachert *et al.*, 2004). Thus, instead of occurring as single receptor units, TNFR appear to exist as pre-formed complexes on the cell surface and form vast clusters after ligand binding. While there is a good understanding of the biological functions of the first three CRD of TNFR1 and TNFR2, only little is known about the role of CRD4.

1.3.2 Transmembrane domain and stalk region

The four CRD and the transmembrane domains of TNFR1 and TNFR2, respectively, are separated from each other by a stretch of aa residues which is here referred to as the stalk region (Figure 2). This stalk region consists of 15 aa residues in TNFR1, whereas the stalk of TNFR2 comprises 56 aa residues. Unfortunately, neither crystallographic data nor information on structural functions is available for the stalk regions so far. Additionally, the high proline content of the stalk region of TNFR2 makes it unlikely that it adopts a defined secondary structure.

However, the stalk region might play an important role in determining the half-life of the receptor. Both TNFR can be shed from the cell surface by membrane-bound TACE (Reddy *et al.*, 2000). For TNFR2 the presence of proline 211 (proline 247 in # P20333), which is located in the stalk region, has been reported to be a requirement for PMA/LPS-induced shedding of the receptor (Herman and Chernajovsky, 1998). Furthermore, O-glycosylation in this region as described by Pennica *et al.* (1993) might play an important role in signalling initiation. Interestingly, O-glycosylation has also been reported in the stalk region of another TNFR superfamily member, TRAIL receptor 2 (TRAILR2/DR5)(Wagner *et al.*, 2007).

Interestingly, the stalk regions of other members of the TNFR superfamily are also relatively diverse with, for example, short stalk regions for CD40, Fas and TRAILR1 and long, proline-rich stalk regions for TRAILR2, NGFR and TACI (Figure 3).

TNFR1:	PQIENVKGTEDSGTT
TNFR2:	STSPTRSMAPGAVHLPQPVSTRSQHTQPTPEPSTAPSTSFLLMGSPSPA EGSTGD
Fas:	EEGSRSN
DR3:	AVCGWRQ
TRAILR1:	VHKESGNGHN
TRAILR2:	VHKESGTKHSGEAPAVEETVTSSPGTPASPCS
DCR1:	PAAEETMNTSPGTPAPAAEETMNTSPGTPAPAAEETMTTSPGTPAPAAEE TMTTSPGTPAPAAEETMITSPGTPA
DCR2:	KNESAASSTGKTPAAEETVTTILGMLASPYH
DR6:	GTLPSFSSSTSPSPGTAIFRPEHMETHEVPSSTYVPKGMNSTESNSSASV RPKVLSSIQEGTVPDNTSSARGKEDVNKTLPNLQVVNHQQGPHHRHILKLL PSMEATGGEKSSTPIKGPKRGHPRQNLHKHFDINEHL
EDAR:	APPNTKECVGATSGASANFPGTSGSSTLSPFQHAHKELSGQGHATA
NGFR:	EIPGRWITRSTPPEGSDSTAPSTQEPEAPPEQDLIASTVAGVVTTVMGSSQ PVVTRGTTDN
RANK:	SSSLPARKPPNEPHVYLP
LTβR:	NPLEPLPPEMSGTMLM
CD27:	PTHLPYVSEMLEARAGHMQTLADFRQLPARTLSTHWPPQRSLSDFIR
CD30:	DTTFEAPPLGTQPCDNPTPENGEAPASTSPTQSLLDVDSQASKTLPIPTSAP VALSSTGK
CD40:	PQDRLR
4-1BB:	PSPADLSPGASSVTPPAPAREPGHSPQ
OX40:	DRDPPATQPQETQGPPARPITVQPTEAWPRTSQQPSTRPVEVPGGRA
GITR:	VPGSPPAEP
BCMA:	NASVTNSVKGTNA
TACI:	CENKLRSPVNLPELRRQRSGEVENNSDNSGRYQGLEHRGSEASPALPG LKLSADQV ALVYS
BAFFR:	GLLRTPRPKPAGASSPAPRTALQPQESVGAGAGEAALPLPGLL
XEDAR:	AFQLSLVEADTPTVPPQEAT
TROY:	ASKVNLVKIASTASSPRDTAL
RELT:	GDCWPGWFGPWGVPRVPCQPCSWAPLGTHGCDEWGRRARRGVEVAA GASSGGETRQPGNGTRAGGPEETAQA

Figure 3. Overview of TNFR superfamily member stalk regions.

Shown are the aa sequences of the indicated TNFR superfamily member stalk regions. Sequences were retrieved from UniProt KB and the corresponding accession numbers are stated in brackets: TNFR1 (P19438), TNFR2 (P20333), Fas (P25445), DR3 (Q93038), TRAILR1 (O00220), TRAILR2 (O14763), DCR1 (O14798), DCR2 (Q9UBN6), DR6 (O75509), EDAR (Q9UNE0), NGFR (P08138), RANK (Q9Y6Q6), LTβR (P36941), CD27 (P26842), CD30 (P28908), CD40 (P25942), 4-1BB (Q07011), OX40 (P43489), GITR (Q9Y5U5), BCMA (Q02223), TACI (O14836), BAFFR (Q96RJ3), XEDAR (Q9HAV5), TROY (Q9NS68), RELT (Q969Z4).

The predicted transmembrane domains (TM) of TNFR1 and TNFR2 are 23 and 30 aa residues long, respectively. Little is known about their function in signalling so far. However, data from erythropoietin receptor/TNFR2 chimaeras showed that the transmembrane domain of TNFR2 is essential for signal transduction (Declercq *et al.*, 1995).

1.3.3 Intracellular domains of TNFR1 and TNFR2

Depending on their intracellular domain, the members of the TNFR superfamily are divided into two groups, the death receptors containing a death domain (DD) and the gene inductive receptors containing at least one binding domain for TNF receptor-associated factor (TRAF) family members. The TNFR1 DD (Figure 2) is 85 aa residues long and located at the intracellular C-terminus of the receptor (Tartaglia *et al.*, 1993a). Furthermore, TNFR1 contains a so called TNFR1 internalisation domain (TRID), which is located adjacent to the TM region. Within this domain a YXXW motif has been found to be essential for ligand-induced receptor internalisation (Schneider-Brachert *et al.*, 2004).

Receptor internalisation upon stimulation has also been described for TNFR2. Here internalisation was found to be mediated by a di-leucine motif (L319/L320; Fischer *et al.*, 2011). In contrast to TNFR1, TNFR2 does not contain a DD but C-terminal TNF receptor associated factor 2 (TRAF2)-binding domains instead (Rothe *et al.*, 1995, Park *et al.*, 1999, Grech *et al.*, 2005). C-terminal of these TRAF2 binding domains a 16 aa domain has been described, which interacts with endothelial/epithelial tyrosine kinase (Etk). Etk is involved in TNF-mediated angiogenic events in vascular endothelial cell migration (Pan *et al.*, 2002). Furthermore, a PEST (proline, glutamic acid, serine, threonine) sequence in the cytoplasmic tail of TNFR2 has been identified. As PEST sequences are thought to mediate proteasomal degradation, the presence of this sequence might affect the half life of the receptor (Carpentier *et al.*, 2004).

The described cytoplasmic domains of the TNFR do not appear to determine the differential responsiveness of the receptors towards sTNF. This could be shown in a TNFR-Fas chimaera cellular system, in which the intracellular domains of TNFR1 and TNFR2 were replaced with an intracellular Fas domain (Krippner-Heidenreich *et al.*, 2002). However, although the cytoplasmic domains play a minor role in differential

responsiveness of the receptors, they are essential for the transmission of initial signals to adaptor proteins and the activation of different signalling pathways.

1.4 TNF/TNFR-mediated signalling

Upon binding of TNF to its receptors a wide range of different signalling pathways can be activated. Depending on which signalling pathway prevails, the cell either undergoes apoptosis or survives through counteracting processes. The signalling events following TNFR1 stimulation are better understood than the ones occurring upon TNFR2 engagement. Due to their complexity, however, only an overview of the three best characterised TNFR1 pathways, namely the caspase- and mitogen-activated protein kinase-(MAPK) dependent pro-apoptotic and the nuclear factor κ B (NF- κ B)-dependent anti-apoptotic signalling pathways, will be given in the following section.

While MAPK and NF- κ B activation have been described to occur while the TNFR1 signalling complex exists at the cell surface, TNFR1-mediated caspase pathway activation only occurs after receptor internalisation (Micheau and Tschopp, 2003, Schneider-Brachert *et al.*, 2004). These signalling complexes differ not only in their cellular localisation but also in their molecular composition. The complex at the plasma membrane contains the signalling adapter molecules TNFR-associated death domain (TRADD) protein, receptor-interacting protein 1 (RIP1) and TRAF2. Data on the signalling complex forming upon TNFR1 internalisation are controversial and two different models have been proposed. In the model described by Micheau and Tschopp TRADD, RIP1 and TRAF2 dissociate from TNFR1 and form a cytoplasmic complex with Fas-associated death domain (FADD) and caspases-8 and -10 (Micheau and Tschopp, 2003). In contrast, in the complex proposed by Schneider-Brachert *et al.* the adaptor proteins TRADD, FADD and caspase-8 associate with the internalised TNFR1 in endosomal compartments which were referred to as TNFR1 receptosomes (Schneider-Brachert *et al.*, 2004, Schütze *et al.*, 2008).

1.4.1 Anti-apoptotic TNFR1 signalling through NF- κ B activation

Binding of TNF to TNFR1 can lead to anti-apoptotic signalling through activation of NF- κ B. In mammalian cells, the five NF- κ B family members RelA (p65), RelB, c-Rel, p50/p105 (NF- κ B1) and p52/p100 (NF- κ B2) can form different NF- κ B complexes from their homo- and heterodimers (reviewed in Hoffmann *et al.*, 2006). In the majority of cell types, these NF- κ B complexes are retained in the cytoplasm by members of the inhibitors of NF- κ B (I κ B) protein family. In mammalian cells the three principal I κ B, I κ B α , I κ B β and I κ B γ , mask NF- κ B DNA binding and nuclear translocation sequences via their ankyrin repeat domain (reviewed in Basak and Hoffmann, 2008).

Activation of TNFR1 leads to the activation of NF- κ B/p50-p65 dimers through the so called canonical pathway (Basak and Hoffmann, 2008). Upon stimulation, TRADD and RIP1 are recruited into the TNFR1 signalling complex at the plasma membrane (Figure 4). The recruitment of RIP1 is mediated through homotypic interactions between the death domains of TRADD and RIP1 (Hsu *et al.*, 1996a). However, also TRADD-independent, competitive association of RIP1 with TNFR1 has been reported (Zheng *et al.*, 2006, Jin and El-Deiry, 2006). In addition, TRAF2 can be recruited to the N-terminus of TRADD via its TRAF2 domain (Hsu *et al.*, 1996b). Upon binding to TRADD, TRAF2 can be auto-ubiquitinated and was thought to induce poly-ubiquitination of RIP1. However, recent studies found the K63-linked poly-ubiquitination of RIP1 to be mediated by the cellular inhibitor of apoptosis proteins (cIAP) 1 and 2 (Varfolomeev *et al.*, 2008), which are associated with TRAF2 via its N-terminal c-IAP interaction motif (Vince *et al.*, 2009). Once ubiquitinated, RIP1 then supports the assembly and activation of a TAK1/TAB (TAK1/TAK1 binding protein) complex (Varfolomeev and Vucic, 2008).

TAK1 is able to phosphorylate and activate the I κ B kinase (IKK) complex. The activation of IKK1 and IKK2 of the IKK-complex leads to the phosphorylation of I κ B α at S32 and S36 and the phosphorylation of I κ B β at S19 and S23 (Mercurio *et al.*, 1997, Woronicz *et al.*, 1997, Zandi *et al.*, 1997, Wu and Ghosh, 2003). The phosphorylation targets I κ B α for K48-linked ubiquitination at K21 and K22 and subsequent proteasomal degradation (Alkalay *et al.*, 1995, Rodriguez *et al.*, 1996, Perkins, 2006). IKK γ , also known as NF- κ B essential modulator (NEMO), functions as regulatory subunit in the NF- κ B activation process (Perkins, 2006) and K63-linked ubiquitination of NEMO has been proposed to be essential for IKK1/IKK2 activation (Zhou *et al.*, 2004).

Furthermore, recently linear ubiquitination of NEMO by a linear ubiquitin chain assembly complex (LUBAC) consisting haem-oxidised IRP2 ubiquitin ligase-1 (HOIL-1) and HOIL-1-interacting protein (HOIP) has been described (Tokunaga *et al.*, 2009). Recruitment of LUBAC to the TNFR1 signalling complex, possibly mediated via cIAP1/2 K63-linked ubiquitin chains, has been proposed to stabilise the TNFR1 signalling complex by acting as a scaffolding platform (Haas *et al.*, 2009).

Proteasomal degradation of I κ B α leads to the release of NF- κ B, which can then translocate to the nucleus and finally induce transcription of TNF/NF- κ B regulated genes such as manganese superoxide dismutase (Mn-SOD) and A20 (Figure 4), which regulate the JNK pathway negatively at different levels. A20, for example, inhibits the activation of JNK by attenuating TRAF2 function (reviewed in Papa *et al.*, 2006). Additionally, NF- κ B induces the transcription of further anti-apoptotic factors such as cellular Fas-associated protein with death domain-like IL-1 β -converting enzyme inhibitory proteins (cFLIP) and X-chromosome linked inhibitor of apoptosis protein (XIAP), thereby promoting cell survival (Kreuz *et al.*, 2001, Micheau *et al.*, 2001, Stehlik *et al.*, 1998).

The importance of RIP1 and TRAF proteins in TNFR1 signalling have been highlighted by data obtained from mouse knockout models. These indicated that RIP1 is absolutely required for NF- κ B and JNK activation (Ting *et al.*, 1996). In contrast, TRAF2 was found to be only crucial for the activation of JNK but appeared to be dispensable for NF- κ B responses (Yeh *et al.*, 1997, Tada *et al.*, 2001a). Another member of the TRAF protein family, TRAF5, has also been implicated in TNFR1-mediated NF- κ B signalling. TNF-induced NF- κ B nuclear translocation is impaired in *traf2^{-/-} traf5^{-/-}* double knockout but not the corresponding single knockout mice, suggesting both, a critical role and a certain redundancy for TRAF2 and TRAF5 (Tada *et al.*, 2001a). TRAF5 was found to interact with RIP1 and, like TRAF2, appears to play a role in both, NF- κ B and JNK activation (Tada *et al.*, 2001a). However, in contrast to data presented by Tada *et al.* (2001a), more recent data indicate that TRAF2 is not dispensable for the activation of the canonical NF- κ B pathway as it is required for efficient recruitment of cIAP and IKK to the TNFR1 signalling complex (Devin *et al.*, 2000, Vince *et al.*, 2009).

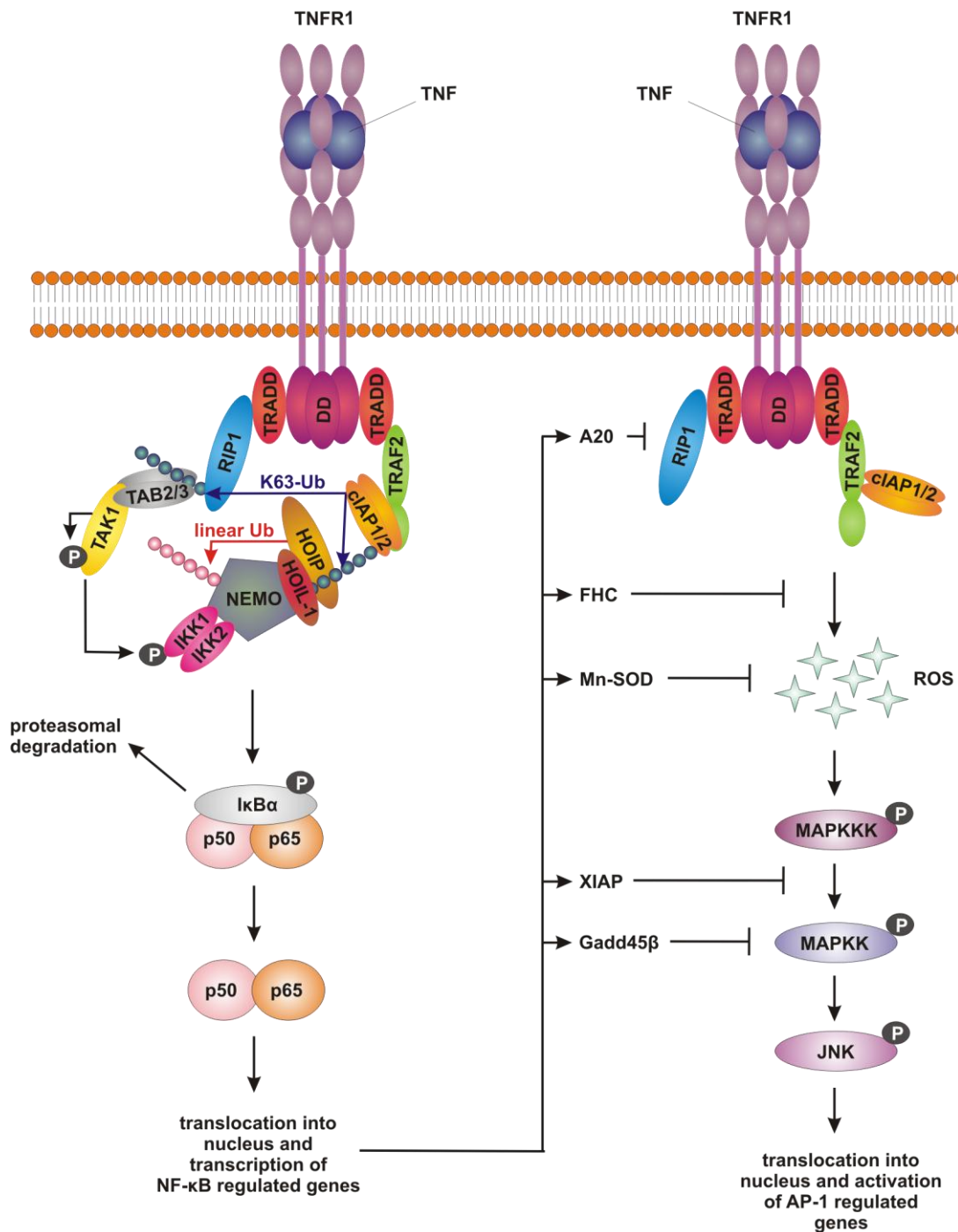


Figure 4. Schematical representation of TNFR1-mediated anti-apoptotic NF- κ B and pro-apoptotic JNK signalling crosstalk.

TNFR-associated death domain (TRADD) is recruited to the TNFR1 death domain (DD) and can recruit receptor interacting protein 1 (RIP1), TNF receptor associated factor 2 (TRAF2) and cellular inhibitor of apoptosis proteins (cIAP1/cIAP2). K63-linked ubiquitination (K63-Ub) of RIP1 by cIAP recruits transforming growth factor β activated kinase 1 (TAK1) and TAK1 binding proteins 2/3 (TAB2/3) to RIP1. Upon recruitment to the TNFR1 signalling complex, TAK1 becomes autophosphorylated and phosphorylates inhibitor of NF- κ B (I- κ B) kinases (IKK). Haem-oxidised IRP2 ubiquitin ligase-1 (HOIL-1) and HOIL-1-interacting protein (HOIP) mediate linear ubiquitination of NF- κ B essential modulator (NEMO), which serves as a regulatory compound. The IKK then cause phosphorylation and subsequent proteasomal degradation of I- κ B α , leading to the release and nuclear translocation of p50/p65.

Alternatively, TNF-stimulation can lead to the activation of the JNK signalling pathway. Here MAPK kinase kinases (MAPKKK) such as MAP/ERK kinase kinase 1 (MEKK1), apoptosis-signal regulating kinase (ASK1) or TAK1 are activated, putatively in a reactive oxygen species (ROS)-dependent manner by TRAF2 (Dhanasekaran and Reddy, 2008), and activate MAPKK such as MKK4 and/or MKK7. The MAPKK then phosphorylate JNK, which translocates to the nucleus and activates AP-1-regulated genes.

NF- κ B regulated gene products such as A20, ferritin heavy chain (FHC), manganese superoxide dismutase (Mn-SOD) and growth arrest and DNA damage protein 45 β (Gadd45 β) function as negative regulators at various levels of the JNK pathway by, for example, counteracting the production of ROS (diagram was adopted from Papa *et al.*, 2006, Varfolomeev and Vucic, 2008, Haas *et al.*, 2009, and modified).

1.4.2 Pro-apoptotic signalling of TNFR1

1.4.2.1 Mitogen-activated protein kinase cascade

Stimulation of TNFR1 with TNF can alternatively lead to MAPK pathway-mediated cell death. Prominent MAPK kinase kinases (MAPKKK) of the c-Jun N-terminal kinase (JNK) cascade comprise apoptosis-signal regulating kinase 1 (ASK-1), MAP/ERK (extracellular signal-regulated kinase) kinase kinases (MEKK) and TAK1. As depicted in Figure 4, these MAPKKK activate MAP kinase kinases (MKK) 4 and/or MKK7, which in turn activate JNK (Derijard *et al.*, 1995, Moriguchi *et al.*, 1997, Tournier *et al.*, 1997, Wu *et al.*, 1997, Yao *et al.*, 1997). Subsequently, the activated JNK translocates to the cell nucleus where it phosphorylates and transactivates c-Jun. c-Jun phosphorylation then leads to the formation of activator protein 1 (AP-1) and transcription of pro-apoptotic AP-1 target genes (reviewed in Dhanasekaran and Reddy, 2008). As reported by Fan *et al.* (2010), K63-linked poly-ubiquitination of TAK1 seems to play a pivotal role in this JNK-mediated activation of AP-1.

Reactive oxygen species (ROS) have been found to function as important mediators in the JNK cascade. The exact mechanism by which ROS trigger TNF induced apoptosis is not clear, but they possibly prolong activation of the JNK cascade (reviewed in Papa *et al.*, 2006) and ROS-dependent activation of ASK1 by TRAF2 appears to play a role (Dhanasekaran and Reddy, 2008).

JNK signalling has been reported to promote apoptosis via the mitochondria-dependent pathway of type II cells (see following section) by inactivating anti-apoptotic and activating pro-apoptotic members of the B-cell lymphoma protein-2 (Bcl-2) family of proteins. UV-induced phosphorylation of JNK was described to lead to release of the pro-apoptotic Bcl2 proteins Bim and Bmf, which link JNK signalling to the Bax/Bak-dependent mitochondrial apoptosis pathway (Lei and Davis, 2003). In addition, JNK can induce an alternative, caspase-8 independent cleavage of Bid to a variant termed j-Bid (Deng *et al.*, 2003). j-Bid leads to the release of Smac (second mitochondrial activator of caspases) from the mitochondria and it has been proposed by Deng *et al.* (2003) that Smac then causes disruption of the TRAF2/cIAP complex and subsequent activation of caspase-8 and induction of apoptosis.

However, activation of the JNK pathway has also been found to be associated with anti-apoptotic functions, such as the deactivation of pro-apoptotic Bcl-2 family

proteins. These controversial findings have been ascribed to the fact, that TNF stimulation does not only induce JNK signalling but also the anti-apoptotic NF- κ B pathway (see section 1.4.1 and Figure 4) and that crosstalk between these two signalling pathways ultimately affects whether cells survive or undergo apoptosis. In this context MKK4 and TAK1 have been proposed to represent nodal points between pro-apoptotic JNK-signalling and activation of the NF- κ B signalling pathway via, for example, Akt/PKB kinases (Sethi *et al.*, 2007, Fan *et al.*, 2010).

Another member of the MAPK family which can be activated by TNF is p38 MAPK. Data obtained from *Mkk3*^{-/-}/*Mkk6*^{-/-} fibroblasts suggest that this TNF-mediated activation requires MKK3 and MKK6 as p38 MAPK activation occurs only in wild type but not the knockout cells (Brancho *et al.*, 2003). p38-mediated activation of transcription factors such as activating transcription factors (ATF) 1, 2 and 6, p53 and myocyte enhance factor 2 C (MEF2C) has been reported and p38 also indirectly regulates AP-1 activity (reviewed in Zarubin and Han, 2005, Nakano *et al.*, 2006).

1.4.2.2 Caspase-dependent pathways

As mentioned above, upon TNF-binding TRADD protein, TRAF2 and RIP1 are recruited to the death domain of TNFR1 and this complex can signal via the NF- κ B and MAPK pathways, respectively (sections 1.4.1 and 1.4.2.1). However, upon subsequent internalisation of the TNFR1 signalling complex the TRADD/TRAF2/RIP1 complex is disrupted (Schütze *et al.*, 2008) and the adaptor proteins FADD (Micheau and Tschopp, 2003) and procaspase-8 (Boldin *et al.*, 1996, Muzio *et al.*, 1996) are recruited to TRADD. TNFR1 and the recruited proteins together constitute the death-inducing signalling complex (DISC, Figure 5). DISC formation has already been described for Fas (Kischkel *et al.*, 1995). However, while Fas-mediated caspase activation can also occur in signalling complexes still located at the plasma membrane, formation of the TNFR1 DISC was found to depend upon the internalisation of TNFR1 after ligand binding (Schneider-Brachert *et al.*, 2004, Schütze *et al.*, 2008).

Caspase-8, a member of a family of cysteine proteases, is expressed as the precursor procaspase-8. As proposed by Chang *et al.* (2003), procaspase-8 becomes auto-proteolytically activated by interdimer processing upon recruitment into the DISC. Caspase-8 then serves as an initiator caspase, which proteolytically cleaves and thereby activates effector caspases (reviewed in Riedl and Shi, 2004). Depending on the cell

type, caspase-8 leads to activation of different signalling pathways (Scaffidi *et al.*, 1998). In type I cells, such as the B-lymphoblastoid SKW6.4 cell line (Algeciras-Schimmich *et al.*, 2003), the high level of caspase-8 directly mediates activation of procaspase-3 to caspase-3, which then leads the proteolytical cleavage of cellular components and eventually to the induction of apoptosis. In contrast, the caspase-8 level in type II cells, such as the T-lymphoblastoid Jurkat cell line (Algeciras-Schimmich *et al.*, 2003) is low and requires an amplification of the signal via the mitochondria. Type II signalling involves cleavage of the Bcl-2 family protein Bid (BH3 interacting domain death agonist) to its truncated form t-Bid by caspase-8 (Li *et al.*, 1998). t-Bid is translocated to the mitochondria where it is thought to directly or indirectly activate the pro-apoptotic Bcl-2 proteins Bax and Bak (Letai *et al.*, 2002, Willis and Adams, 2005, Willis *et al.*, 2005, Willis *et al.*, 2007). This activation leads to the release of cytochrome C from the mitochondria. Cytochrome C can bind to the WD40 region of apoptotic protease activating factor 1 (Apaf-1), thereby releasing Apaf-1 from its auto-inhibited state. Seven of the Apaf-1 molecules, which have bound cytochrome C, can then assemble into a wheel-like structure termed the apoptosome (Riedl and Salvesen, 2007). Caspase-9 becomes activated within the apoptosome and in turn activates caspase-3 and caspase-7, which then, as described for type I cells, can initiate apoptosis (reviewed in Riedl and Salvesen, 2007, Schütze *et al.*, 2008).

Both, the type I and type II signalling pathways can be regulated at the level of DISC formation by cFLIP. The three cFLIP isoforms, cFLIP_L, cFLIP_S and cFLIP_R, have been reported to inhibit death receptor mediated apoptosis by modulating caspase-8 activation, although also pro-apoptotic functions of cFLIP_L have been described (Yu and Shi, 2008). XIAP can directly inhibit the activation of caspase-9 (Eckelman *et al.*, 2006) while this appears not to be the case for cellular inhibitor of apoptosis proteins (cIAP) 1 and 2, which rather counteract apoptosis via their E3 ubiquitin ligase activity. cIAP1-mediated proteasomal degradation of caspase-3 and caspase-7 has been reported (Choi *et al.*, 2009) and data from IAP inhibitor experiments indicate that cIAP1 also controls the non-canonical NF- κ B pathway at the level of NF- κ B-inducing kinase stability (NIK; Varfolomeev *et al.*, 2007, Vince *et al.*, 2007). Furthermore, cIAP1 and cIAP2 mediate K63-linked ubiquitination of RIP1, which is in turn required for binding of transforming growth factor- β activated kinase 1 (TAK1) and activation of anti-apoptotic pathways (Bertrand *et al.*, 2008).

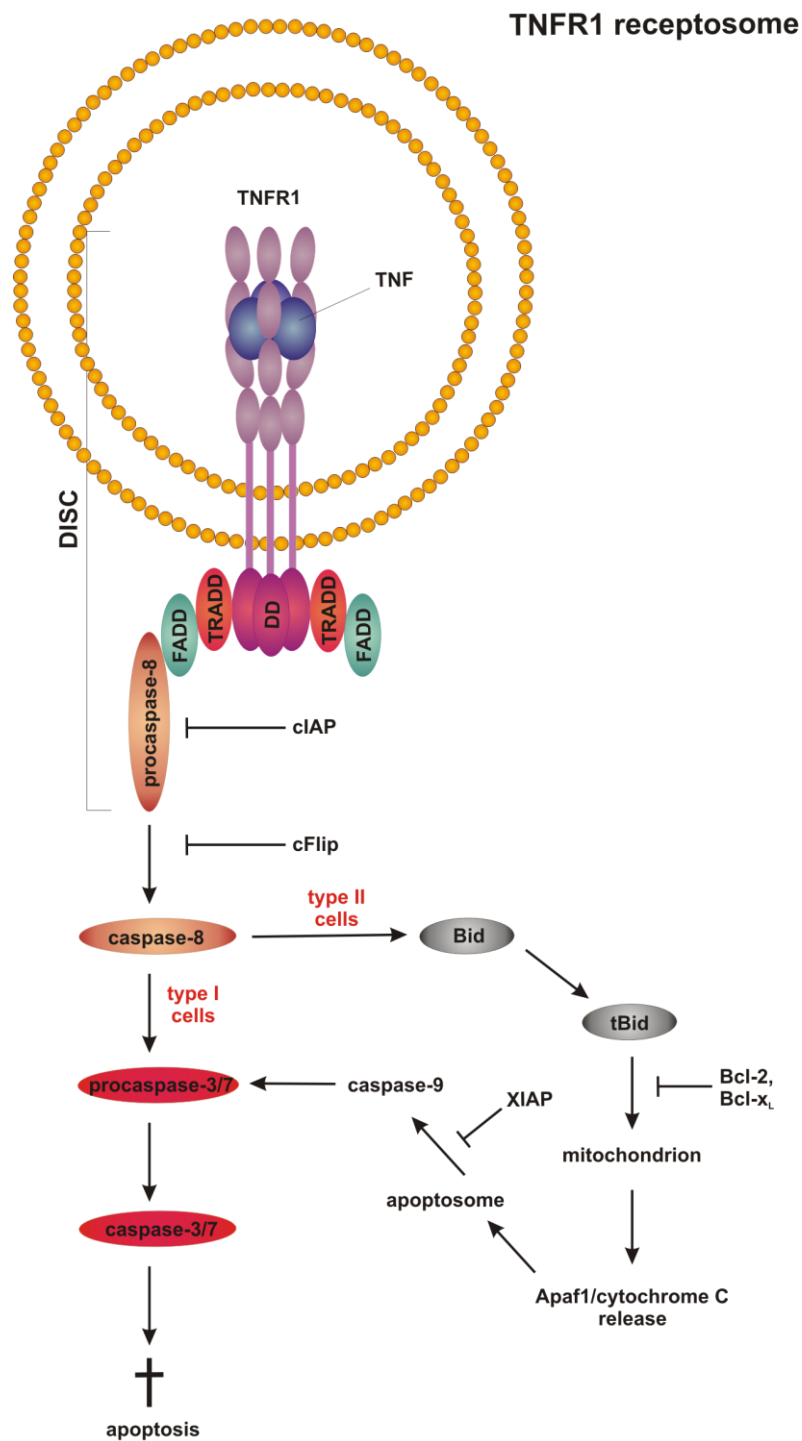


Figure 5. DISC formation and caspase-dependent signalling of TNFR1.

Upon TNF-mediated receptor endocytosis TNFR1 receptosomes are formed, in which the death inducing signalling complex (DISC) is assembled. The DISC consists of TNFR1, TNFR-associated death domain (TRADD) and Fas-associated death domain (FADD), which all three contain a DD, and caspase-8. In both, type I cells and type II cells, DISC formation leads to the activation of caspases and apoptosis. Caspase activation in type II cells, however, does require an amplification of the signal via the mitochondrial pathway with apoptotic protease activating factor 1 (Apaf-1) and truncated Bid (tBid) being important components. X-chromosome linked inhibitor of apoptosis protein (XIAP), cellular inhibitor of apoptosis protein (cIAP), cellular FLICE inhibitor protein (cFLIP), B-cell lymphoma protein-2 (Bcl-2) and B-cell lymphoma-extra large protein (Bcl-x_L) regulate the apoptotic pathway negatively (Graphic was adopted from Schneider-Brachert *et al.*, 2004, Schütze *et al.*, 2008).

1.5 TNFR2-mediated signalling and crosstalk between TNFR1 and TNFR2

Similar to TNFR1, for TNFR2 TRAF2-dependent activation of the NF- κ B and JNK pathways has been described (Rothe *et al.*, 1995, Reinhard *et al.*, 1997) and, furthermore, data from *tnfr1*^{-/-} knockout murine fibroblasts revealed TNFR2-mediated activation of ERK1/ERK2 (Kalb *et al.*, 1996, Reinhard *et al.*, 1997). In TNFR2-mediated MAPK signalling c-IAP1 appears to play an important role. c-IAP1 gets activated upon stimulation of TNFR2 and mediates ubiquitination and degradation of TRAF2 (Li *et al.*, 2002). In addition, TNFR2 stimulation leads to degradation of ASK1 in Jurkat cells as well as B-cells from *c-iap1*^{-/-} knockout mice, further showcasing TNFR2-mediated activation of the MAPK pathways (Zhao *et al.*, 2007).

Recent evidence emerged, that the ability of TNFR2 to induce the JNK signalling pathway might be affected by its ubiquitination through the E3 ubiquitin ligase Smurf2 (Carpentier *et al.*, 2008). In an overexpression system, Smurf2-mediated ubiquitination was found to cause a redistribution of the receptor within the membrane to detergent-insoluble cell fractions and this redistribution seemed to effect the selective activation of the JNK pathway.

Furthermore, TNFR2 is capable of facilitating or inducing apoptosis indirectly and two possible mechanisms have been described so far. Firstly, TNFR2 was described to exert its apoptotic action via the induction of endogenous TNF, which then subsequently activates TNFR1 (Vercammen *et al.*, 1995, Grell *et al.*, 1999). Secondly, a TRAF2-dependent intracellular mechanism, which is independent of endogenous TNF but also enhances TNFR1-mediated signalling for apoptosis, has been described (Declercq *et al.*, 1998, Chan and Lenardo, 2000). Fotin-Mleczek *et al.* (2002) showed that co- and pre-stimulation of TNFR2 enhanced TNFR1-induced caspase-8 activation and proposed that this is due to a TNFR2-mediated depletion of TRAF2. In several publications TRAF2 recruitment to detergent-insoluble membrane compartments upon TNFR2 stimulation has been described (Li *et al.*, 2002, Wu *et al.*, 2005, Wicovsky *et al.*, 2009). TRAF2 recruitment to TNFR2 would consequently lead to a decreased availability of the TRAF2-cIAP complex for TNFR1. As this complex is required for efficient induction of anti-apoptotic NF- κ B activation of the latter (section 1.4.1), this decreased availability promotes the caspase-dependent TNFR1 signalling pathways. A TRAF family member which has recently been described to antagonise the recruitment-

dependent depletion and subsequent proteasomal degradation of TRAF2 is TRAF1. TRAF1 can rescue TNFR1-mediated activation of NF- κ B and JNK in TNFR2-prestimulated Colo205 cells to at least some extent (Wicovsky *et al.*, 2009).

In contrast to TNFR1, for TNFR2 in addition to activation of the canonical NF- κ B pathway (Rothe *et al.*, 1995, Krippner-Heidenreich *et al.*, 2002, Marchetti *et al.*, 2004, Fischer *et al.*, 2011) also TNFR2-mediated signalling via the non-canonical NF- κ B pathway has been reported. Stimulation with oligomerised TNFR2-selective TNF has been proposed to result in the accumulation of NIK by preventing TRAF2/cIAP1/cIAP2-mediated NIK degradation in HeLa cells expressing exogenous TNFR2 (NIK; Rauert *et al.*, 2010). This accumulation of NIK was further described to lead to NEMO-mediated processing of the NF- κ B subunit p100 to p52 and to the nuclear translocation of the latter.

1.6 TNF and TNFR in health and disease

1.6.1 Physiological implications for sTNF and membrane-bound TNF

As mentioned in section 1.2, TNF can exert its biological functions as both soluble and membrane-bound ligand. However, depending on which form TNF exists in these functions can differ. TNF has, for example, been implicated to be an important regulator of the micro-architecture and function of secondary lymphoid tissues. Studies from *tnf*^{-/-} mice showed that TNF is required for the formation of germinal centres as well as development and organisation of lymph nodes and spleen (Marino *et al.*, 1997, Körner *et al.*, 1997). Like *tnf*^{-/-} mice, transgenic mice which only express membrane-bound TNF fail to form organised germinal centres and follicular dendritic cell networks, highlighting not only an important role for sTNF in lymphoid tissue development (Alexopoulou *et al.*, 2006) but also the divergent biological functions of the soluble and membrane-bound forms of the ligand.

Moreover, the divergent roles for sTNF and membrane-bound TNF become apparent in the context of host defence against pathogens. Transmembrane TNF was found to be sufficient to mediate immunity and resistance to infections with *Bacillus Calmette-Guérin* (BCG), a strain of the attenuated *Mycobacterium bovis* (Olleros *et al.*, 2002). In the absence of sTNF, membrane-bound TNF was capable of sufficiently

controlling acute but not chronic infections with *Mycobacterium tuberculosis* (Saunders *et al.*, 2005). Furthermore, studies on D-galactosamine/LPS-induced and BCG/LPS-induced liver injury in transgenic mice together with TNF inhibitor data support a role for sTNF but not membrane-bound TNF in liver granuloma formation and hepatitis (Nowak *et al.*, 2000, Olleros *et al.*, 2010). Similarly, membrane-bound TNF was able to confer immunity against low doses of *Listeria monocytogene*, but sTNF was found to be required for a full protective inflammatory response to the pathogen (Torres *et al.*, 2005, Musicki *et al.*, 2006).

While these data demonstrate the diversity of sTNF and membrane-bound TNF functions, the underlying mechanisms for these differences are not very well understood to date.

1.6.2 Divergent roles of TNFR1 and TNFR2 in health and disease

As already indicated above, TNF and its receptors play important roles in the immune system. In animal studies it was shown that TNF, TNFR1 and TNFR2 are involved in the development of germinal centres and Peyer's patches (Marino *et al.*, 1997, Neumann *et al.*, 1996) and important roles in the proliferation and migration of immune cells have been described. While some of the biological functions of TNF are mediated by both of its receptors, also divergent roles have been reported for TNFR1 and TNFR2.

1.6.2.1 Modulation of immune tolerance by TNFR2

Given that cells of the immune system represent one of the few cellular subsets where TNFR2 expression can be observed (reviewed in Faustman and Davis, 2010), it is not surprising that this receptor exerts specific functions in immunity. Results from mouse knockout models, for example, indicate a role for TNFR2 but not TNFR1 in the promotion of thymocyte proliferation (Tartaglia *et al.*, 1991, Tartaglia *et al.*, 1993b, Grell *et al.*, 1998a) and TNFR2 has been described to function as an important co-stimulator during antigen-driven differentiation and expansion of CD4⁺ and CD8⁺ T-cells (Kim and Teh, 2001, Aspalter *et al.*, 2003, Kim *et al.*, 2006). Kim *et al.* (2006) propose an anti-apoptotic role for TNFR2 and suggest that this receptor controls T-cell survival after T-cell expansion is initiated.

Furthermore, involvement of TNFR2 in the maintenance and balance of immune tolerance has been reported. Forkhead box P3 (FoxP3) protein positive CD4⁺CD25⁺ regulatory T-cells (T_{reg}) constitute the major T_{reg} population in the human immune system, which controls maintenance of self-tolerance and immune homeostasis. Studies on FoxP3⁺-deficient mice and humans who carry mutations in the *foxp3* gene, respectively, showed that the absence of functional FoxP3⁺CD4⁺CD25⁺ T_{reg} results in immune system dysregulation and the development of autoimmunity. This autoimmunity has been proposed to arise as a result of an imbalance in the control of pathogenic auto-reactive T-cells by FoxP3⁺CD4⁺CD25⁺ T_{reg} (reviewed in Miyara and Sakaguchi, 2011). In the context of regulatory and auto-reactive T-cells divergent roles have been proposed for TNFR2. Valencia *et al.* (2006) found TNF- and TNFR2-agonistic antibody-mediated stimulation of TNFR2 to down-regulate FoxP3 expression and inhibit the suppressive function of human FoxP3⁺CD4⁺CD25⁺ T_{reg}, thereby modulating immune reactivity. This down-regulation of the suppressive FoxP3⁺CD4⁺CD25⁺ T_{reg} function appears to result from TNFR2-mediated activation of the canonical NF-κB pathway and can be inhibited through co-treatment with anti-TNFR2 blocking antibodies (Nagar *et al.*, 2010). In contrast, TNFR2 was described to be a cell surface marker for a more suppressive subset of the FoxP3⁺CD4⁺CD25⁺ T_{reg} population in a murine model of lung carcinoma (Chen *et al.*, 2008). In this model, TNFR2 cell surface expression on a CD4⁺FoxP3⁻ subset of conventional T-cells (T_{conv}) was described to lead to an increased resistance of these T_{conv} cells towards suppression by T_{reg} cells. This resistance could, however, be overcome by the aforementioned TNFR2-positive subset of FoxP3⁺CD4⁺CD25⁺ T_{reg} cells (Chen *et al.*, 2010). How the different findings from these studies relate to each other remains yet to be determined. However, together with data from Ban *et al.* (2008), who observed TNFR2-mediated killing of insulin-specific auto-reactive CD8⁺ T-cells of type I diabetes patients, these studies highlight the role of TNFR2 as an important regulatory modulator in immunity and suggest that TNFR2 might be a promising target in the therapy of autoimmune diseases and cancer.

1.6.2.2 Involvement of TNFR1 and TNFR2 in host defence

In addition to its well described function as a pro-inflammatory cytokine, TNF has been found to be involved in mediating resistance against various bacterial infections (see also section 1.6.1). Studies on mice deficient in TNFR1 revealed that this receptor is

required to clear infections with intracellular pathogens such as *Listeria monocytogenes*, *Mycobacterium tuberculosis*, *Leishmania major* and *Trypanosoma cruzi* (Rothe *et al.*, 1993, Pfeffer *et al.*, 1993, Nashleanas *et al.*, 1998, Castanos-Velez *et al.*, 1998).

Granuloma formation, which is important for modulating the growth of *Mycobacterium* and clearing the infection, was found to be impaired in *tnfr1*^{-/-} mice (Ehlers *et al.*, 2000). As shown recently by Clay and co-workers (2008), similar protective effects of TNF in early infection with *Mycobacterium tuberculosis*, involving modulation of bacterial growth and macrophage death, also hold true in a zebra fish tuberculosis model. Unfortunately, it has not yet been described, whether these functions involve TNFR1, TNFR2 or are mediated by both TNFR. Increased severity of inflammatory lesions has been reported in *tnfr1*^{-/-} mice after infection with *Trypanosoma cruzi* and *Legionella pneumophila*, respectively (Fujita *et al.*, 2008, Nashleanas *et al.*, 1998). The lesions upon infection with *Legionella pneumophila* have been proposed to be a result of a delayed clearance of the pathogens from the lung leading to severe inflammation (Fujita *et al.*, 2008). Therefore, in these studies TNFR1 was proposed to play an important role in the control of the infection (Castanos-Velez *et al.*, 1998, Fujita *et al.*, 2008). In contrast, corresponding experiments with *tnfr2*^{-/-} mice indicated that TNFR2 is required to control inflammation and appears to rather have an anti-inflammatory function during infections with *Legionella pneumophila* (Fujita *et al.*, 2008).

While TNF is helping to contain and remove local infections, its actions have, however, been found to be detrimental when infections become systemic as the cytokine was discovered to trigger septic shock (Beutler *et al.*, 1985, Tracey *et al.*, 1987). Studies on *tnfr1*^{-/-} mice showed that it is TNFR1 which is critically involved in mediating septic shock (Pfeffer *et al.*, 1993, Rothe *et al.*, 1993).

1.6.3 TNFR1 and TNFR2 in the central nervous system

In the central nervous system (CNS), TNF regulates physiological processes such as neuronal development, cell survival and synaptic transmission and, furthermore, represents an important mediator of inflammation (reviewed in Park and Bowers, 2010). It is produced in response to various insults to the CNS, including bacterial and viral infections, physical damage and oxygen-glucose deprivation, the latter occurring during ischaemic conditions associated with stroke. Dysregulation of inflammatory responses

in the CNS has been proposed to underlie the pathogenesis of neuronal diseases (Park and Bowers, 2010).

Primary demyelination is a hallmark of several inflammatory diseases of the CNS, such as multiple sclerosis (MS). It involves the destruction and phagocytosis of myelin by activated microglia/macrophages (Martin *et al.*, 1992) and can be accompanied by apoptosis of the myelin sheath-forming oligodendrocytes. Earlier studies had shown that the expression of TNF is up-regulated in active MS lesions (Hofman *et al.*, 1989) and, that TNF levels in the cerebrospinal fluid of patients correlated with MS disease severity (Sharief and Hentges, 1991). Using transgenic mice which were deficient in TNFR1 and expressed human membrane-bound TNF on astrocytes, Akassoglou *et al.* (1998) could show that it is TNFR1 which mediates oligodendrocyte apoptosis, primary inflammatory demyelination and the generation of MS-type plaques. Moreover, in a humanised model, in which membrane-bound human TNF was also expressed by astrocytes, Akassoglou *et al.* (2003) went on to show that the inflammation is mediated through both, TNFR1 and TNFR2. The activation of TNFR2 expressed by endothelial cells was described to cause inflammation and development of neuropathology. In contrast, using mice which were deficient in TNFR1 but expressed human TNFR2 together with the non-cleavable membrane-bound TNF variant on astrocytes, the exclusive role for TNFR1 in TNF-mediated apoptosis of oligodendrocytes and primary demyelination could be further confirmed (Akassoglou *et al.*, 2003). In line with these findings, data from a murine experimental autoimmune encephalomyelitis model indicate that rather sTNF than membrane-bound TNF determines MS pathology (Alexopoulou *et al.*, 2006). Exclusive expression of membrane-bound TNF was found to suppress disease onset and progression while TNF-mediated suppression of autoimmunity and resistance to infections with intracellular pathogens was sustained.

In contrast to the inflammatory diseases affecting the CNS, inflammation has been reported to play a positive role in ischaemia-induced neurogenesis and increased neurogenesis has been described for several models of inflammation (reviewed in Whitney *et al.*, 2009). An involvement of TNF in neuroregeneration after ischaemic injury has been suggested as treatment with anti-TNF antibodies two weeks after the ischaemic insult was shown to abolish hippocampal neurogenesis in a rat model for stroke (Heldmann *et al.*, 2005). Based on experiments with *tnfr1^{-/-}/tnfr2^{-/-}* mice, TNFR had already been implicated in providing protection of neurons during brain injury (Bruce *et al.*, 1996) and TNFR1 and TNFR2 have both been described to be up-regulated in

response to ischaemic insults (Botchkina *et al.*, 1997). However, the roles of the two TNFR in ischaemia appear to be opposing. In a retina ischaemia-reperfusion mouse model TNFR2 was found to promote neuroprotection, whereas TNFR1 aggravated neuronal damage (Fontaine *et al.*, 2002).

Further evidence supporting a neuroprotective role for TNFR2 was provided by a study on neurons from *tnfr1*^{-/-} mice expressing moderate levels of TNF in the cortex and hippocampus (Marchetti *et al.*, 2004). Here, TNFR2 was found to counteract excitotoxicity, i.e. killing of neurons through excessive stimulation by neurotransmitters such as glutamate, through a NF- κ B dependent signalling mechanism. Furthermore, the use of TNFR antagonists revealed that the inhibition of excitotoxicity was exclusively conferred by TNFR2 but not TNFR1.

1.6.4 Anti-TNF treatment in autoimmune diseases

With TNF being a potent immunostimulatory agent, defects in the production and regulation of this cytokine and its receptors can cause severe problems. TNF has been reported to play an important role in a large number of autoimmune diseases such as rheumatoid arthritis (RA), Crohn's inflammatory bowel disease (IBD), type I diabetes, psoriasis and SLE (reviewed in Bradley, 2008, Faustman and Davis, 2010). Together with many other pro-inflammatory cytokines, TNF is produced in the inflamed joints of RA patients and was reported to play a dominant role in this disease (Bradley, 2008).

Neutralisation of TNF with recombinant soluble TNFR or anti-TNF antibodies ameliorated joint disease in a mouse model of collagen induced arthritis (Piguet *et al.*, 1992, Thorbecke *et al.*, 1992, Williams *et al.*, 1992). After these promising results, a pilot study was performed in which RA patients were treated with a monoclonal, neutralising, mouse/human chimaeric anti-TNF antibody that today is known as infliximab (Elliott *et al.*, 1993). A multi-centre study with infliximab confirmed the ameliorating effect of the antibody on disease activity and symptoms (Elliott *et al.*, 1994). Since then, four more TNF antagonists have been authorised for the treatment of RA: etanercept, adalimumab, golimumab and certolizumab. Etanercept is a fusion protein of the TNFR2 Fc region and human IgG1, whereas adalimumab and golimumab are fully human IgG1 monoclonal anti-TNF antibodies. Finally, certolizumab is a polyethylene glycol-coupled Fab fragment of a humanised IgG1 monoclonal anti-TNF antibody (reviewed in Caminero *et al.*, 2011). Randomised controlled trials found anti-

TNF therapeutics to be efficient in the treatment of RA and demonstrated that a long-term treatment in combination with the anti-folate drug methotrexate is feasible (Bradley, 2008). Hence, anti-TNF treatment has been one of the major successes in the treatment of RA and has, in addition, been successfully applied in various other autoimmune diseases such as psoriasis or IBD.

The above-mentioned TNF antagonists have been shown to bind sTNF with high affinity (Tracey *et al.*, 2008) but can also bind membrane-bound TNF. As a consequence of the latter, these therapeutic agents have been reported to not only function as TNF-antagonist by neutralising TNF, but also show agonistic effects by causing so-called reverse signalling (reviewed in Caminero *et al.*, 2011). Reverse signalling through TNF occurs when membrane-bound TNF binds either endogenous soluble and membrane-bound TNFR or exogenous soluble TNFR, such as etanercept, and anti-TNF antibodies. The function of TNF as a receptor has been demonstrated in T-cells, monocytes/macrophages and natural killer cells (reviewed in Horiuchi *et al.*, 2010). Interaction of membrane-bound TNF expressed on monocytes with TNFR2 expressed on T-cells, for example, was shown to lead to phosphorylation of ERK1/ERK2 and to upregulate TNF production in the monocytes via reverse signalling (Rossol *et al.*, 2007). As mentioned above, reverse signalling can also be induced by TNF antagonists. Infliximab was found to induce apoptosis in membrane-bound TNF-expressing Jurkat T-cells and monocytes of RA patients, respectively (Mitoma *et al.*, 2005, Meusch *et al.*, 2009). However, no such effect could be detected for etanercept and it has been proposed that this difference in reverse signalling induction is determined by the ability of the TNF antagonist to form oligomers/multimers with the membrane-bound ligand (reviewed in Horiuchi *et al.*, 2010).

Alexopoulou *et al.* (2006) suggested, based on data obtained from mice which only expressed a membrane-bound TNF variant, that it is rather sTNF than membrane-bound TNF which plays a role in the development of arthritis. This idea is further supported by observations made in a mouse model of collagen-induced arthritis, in which dominant-negative TNF (DN-TNF) was able to neutralise sTNF but not membrane-bound TNF (Steed *et al.*, 2003). This neutralising effect of DN-TNF was based on the formation of heterotrimers from DN-TNF and endogenous sTNF. These heterotrimers exhibited a strongly reduced affinity to the TNFR. Another advantage of this therapeutic approach was that, while the neutralisation of sTNF did ameliorate the disease symptoms of experimental arthritis, it did not impair the TNF-mediated resistance to infections

(Zalevsky *et al.*, 2007). Similar observations have been made in an LPS-induced hepatitis model, where DN-TNF was also capable to protect mice from liver injury (Olleros *et al.*, 2010). However, Olleros *et al.* (2010) also demonstrated that the inhibitory effect of DN-TNF biologics wears off quicker than the one seen with etanercept.

Given their involvement in immune defence and regulation of the immune system (see section 1.6.2) it is not surprising that TNFR1 and TNFR2 have been reported to play certain roles in several autoimmune diseases. In addition to their involvement in the pathogenesis of MS and type I diabetes (sections 1.6.2.1 and 1.6.3), distinct roles have been suggested for the two TNFR in RA and IBD. Data from a collagen-induced arthritis mouse model of *tnfr1*^{-/-} mice suggested a pro-inflammatory role for TNFR1 (Mori *et al.*, 1996) and opposing roles for TNFR2 (Tada *et al.*, 2001b). TNFR2 was found to accelerate the induction of arthritis during the early stage of the disease, while suppressing it at the late stage and in transplantation experiments with bone marrow from *tnfr1*^{-/-}, *tnfr2*^{-/-} and *tnfr1*^{-/-}/*tnfr2*^{-/-} mice also an anti-inflammatory role was observed for TNFR2 (Blüml *et al.*, 2010). Moreover, in myofibroblasts from IBD patients TNFR2 seems to be involved in mediating TNF-induced collagen accumulation through induction of tissue inhibitor of matrix metalloproteinase-1 (TIMP-1) and ERK1/ERK2 mediated proliferation (Theiss *et al.*, 2005).

This highlights not only the opposing functions of TNFR1 and TNFR2 further but also implies that it may not always be beneficial to abrogate TNF-mediated signalling altogether. Indeed anti-TNF treatment with anti-TNF antibodies and etanercept has been found to be occasionally associated with certain adverse effects such as serious bacterial infections (including tuberculosis), demyelinating syndromes and SLE-like reactions (reviewed in Bradley, 2008) and the development of cancer. These adverse effects, together with the fact that not all patients respond to anti-TNF treatment, suggest that different approaches are required in the treatment of autoimmune diseases. A TNFR-selective therapy could be superior to an overall blockage of TNF. Findings by Ban *et al.* (2008) support such an approach. Here, in *in vitro* experiments with selective agonistic TNFR-antibodies a TNFR2-specific killing of auto-reactive CD8⁺ T-cells could be achieved not only in cells from type I diabetes patients, but also in CD8⁺ T-cells of patients suffering from SLE, psoriasis, MS and Graves' disease.

An alternative way, which has been considered to specifically target TNFR1 and TNFR2, respectively, is the use of soluble PLAD protein. A soluble version of the

TNFR1 PLAD was found to have an inhibitory effect on disease development in mouse models of TNF-, CpG-DNA- and collagen-induced of arthritis, while no such effect could be observed when a soluble version of the TNFR2 PLAD was used (Deng *et al.*, 2005). Since both PLAD proteins used in this study were capable to block TNF-mediated signalling Deng *et al.* (2005) proposed that soluble TNFR PLAD could serve as TNFR-selective therapeutics. However, this would require the design of more stable versions of these proteins as their half-life was measured to be only 5 h in the blood. Moreover, more recent evidence emerged which suggested the use of PLAD proteins might not always be beneficial. In an SLE mouse model TNFR1 PLAD protein was found to improve facial skin lesions and to prevent infiltration by inflammatory cells (Deng *et al.*, 2010). However, a trend towards increased levels of IgG and auto-antibodies against double-stranded DNA could be observed in animals treated with either TNFR1 or TNFR2 PLAD protein, indicating that the overall systemic autoimmunity got rather worse upon treatment. In addition, treatment with TNFR1 PLAD protein aggravated SLE kidney pathology, further highlighting the limitations of PLAD protein use in the treatment of autoimmune diseases.

Taken together, the anti-inflammatory functions of TNFR2 as outlined above together with the described pro-inflammatory functions of TNFR1 indicate that selectively blocking TNFR1 while specifically activating TNFR2 may be a promising approach in the treatment of autoimmune diseases and could be superior to an overall blockage of TNF. However, a more profound understanding of the TNF-mediated receptor activation seems to be required as mere interruption of TNFR signalling with, for example, PLAD protein has not proven to be suitable for the treatment of all autoimmune diseases.

1.7 Scope of this thesis

Membrane-bound TNF and sTNF play different roles in immunity and data from mouse models indicate that rather the soluble than the membrane-bound form plays a role in the development of autoimmune diseases such as RA and MS (Steed *et al.*, 2003, Alexopoulou *et al.*, 2006). Therapy with biological antagonists of TNF action has proven to be a successful way of treating various autoimmune diseases (Caminero *et al.*, 2011). In addition, a role for sTNF in autoimmunity has been highlighted by findings that especially neutralisation of this soluble form of TNF can ameliorate disease symptoms in experimental arthritis (Steed *et al.*, 2003).

Like its membrane-bound form sTNF can bind both TNFR with high affinity (Grell *et al.*, 1998b). However, while TNFR1 and TNFR2 are both efficiently activated by membrane-bound TNF, sTNF only fully activates TNFR1 (Grell *et al.*, 1995). This differential receptor responsiveness to sTNF, together with the opposing functions described for TNFR1 and TNFR2 in immunity (section 1.6.2), suggests that selective targeting of the TNFR could be a promising therapeutic approach in the treatment of autoimmune diseases and may help to avoid the anti-TNF treatment-associated adverse effects which have been reported in some patients (reviewed in Bradley, 2008). However, the development of TNFR selective drugs requires a profound understanding of the molecular basis of functional differences between TNFR1 and TNFR2.

A cellular system, which comprises immortalised embryonic fibroblasts from *tnfr1*^{-/-}/*tnfr2*^{-/-} mice stably expressing TNFR-Fas chimaeras (consisting of the extracellular part of the TNFR and the cytoplasmic part of Fas), has been established in our group previously. By using these cells in combination with sTNF and a membrane-bound TNF mimic, respectively, differential responsiveness of TNFR1 and TNFR2 towards sTNF can be investigated in the absence of TNFR1/TNFR2 crosstalk. Data generated with the help of this cellular system indicated that differential responsiveness to sTNF is not controlled by the cytoplasmic part of the receptors (Krippner-Heidenreich *et al.*, 2002) and is only to a minor extent determined by the CRD1 (Branschädel *et al.*, 2010) and the TM region (Dr Anja Krippner-Heidenreich, personal communication). In contrast, preliminary data suggest that rather the TNFR stalk region, potentially in combination with the TM region, controls receptor responsiveness to sTNF (Dr Anja Krippner-Heidenreich, personal communication).

Furthermore, it has been observed that efficient activation of TNFR by sTNF correlates with the strength of ligand-independent receptor pre-assembly (Branschädel *et al.*, 2010, Boschert *et al.*, 2010) and the ability of the receptors to form higher molecular TNF/TNFR clusters (Krippner-Heidenreich *et al.*, 2002). These observations, together with the aforementioned preliminary data on sTNF responsiveness, raised the question whether the TNFR stalk region could influence cluster formation and receptor pre-assembly in the plasma membrane. Taken together, we hypothesise that the TNFR stalk region is the major determinant for sTNF responsiveness by controlling signalling complex formation at the level of receptor pre-assembly and cluster formation.

Moreover, investigations into the potential control of TNFR responsiveness towards sTNF by the TNFR stalk region will help elucidate whether this region represents a potential target for the design of TNFR-selective therapeutics.

In the absence of functional FoxP3⁺CD4⁺CD25⁺ T_{reg} cells immune system dysregulation and development of autoimmunity have been demonstrated to arise as a result of insufficient suppression of pathogenic auto-reactive T-cells (reviewed in Miyara and Sakaguchi, 2011). In the murine system TNFR2 signalling has been shown to promote the expansion of T_{reg} cells (Chen and Oppenheim, 2010) and in the human system TNFR2 has been also been implicated in the control of T_{reg} cell survival and function under inflammatory conditions (reviewed in Chen and Oppenheim, 2011). However, as mentioned above, despite its ability to bind sTNF with high affinity, TNFR2 is only efficiently activated upon the engagement with membrane-bound TNF (Grell *et al.*, 1995). Therefore, it is conceivable that at the high sTNF concentrations present in acute and chronic inflammatory diseases membrane-bound TNF competes with sTNF for TNFR2 binding. This in turn would lead to insufficient activation of TNFR2 on T_{reg} cells and, consequently, the aggravation of the disease. Hence, targeting the TNFR2 stalk region with, for example, stabilising antibodies or small stabilising molecules which help to overcome its inhibitory effect on sTNF responsiveness may enhance TNFR2 signalling and promote suppressive T_{reg} cell function.

In addition, differential responsiveness towards soluble and membrane-bound ligands is a characteristic which can also be observed for other TNFR superfamily members such as Fas (Suda *et al.*, 1997, Schneider *et al.*, 1998), TRAILR2 (Wajant *et al.*, 2001), TACI (Bossen *et al.*, 2008), CD27 (Wyzgol *et al.*, 2009) and OX40 (Müller *et al.*, 2008). With the exception of Fas, all of these receptors contain relatively long proline-rich stalk regions (Figure 3). Therefore, understanding the mechanisms by

which the TNFR2 stalk region determines sTNF responsiveness may also provide insight into how the differential responsiveness of other TNFR superfamily members is controlled.

Therefore, the aims of this project are to:

- Determine whether the stalk region, alone or in combination with the TM region, determines differential receptor responsiveness to sTNF;
- Identify the molecular feature(s) in the TNFR stalk region controlling sTNF responsiveness;
- Determine whether ligand-independent pre-assembly and multimerisation/cluster formation of the receptors are determined by the TNFR stalk region;
- Investigate whether observations made using the TNFR-Fas cell system are also valid for wild type TNFR2 and, hopefully, to provide new insights into the control of TNFR signalling initiation.

CHAPTER 2

Materials and methods

2.1 Materials

2.1.1 Chemicals and reagents

Overall, chemicals and biochemicals used for this PhD project were commercially available analytical grade reagents obtained from Sigma-Aldrich Company Ltd. (Poole, UK), Fisher Scientific (Loughborough, UK), Life Technologies (Paisley, UK) or BDH (Poole, UK). Chemicals and reagents obtained elsewhere are listed in Table 1 together with the appropriate suppliers.

Table 1. Chemicals and reagents

Chemical/reagent	Supplier
40 % (w/v) Acrylamide/bis-acrylamide (37.5:1) solution	Anachem (Luton, UK)
Agarose (electrophoretic grade)	Invitrogen Ltd. (Paisley, UK)
Ammonium peroxodisulphate (APS)	BDH (Poole, UK)
BactoAgar	Difco™ (West Molesey, UK)
BactoTryptone	Difco™ (West Molesey, UK)
Benzyl-2-acetamido-2-deoxy- α -D-galactopyranoside (Benzyl- α -GalNAc)	Calbiochem (San Francisco, USA)
Bis[sulfosuccinimidyl]suberate (BS ³)	Perbio (Erembodegem, Belgium)
BradfordUltra reagent	Expedeon (Harston Cambridgeshire, UK)
Broad range prestained protein marker	New England Biolabs Inc. (Hertfordshire, UK)
Complete, Mini, EDTA-free protease inhibitor cocktail tablets	Roche Applied Science (Burgess Hill, UK)
Deoxynucleotide mix (10 mM dNTP mix)	New England Biolabs Inc. (Hertfordshire, UK)

Fluoromount G	Southern Biotech (Birmingham Alabama, USA)
Recombinant protein G-sepharose 4B conjugate	Invitrogen Ltd. (Paisley, UK)
PROTRAN nitrocellulose transfer membrane	Whatman International Ltd. (Maidstone, UK)
Oregon Green-conjugated wheat germ agglutinin (WGA)	Invitrogen Ltd. (Paisley, UK)
QIAprep Spin Miniprep kit	Qiagen (Crawley, UK)
Qiagen HiSpeed Plasmid Midiprep kit	Qiagen (Crawley, UK)
QIAquick Gel Extraction kit	Qiagen (Crawley, UK)
Sodium dodecyl sulphate (SDS)	BDH (Poole, UK)
SuperSignal® West Pico chemiluminescent substrate	Thermo Scientific/Pierce (Loughborough, UK)
SuperSignal® West Dura extended duration chemiluminescent substrate	Thermo Scientific/Pierce (Loughborough, UK)
Vectashield® mounting medium with DAPI	Vector Laboratories Ltd. (Peterborough, UK)
Z-Val-Ala-DL-Asp-fluoromethylketone (zVADfmk)	Bachem Ltd. (St. Helens, UK)

2.1.2 Cell culture media and reagents

75 cm² vented cell culture flasks were obtained from Greiner Bio-One Ltd. (Stonehouse, Gloucestershire, UK). Cryo vials, 96-well tissue culture plates and 6-well tissue culture plates were obtained from Corning/Costar UK Ltd. (High Wycombe, UK). Cell culture reagents and media used are listed in Table 2 together with the appropriate suppliers.

Table 2. Cell culture reagents and media

Reagent/medium	Supplier
Blasticidin S	Invitrogen Ltd. (Paisley, UK)
Dimethyl Sulfoxide (DMSO) Hybri-Max™	Sigma-Aldrich Company Ltd. (Poole, UK)
Dulbecco's Modified Eagle Medium (DMEM)	Invitrogen Ltd. (Paisley, UK)
Dulbeccos's phosphate buffered saline (DPBS)	Lonza (Workingham, UK)
Doxycycline	Sigma-Aldrich Company Ltd. (Poole, UK)
Effectene® transfection reagent	Qiagen (Hilden, Germany)
Foetal calf serum (FCS)	Gibco BRL (Paisley, UK)
200 mM L-glutamine solution	Sigma-Aldrich Company Ltd. (Poole, UK)
HiPerFect transfection reagent	Qiagen (Hilden, Germany)
Hygromycin B	Invitrogen Ltd. (Paisley, UK)
Lipofectamine™2000 transfection reagent	Invitrogen Ltd. (Paisley, UK)
MycoAlert® Mycoplasma Detection Kit	Lonza (Workingham, UK)
Opti-MEM 1 reduced serum medium with L-glutamine	Invitrogen Ltd. (Paisley, UK)
10x Penicillin-streptomycin solution (10 ⁴ units (U) per ml penicillin, 10 mg/ml streptomycin)	Sigma-Aldrich Company Ltd. (Poole, UK)
Poly-L-lysine (MW : 70000 – 150000)	Sigma-Aldrich Company Ltd. (Poole, UK)
Puromycin A	Calbiochem (San Francisco, USA)
RPMI-1640 medium	Sigma-Aldrich Company Ltd. (Poole, UK)
TransIt®-293 transfection reagent	Mirus Bio Corporation (Madison, USA)
0.4 % (w/v) Trypan Blue solution	Sigma-Aldrich Company Ltd. (Poole, UK)
10x Trypsin-EDTA solution (0.5 % (w/v) trypsin, 0.2 % (w/v) EDTA)	Sigma-Aldrich Company Ltd. (Poole, UK)
Zeocin	Invitrogen Ltd. (Paisley, UK)

2.1.3 Molecular biology enzymes

Antarctic Phosphatase, Phusion deoxyribonucleic acid (DNA)-polymerase, *Thermus aquaticus* (*Taq*) DNA polymerase, T4 DNA ligase, T4 polynucleotide kinase and all restriction endonucleases were obtained from New England Biolabs Inc. (Hertfordshire, UK).

2.1.4 Antibodies

Antibodies and antibody conjugates used are listed in Table 3 together with the appropriate suppliers.

Table 3. Antibodies

Antibody	Supplier
Biotin-conjugated rat anti-mouse immunoglobulin G (IgG) (H+L)	eBioscience Ltd. (Hatfield, UK)
Monoclonal mouse anti-human β -actin antibodies AC-15	Abcam (Cambridge, UK)
Monoclonal mouse anti-human cytoplasmic-Fas antibody clone B10	Santa Cruz Biotechnology Inc. (Santa Cruz, USA)
Polyclonal rabbit anti-human p65 antibodies C-20	Santa Cruz Biotechnology Inc. (Santa Cruz, USA)
Monoclonal mouse anti-human TRAF2 clone C90–481	BD/Pharmingen (Oxford, UK)
Monoclonal mouse anti-human TNFR1 antibody clone H398	Institute of Cell Biology and Immunology, University of Stuttgart (Stuttgart, Germany)
Polyclonal goat anti-soluble human TNFR2 antibodies	R&D Systems Europe Ltd. (Abingdon, UK)
Monoclonal mouse anti-human TNFR2 antibody clone 80M2	Institute of Cell Biology and Immunology, University of Stuttgart (Stuttgart, Germany)
Monoclonal mouse anti-human TNFR2 antibody clone MR2-1	Hbt HyCult (Uden, Netherlands)
Phycoerythrin-conjugated monoclonal	R&D Systems Europe Ltd. (Abingdon, UK)

mouse anti-human TNFR2 antibody clone # 22235	
FITC-conjugated goat anti-mouse IgG + IgM (H+L) antibody	Jackson ImmunoResearch Laboratories Inc. (West Grove, USA)
Goat anti-mouse IgG-HRP antibody	Dianova (Hamburg, Germany)
Alexa594-conjugated goat anti-rabbit IgG (H+L) antibody	Molecular Probes/Invitrogen Ltd. (Paisley, UK)
Rabbit anti-goat IgG (whole molecule)- HRP antibody	Sigma-Aldrich Company Ltd. (Poole, UK)
Streptavidin-phycoerythrin	BD/Pharmingen (Oxford, UK)

2.1.5 Ligands

Recombinant soluble TNF (sTNF; 2×10^7 U/mg) was obtained from Knoll AG (Ludwigshafen, Germany). The cloning, expression and purification of recombinant, endotoxin-free Cysteine-TNF (CysTNF) has been described previously (Bryde *et al.*, 2005). CysTNF contains an N-terminal histidine tag and a free cysteine residue, which leads to the preferential oligomerisation into TNF hexamers. It was produced at the University of Stuttgart's institute of natural sciences, Germany, by bacterial expression and subsequent purification via a nickel column. Stock solutions of sTNF and CysTNF were stored at -80 °C; aliquots for the day to day use were stored at 4 °C. Recombinant human sTNF had been labelled with AlexaFluor546 (Molecular Probes Inc., Eugene, Oregon, USA) at the Institute of Cell Biology and Immunology of the University of Stuttgart, Germany, according to the manufacturer's instructions and was stored at -80 °C. Flag-tagged TNFR2-selective sTNF (Flag-sTNF(143N/145R)) and Flag-tagged TNFR2-selective single-chain TNF containing the trimerisation domain of chicken tenascin-C (Flag-TNC-scTNF(143N/145R)) have been described previously (Rauert *et al.*, 2010) and were kindly gifted by Prof. Dr. Harald Wajant, University of Würzburg, Germany.

2.1.6 Plasmids

The bacterial plasmid pBlueScript SK (+) (pBS SK (+)) from Stratagene was used as a subcloning vector. Receptor constructs and chimaeras were cloned into the mammalian expression vector pEF-pGK/puro polyA (Huang *et al.*, 1997). For the generation of inducible cells the expression plasmid pcDNA/FRT/TO and the Flp recombinase encoding pOG44 vector of the Flp-IN T-Rex system from Invitrogen Ltd (Paisley, UK) were used. For plasmid maps please see appendix.

2.1.7 Oligonucleotides

Desalted or poly-acrylamide gel electrophoresis (PAGE)-purified oligonucleotides were obtained from Sigma-Aldrich Company Ltd. (Poole, UK) and resuspended in ddH₂O to a final concentration of 100 µM unless stated otherwise. Oligonucleotides that served as sequencing primers are listed in Table 4.

Table 4. Sequencing primers

Number	Nucleotide sequence (5' → 3')
#O-213	CAA CAC GAC TTC ATC CAC GG
#O-231	TTT TTC TTC CAT TTC AGG TGT C
#O-500	GAA AAC GAG TGT GTC TCC TGT AG
#O-501	AAT TAA CCC TCA CTA AAG GG
#O-502	GTA ATA CGA CTC ACT ATA GGG C
CMV fw	CGC AAA TGG GCG GTA GGC GTG

2.1.8 Competent cells

Subcloning EfficiencyTM DH5α chemically competent *Escherichia coli* (*E. coli*) cells were obtained from Invitrogen Ltd. (Paisley, UK).

2.1.9 Small interfering RNA

ON-TARGETplus SMARTpool TNFRSF1A small interfering RNA (siRNA) was obtained from Dharmacon (Lafayette, CO, USA). The four pooled target siRNA strands are depicted below. Lyophilised siRNA was dissolved in RNase-free siRNA buffer (Dharmacon) to receive a 100 μ M stock solution. Non-specific siRNA (5'-AGG UAG UGU AAU CGC CUU GTT-3') was purchased from MWG-Biotech AG (Ebersberg, Germany).

Table 5: ON-TARGETplus SMARTpool TNFRSF1A siRNA strands

No.	Sense strand (5' \rightarrow 3')	Antisense strand (5' \rightarrow 3')
1	CAA AGG AAC CUA CUU GUA CUU	pGUA CAA GUA GGU UCC UUU GUU
2	GAG CUU GAA GGA ACU ACU AUU	pUAG UAG UUC CUU CAA GCU CUU
3	AAG CUC UAC UCC AUU GUU UUU	pAAA CAA UGG AGU AGA GCU UUU
4	CCC UUG CGC UGG AAG GAA UUU	pAUU CCU UCC AGC GCA ACG GUU

2.1.10 Software

Sequence similarity searches were carried out using ClustalW (based on the algorithms described in Wilbur and Lipman, 1983, Myers and Miller, 1988). OLIGO primer analysis software (Molecular Biology Insights Inc.; Cascade, USA) was used to ensure optimal oligonucleotide design. The online sequence alignment tool LALIGN (based on the algorithm described in Myers and Miller, 1988) was used to compare DNA sequences of parental and mutated receptor constructs. Plasmid maps were created using the Clone Manager 9 software (Scientific & Educational Software; Cary, USA). Photographs were formatted and figures created with the help of the Corel DRAW Graphics Suite X4. Chemical structures were drawn using the ACD/Labs Software version 12.0 (Advanced Chemistry Development Inc., Toronto, Canada).

Statistical difference between non-parametric samples was assessed by Mann-Whitney U test. The GraphPad Prism 5 software (GraphPad Software, Inc.; La Jolla, USA) was used in all instances. Significance levels were indicated as * = $p \leq 0.05$, ** $p \leq 0.01$ and *** = $p \leq 0.001$.

2.2 Molecular biology methods

To obtain TNFR2-Fas chimaeras with point mutations in the stalk region, inserts were constructed via two-step site-directed mutagenesis. TNFR-Fas chimaeras, in which parts of the stalk region had been replaced with artificial glycine-serine-linkers, were also constructed via two-step site-directed mutagenesis.

For complete replacement of the stalk region with artificial linkers of different lengths, oligonucleotides with complementary 3'-ends were heat-denatured, annealed and the resulting 5'-overhangs were filled in using Phusion DNA polymerase. The plasmid pBS SK (+) was used in subcloning steps for the construction of chimaeras with GSL of different lengths. All constructs were finally cloned into the mammalian expression vector pEF-PGK/puro polyA. pEF-PGK/puro polyA contains an elongation factor 1 promoter, a puromycin A resistance gene and a poly adenosine (polyA) sequence.

2.2.1 Determination of DNA concentrations

Concentrations of plasmid and insert DNA were determined by measuring the absorbance at 260 nm ($A_{260\text{nm}}$) using a ND1000 spectrophotometer (Nanodrop, USA). The ratio $A_{260\text{nm}}/A_{280\text{nm}}$ was used to determine DNA purity.

2.2.2 Agarose gel electrophoresis

6x Sample buffer

30 % (v/v) Glycerol
0.25 % (w/v) Bromophenol blue

10x Tris-boric acid-EDTA buffer (TBE) pH 8.0

900 mM Tris base
900 mM Boric acid
20 mM $\text{Na}_2\text{-EDTA}$

50x Tris-acetate-EDTA buffer (TAE) pH 8.0

2 M	Tris base
1 M	Glacial acetic acid
50 mM	Na ₂ -EDTA (from 0.5 M stock solution pH 8.0)

Vector DNA and insert DNA for cloning were separated by 1 - 3 % horizontal agarose gel electrophoresis. TBE buffer was used for gels containing 2 % (w/v) agarose or more, TAE was used for gels containing up to 2 % (w/v) agarose. Samples were mixed with sample buffer, loaded onto the gels containing 0.1 µg/ml of ethidium bromide and electrophoresis was performed at constant 80 V for 1 - 2.5 h. For DNA detection a ChemiGenius² bioimaging system (Syngene, Cambridge, UK) was used.

2.2.3 Agarose gel extraction

For the extraction of plasmid and insert DNA from agarose gels buffers are used that contain guanidine thiocyanate. Guanidine thiocyanate is a chaotropic salt which creates a hydrophobic environment in which the DNA can bind to silica membranes via cation-bridges.

DNA in agarose gels was visualised with UV_{300nm} light and cut out of the gel using a sharp, clean scalpel blade. DNA was extracted using the QIAquick Gel Extraction kit as described by the supplier. Briefly, the gel slice was dissolved in three gel slice volumes of the guanidine thiocyanate-containing buffer QG. DNA was precipitated by adding one gel slice volume of propan-2-ol to the mixture and was then allowed to bind to the silica membrane. Columns were washed with buffer PE and DNA was eluted in 30-50 µl ddH₂O.

2.2.4 Enzymatic modifications of DNA

2.2.4.1 Restriction digests and dephosphorylation of vector DNA

Unless stated otherwise, restriction digests were performed as 40 µl reactions in 1.5 ml Eppendorf reaction tubes in a 37 °C water bath for 2 h. For 0.7 pmol of double-stranded DNA (dsDNA) 5 U of restriction enzyme were used in the buffer recommended by the supplier. For partial restrictions, 1-2 U per 0.7 pmol of dsDNA were used.

Restriction samples of vector DNA were supplemented with 1x Antarctic Phosphatase reaction buffer and de-phosphorylation of the 3'- and 5'-ends of the DNA was performed using 5 U of Antarctic Phosphatase. Samples were incubated at 37 °C for 30 min and were then purified via agarose gel extraction.

2.2.4.2 Ligation of vector and insert DNA

Approximately 14 fmol of vector DNA and a 5-fold excess of insert DNA were ligated using 20 U of T4 DNA ligase in 1x T4 DNA ligase reaction buffer for 3 h or over night in a 16 °C water bath.

2.2.5 Heat shock transformation of chemically competent *E. coli* DH5a cells

SOC++ medium

2 % (w/v) BactoTryptone
0.5 % (w/v) Yeast extract
10 mM Sodium chloride (NaCl)
2.5 mM KCl
200 mM Glucose (sterile filtered)
10 mM MgCl₂ (sterile filtered)
pH adjusted to 7.0

Lysogeny broth medium (LB)

1 % (w/v) BactoTryptone
0.5 % (w/v) Yeast extract
0.5 % (w/v) NaCl
pH adjusted to 7.5

LB ampicillin agar plates

1 % (w/v)	BactoTryptone
0.5 % (w/v)	Yeast extract
0.5 % (w/v)	NaCl
1.5 % (w/v)	Bacto agar
100 µg/ml	Ampicillin

LB ampicillin medium

1 % (w/v)	BactoTryptone
0.5 % (w/v)	Yeast extract
0.5 % (w/v)	NaCl
100 µg/ml	Ampicillin

Heat shock transformation in the presence of calcium chloride (CaCl₂) is a commonly used method to deliver DNA into *E. coli* cells. CaCl₂ is believed to facilitate DNA binding to the cell surface. The bacteria are subjected to a heat-pulse (transfer from 0 °C to 42 °C) followed by a cold-shock (transfer from 42 °C to 0 °C). The heat-pulse has been reported to lead to the formation of pores in the outer cell membrane and a decrease in membrane potential of the inner cell membrane, while the cold-shock decreases the inner cell membrane potential further. Both, pore formation and reduction of membrane potential, facilitate the DNA to cross the *E. coli* cell membranes (Panja *et al.*, 2006, Panja *et al.*, 2008).

50 µl of chemically competent Subcloning Efficiency™ DH5α chemically competent *E. coli* cells were incubated with 5 µl of ligation reaction sample on ice for 30 min. Cells were then transferred to a 42 °C water bath for 45 sec and afterwards immediately placed on ice for 2 min. 550 µl of pre-warmed SOC ++ medium were added to each sample and samples were incubated at 37 °C under vigorous shaking for 1 h. Bacteria were pelleted in an Eppendorf microcentrifuge 5418 at 2500 x *g* for 3 min. The supernatant was discarded; bacteria were resuspended in 100 µl of SOC++ medium and plated onto LB ampicillin plates. Plates were incubated at 37 °C over night. The next day, single colonies were used to inoculate 5 ml of LB ampicillin medium for mini plasmid DNA preparations.

2.2.6 Preparation of plasmid DNA from *E. coli* DH5 α cells

Preparation of plasmid DNA for cloning, DNA sequencing and transfection of mammalian cells was performed using kits obtained from Qiagen. Plasmid preparation with these kits is based on the principle of alkaline lysis (as described in Birnboim and Doly, 1979) using three different buffers: a resuspension buffer (P1), a lysis buffer (P2) and a neutralisation buffer (P3).

The EDTA in buffer P1 destabilises the cell membrane and inhibits DNases by chelating bivalent cations. Buffer P2 contains sodium dodecyl sulphate (SDS), which breaks up the cell membranes, and sodium hydroxide (NaOH), which denatures the chromosomal DNA in the lysates. In contrast, the covalently closed circular plasmid DNA remains intact at pH 12-12.5. Buffer P3 contains potassium acetate (KAc) and stops the cell lysis. KAc neutralises the sample and causes renaturation and aggregation of chromosomal DNA. Addition of KAc also allows the formation of water-insoluble potassium dodecyl sulphate and, therefore, leads to the precipitation of SDS/protein complexes and high molecular weight RNA. Precipitated chromosomal DNA, protein and RNA can then be removed via a centrifugation step and plasmid DNA can be purified from the supernatant with the help of a silica column.

2.2.6.1 Mini plasmid preparation

The Qiagen Mini Plasmid Kit was used for the preparation of up to 20 μg of plasmid DNA from *E. coli* DH5 α cells. 5 ml of LB ampicillin medium (see section 2.2.5) were inoculated and bacteria were grown over night. The next day, bacteria from 4 ml of the cell suspension were pelleted at 7000 x *g* for 3 min and the supernatant was discarded. The bacterial pellet was resuspended in 250 μl of buffer P1. In order to lyse the bacteria, 250 μl of buffer P2 were added to the resuspended cells. Finally, 350 μl buffer P3 were added to the lysates. Samples were applied to Qiagen columns, columns were washed as recommended by the supplier and DNA was eluted in 50 μl ddH₂O.

2.2.6.2 Midi plasmid preparation

Buffer TE (Qiagen)

10 mM Tris-HCl pH 8.0

0.1 mM EDTA

The Qiagen HiSpeed Plasmid Midiprep kit was used for preparation of plasmids for transfections of mammalian cells. 120 ml of LB ampicillin medium (see section 2.2.5) were inoculated with 1 ml of a 5 ml pre-culture of *E. coli* DH5 α cells and bacteria were grown at 37 °C over night. The next day, bacteria were pelleted at 4 °C at 6000 x *g* for 15 min in a Sorvall RC 5C PLUS centrifuge using a SLA-1500 Superlite rotor. Afterwards, the supernatant was discarded and the bacterial pellet was resuspended in 6 ml buffer P1. The bacteria were lysed by adding 6 ml of buffer P2 and incubation at room temperature for 5 min. 6 ml of buffer P3 were added to the lysates and samples were applied to equilibrated Qiagen columns. Washing steps and DNA precipitation were carried out as recommended by the supplier. Plasmid DNA was eluted in 600 μ l of endotoxin-free buffer TE.

2.2.7 Replacement of the complete stalk region with glycine-serine-linkers

The stalk region of TNFR1 is 15 aa long whereas the stalk region of TNFR2 consists of 56 aa. In order to assess whether the length of the stalk region could account for the difference in receptor responsiveness towards sTNF, the stalk regions of TNFR1-Fas and TNFR2-Fas chimaeras were replaced with artificial linkers. These linkers (S_{GSL}) were 15 and 56 aa residues long, respectively, and consisted of glycine and serine residues (for aa sequences see Table 6). Glycine-serine-linkers were chosen as they are predicted to adopt no distinct secondary structure but a random coil fold (Evers *et al.*, 2006), thereby ensuring that changes in sTNF responsiveness are not due to the introduction of any secondary structures.

For the generation of short linkers (S_{GSL15}) for TNFR1 and TNFR2, two pairs of overlapping oligonucleotides were used. Their sequences were designed so they encoded the linker itself, (parts of) the TM, an *Acc65I* restriction site, an *XbaI* restriction site as well as a *BglII* restriction site. Due to the required length and the limitation in possible codons, overlapping oligonucleotides were chosen instead of full-length oligonucleotides to reduce their tendency to self-anneal and/or form strong secondary structure.

The sequences of the used oligonucleotide pairs were complementary in their 3'-ends and, after the annealing step, the 5'-overhangs could be filled in using PhusionTM High-Fidelity DNA Polymerase. The resulting dsDNA was cut with the restriction enzymes *XbaI* and *Acc65I* and was cloned into the plasmid pBS SK (+), which had been cut with *XbaI* and *Acc65I* (Figure 6).

In order to subsequently generate longer S_{GSL} , two more combinations of overlapping oligonucleotides were used. dsDNA was generated by fill-in reactions and was then cut with the restriction enzymes *BamHI* and *XbaI* and cloned into the previously generated pBS SK (+) plasmid, which had been cut with *XbaI* and *BglII* (Figure 7).

Being isocaudamers, *BamHI* and *BglII* differ slightly in their recognition sites but create DNA 5'-overhangs which are compatible with each other. This permits the ligation of vector DNA cut with *BglII* and oligonucleotide dsDNA cut with *BamHI* and, eventually, leads to the loss of both restriction sites.

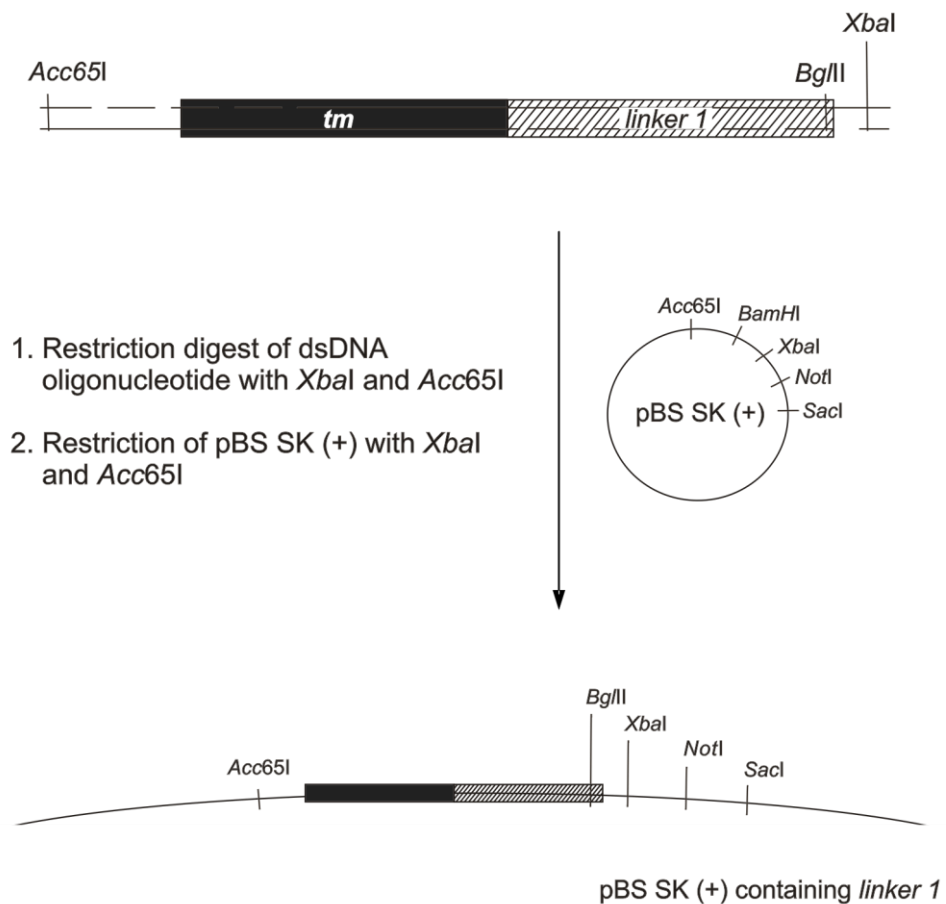


Figure 6. Construction of the 15 aa glycine-serine-linker for TNFR.

Two DNA oligonucleotides, which overlap in their 3'-ends, were annealed and the 5'-overhangs were filled in using PhusionTM High-Fidelity DNA polymerase. This dsDNA oligonucleotide encoded for the transmembrane domain (tm) of the receptor and the linker sequence (linker 1). The TM/linker sequence was cloned into a pBS SK (+) plasmid using the restriction enzymes *XbaI* and *Acc65I*.

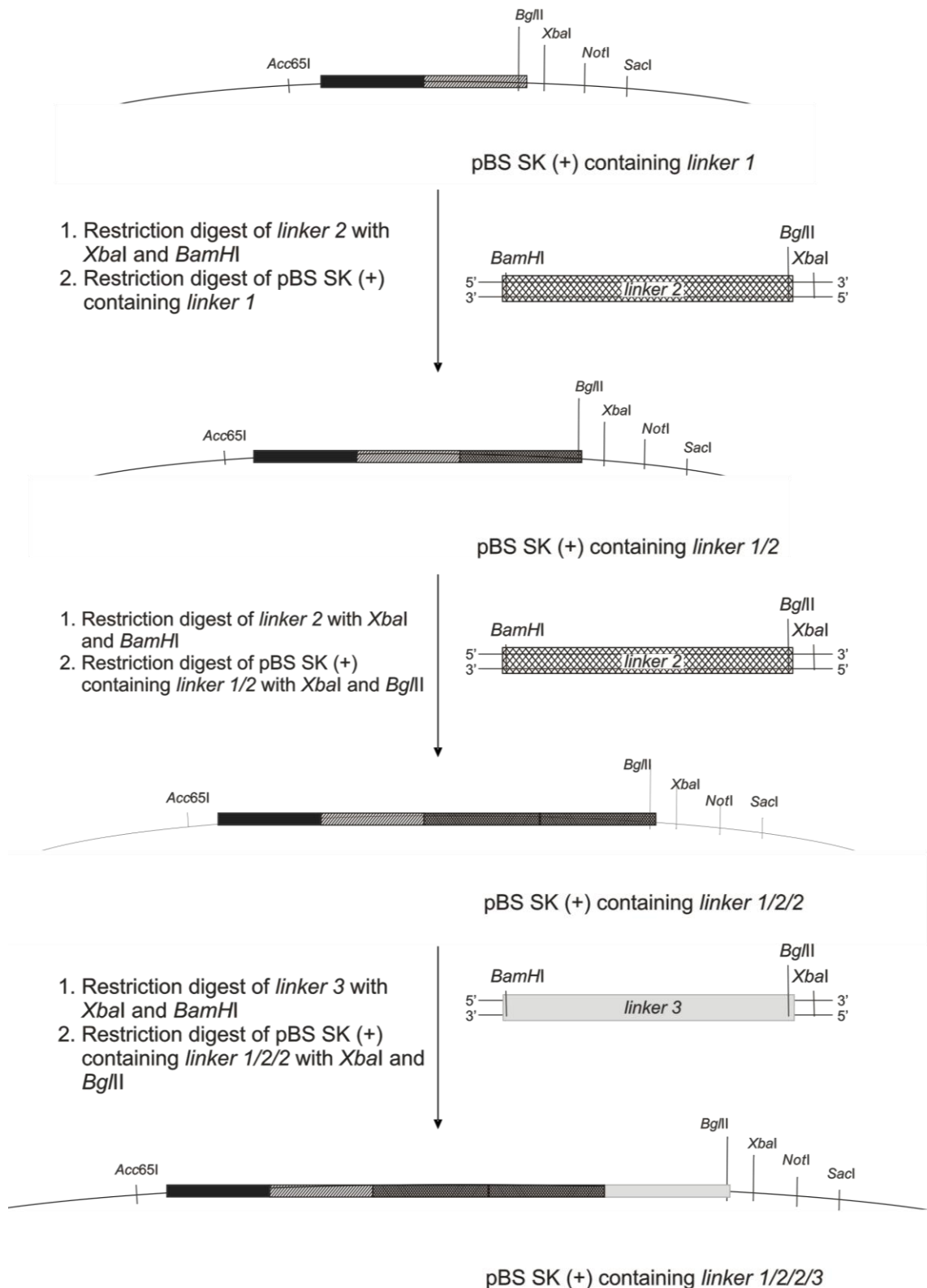


Figure 7. Subsequent cloning of glycine-serine-linker sequences for TNFR.

Linker 1 generated earlier (Figure 6) was extended by inserting a further linker sequence (*linker 2*). Vector DNA was cut with *BglII* and *XbaI*, dsDNA oligonucleotides were cut with *BamHI* and *XbaI*. Ligation of the vector and fragment DNA led to the loss of the *BamHI* and *BglII* restriction sites, allowing the introduction of another *linker 2* fragment applying the same technique. Finally, using the same approach the *linker 3* fragment could be introduced resulting in the full-length 56 aa artificial linker sequence.

Once generated, the S_{GSL} sequences could be cut out of the pBS SK (+) subcloning vectors and be cloned into the TNFR sequences using the restriction enzymes *BamHI* and *BstBI*. The resulting, modified TNFR sequences could then be transferred into pEF PGKpuro polyA expression plasmids. Table 6 shows the aa compositions of the different S_{GSL} for TNFR1 and TNFR2.

Table 6. Amino acid composition of S_{GSL} for TNFR1 and TNFR2

Insert combinations	S_{GSL}	aa sequence S_{GSL} for TNFR1	aa sequence S_{GSL} for TNFR2
<i>linker1</i>	S_{GSL15}	PGS[GGGS] ₃	GSG[GGGS] ₃
<i>linker1/2</i>	S_{GSL31}	PGS[GGGS] ₇	GS[GGGS] ₄ G[GGGS] ₃
<i>linker1/2/2</i>	S_{GSL47}	PGS[GGGS] ₁₁	GS[GGGS] ₈ G[GGGS] ₃
<i>linker1/2/2/3</i>	S_{GSL56}	PGSG[GGGS] ₁₃	GSG[GGGS] ₁₀ G[GGGS] ₃

2.2.7.1 Subcloning of linker sequences

Fill-in reaction of linker inserts for the generation of S_{GSL}

For the subcloning of S_{GSL} sequences pairs of PAGE-purified oligonucleotides were used. The oligonucleotides of these pairs (see Table 7) were complementary in their 3'-ends. Annealing of the oligonucleotides of the respective pairs resulted in 5'-overhangs which could be filled in using PhusionTM High-Fidelity DNA Polymerase.

Oligonucleotides were dissolved in ddH₂O to a final concentration of 50 μ M. For fill-in reactions, 50 μ l reaction samples containing 50 pmol of each of the two oligonucleotides, 1x Phusion reaction buffer HF and 200 μ M of dNTPs (10 mM deoxynucleotide mix, NEB) were prepared. The reaction was performed in a TaKaRa polymerase chain reaction (PCR) Thermal Cycler DiceTM TP600. After a 3 min denaturing step at 98 °C, the samples were gradually cooled down (respective annealing temperatures see Table 8) to allow annealing of the oligonucleotides. After the annealing step 1 U of PhusionTM High-Fidelity DNA Polymerase was added per reaction tube and the 3'-ends were extended at 72 °C for 10 sec. Afterwards, the samples were cooled down to 4 °C.

Four different linker inserts were generated via fill-in reactions: *linker 1* for TNFR1 and *linker 1* for TNFR2 as well as *linker 2* and *linker 3*, which were compatible for both TNFR.

Table 7. Oligonucleotides for the replacement of the complete stalk region with S_{GSL}

	Number	Nucleotide sequence (5' → 3')
<i>linker 1</i> for TNFR1	#O-505	CTT CAG GTA CCG ATA CAT TAA ACC AAT GAA GAG GAG GGA TAA AAG GCA AAG ACC AAA GAA AAT GAC CAG GGG CAA CAG CAC
	#O-506	TTG GGC TCT AGA CTG CAG AGA TCT GGC GGT GGT TCC GGA GGT GGA AGT GGA GGA GGC AGC GTG CTG TTG CCC CTG GTC ATT TTC TTT GGT C
<i>linker 1</i> for TNFR2	#O-507	GTT CAC GGT ACC TAT TAT TAG TAG ACC CAA GGC TGT CAC ACC CAC AAT CAG TCC AAC TGG AAG AGC GAA GC
	#O-508	GGC TCT AGA CTG CAG AGA TCT GGC GGC GGT GGT TCC GGA GGT GGA AGT GGA GGA GGC AGC TTC GCT CTT CCA GTT GGA CTG ATT GTG
<i>linker 2</i> for TNFR1 and TNFR2	#O-509	GTT CAC GGT ACC CAC AAT CAG TCC AAC TGG AAG AGC GAA GG
	#O-510	GCT CTA GAG TTC TGC AGA GAT CTG GCG GCG GTT CCG GTG GTG GAA GTG GCG GAG GTA GCG GCG GAG GAT CCT TCG CTC TTC CAG TTG GAC TGA TTG
<i>linker 3</i> for TNFR1 and TNFR2	#O-509	GTT CAC GGT ACC CAC AAT CAG TCC AAC TGG AAG AGC GAA GG
	#O-511	GCT CTA GAG TTG GCG GCG GTT CCG GTG GTC TGC AGA GAT CTG GAG GTG GAG GAA GTG GAG GTG GAT CCT TCG CTC TTC CAG TTG GAC TGA TTG

Table 8. Oligonucleotide annealing temperatures for complete stalk region replacement with S_{GSL}

	Oligonucleotide	Annealing temperature and times	Insert generated
Pair 1	#O-505 and #O-506	72.4 °C for 5 min, 67.4 °C for 5 min, 66.1 °C for 6 min;	<i>linker 1</i> for TNFR1
Pair 2	#O-507 and #O-508	73.0 °C for 5 min, 68.0 °C for 5 min, 59.4 °C for 6 min;	<i>linker 1</i> for TNFR2
Pair 3	#O-509 and #O-510	70.6 °C for 5 min, 65.6 °C for 5 min, 60.6 °C for 6 min;	<i>linker 2</i>
Pair 4	#O-509 and #O-511	70.6 °C for 5 min, 65.6 °C for 5 min, 60.6 °C for 6 min;	<i>linker 3</i>

Cloning of the linker sequences into pBS SK (+)

The *linker 1* sequences for TNFR1 and TNFR2 were introduced into the subcloning vector pBS SK(+) (internally referred to as plasmid #86) and the resulting plasmids were used for the introduction of further linker sequences (see Figure 7). Restriction digests of the pBS SK(+) plasmids were performed with *Xba*I and *Acc*65I. The cut vector DNA was then de-phosphorylated with Antarctic Phosphatase and purified by agarose gel extraction.

65 pmol of the *linker 1*, *linker 2* and *linker 3* fill-in products, respectively, were used in 60 µl restriction samples containing 26 U *Xba*I and 20 U *Bam*HI. After purification via agarose gel extraction, insert DNA was ligated into the pBS SK(+) plasmids. The resulting plasmids were transformed into *E. coli* DH5a via heat shock transformation. The DNA sequence was verified by sequencing at GATC (Konstanz, Germany) using the sequencing primer #O-501 (Table 4). Generated plasmids are listed in Table 9.

Table 9. Subcloning plasmids generated for S_{GSL} introduction into TNFR1 and TNFR2

Subcloning vector generated	Linkers inserted	Resulting S _{GSL}	Subcloning vector for
#501	<i>linker1</i>	S _{GSL15}	TNFR2
#502	<i>linker1</i>	S _{GSL15}	TNFR1
#507	<i>linker1/2</i>	S _{GSL31}	TNFR2
#508	<i>linker1/2</i>	S _{GSL31}	TNFR1
#513	<i>linker1/2/2</i>	S _{GSL47}	TNFR2
#514	<i>linker1/2/2</i>	S _{GSL47}	TNFR1
#519	<i>linker1/2/2/3</i>	S _{GSL56}	TNFR2
#520	<i>linker1/2/2/3</i>	S _{GSL56}	TNFR1

2.2.7.2 Cloning of S_{GSL} sequences into pBS SK (+) TNFR-BamHI-Fas

In order to exchange the stalk region in TNFR2-Fas with the artificial S_{GSL15} and S_{GSL56} sequences, which had been subcloned previously, the S_{GSL} inserts of plasmids #501, #502, #519 and #520 were cut out and transferred into plasmid pBS SK(+) TNFR1-BamHI-Fas -*KpnI* (#500) and pBS SK(+) TNFR2-BamHI-Fas (#345), respectively. Plasmid #345 had been generated previously by Krippner-Heidenreich *et al.* (2002).

For the introduction of the S_{GSL} into TNFR1-Fas, the plasmids #502 and #520 were cut using the restriction enzymes *BglIII* and *Acc65I* and the insert DNA was purified via agarose gel extraction. A partial restriction digest of 0.7 pmol vector DNA (#500) was performed in a 40 µl restriction sample using 12.5 U *Acc65I* and 1.4 U *BamHI*. The vector DNA was dephosphorylated and purified using agarose gel extraction.

For the introduction of the S_{GSL} into TNFR2-Fas, the plasmids #501 and #519 were sequentially cut using the restriction enzymes *BglIII* and *AccI*. 7.7 pmol of plasmid DNA was fully digested with *BglIII* and, after 2 h of incubation at 37 °C, ethanol-precipitated and subjected to another restriction digest with *AccI*. The insert DNA was purified via agarose gel extraction. A partial restriction with 5 U *AccI* and 1.4 U *BamHI* was performed with 0.7 pmol of vector DNA (#345) in a 40 µl restriction sample. The vector DNA was dephosphorylated and purified using agarose gel extraction. Insert and

vector DNA were ligated and transformed into *E. coli* DH5 α . The resulting plasmids are listed in Table 10.

Table 10. pBS SK(+) TNFR-S_{GSL}-Fas plasmids

plasmid	plasmid name	linker
#503	pBS SK(+) TNFR1-S _{GSL15} -Fas	S _{GSL15}
#504	pBS SK(+) TNFR2-S _{GSL15} -Fas	S _{GSL15}
#521	pBS SK(+) TNFR1-S _{GSL56} -Fas	S _{GSL56}
#522	pBS SK(+) TNFR2-S _{GSL56} -Fas	S _{GSL56}

2.2.7.3 Cloning of S_{GSL} sequences into pEF-PGK/puro polyA TNFR-Fas

The TNFR-S_{GSL}-Fas constructs, generated as described in section 2.2.7.2, were transferred from the pBS SK(+) plasmids into the mammalian expression plasmids pEF-PGK/puro polyA TNFR1-Fas (#113) and pEF-PGK/puro polyA TNFR2-Fas (#114), respectively. The generation of plasmids #113 and #114 has been described previously (Krippner-Heidenreich *et al.*, 2002).

Restriction digests of plasmids #113, #114, #503, #504, #521 and #522 with the restriction enzymes *Bam*HI and *Bst*BI were performed as described in section 2.2.4.1. The plasmid DNA of plasmids #113 and #114 was treated with Antarctic Phosphatase and purified by gel extraction. The insert DNA of plasmids #503, #504, #521 and #522 was purified via gel extraction.

The ligation of the insert DNA of plasmids #503 and #521 into the purified vector DNA #113 resulted in the plasmids pEF-PGK/puro polyA TNFR1-S_{GSL15}-Fas (#505) and pEF-PGK/puro polyA TNFR1-S_{GSL56}-Fas (#523), respectively. The ligation of the insert DNA of plasmids #504 and #522 into the purified plasmid #114 resulted in the plasmids pEF-PGK/puro polyA TNFR2-S_{GSL15}-Fas (#506) and pEF-PGK/puro polyA TNFR2-S_{GSL56}-Fas (#524), respectively. DNA sequences were verified via sequencing at GATC (Konstanz, Germany) using the sequencing primers #O-213, #O-231 and #O-500, respectively.

2.2.8 Partial replacement of the TNFR2 stalk region with glycine-serine-linkers

In order to locate which part of the TNFR2 stalk region could account for the lack of sTNF responsiveness of TNFR2, the stalk region of TNFR2-Fas chimaeras was partially replaced with glycine-serine-linkers. Four different exchange mutants, TNFR2-(S_{Exaa202-219}/TM)_{R2}-Fas, TNFR2-(S_{Exaa215-232}/TM)_{R2}-Fas, TNFR2-(S_{Exaa228-249}/TM)_{R2}-Fas and TNFR2-(S_{Exaa241-257}/TM)_{R2}-Fas, were generated by a two step site directed mutagenesis approach. The aa sequences for the stalk regions of wild type TNFR2 (wt; aa 202-257) and the four exchange mutants (Ex_{aa202-219}, Ex_{aa215-232}, Ex_{aa228-249} and Ex_{aa241-257}) are depicted in Table 11.

Table 11. Amino acid sequences of the wild type and partially replaced TNFR2 stalk regions

wt:	STSPTRSMAPGAVHLPQPVSTRSQHTQPTPEPSTAPSTSFLLLPMGSPPPAEGSTGD
Ex_{aa202-219}:	<u>GSGGSGGSGGSGGSGGSGV</u>STRSQHTQPTPEPSTAPSTSFLLLPMGSPPPAEGSTGD
Ex_{aa215-232}:	STSPTRSMAPGAV<u>GSGGSGGSGGSGGSGGSGP</u>STAPSTSFLLLPMGSPPPAEGSTGD
Ex_{aa228-249}:	STSPTRSMAPGAVHLPQPVSTRSQHT<u>GSGGSGGSGGSGGSGGSGGSGG</u>PPAEGSTGD
Ex_{aa241-257}:	STSPTRSMAPGAVHLPQPVSTRSQHTQPTPEPSTAPSTS<u>GSGGSGGSGGSGGSGGSGG</u>

Pairs of PAGE-purified oligonucleotides were used, in which the 3'-ends were complementary to the sequences flanking the region which was to be replaced (for pairs see Table 12). The remaining bases encoded the glycine-serine-linker sequence and were complementary between the oligonucleotides of the respective oligonucleotide pair (Table 12, bold letters).

Table 12. Oligonucleotides for partial stalk replacements in TNFR2-Fas

	Number	Nucleotide sequence (5' → 3')
Forward primer 1	#O-524	GT GAG GAA TTC TAG GAT CCC CCA GCT TCT AGA GAT C
Forward primer 2	#O-525	GAT CTC ATC TAT TTT GGC TTC ATT GAC ACC ATT CTT TCG
Pair 1 for TNFR2-(S_{Exaa202-219}/TM)_{R2}-Fas	#O-526	GAA GCG GGG GAA GCG GAG GAT CAG GCG GCA GCG GAG TGT CCA CAC GAT CCC AAC ACA CG
	#O-527	CGC TGC CGC CTG ATC CTC CGC TTC CCC CGC TTC CAC CAG AAC CAC CAC TTC CCG TGC AGA CCG CAT CCA TGC TTG CAT TCC CAG
Pair 2 for TNFR2-(S_{Exaa215-232}/TM)_{R2}-Fas	#O-528	GGT GGT TCT GGT GGA AGC GGT GGA AGC GGC GGA TCA GGC GGT AGC GGA CCC AGC ACT GCT CCA AGT ACC TCC TTC CTG CT
	#O-529	CTG ATC CGC CGC TTC CAC CGC TTC CAC CAG AAC CAC CGG AAC CTA CTG CTC CTG GGG CCA TAC TCC
Pair 3 for TNFR2-(S_{Exaa228-249}/TM)_{R2}-Fas	#O-530	GGA GGA TCA GGC GGC AGC GGA GGC AGT GGA GGT CCA GCT GAA GGG AGC ACT GGC GAC TTC
	#O-531	GAC CTC CAC TGC CTC CGC TGC CGC CTG ATC CTC CGC TTC CCC CGC TTC CAC CAG AAC CTC CAG AAC CGG TGT GTT GGG ATC GTG TGG ACA CTG
Pair 4 for TNFR2-(S_{Exaa241-257}/TM)_{R2}-Fas	#O-532	TCA GGT GGA AGC GGT GGA AGT GGA GGA TCT GGA GGC AGC TTC GCT CTT CCA GTT GGA CTG ATT G
	#O-533	CAG ATC CTC CAC TTC CAC CGC TTC CAC CTG ATC CGC CGG AGC CAG AGG TGC TTG GAG CAG TGC TGG GTT CTG
Reverse primer	#O-534	CTT GGT TCA TTC TCA AGC CTC AGA CAG TGG TTC AAA G

As a first step in the mutagenesis procedure, two separate PCR were performed. For one of these PCR an oligonucleotide of the oligonucleotide pair in combination with a forward primer (primers #O-524 and #O-534, respectively), while for the other PCR the second oligonucleotide of the pair and the reverse primer #O-525 were used (see Figure 8 A). A summary of the appropriate oligonucleotide combinations and annealing temperatures is given in Table 13.

Each of the 25 μ l PCR samples contained 200 μ M dNTPs, 0.4 μ M forward primer, 0.4 μ M reverse primer, 1.8 fmol template DNA (#114) and 0.5 U PhusionTM High-Fidelity DNA Polymerase in 1x Phusion reaction buffer HF. Cycling conditions were as follows: 30 sec at 98 °C; 30 cycles of 10 sec 98 °C, 20 sec 55.8-64.7 °C (appropriate annealing temperatures see Table 13) and 15 sec at 72 °C; 5 min 72 °C; hold 4 °C. Resulting PCR products were purified via agarose gel extraction and resuspended in 30 μ l ddH₂O.

Table 13. Oligonucleotide combinations and annealing temperatures for partial stalk replacements

	Oligonucleotides	Annealing temperature
PCR 1	#O-526 and #O-525	58.2 °C
PCR 2	#O-527 and #O-534	64.7 °C
PCR 3	#O-528 and #O-525	58.9 °C
PCR 4	#O-529 and #O-524	62.5 °C
PCR 5	#O-530 and #O-525	57.6 °C
PCR 6	#O-531 and #O-524	61.2 °C
PCR 7	#O-532 and #O-525	55.8 °C
PCR 8	#O-533 and #O-534	64.5 °C

In the second part of the mutagenesis procedure, the purified PCR products were combined in four parallel PCR as follows: products PCR1 and PCR2; products PCR3 and PCR4; products PCR5 and PCR6; products PCR7 and PCR8.

The 25 μ l PCR samples contained 3 μ l of each of the respective purified PCR products, 200 μ M dNTPs and 0.5 U PhusionTM High-Fidelity DNA Polymerase in 1x Phusion reaction buffer HF. As depicted in Figure 8 D, the 3'-ends of the PCR products are complementary and, therefore, could act as primers for each other. The resulting 5'-overhangs were filled-in by the PhusionTM High-Fidelity DNA polymerase and one long

product, which contained the desired mutation in the middle, was generated. This PCR product could then be amplified by addition of primers which were complementary to the 3'-ends of the full PCR product (Figure 8 E). The cycling conditions for the fill-in reaction and amplification were as follows: 30 sec 98 °C; 10 cycles of 10 sec 98 °C, 20 sec 58.8 °C, 20 sec 72 °C; cool down to 4 °C for 6 min and addition of primers #O-524 and #O-525 to a final concentration of 0.4 μM; 20 sec 98 °C; 30 cycles of 10 sec 98 °C, 20 sec 55.0 °C, 20 sec 72 °C; 5 min 72 °C; cool down to 4 °C.

The resulting PCR products were purified using the Qiagen gel extraction kit. Briefly, 600 μl buffer QC and 200 μl propan-2-ol were added to the PCR samples and the mixture was applied to a silica column. The following steps were identical to the gel extraction procedure described in section 2.2.3. Samples were eluted in 30 μl ddH₂O. The primers used to generate the PCR products contained a *Bam*HI and a *Bst*BI restriction site, respectively. Therefore, after the purification the PCR products could be cut with these restriction enzymes and could, after purification via gel extraction, be cloned into the mammalian expression plasmid pEF-PGK/puro polyA. DNA sequences were verified via sequencing at Genome Enterprise Ltd. (Norwich, UK) using the sequencing primers #O-213 and #O-231 (Table 4), respectively. A summary of the generated plasmids is given in Table 14.

Table 14. Mammalian expression vectors encoding for partial stalk exchange mutants of TNFR2-Fas

Number	Plasmid name
#532	pEF-PGK/puro polyA TNFR2-(S _{Exaa202-219} /TM) _{R2} -Fas
#533	pEF-PGK/puro polyA TNFR2-(S _{Exaa215-232} /TM) _{R2} -Fas
#534	pEF-PGK/puro polyA TNFR2-(S _{Exaa228-249} /TM) _{R2} -Fas
#535	pEF-PGK/puro polyA TNFR2-(S _{Exaa241-257} /TM) _{R2} -Fas

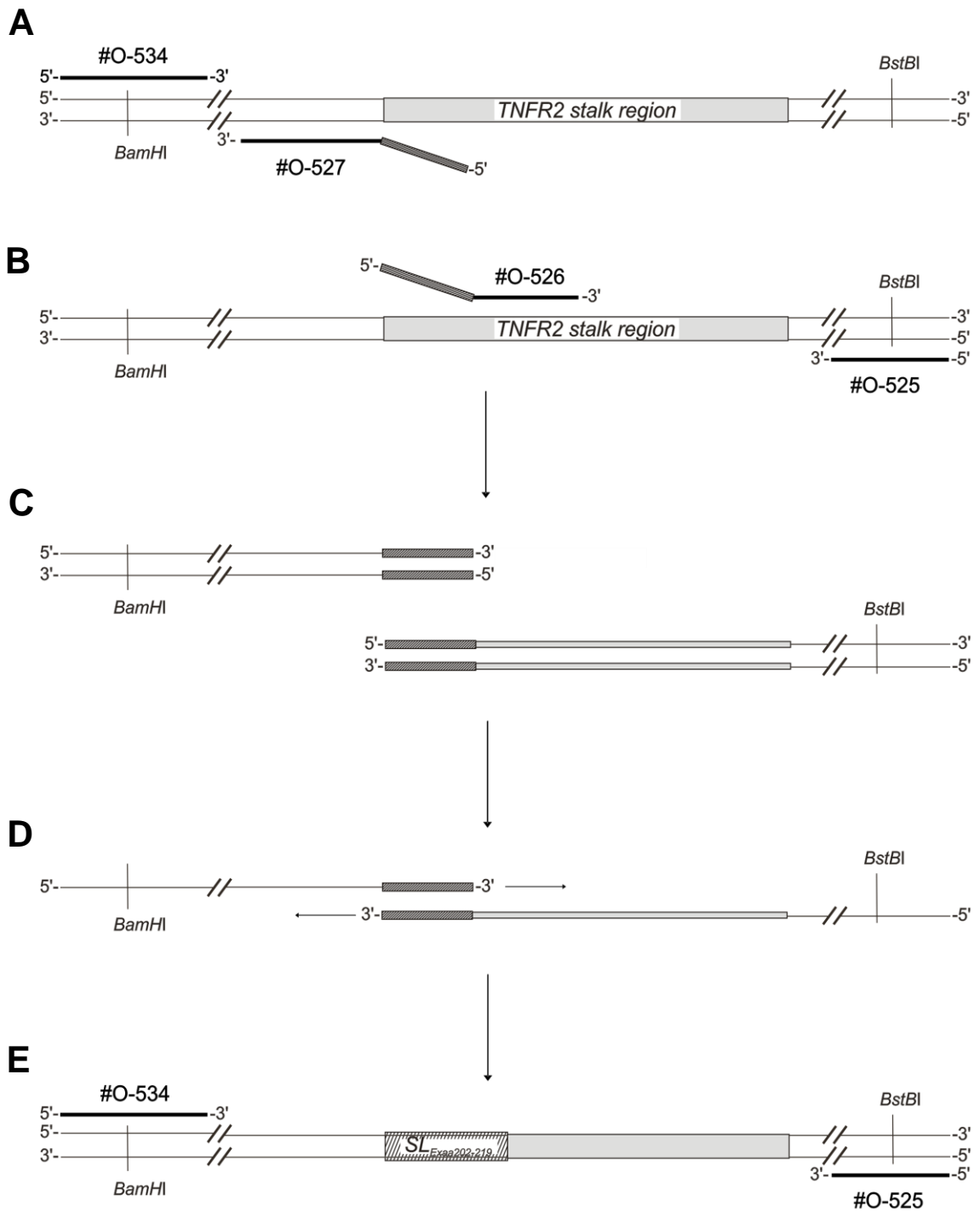


Figure 8. Schematic representation of the partial replacement of the TNFR2 stalk region with an artificial glycine-serine linker (Ex_{aa} 202-219).

PCR were performed using oligonucleotides complementary to the region **A**) upstream of the TNFR2-Fas insert (#O-534) and **B**) downstream of the TNFR2-Fas insert (#O-525), respectively. These were combined with oligonucleotides of which the 5'-part encoded a glycine-serine-linker and the 3'-part was complementary to either the region **A**) upstream (#O-527) or **B**) downstream (#O-526) of the part which was to be replaced. **C**) Amplification resulted in two PCR products which carried the glycine-serine-linker sequence at the 3'-end and 5'-end, respectively. **D**) In a fill-in reaction the 3'-ends of the PCR products could be annealed and extended. This resulted in a product in which the desired part of the TNFR2 stalk region was replaced with a glycine-serine-linker sequence. **E**) The filled-in product could be amplified via PCR using the primers #O-534 and #O-525 and cloned into pEF-PGK/puro polyA via *Bam*HI and *Bst*BI.

2.2.9 Mutagenesis of conserved proline residues in the TNFR2 stalk region

Sequence alignment of the TNFR2 from different mammalian species (*homo sapiens*, *macaca mulatta*, *mus musculus*, *rattus norvegicus*, *canis familiaris* and *equus caballus*) revealed seven conserved proline residues in the TNFR2 stalk region: P205, P211, P219, P231, P233, P237 and P249. To assess the role of these prolines in sTNF responsiveness of TNFR2, the proline residues were mutated to alanines via two step site directed mutagenesis.

The mutagenesis approach was similar to the one described in section 2.2.8. Here pairs of desalted oligonucleotides were used which were complementary to each other (for pairs see Table 15). These oligonucleotides encoded proline to alanine mutations (Table 15, bold letters). Where necessary, silent mutations were introduced for cloning purposes (Table 15, underlined).

Table 15. Oligonucleotides for proline mutants of TNFR2-Fas

	Number	Nucleotide sequence (5'→3')
Pair 1	#O-512	C ACG TCC ACG TCT GCC ACC CGG AGT ATG G
	#O-513	C CAT ACT CCG GGT GGC AGA CGT GGA CGT G
Pair 2	#O-514	G AGT ATG GCA GCA GGG GCA GTA CAC TTA C
	#O-515	G TAA GTG TAC TGC CCC TGC TGC CAT ACT C
Pair 3	#O-516	GTA CAC TTA CCC CAG GCA <u>GTT</u> TCC ACA CGA
	#O-517	TCG TGT GGA <u>AAC</u> TGC CTG GGG TAA GTG TAC
Pair 4	#O-518	<u>ACA</u> CAG CCA ACT GCA GAA GCT AGC <u>ACG</u> GCT CCA
	#O-519	TGG AGC <u>CGT</u> GCT AGC TTC TGC AGT TGG CTG <u>TGT</u>
Pair 5	#O-520	GAA CCC <u>AGT</u> ACT GCT GCA AGC ACC TCC TTC C
	#O-521	G GAA GGA GGT GCT TGC AGC AGT <u>ACT</u> GGG TTC
Pair 6	#O-522	A ATG GGC CCC AGC GCA CCA GCA GAA GGG AGC A
	#O-523	T GCT CCC TTC TGC TGG TGC GCT GGG GCC CAT T

As a first step, two separate PCR were performed. With one oligonucleotide of the oligonucleotide pair a PCR was performed in combination with the forward primer #O-524, while for the other PCR the second oligonucleotide of the pair and the reverse primer #O-525 were used. A summary of the appropriate oligonucleotide combinations and annealing temperatures is given in Table 16.

The 25 μ l reaction samples contained 200 μ M dNTPs, 0.4 μ M forward primer, 0.4 μ M reverse primer, 1.8 fmol template DNA (#114) and 0.5 U PhusionTM High-Fidelity DNA Polymerase in 1x Phusion reaction buffer HF. Cycling conditions were as follows: 30 sec at 98 $^{\circ}$ C; 30 cycles of 10 sec 98 $^{\circ}$ C, 15 sec 58.2-65 $^{\circ}$ C (appropriate annealing temperatures see Table 16) and 15 sec at 72 $^{\circ}$ C; 5 min 72 $^{\circ}$ C; hold 4 $^{\circ}$ C. Resulting PCR products were purified via agarose gel extraction and resuspended in 40 μ l ddH₂O.

Table 16. Two step site directed mutagenesis of conserved proline residues in the TNFR2 stalk region - oligonucleotide combinations and annealing temperatures

	Oligonucleotides	Annealing temperature
PCR 1	#O-512 and #O-525	61.1 $^{\circ}$ C
PCR 2	#O-513 and #O-524	64.9 $^{\circ}$ C
PCR 3	#O-514 and #O-525	58.9 $^{\circ}$ C
PCR 4	#O-515 and #O-524	63.5 $^{\circ}$ C
PCR 5	#O-516 and #O-525	59.6 $^{\circ}$ C
PCR 6	#O-517 and #O-524	64.5 $^{\circ}$ C
PCR 7	#O-518 and #O-525	64.9 $^{\circ}$ C
PCR 8	#O-519 and #O-524	59.0 $^{\circ}$ C
PCR 9	#O-520 and #O-525	58.8 $^{\circ}$ C
PCR 10	#O-521 and #O-524	64.9 $^{\circ}$ C
PCR 11	#O-522 and #O-525	58.2 $^{\circ}$ C
PCR 12	#O-523 and #O-524	65.0 $^{\circ}$ C

In the second part of the mutagenesis procedure, the purified PCR products were combined in six parallel PCR as follows: products PCR1 and PCR2; products PCR3 and PCR4; products PCR5 and PCR6; products PCR7 and PCR8; products PCR9 and PCR10; products PCR11 and PCR12.

The 25 μ l PCR samples contained 3 μ l of each of the respective purified PCR products, 200 μ M dNTPs and 0.5 U PhusionTM High-Fidelity DNA Polymerase in 1x Phusion reaction buffer HF. The same principle was applied to generate the full-length inserts as has been described in section 2.2.8. The cycling conditions for the fill-in reaction and amplification were as follows: 30 sec 98 $^{\circ}$ C; 10 cycles of 10 sec 98 $^{\circ}$ C, 20 sec 58.0 $^{\circ}$ C, 20 sec 72 $^{\circ}$ C; cool down to 4 $^{\circ}$ C for 6 min and addition of primers #O-524

and #O-525; 20 sec 98 °C; 30 cycles of 10 sec 98 °C, 20 sec 55.0 °C, 20 sec 72 °C; 5 min 72 °C; cool down to 4 °C.

The PCR products were purified using the Qiagen gel extraction kit. 600 µl buffer QC and 200 µl propan-2-ol were added to the PCR samples and the mixture was applied to a silica column. The following steps were identical to the gel extraction procedure described in section 2.2.3. Samples were eluted in 30 µl ddH₂O.

The PCR products could be cloned into the mammalian expression plasmid pEF-PGK/puro polyA via *Bam*HI and *Bst*BI as described previously. DNA sequences were verified via sequencing at Genome Enterprise Ltd. (Norwich, UK) using the sequencing primers #O-213 and #O-231 (Table 4), respectively. A summary of the generated plasmids is given in Table 17.

Table 17. Mammalian expression vectors encoding for proline mutants of TNFR2-Fas

Number	Plasmid name
#525	pEF-PGK/puro polyA TNFR2-Fas P205A
#526	pEF-PGK/puro polyA TNFR2-Fas P211A
#527	pEF-PGK/puro polyA TNFR2-Fas P219A
#528	pEF-PGK/puro polyA TNFR2-Fas P231A/P233A
#529	pEF-PGK/puro polyA TNFR2-Fas P237A
#530	pEF-PGK/puro polyA TNFR2-Fas P249A

2.2.10 Generation of TNFR2-(S/TM)_{R1}-R2 and TNFR2-(S_{Δ42}/TM)_{R2}-R2 constructs

To create a TNFR2 variant, in which 42 aa residues of the stalk region are deleted (TNFR2-(S_{Δ42}/TM)_{R2}-R2), the sequences encoding the extracellular portion and transmembrane region of the corresponding TNFR2-Fas chimaera (TNFR2-(S_{Δ42}/TM)_{R2}-Fas) were cloned from plasmid #436 (generated by Dr Andrea Zappe, University of Stuttgart, Germany) into plasmid pEF-PGK/puro polyA TNFR2 + *KpnI* (#81). For this purpose a partial restriction with *Acc65I* and a full restriction with *EcoRV* were performed with these plasmids. The products were ligated to receive plasmid pEF-PGK/puro polyA TNFR2-(S_{Δ42}/TM)_{R2}-R2 (#450).

The expression plasmid for TNFR2 with the stalk and transmembrane regions of TNFR1 (pEF-PGK/puro polyA TNFR2-(S/TM)_{R1}-R2, #451) was generated by using a set of three primers: #O-564 (PAGE-purified), #O-562 and #O-563 (sequences see Table 18).

Primer #O-562 is complementary to the sequence around the *KpnI* restriction site of the intracellular portion of TNFR2 and primer #O-563 encodes for the plasmid #81 sequence downstream of the TNFR2 stop codon. Therefore, with #O-564 as forward primer and #O-563 as reverse primer the DNA sequence encoding aa 293-461 of TNFR2, the Stop codon and the 59 DNA base pairs downstream of the Stop codon could be amplified from plasmid #81.

Primer #O-564 is complementary to the plasmid sequence encoding for the 12 membrane-proximal aa of the intracellular portion of TNFR2 (Table 18 bold letters) and parts of the TNFR1 TM region. Using plasmid pEF-PGK/puro polyA TNFR2-(S/TM)_{R1}-Fas (#449), primer #O-564 as reverse primer and the forward primer #O-524 (Table 12) a PCR product could be generated which comprised the extracellular portion of TNFR2, the stalk and TM regions of TNFR1 and the 12 membrane-proximal intracellular aa of TNFR2.

The 25 µl reaction samples contained 200 µM dNTPs, 0.4 µM of each primer, 1.8 fmol template DNA and 0.5 U PhusionTM High-Fidelity DNA Polymerase in 1x Phusion reaction buffer HF. Cycling conditions were as follows: 30 sec at 98 °C; 30 cycles of 10 sec 98 °C, 15 sec 64 °C and 15 sec at 72 °C; 5 min 72 °C; hold 4 °C. PCR products were gel purified as described in section 2.2.8.

Table 18. Oligonucleotides for the generation of TNFR2-(S/TM)_{R1}-R2

Number	Nucleotide sequence (5'→3')
#O-562	GTG CCT GCA GAG AGA AGC CAA GGT ACC
#O-563	GGG TCA TCC TGC CAG GGC TCA G
#O-564	CCT TGG CTT CTC TCT GCA GGC ACA AGG GCT TCT TTT TCC GAT ACA TTA AAC CAA TGA AGA GG

The two PCR products generated from plasmids #81 and #449, respectively, could then be used in a third PCR. 23 bases of the 3'-regions of these PCR products were complementary to each other, could be annealed with each other and the 5'-overhangs could be filled-in with the help of the PhusionTM High-Fidelity DNA Polymerase. The resulting full-length TNFR2 constructs carried the stalk and transmembrane regions of TNFR1 and the intracellular portion of wild type TNFR2.

For this third PCR, 3 µl of each of the purified PCR products, 200 µM dNTPs and 0.5 U PhusionTM High-Fidelity DNA Polymerase in 1x Phusion reaction buffer HF were used. The cycling conditions for the fill-in reaction and amplification were as follows: 30 sec 98 °C; 10 cycles of 10 sec 98 °C, 15 sec 53.6 °C, 40 sec 72 °C; cool-down to 4 °C for 5 min and addition of primers #O-524 and #O-563 to a final concentration of 0.4 µM; 10 sec 98 °C; 30 cycles of 10 sec 98 °C, 15 sec 55.0 °C, 40 sec 72 °C; 5 min 72 °C; cool down to 4 °C. The following steps were identical to the gel extraction procedure described in section 2.2.3. Samples were eluted in 50 µl ddH₂O.

The PCR products were cloned into the mammalian expression plasmid pEF-PGK/puro polyA via *Bam*HI and *Eco*RV. DNA sequences were verified via sequencing at Genome Enterprise Ltd. (Norwich, UK) using the sequencing primers #O-213 and #O-231 (Table 4), respectively.

2.2.11 Generation of vectors for inducible HEK 293 Flp-IN T-Rex cells

For the generation of inducible HEK 293 Flp-IN T-Rex cells cloning of the construct of interest into the pcDNA5/FRT/TO vector of the Flp-IN T-Rex system (Invitrogen) was required. The pcDNA5/FRT/TO plasmid encodes for a CMV/TetO₂ promoter, which is located upstream of the insert DNA and ensures doxycycline-inducible expression of the insert DNA. The CMV/TetO₂ promoter and insert DNA in the pcDNA5/FRT/TO vector are flanked by FRT sites of recombination at the 3'- and 5'-ends, which allows site-specific recombination in HEK 293 Flp-IN T-Rex cells by Flp recombinase.

A pcDNA5/FRT/TO vector carrying the TNFR1-Fas chimera as insert (plasmid # 358) had been generated previously (Branschädel *et al.*, 2010). This vector was used to generate pcDNA5/FRT/TO vectors encoding for TNFR2, TNFR2-(S/TM)_{R1}-R2, TNFR2-(S_{Δ42}/TM)_{R2}-R2 and TNFR2-(S_{Δ42}/TM)_{R2}-Fas. For this purpose, the TNFR1-Fas insert was removed from plasmid #358 by cutting the vector DNA with the restriction enzymes *Bam*HI and *Eco*RV, dephosphorylating with Antarctic Phosphatase (section 2.2.4.1) and purifying it via gel extraction (section 2.2.3).

A full restriction digest with these enzymes was performed with plasmid pEF-PGK/puro polyA TNFR2 + *Kpn*I (plasmid #81). With the plasmids pEF-PGK/puro polyA TNFR2-(S/TM)_{R1}-R2 (# 451), pEF-PGK/puro polyA TNFR2-(S_{Δ42}/TM)_{R2}-R2 (# 450) and pEF-PGK/puro polyA TNFR2-(S_{Δ42}/TM)_{R2}-Fas (#436) a partial restriction with *Bam*HI and full restriction with *Eco*RV were performed. Full-length inserts were purified by gel extraction (section 2.2.3) and were ligated into plasmid #358 (section 2.2.4.2). DNA sequences were verified via sequencing at Genome Enterprise Ltd. (Norwich, UK) using the sequencing primers #O-213 and CMV fw (Table 4), respectively. A summary of the generated plasmids is given in Table 19.

Table 19. pcDNA5/FRT/TO vectors for the generation of HEK 293 Flp-IN T-Rex cells

Number	Plasmid name
#539	pcDNA5/FRT/TO TNFR2
#540	pcDNA5/FRT/TO TNFR2-(S/TM) _{R1} -R2
#541	pcDNA5/FRT/TO TNFR2-(S _{Δ42} /TM) _{R2} -R2
#546	pcDNA5/FRT/TO TNFR2-(S _{Δ42} /TM) _{R2} -Fas

2.3 Cell culture

Cell lines

HeLa cells (human cervix carcinoma cell line; ATCC, Manassas, USA);

SV40 large T immortalised *tnfr1*^{-/-}/*tnfr2*^{-/-} murine embryonic fibroblasts (MF)(kindly provided by Daniela Maennel, University of Regensburg, Germany);

Human embryonic kidney (HEK) 293 Flp-IN T-Rex cells (Invitrogen Ltd., Paisley, UK)

Cell culture medium

2 mM L-glutamine

5 % (v/v) Foetal calf serum

in RPMI-1640

HEK 293 Flp-IN T-Rex cell culture medium

10 % (v/v) Foetal calf serum

in DMEM

Mammalian cell lines were cultivated at 37 °C in 5 % CO₂ humidified air. For harvesting, adherent cells were washed with DPBS and detached with 1x trypsin-EDTA (diluted in DPBS from 10x stock solution,). Trypsin was inactivated by the addition of cell culture medium. Cells were then pelleted at 400 x g for 5 min and resuspended in buffer or cell culture medium. To determine the cell concentration, 0.4 % (w/v) Trypan-Blue solution was added to the cells in a 1:1 ratio and cells were counted in a Neubauer counting chamber.

Mycoplasma infection of cell cultures can alter cell proliferation and cellular responses. Therefore, the cell lines were routinely tested for contamination with *Mycoplasma* using the MycoAlert® mycoplasma detection kit. In the presence of *Mycoplasma*, mycoplasmal enzymes react with the MycoAlert substrate and ATP is produced. ATP levels can then be measured via the ATP-dependent conversion of luciferin to oxyluciferin by luciferase and the resulting luminescence could be detected on a Berthold Microlumat Plus LB96V luminometer.

2.4 Transfection of mammalian cells

Four different transfection reagents were used for the transfection of mammalian cells. TransIT®-293 (Mirus), HiPerFect (Qiagen) and Lipofectamine™2000 (Invitrogen) are all cationic, lipid-based transfection reagents. These reagents form liposomes which carry a positively charged head group. This head group interacts with negatively charged DNA leading to the condensation of the DNA and the formation of DNA:liposome complexes. The positive charge of the liposomes allows them to interact with the cell membrane and the uptake of the DNA:liposome complex into the cell is believed to happen via endocytosis (reviewed in Chesnoy and Huang, 2000).

In contrast, transfection with the reagent Effectene® (Qiagen) is based on the formation of positively charged micelles. At first, the DNA is condensed using an enhancer and is then coated with the cationic Effectene micelle. Similar to the liposomes, the DNA-loaded micelles can then bind to the cell membrane and are also believed to be taken up into the cell via endocytosis.

2.4.1 Transfection of mammalian cells with mammalian expression plasmids

Transfection of HEK 293 Flp-IN T-Rex cells

HEK 293 Flp-IN T-Rex selection medium A

2 mM	L-glutamine
10 % (v/v)	Foetal calf serum
100 µg/ml	Zeocin
15 µg/ml	Blasticidin S

in DMEM

HEK 293 Flp-IN T-Rex selection medium B

2 mM	L-glutamine
10 % (v/v)	Tetracycline-free foetal calf serum
100 µg/ml	Hygromycin B
15 µg/ml	Blasticidin S

in DMEM

Opti-MEM 1 reduced serum medium with L-glutamine (Invitrogen)

Doxycycline-inducible stable HEK 293 Flp-IN T-Rex cells expressing TNFR2 variants were generated using the Flp-IN T-Rex system (Invitrogen). Cells were grown in HEK 293 Flp-IN T-Rex selection medium A for 10 days prior to transfection to ensure cells carried the FRT recombination site and were expressing the Tet repressor. After this first selection, for each construct 8×10^5 cells/flask were seeded in 7 ml of HEK 293 Flp-IN T-Rex cell culture medium into three parallel 75 cm^2 vented cell culture flasks and grown for 48 h. Cells were then co-transfected on day 3 with pcDNA5/FRT/TO (containing the insert of interest) and the pOG44 vector (encoding the Flp recombinase) in a 1:11 ratio. Briefly, 500 μl of Opti-MEM 1 reduced serum medium with L-glutamine were mixed with 25 μl of TransIT®-293 transfection reagent and 11 μg of total plasmid DNA and incubated at room temperature for 15 min. Cells were washed once with pre-warmed DPBS and 180 μl of the transfection sample were added to each of the 75 cm^2 flasks. Cells were selected the next day with HEK 293 Flp-In T-Rex selection medium B. Cell culture medium was changed every 2-3 days and, in general, it took about 10 days until stable cell clones were obtained.

Transfection of HeLa cells using Effectene

For transient and stable transfections of HeLa cells with expression plasmids the Effectene® transfection reagent kit was used. 2.5×10^5 HeLa cells/well were seeded in 2.5 ml of cell culture medium into a 6-well plate. The next day, 86 μl of buffer EC were combined with 750 ng of plasmid DNA and 6 μl of enhancer in a 1.5 ml reaction tube and incubated at room temperature for 5 min. After addition of 7.5 μl Effectene, the sample was mixed briefly and incubated at room temperature for 10 min. After the incubation, 261 μl of cell culture medium were added. Meanwhile, cells were washed once with pre-warmed DPBS and 670 μl of cell culture medium were added per well. The transfection sample was added to the cells drop by drop and cells were cultivated over night. The next day, cells were either harvested or, for stably transfected HeLa cells, selected with 3 $\mu\text{g}/\text{ml}$ puromycin A. Cell culture medium was changed every 2-3 days and, in general, it took about 7 days until stable cell clones were obtained.

Transfection of MF using Lipofectamine

Transfection medium

2 mM L-Glutamine
in RPMI-1640

Simian virus 40 large T immortalised mouse embryonic fibroblasts (MF) generated from TNFR1/TNFR2 double-knockout mice were kindly provided by Prof. Daniela Männel (University of Regensburg, Germany). The generation of MF stably expressing TNFR-Fas chimaeric receptors using the LipofectamineTM method has been described previously (Krippner-Heidenreich *et al.*, 2002).

Briefly, 2.5×10^5 cells/well were seeded in 6-well plates. The following day, 2.0 µg of DNA were combined with 100 µl of transfection medium. In a separate reaction tube 6.0 µl of Lipofectamine reagent were added to 100 µl of transfection medium. After 15 min of incubation at room temperature, both samples were combined and incubated at room temperature for another 15 min. In the meantime, cells were washed with pre-warmed DPBS and covered with 800 µl of transfection medium. The transfection mixture was added to the cells drop by drop and cells were cultivated for 6 h. The transfection mixture was then replaced with normal cell culture medium. The medium was changed the next day and puromycin A was added to a final concentration of 3 µg/ml. The cell culture medium was changed every 2-3 days and, in general, it took about 7 days until stable cell clones were obtained.

2.4.2 Transfection of HeLa cells with siRNA

HeLa cells were transfected with siRNA using the Qiagen transfection reagent HiPerFect. 3×10^5 cells/well were seeded in 2.3 ml of cell culture medium into a 6-well plate and grown over night. The next day, 12 µl of HiPerFect transfection reagent were added to 100 µl of serum-free medium. 3 µl of 20 µM siRNA were added to this mixture and samples were incubated at room temperature for 10 min. Afterwards, the transfection samples were added to the cells drop by drop, resulting in a final siRNA concentration of 25 nM, and cells were cultivated over night. After 24 h and 48 h, respectively, HeLa cells were harvested for flow cytometry analysis (see section 2.5.2) or were used for co-immunoprecipitation (co-IP) experiments.

2.5 Cell sorting and flow cytometry

PBS-BSA-sodium azide buffer (PBA)

0.025 % (w/v) Bovine serum albumine (BSA)

0.02 % (w/v) Sodium azide (NaN_3)

DPBS

sterile filtered

Antibodies

Biotin rat anti-mouse IgG (H+L) (eBioscience);

Mouse anti-human TNFR1 antibody clone H398 (Institute of Cell Biology and Immunology, University of Stuttgart, Germany);

Mouse anti-human TNFR2 antibody clone MR2-1 (Hycult);

Goat anti-mouse IgG + IgM (H + L)-FITC (Dianova);

Streptavidin-phycoerythrin (BD);

2.5.1 Cell sorting

Previously transfected and puromycin A-selected cells were harvested (at least 5×10^6), washed once with ice-cold PBA and resuspended in 500 μl of ice-cold PBA containing the primary antibodies mouse anti-human TNFR1 clone H398 (5 $\mu\text{g}/\text{ml}$) and mouse anti-human TNFR2 clone MR2-1 (2 $\mu\text{g}/\text{ml}$), respectively. After one hour of incubation on ice, the cells were washed once more and resuspended in ice-cold PBA containing the fluorescein isothiocyanate (FITC)-labelled secondary antibodies (goat anti-mouse IgG + IgM (H + L)-FITC, 1:200). After 45 min of incubation in the dark, the cells were washed once and were resuspended in ice-cold PBA to a concentration of approximately 3×10^6 cells/ml. 40,000 cells were sorted into sterile FACS-tubes containing 3 ml cell culture medium. The cell culture medium was supplemented with 20 μM zVADfmk, a pan caspase-inhibitor, to prevent induction of cell apoptosis by the antibody staining and/or sorting process. Cells were then transferred to a 6-well plate and selected with 3 $\mu\text{g}/\text{ml}$ puromycin A the next day. The selection medium was changed every 2-3 days and after approximately 10 days cells could be used for further analyses.

2.5.2 Flow cytometry

For the detection of exogenously expressed TNFR2, TNFR2 variants and TNFR-Fas chimaeras on the cell surface 5×10^5 cells were harvested, washed once with ice-cold PBA and transferred into V-bottom 96-well plates. Cells were incubated in 100 μ l PBA containing 2 μ g/ml of TNFR2 specific antibodies (mouse anti-human TNFR2 clone MR2-1) or 5 μ g/ml of TNFR1 specific antibodies (mouse anti-human TNFR1 clone H398) on ice for 1 h. After washing with 200 μ l PBA, cells were incubated on ice with FITC-labelled secondary antibodies (goat anti-mouse IgG + IgM (H + L)-FITC, 1:200) for 1 h, washed again with ice-cold PBA and analysed by flow cytometry on a Becton Dickinson FACScan or FACSCanto II. Cells incubated with PBA or secondary antibodies only served as controls.

For the detection of endogenously expressed TNFR1 on HeLa cells, the protocol described above with the following changes was used: Cells were resuspended in 100 μ l PBA containing 2 μ g/ml human IgG and 5 μ g/ml primary mouse anti-human TNFR1 antibodies H398. Cells were incubated on ice for 1 h and were then washed twice with 150 μ l of ice-cold PBA. Cells were resuspended in ice-cold 50 μ l PBA containing 2 % (v/v) rat serum and incubated on ice for 15 min. 1 μ l of biotin rat anti-mouse IgG (H+L) (1:50) was added to each well and samples were incubated on ice for 30 min. Cells were washed twice with 100 μ l PBA and resuspended in 70 μ l PBA containing 5 μ l of streptavidin-phycoerythrin. After a 20 min incubation on ice in the dark, cells were washed twice with ice-cold PBA, resuspended in PBA and analysed on a Becton Dickinson FACSCanto II flow cytometer.

2.6 Cell viability assay using crystal violet staining

10x Phosphate buffered saline (PBS)

160.8 mM Na_2HPO_4

39.5 mM NaH_2PO_4

1.2 M NaCl

pH adjusted to 7.2

Crystal violet solution

0.5 % (w/v) Crystal violet powder

20 % (v/v) Methanol

ddH₂O

For cell viability assays of MF TNFR-Fas, 1×10^4 cells/well were seeded in 100 μl of cell culture medium into a flat bottom 96 well plate. The next morning, cells were treated with serial dilutions of sTNF and CysTNF (0.015-100 ng/ml), respectively. After 8 h of cultivation, the medium was removed and cells were washed three times with 1x PBS. Cells were then stained with 70 μl /well of crystal violet solution for 20 min at room temperature. After removing the crystal violet solution, plates were washed with ddH₂O and left to air-dry over night. 100 μl of 100 % methanol were added per well and the absorbance at 550 nm was determined using a TECAN sunrise basic microplate reader.

2.7 Bradford protein assay

The determination of protein concentrations with the Bradford protein assay is based on the shift in absorbance (465 nm to 595 nm) the Coomassie Brilliant Blue G-250 dye undergoes upon binding to proteins. The protein-dye complex formation stabilises the negatively charged, blue form of the dye in acidic solution. The protein concentration correlates with the absorbance and can be determined via comparison with a solution of a protein, such as BSA, of known concentration.

Cell lysates were prepared using solubilisation buffers as described in sections 2.10 and 2.12. 20 µl of the cell lysates were transferred into the wells of a flat-bottom 96-well plate and 300 µl of room temperature BradfordUltra reagent were added to each well. The plate was incubated at room temperature for 5 min and then the absorbance at 595 nm was determined on a TECAN sunrise basic microplate reader. Samples were prepared in duplicates or triplicates.

2.8 SDS-polyacrylamide gel electrophoresis

4x Resolving gel buffer

1.5 M Tris-HCl pH 8.8

0.4 % (w/v) SDS

10 % SDS polyacrylamide gel solution

1x Resolving gel buffer

10 % (w/v) Acrylamide/bis-acrylamide (37.5:1)

0.1 % (w/v) Ammonium persulphate (APS)

0.17 % (w/v) N,N,N',N'-tetramethylethylenediamine (TEMED)

4x Stacking gel buffer

0.5 M Tris-HCl pH 6.8

0.4 % (w/v) SDS

4.5 % Stacking gel solution

1x	Stacking gel buffer
4.5 % (w/v)	Acrylamide/bis-acrylamide (37.5:1)
0.1 % (w/v)	Ammonium persulphate (APS)
0.17 % (w/v)	N,N,N',N'-tetramethylethylenediamine (TEMED)

4x Sample buffer

0.25 M	Tris-HCl pH 6.8
0.28 M	SDS
0.4 % (w/v)	Bromophenol blue
40 % (v/v)	Glycerol
20 % (v/v)	β -mercaptoethanol (added just before use)

10x Running buffer

250 mM	Tris
2 M	Glycine
10 % (w/v)	SDS

Sealing agarose

0.5 % (w/v)	Agarose
	ddH ₂ O

SDS-PAGE gels consist of a fine mesh of acrylamide and bisacrylamide, which is generated in a co-polymerisation reaction. TEMED accelerates formation of free radicals from APS. APS radicals in turn catalyse the polymerisation of acrylamide and bisacrylamide. SDS present in the SDS-PAGE gels and buffers provides denaturing conditions during electrophoresis and, furthermore, ensures that all proteins are negatively charged and can be resolved in the gel solely according to their molecular weight irrespective of their other electrochemical properties.

The stacking gel has a lower pH of 6.8 at which glycine exists as zwitterion. During electrophoresis, proteins are concentrated into a thin band between the neutrally charged glycine zwitterions and the negatively charged chloride ions in the stacking gel. Entering into the resolving gel, the pH increases to 8.8. Glycine becomes negatively charged and overtakes the proteins in the resolving gel, leading to a further concentration of

the protein bands. In the resolving gel proteins are separated based on their molecular weight.

Discontinuous Tris/glycine SDS-PAGE was performed using a vertical PROT-RESOLV MAXI-LC gel electrophoresis chamber (Phase GmbH, Lübeck) with 1.5 mm spacers and combs (immunoprecipitation samples) or 1.0 mm spacers and combs (all other samples). Glass plates and spacers were assembled and sealing agarose was applied to prevent leakage of the gel solution during pouring. For the resolving gel, 10 % SDS polyacrylamide gel solution was poured between the plates and overlaid with propan-2-ol to exclude oxygen. The gel was allowed to polymerise. After the gel had set, the propan-2-ol was removed, a 4.5 % stacking gel was poured on top and the comb was inserted. After the stacking gel had set, the comb was removed and the gel kit was assembled into the device. Both gel chambers were filled with 1x running buffer.

Cell lysates supplemented with 1x sample buffer were denatured at 105 °C for 3 min. Samples were then loaded onto the gel together with a broad range prestained protein marker (NEB). For the stacking of the proteins electrophoresis was performed at constant 90 V and for the separation at constant 180 V. The gel run was stopped when the bromophenol blue front had reached the bottom of the gel and the gel was analysed using Western Blot analysis.

2.9 Western Blot analysis

Transfer buffer

192 mM Glycine
25 mM Tris-HCl pH 8.3
20 % (v/v) Methanol
ddH₂O

1x phosphate buffered saline-Tween 20 (PBS-T)

16.08 mM Na₂HPO₄
3.95 mM NaH₂PO₄
120 mM NaCl
0.05 % (v/v) Tween 20
pH adjusted to 7.2

Blocking solution

5 % (w/v) Non-fat milk powder

PBS-T

PBA

0.025 % (w/v) BSA

0.02 % (w/v) NaN_3

DPBS

Proteins were transferred from SDS-polyacrylamide gels onto PVDF membranes (immunoprecipitation samples) or nitrocellulose membranes (all other samples) using a Pegasus S semi-dry blotting chamber (Phase, Lübeck).

The blotting chamber was assembled as follows: a layer of three 1.0 mm thick Whatman papers soaked in transfer buffer was placed on the cathode plate and the gel was placed on top of the Whatman papers, followed by the nitrocellulose membrane, which had been bathed briefly in transfer buffer. When PVDF membranes were used, the membrane was briefly soaked in methanol, was washed in ddH₂O and a finally soaked in transfer buffer. Another layer of three soaked Whatman papers was placed on top of the membrane.

The anode plate was placed on top of the second Whatman paper layer and protein transfer was performed for 80 min at 1.4 mA/cm². After the transfer, the membrane was incubated in blocking buffer on a rocking table at room temperature for 1 h. Then the membrane was washed four times for 10 min with PBS-T and incubated with the primary antibodies at 4 °C over night. The next day, the membrane was washed four times for 10 min with PBS-T and incubated with the secondary antibodies for 2 h at room temperature on a rocking table. The membrane was washed again and overlaid with SuperSignal® West Pico or SuperSignal® West Dura chemiluminescence substrate (Thermo Scientific/Pierce) and transferred between two layers of clear-transparent plastic film. The secondary antibodies were labelled with horseradish peroxidase (HRP). This enzyme cleaved the West Pico and West Dura substrates, respectively, and the resulting chemiluminescence was captured on Kodak® BioMax™ MR autoradiography films (Sigma-Aldrich) or detected using a Syngene G:Box and the GeneSnap V7.09 acquisition software (Syngene UK, Cambridge). Western Blot band quantification was performed using the GeneTools V4.01 analysis software (Syngene UK, Cambridge).

2.10 Protein crosslinking with bis[sulfosuccinimidyl]suberate

Solubilisation buffer

20 mM	Tris-HCl pH 7.4
150 mM	NaCl
1 mM	EDTA
1 % (v/v)	Triton X-100
1x	Complete, Mini, EDTA-free protease inhibitor cocktail tablets (Roche Applied Science, Burgess Hill, UK; added just before use)

Bis[sulfosuccinimidyl]suberate (BS³) stock solution

500 µM	Bis[sulfosuccinimidyl]suberate
--------	--------------------------------

in DPBS

10x Tris-buffered saline (TBS)

200 mM	Tris-HCl pH 7.6
1.37 M	NaCl

in ddH₂O

3×10^5 cells/well of MF TNFR-Fas were seeded into 6-well plates and grown over night. For each concentration of the chemical crosslinking reagent bis[sulfosuccinimidyl]suberate (BS³) two parallel wells were seeded. The next day, cells were transferred onto ice and washed once with ice-cold DPBS. Afterwards, cells were incubated with 0.8 ml/well of freshly prepared dilutions of BS³ (0 µM, 33 µM, 64 µM, 125 µM, 250 µM and 500 µM, respectively) for 30 min on ice. The crosslinking reaction was stopped by addition of Tris-HCl pH 7.2 to a final concentration of 10 mM and incubation at room temperature for 15 min. Cells were washed once with 1 ml of ice-cold 1x TBS and harvested on ice using a rubber cell scraper. Cells were pelleted at 400 x g at 4 °C for 5 min and resuspended in 200 µl of solubilisation buffer. Samples were vortexed for 30 sec and incubated on ice for 5 min afterwards. This step was repeated six times. Finally, the samples were centrifuged at 13000 x g at 4 °C for 10 min. Supernatants were transferred to new 1.5 ml reaction tubes and protein concentrations were determined via Bradford analysis. Samples were normalised for protein concentrations and receptor cell surface expression as determined by parallel FACS analyses. Chimaeric receptors were detected using the mouse anti-human

cytoplasmic Fas antibody clone B10 (Santa Cruz; 1:2000) and goat anti-mouse IgG-HRP antibodies (Dianova; 1:20000).

2.11 Inhibition of core 1 and core 2 O-glycosylation in MF TNFR-Fas cells

Mucin-type O-glycosylation is initiated by the addition of an N-acetyl-galactosamine (GalNAc) residue to the hydroxyl group of a serine or threonine residue of the protein substrate. Benzyl-2-acetamido-2-deoxy- α -D-galactopyranoside (Benzyl- α -GalNAc) is a structural analog of GalNAc (Figure 9) and can function as a competitive inhibitor for β -1,3-galactosyltransferase-dependent core 1 and core 2 O-glycosylation (Kuan *et al.*, 1989).

MF TNFR1-Fas and MF TNFR2-Fas were cultivated in cell culture medium containing 3.5 mM Benzyl- α -GalNAc until day 3 or day 4. TNFR2-S_{L56}-Fas were cultivated in cell culture medium containing 3.5 mM Benzyl- α -GalNAc until day 4. The cell culture medium was replaced with fresh medium containing 3.5 mM Benzyl- α -GalNAc on day 2.

For flow cytometry and Western Blot experiments 2.5×10^5 cells/well were seeded into a 6-well plate on day 3 and 4, respectively. For cell viability assays 1×10^5 cells/well were seeded into a 96-well plate on day 3 and day 4. The cell culture medium was supplemented with 3.5 mM Benzyl- α -GalNAc. 0.55 % (v/v) DMSO served as solvent control. Chimaeric receptors were detected using the mouse anti-human cytoplasmic Fas antibody clone B10 (Santa Cruz; 1:2000) and goat anti-mouse IgG-HRP antibodies (Dianova; 1:20000).

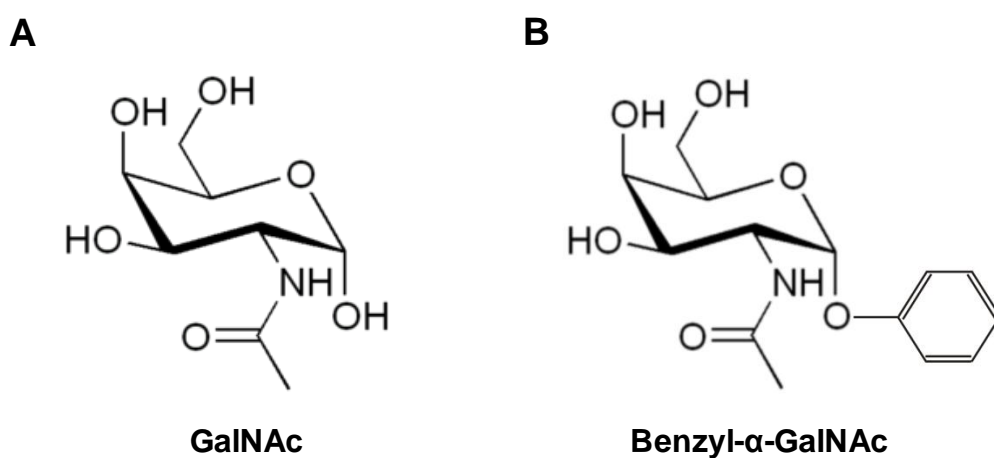


Figure 9. Chemical Structure of Benzyl-2-acetamido-2-deoxy- α -D-galactopyranoside. Shown are the chemical structures of **A**) 2-Acetamido-2-deoxy-D-galactose (GalNAc) and **B**) Benzyl-2-acetamido-2-deoxy- α -D-galactopyranoside (Benzyl- α -GalNAc). Both, GalNAc and Benzyl- α -GalNAc can act as substrates for β -1,3-galactosyltransferase.

2.12 TNFR2/TRAF2 co-immunoprecipitation from HeLa cell lysates

Solubilisation buffer Shu

20 mM	Tris-HCl pH 7.5
150 mM	NaCl
1 mM	EDTA
1 % (v/v)	Triton X-100
30 mM	NaF
1x	Complete, Mini, EDTA-free protease inhibitor cocktail tablets (Roche Applied Science, Burgess Hill, UK; added just before use)
0.5 mM	PMSF (added just before use)

Antibodies

Mouse anti-human TRAF2 antibody clone C90–481 (BD/Pharmingen, Oxford, UK)

Polyclonal goat anti-human soluble TNFR2 antibodies (R&D Systems Europe Ltd., Abingdon, UK)

Goat anti-mouse IgG-HRP antibody (Dianova, Hamburg, Germany)

Rabbit anti-goat IgG-HRP antibody (Sigma-Aldrich Company Ltd., Poole, UK)

Co-immunoprecipitation allows the purification of intact protein complexes from cell lysates. Antibodies against a specific protein are coupled to a solid matrix and can bind their target protein from cell lysates. The matrix, here protein G sepharose beads, can then be pelleted together with the protein of interest. Associated proteins present in the target protein complex will be precipitated together with the protein of interest and can be analysed, e.g. by Western Blotting.

For each immunoprecipitation sample 2.5×10^5 HeLa cells/well were seeded into 6-well plates. The next day, the medium was replaced with 1 ml of pre-warmed cell culture medium containing 10 ng/ml of sTNF and CysTNF, respectively. Cells were stimulated at 37 °C for 5 min, 10 min or 15 min. After stimulation the cells were transferred onto ice and washed with 3 ml of ice-cold DPBS. Cells were harvested in 750 µl of ice-cold DPBS using a cell scraper and pelleted at 400 x g at 4 °C for 5 min. The cell pellets were resuspended in 300 µl of solubilisation buffer Shu. The resulting lysates were vortexed three times for 45 sec with 5 min incubations on ice in between. Cell lysates were centrifuged at 13000 x g at 4 °C for 10 min and the supernatants were transferred into fresh 1.5 ml Eppendorf reaction tubes. For each immunoprecipitation

sample an equivalent of 5×10^5 cells was used. The use of equal amounts of protein was ensured by Bradford analysis. 2 μg of monoclonal goat anti-human soluble TNFR2 antibodies (R&D) were added to each lysate and samples were incubated on a rotary mix at 4 °C for 2 h. The lysates were then added to 10 μl of equilibrated slurry (1:1) protein G sepharose beads and incubated at 4 °C on the rotary mix for 1 h. Beads were washed three times with 1 ml of solubilisation buffer Shu and pelleted at 14000 x g. 50 μl of 1x SDS PAGE sample buffer were added to the pelleted beads and the mixture was vortexed briefly. The samples were denatured at 105 °C for 3 min, the beads were pelleted and supernatants were loaded onto a 10 % SDS gel. TRAF2 was detected using mouse anti-human TRAF2 antibodies (BD/Pharmingen; 1:2000) and goat anti-mouse IgG-HRP antibodies (Dianova; 1:20000).

Precipitated TNFR2 was detected using polyclonal goat anti-human soluble TNFR2 antibodies (R&D; 1:2000) and rabbit anti-goat IgG-HRP antibodies (Sigma-Aldrich; 1:20000). β -actin from the supernatants of the co-immunoprecipitation samples was detected on a separate gel using mouse anti-human β -actin antibodies AC-15 (Abcam; 1:50000) and goat anti-mouse IgG-HRP antibodies (Dianova; 1:20000).

2.13 Analysis of p65 translocation in MF via immunofluorescence

Antibodies

Polyclonal rabbit anti-human p65 antibody clone C-20 (Santa Cruz Biotechnology Inc., Santa Cruz, USA)

Alexa594-conjugated goat anti-rabbit IgG (H+L) antibody (Molecular Probes/Invitrogen Ltd., Paisley, UK)

5×10^4 MF were seeded onto ethanol-sterilised glass cover slips in a 24-well plate. The next day, some of the cells were pre-treated with 1.25 $\mu\text{g}/\text{ml}$ mouse anti-human TNFR2 antibody clone 80M2 for 30 min prior to stimulation. Cells were then stimulated by adding sTNF and CysTNF, respectively, to a final concentration of 100 ng/ml. Cells were stimulated for 30 min or 60 min and then transferred onto ice. The medium was removed using an aspirator, cells were washed once with ice-cold DPBS and fixed with 300 $\mu\text{l}/\text{well}$ of 3.7 % formaldehyde for 10 min at room temperature. Cells were washed once with DPBS and permeabilised for 10 min at room temperature using 1 ml 0.1 % (w/v) saponin/0.5 % (w/v) BSA/DPBS per cover slip. The saponin solution was removed and the cells were blocked with 3 % (w/v) BSA/DPBS for 45 min at room

temperature. Each cover slip was stained with 75 μ l of primary antibody solution (polyclonal rabbit anti-human p65 IgG (C-20) sc-372 1:100 in 1 % (w/v) BSA/DPBS) in a wet chamber for 2 h at room temperature. Cover slips were washed three times with DPBS and were then incubated in 75 μ l of secondary antibody solution (Alexa594-conjugated goat anti-rabbit IgG (H+L) 1:100 in 1 % (w/v) BSA/DPBS) in a wet chamber for 1 h at room temperature in the dark. Cover slips were washed three times with DPBS and then mounted onto microscope slides with Vectashield® DAPI-containing mounting medium (Vector Laboratories Ltd., Peterborough, UK). Images were acquired on a Zeiss Axio Imager 2 fluorescence microscope using the AxioVision 4.7.2 software.

2.14 Confocal microscopy of HEK FlpIN T-Rex cells over-expressing TNFR2 and TNFR2 variants

Distribution of the TNFR on the cell surface was investigated by confocal microscopy of doxycycline-induced HEK Flp-IN T-Rex cells, which had been stained with either AlexaFluor546-labelled recombinant human sTNF or phycoerythrin-conjugated TNFR2-specific antibodies clone # 22235 (R&D Systems Europe Ltd., Abingdon, UK). Ethanol-sterilised glass cover slips were coated with poly-L-lysine. Briefly, cover slips were incubated with the 0.01% (w/v) poly-L-lysine solution (MW: 70 - 150 kDa; Sigma-Aldrich Company Ltd. (Poole, UK)) for 5 min and the excess solution was removed. Cover slips were left to air-dry at room temperature in a laminar flow.

8×10^4 HEK Flp-In T-Rex cells/well were seeded onto the poly-L-lysine coated cover slips in 12-well plates. After 6 h, TNFR expression was induced by adding doxycycline to a final concentration of 6 ng/ml. After 18 h of induction cells were transferred onto ice and washed three times with ice-cold DPBS. Cover slips were then stained with 50 μ l 1.7 μ g/ml AlexaFluor546-labelled recombinant human sTNF diluted in HEK cell culture medium on ice for 5 min. Cells were washed three times with ice-cold DPBS and were fixed with 4 % formaldehyde at room temperature for 20 min. Cover slips were washed three times with DPBS and incubated with 200 μ l of 1 μ g/ml DAPI/1 % (w/v) BSA/DPBS at room temperature for 30 min. Cover slips were washed three times with DPBS, mounted onto glass microscope slides using Fluoromount G mounting medium and sealed with clear nail varnish. Images were acquired on an

Andor Revolution XD confocal microscope using the Andor iQ 1.9.1 software (Welcome Trust Grant reference number 087961).

For the staining with the phycoerythrin-conjugated TNFR2-specific antibodies (clone # 22235), cells were seeded as described above and fixed with 4 % formaldehyde at room temperature for 20 min. TNFR2-specific antibodies were diluted 1:75 in HEK Flp-IN T-Rex cell culture medium. Cells were stained with of 50 μ l of this dilution for 1 h at room temperature in a wet chamber. Afterwards, cells were washed three times with DPBS and mounted onto glass microscope slides and analysed as described above.

To demonstrate cell membrane localisation of the TNFR, co-localisation with Oregon Green-conjugated wheat germ agglutinin (WGA) staining was assessed. The lectin WGA selectively recognises sialic acid and N-acetylglucosaminyl sugars, which are predominantly found in the cell membrane. Cells were stained as described above and the DAPI staining solution was supplemented with 5 μ g/ml of Oregon Green-conjugated wheat germ agglutinin.

CHAPTER 3

Results I: Control of sTNF responsiveness by the TNFR1 and TNFR2 stalk regions

3.1 Introduction

TNFR1 and TNFR2 can bind membrane-bound TNF and sTNF with high affinity (Grell *et al.*, 1998b). However, while TNFR1 can be efficiently activated by both forms of TNF, efficient activation of TNFR2 only occurs upon stimulation with membrane-bound TNF (Grell *et al.*, 1995). A cellular system to investigate differential responsiveness of TNFR1 and TNFR2 has been described previously (Krippner-Heidenreich *et al.*, 2002). Krippner-Heidenreich *et al.* (2002) stably transfected embryonic fibroblasts from *tnfr1^{-/-}/tnfr2^{-/-}* double knockout mice (MF) with TNFR-Fas chimaeras, which consisted of the extracellular and transmembrane part of the TNFR and the cytoplasmic part of Fas (a potent inducer of apoptosis in MF)(Figure 10). The intracellular domain of Fas ensures that the signalling outcome upon activation is identical between TNFR-Fas chimaeras. Therefore, this cellular system allows comparing activation of TNFR1 and TNFR2 while it also eliminates the major technical problem that TNFR1 tends to induce ligand-independent toxicity when expressed exogenously.

MF TNFR-Fas can be stimulated with sTNF or CysTNF, a mutant variant of sTNF which forms oligomers via an N-terminal cysteine residue and displays activity similar to membrane-bound TNF (Bryde *et al.*, 2005). Cell viability can then be determined by crystal violet staining and reflects the responsiveness of TNFR-Fas chimaeras towards the respective ligand. Pilot data obtained with this cellular system showed that responsiveness to sTNF is not determined by the intracellular portion of either TNFR (Krippner-Heidenreich *et al.*, 2002)(see also Figure 11 A and D).

Preliminary data from MF transfected with TNFR-Fas chimaeras in which stalk (S) and transmembrane (TM) regions had been exchanged between receptors (TNFR1-(S/TM)_{R2}-Fas and TNFR2-(S/TM)_{R1}-Fas, Figure 10) suggest a role for these regions in determining the differential responsiveness to sTNF (Figure 11 B and E, obtained in our

group previously). Analysis of chimaeras, in which only the TM had been exchanged between TNFR1-Fas and TNFR2-Fas, indicates that the TM regions play only a minor role in differential responsiveness towards sTNF (data not shown, diploma thesis Gerlinde Holeiter 2005, Stuttgart University, Germany). This implies that the stalk region plays a major role in determining sTNF responsiveness.

The stalk regions of TNFR1 and TNFR2 do not only differ in their aa composition but, with 15 aa for TNFR1 and 56 aa for TNFR2, also in their length. To investigate whether a component within the stalk region determines responsiveness towards sTNF, the TNFR2 stalk region in the TNFR1-(S/TM)_{R2}-Fas chimaeras was shortened by 42 amino acids (TNFR1-(S_{Δ42}/TM)_{R2}-Fas, Figure 10). These chimaeras, in which the stalk length is comparable to the one of TNFR1, were responsive to sTNF (Figure 11 C), supporting a role for the stalk regions of TNFR1 and TNFR2 in differential sTNF responsiveness.

Therefore, the aims in this chapter were to:

- Investigate whether the TNFR2 stalk region has an inhibitory effect on the sTNF responsiveness of TNFR2-Fas chimaeras;
- Determine whether the TNFR2 stalk region controls sTNF responsiveness of wild type TNFR2;
- Establish a read-out system for sTNF-mediated downstream signalling of wild type TNFR2.

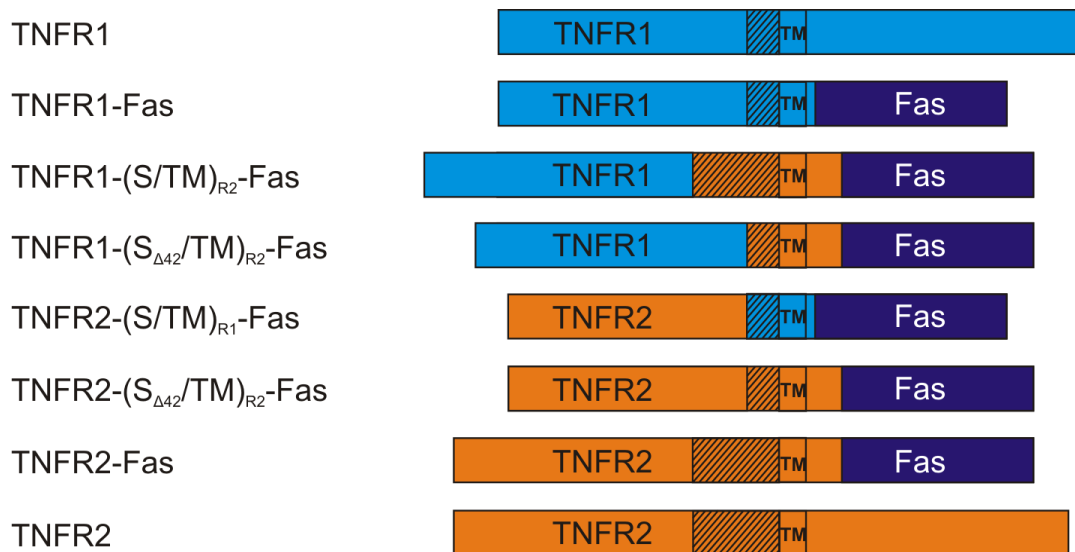


Figure 10. Schematic representation of TNFR-Fas chimaeras.

Wild type TNFR1 and TNFR2, chimaeric receptors TNFR1-Fas and TNFR2-Fas as well as four TNFR-Fas variants are shown schematically. TNFR-Fas chimaeras consist of the extracellular and transmembrane (TM) domain of TNFR1 (aa 1-236, light blue) and TNFR2 (aa 1-301, orange), respectively, and the intracellular portion of Fas (aa 191-335, dark blue)(Krippner-Heidenreich *et al.*, 2002). The TM and stalk regions (S, shaded) are indicated. Exchange of aa 197-236 of TNFR1 and aa 202-301 of TNFR2 between TNFR-Fas resulted in the TNFR1-(S/TM)_{R2}-Fas and TNFR2-(S/TM)_{R1}-Fas chimaeras. TNFR1-(S_{Δ42}/TM)_{R2}-Fas and TNFR2-(S_{Δ42}/TM)_{R2}-Fas represent chimaeras in which the TNFR2 stalk region had been shortened to the same length as the TNFR1 stalk region. The deletion comprised aa 202-243 of TNFR2.

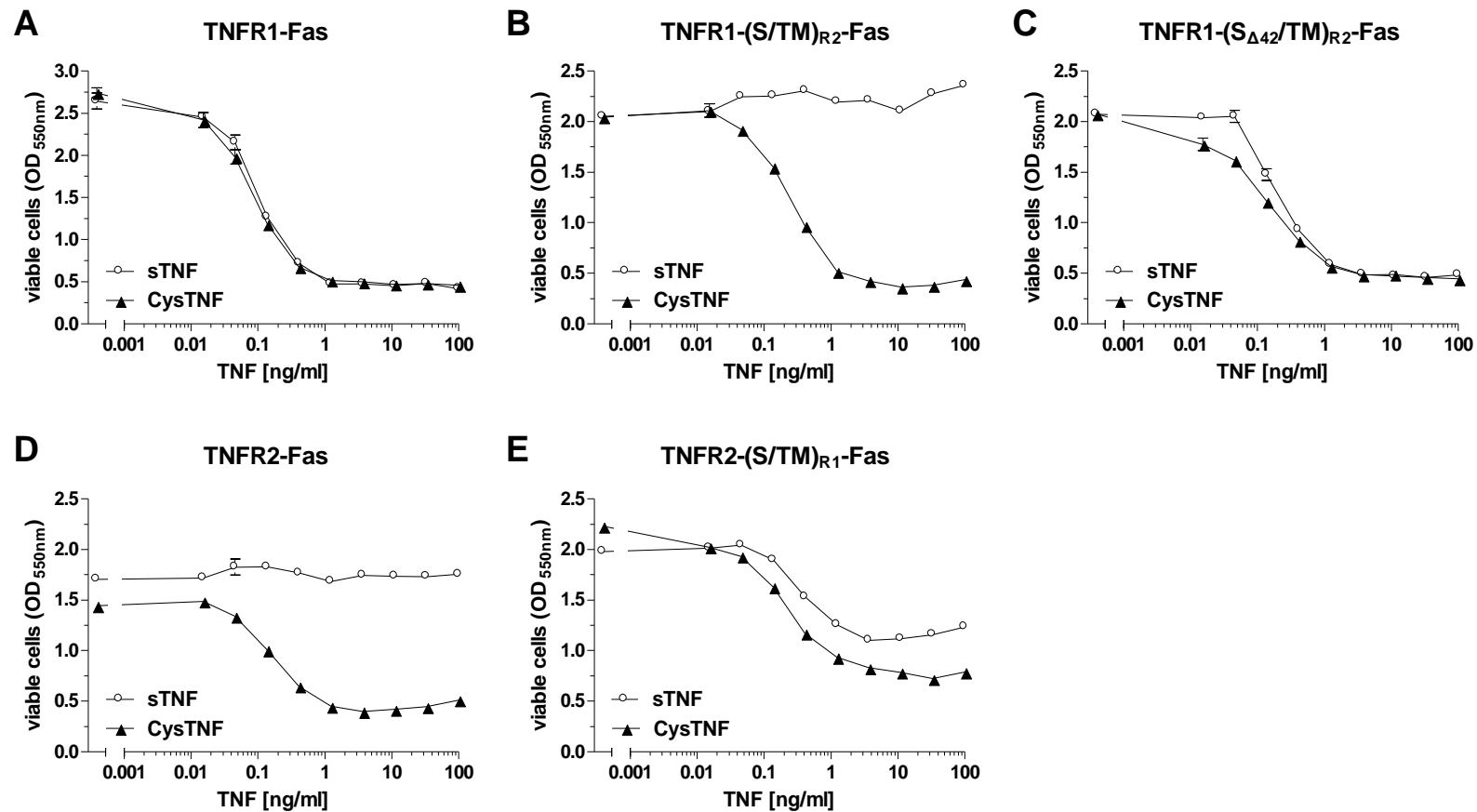


Figure 11. Preliminary data suggest a role for stalk and/or TM regions of TNFR in sTNF responsiveness.

MF were stably transfected with **A**) TNFR1-Fas, **B**) TNFR1-(S/TM)_{R2}-Fas, **C**) TNFR1-(S_{Δ42}/TM)_{R2}-Fas, **D**) TNFR2-Fas or **E**) TNFR2-(S/TM)_{R1}-Fas. Cells remained untreated or were stimulated with increasing concentrations (0.015-100 ng/ml) of sTNF and CysTNF, a TNF variant that mimics membrane-bound TNF (Bryde *et al.*, 2005). Data shown represent more than three independent experiments and were kindly provided by Dr Anja Krippner-Heidenreich, Newcastle University, UK.

3.2 The TNFR2 stalk region inhibits sTNF responsiveness in TNFR2-Fas chimaeras

Preliminary data obtained from MF stably transfected with the TNFR1-(S/TM)_{R2}-Fas and TNFR1-(S_{Δ42}/TM)_{R2}-Fas chimaeras suggested that the TNFR stalk regions are determining receptor responsiveness to sTNF (Figure 11 B and C). In order to elucidate whether the TNFR2 stalk region also controls sTNF responsiveness of the TNFR2-Fas chimaera, the stalk region of this construct was shortened by the same 42 aa residues as in TNFR1-(S_{Δ42}/TM)_{R2}-Fas. The aa sequence of the stalk region of the resulting TNFR2-(S_{Δ42}/TM)_{R2}-Fas construct is depicted in Figure 12. The two N-terminal aa residues of the TNFR2-(S_{Δ42}/TM)_{R2}-Fas stalk region (GS) represent the *Bam*HI restriction site used for the generation of this construct. MF stably transfected with this chimaera (MF TNFR2-(S_{Δ42}/TM)_{R2}-Fas) were generated by Dr Andrea Zappe, University of Stuttgart, Germany, and were analysed at Newcastle University.

MF TNFR2-(S_{Δ42}/TM)_{R2}-Fas were characterised by FACS analysis (Figure 13 A) and Western Blotting (Figure 13 B). The TNFR2-(S_{Δ42}/TM)_{R2}-Fas chimaera was expressed on the cell surface of MF with a mean fluorescence intensity (MnX) of 187. 80 % of the cells could be gated positive for the construct (Figure 13 A).

The correct molecular weight of the stably transfected constructs was confirmed via Western Blot analysis using whole cell lysates from both transiently transfected HeLa cells and stably transfected MF (Figure 13 B). The predicted molecular weight for the TNFR2-Fas construct is 48 kDa whereas the one for TNFR2-(S_{Δ42}/TM)_{R2}-Fas is 44 kDa (both determined using the ProtParam tool on the ExPaSy proteomics server)(Gasteiger *et al.*, 2005). For both constructs two bands could be observed in Western Blot analysis, of which the faster migrating bands correlated with the predicted molecular weights for the constructs (Figure 13 B).

As whole cell lysates were used in this Western Blot, the faster migrating protein bands presumably represent receptors which had been translated but had not undergone any post-translational modification yet, whereas the slower migrating bands probably represent the mature form of the receptor. This assumption is supported by the fact that more of the putatively un-modified forms of the TNFR-Fas chimaeras can be found in lysates from transiently transfected HeLa cells than in lysates from stably transfected MF (Figure 13 B).

TNFR1: PQIENVKGTEDSGTT

TNFR2: STSPTRSMAPGAVHLPQPVSTRSQHTQPTPEPSTAPSTSFLLPMGPPPAEGSTGD

TNFR2-(S_{Δ42}/TM)_{R2}-Fas: GSPMGPPPAEGSTGD

Figure 12. The aa sequences of the TNFR1, TNFR2 and TNFR2-(S_{Δ42}/TM)_{R2}-Fas stalk regions.

Shown are the aa sequences of the stalk regions of TNFR1 (aa 197-211) and TNFR2 (aa 202-257). The aa sequence of the TNFR2 stalk region, in which aa 202-243 had been deleted, is also shown (TNFR2-(S_{Δ42}/TM)_{R2}-Fas). The two N-terminal aa residues of the TNFR2-(S_{Δ42}/TM)_{R2}-Fas stalk region (GS) represent the *Bam*HI restriction site used for the generation of this construct.

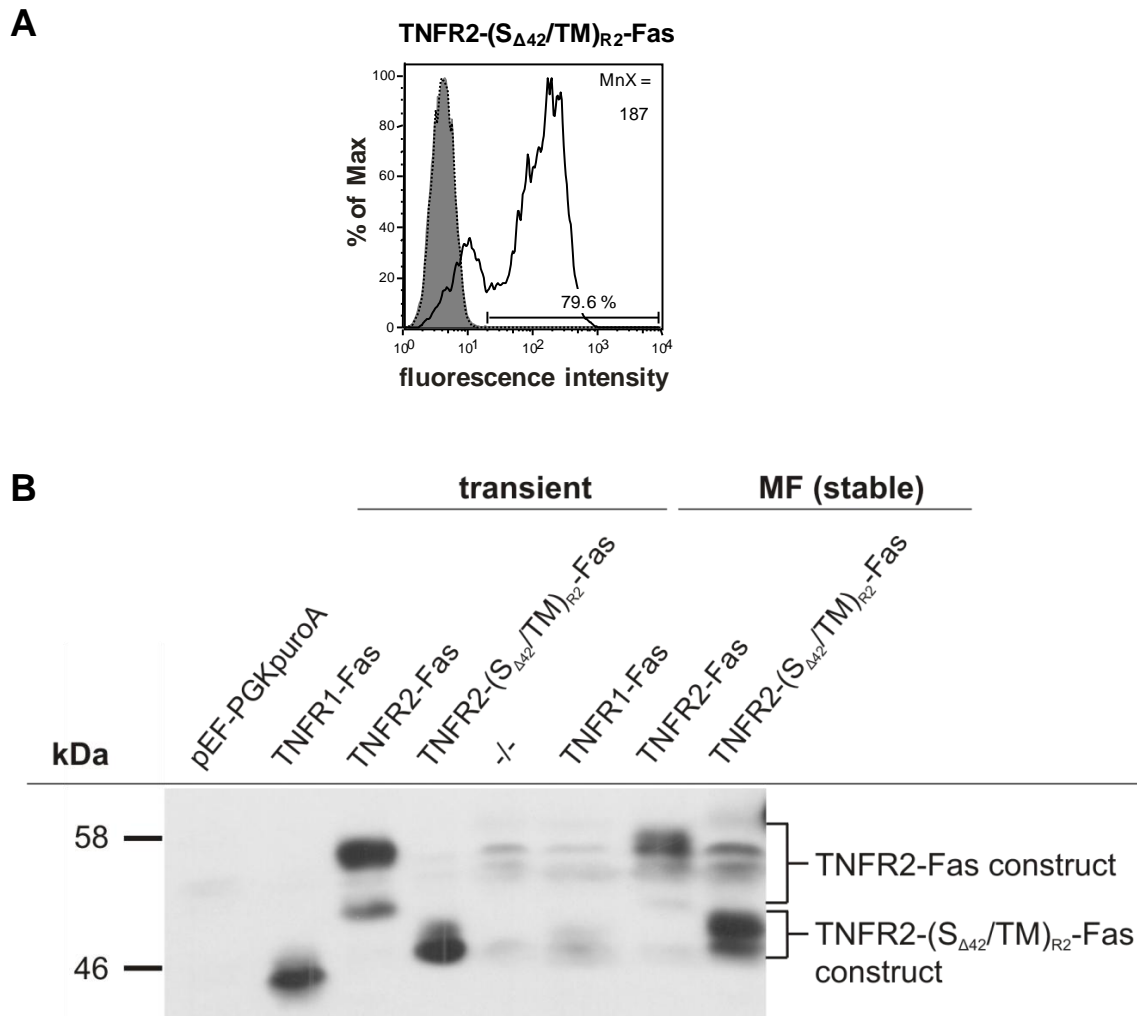


Figure 13. Characterisation of TNFR2-Fas chimaeras with a shortened stalk region.

MF had been stably transfected with the TNFR2-(S_{Δ42}/TM)_{R2}-Fas chimaera. After selection with puromycin A the cells were characterised by FACS and Western Blot analyses. **A)** FACS analysis of MF TNFR2-(S_{Δ42}/TM)_{R2}-Fas. Chimaeras were stained on the cell surface using mouse anti-human TNFR2 antibodies (clone MR2-1) and goat anti-mouse IgG-FITC antibodies (black line). Unstained cells (dotted line); cells only incubated with goat anti-mouse IgG-FITC antibodies (grey). 80 % of the MF were gated positive for TNFR2-(S_{Δ42}/TM)_{R2}-Fas. Acquisition was performed on a Becton Dickinson FACScan flow cytometer. **B)** Western Blot analysis of MF TNFR2-(S_{Δ42}/TM)_{R2}-Fas. Whole cell lysates from 1 x 10⁵ cells were subjected to SDS-PAGE and Western Blot analysis. Mouse anti-human Fas antibodies (clone B10, 1:2000) were used as primary and goat anti-mouse-IgG-HRP (1:20000) as secondary antibodies. HeLa cells transiently transfected with indicated TNFR-Fas chimaeras, untransfected MF, MF TNFR1-Fas and MF TNFR2-Fas served as controls. Data shown represent one experiment.

To determine the effect the shortening of the TNFR2 stalk region had on sTNF responsiveness of TNFR2-Fas, cell viability assays were performed with MF TNFR2-(S_{Δ42}/TM)_{R2}-Fas. For this purpose MF TNFR2-(S_{Δ42}/TM)_{R2}-Fas were treated with increasing concentrations of CysTNF and sTNF, respectively, and cell viability was determined using crystal violet staining. About 75 % of the cells were responsive towards CysTNF (Figure 14 A and B), which correlated with the receptor positive cell population determined by FACS analysis (Figure 13 A). The responsiveness towards CysTNF with a half-maximal effective dose (ED₅₀) of 0.3 ng/ml was comparable to that of MF TNFR2-Fas cells (ED₅₀ = 0.2 ng/ml, Figure 11 D). This indicates that CysTNF-mediated activation of this chimaera is not compromised by the deletion of the 42 aa in the TNFR2 stalk region.

In contrast to TNFR2-Fas, TNFR2-(S_{Δ42}/TM)_{R2}-Fas was activated by sTNF, although the responsiveness towards sTNF was somewhat reduced (ED₅₀ = 3 ng/ml) compared to the one seen for CysTNF (ED₅₀ = 0.3 ng/ml). This, together with the data from the TNFR1-(S_{Δ42}/TM)_{R2}-Fas chimaera, shows that the inhibitory effect of the TNFR2 stalk region on sTNF responsiveness can be overcome when this stalk region is shortened by 42 aa residues (see Figure 11 C and Figure 14 C). Therefore, one or more feature(s) that is (are) encoded by these 42 aa appears to inhibit sTNF responsiveness of TNFR2.

Interestingly, only about 50 % of the cells were responsive to saturating concentrations of sTNF (Figure 14 A and B), suggesting that a subpopulation of the cells was resistant to sTNF. When cells were treated with 100 ng/ml sTNF for 8 h and the surviving cells were challenged again after 2 days of cultivation, no difference in receptor cell surface expression (Figure 15 A and C) and responsiveness to TNF (Figure 15 B and D) between pretreated and non-pretreated cells could be detected. Therefore, we could exclude the possibility that during the selection process of this cell line an sTNF-resistant sub-population had been generated. Our observations rather suggest that an unknown intrinsic mechanism leads to a certain percentage of sTNF-unresponsive cells. However, this mechanism has not been further investigated in this project and remains as future work.

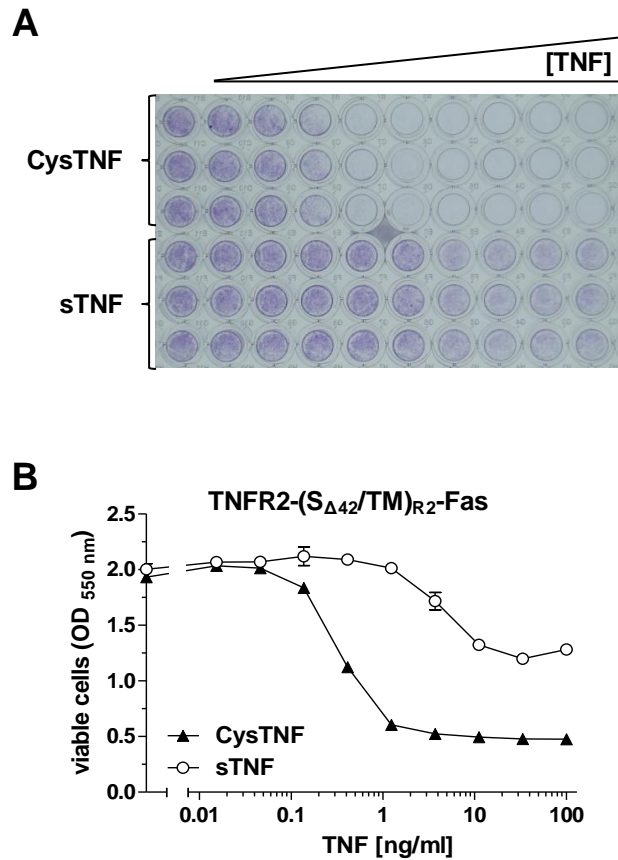


Figure 14. MF TNFR2-(S_{Δ42}/TM)_{R2}-Fas are responsive to sTNF.

MF stably transfected with TNFR2-(S_{Δ42}/TM)_{R2}-Fas remained untreated or were stimulated with increasing concentrations of sTNF and CysTNF (0.015-100 ng/ml) for 8 h. Adherent cells were stained using crystal violet solution. **A)** Photograph of a 96-well plate after crystal violet staining; **B)** Corresponding absorbances at 550 nm were determined for quantitative analysis of cell viability. Data shown represent five independent experiments.

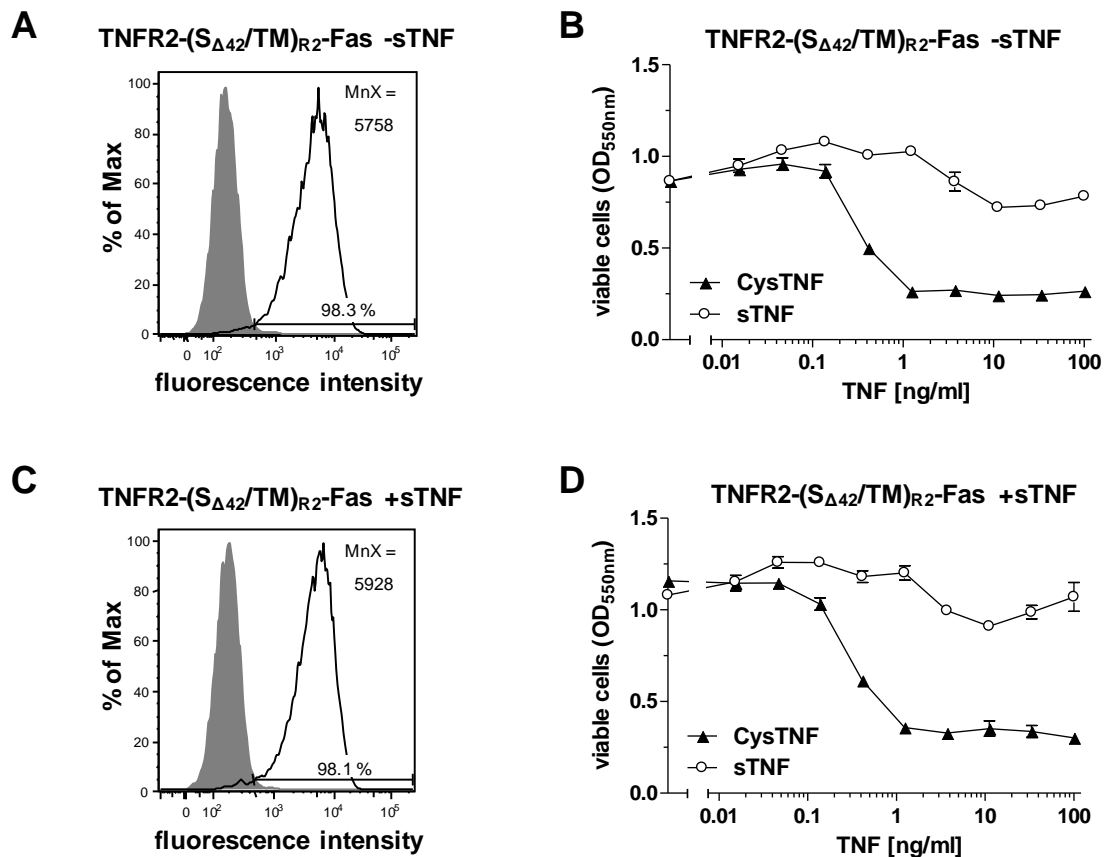


Figure 15. Partial responsiveness of MF TNFR2-(S Δ 42/TM)_{R2}-Fas to sTNF is an intrinsically regulated phenomenon.

MF stably transfected with TNFR2-(S Δ 42/TM)_{R2}-Fas were **A and B**) left untreated or **C and D**) pre-selected with sTNF. Cells were analysed 48 h post pre-selection. **A and C**) FACS analysis; chimaeras were stained on the cell surface using mouse anti-human TNFR2 antibodies (clone MR2-1) and goat anti-mouse IgG-FITC antibodies (black line). Cells only incubated with goat anti-mouse IgG-FITC antibodies are depicted in grey. 98 % of the MF were gated positive for TNFR2-(S Δ 42/TM)_{R2}-Fas. Acquisition was performed on a Becton Dickinson FACSCanto II flow cytometer. **B and D**) Cell viability assay; cells remained unstimulated or were stimulated with increasing concentrations of sTNF and CysTNF (0.015-100 ng/ml), respectively, and viable cells were stained using crystal violet. Data shown represent three independent experiments.

3.3 Influence of the stalk region on sTNF-mediated TNFR2 complex formation

Data obtained from the MF TNFR-Fas cell system suggest an important role for the TNFR stalk regions in the control of receptor responsiveness to sTNF (see sections 3.1 and 3.2). However, while the use of this cell system allowed us to assess TNFR-Fas activation in an easy and reproducible manner, the question remained how these data would apply to wild type receptors. Therefore, the aim was to investigate whether an inhibitory effect of the stalk region could also be observed when TNFR2 wild type constructs were used instead of TNFR-Fas chimaeras. Unfortunately, to date the downstream signalling of TNFR2 in MF is not very well understood and data on TNFR2-mediated IL-6 production, I κ B α degradation, p65 phosphorylation and real-time PCR analysis for potential NF- κ B downstream target genes, which had been generated in our group, were inconclusive (Dr Anja Krippner-Heidenreich, personal communication).

Furthermore, I wanted to investigate whether the TNFR stalk region would also control differential responsiveness when different cell types were used. This was of particular importance as we used mouse cells to investigate signalling of human receptors and, despite the high homology between murine and human TNFR, processes in receptor activation might differ between species.

3.3.1 The TNFR2 stalk region inhibits sTNF-mediated TRAF2 recruitment

TRAF2 recruitment to the TNF/TNFR2 signalling complex occurs as an early event during TNFR2 activation. The TNF-mediated recruitment of TRAF2 to TNFR2 and the subsequent poly-ubiquitination of TRAF2 have already been described for HeLa cells stably transfected with TNFR2 (Krippner-Heidenreich *et al.*, 2002, Habelhah *et al.*, 2004). These interactions are required for the activation of both, the NF- κ B and JNK signalling pathways (Rothe *et al.*, 1995, Reinhard *et al.*, 1997). Furthermore, in agreement with observations made in the MF TNFR-Fas system, sTNF-induced recruitment of TRAF2 to wild type TNFR2 was found to be markedly reduced compared to recruitment upon stimulation with a TNFR2-selective CysTNF variant (Krippner-Heidenreich *et al.*, 2002). Therefore, HeLa cells stably transfected with expression constructs of TNFR2 variants, which contained different stalk and/or

transmembrane regions and the intracellular portion of wild type TNFR2, represented a system to investigate the role of the stalk region in differential sTNF responsiveness of wild type TNFR2.

HeLa cells stably transfected with wild type TNFR2 have been generated previously by Regina Pfeiffer (University of Stuttgart, Germany). HeLa transfectants stably expressing the mutants TNFR2-(S/TM)_{R1}-R2 and TNFR2-(S_{Δ42}/TM)_{R2}-R2, respectively, have been generated. These TNFR2 constructs contain either the stalk and transmembrane regions (aa 197-236) of TNFR1 (TNFR2-(S/TM)_{R1}-R2) or the TNFR2 stalk region shortened by 42 aa residues (aa 244-257; TNFR2-(S_{Δ42}/TM)_{R2}-R2). TNFR2 and variants thereof were expressed on the cell surface (Figure 16) with a comparable MnX (MnX = 7816 for TNFR2, MnX = 9037 for TNFR2-(S/TM)_{R1}-R2 and MnX = 5843 for TNFR2-(S_{Δ42}/TM)_{R2}-R2). All three cell lines showed homogenous cell populations which could be gated positive for the respective TNFR2 variants (94 % for TNFR2 (Figure 16 A), 98 % for TNFR2-(S/TM)_{R1}-R2 (Figure 16 B) and 88 % for TNFR2-(S_{Δ42}/TM)_{R2}-R2 (Figure 16 C)).

In addition the correct molecular size of the TNFR2 variants was confirmed via Western Blot analysis using whole cell lysates from both transiently and stably transfected HeLa cells (Figure 16 D). The predicted molecular weight for wild type TNFR2 is 48 kDa, whereas TNFR2-(S/TM)_{R1}-R2 and TNFR2-(S_{Δ42}/TM)_{R2}-R2 are predicted to be approximately 44 kDa in size (determined using the ProtParam tool on the ExPaSy proteomics server)(Gasteiger *et al.*, 2005). For all constructs two bands in the range of the predicted molecular weight could be observed in the Western Blot (approximately 70 kDa and 50 kDa for TNFR2 and approximately 50 kDa and 48 kDa for TNFR2-(S/TM)_{R1}-R2 and TNFR2-(S_{Δ42}/TM)_{R2}-R2 (Figure 16 D)). Similar to the TNFR-Fas constructs analysed in results section 3.2, the faster migrating protein bands are likely to represent receptors which had been translated but not post-translationally modified yet, whereas the slower migrating bands probably represent the mature forms of the receptors.

To ensure that any differences in TRAF2 recruitment of the three HeLa cell lines, HeLa TNFR2, HeLa TNFR2-(S/TM)_{R1}-R2 and HeLa TNFR2-(S_{Δ42}/TM)_{R2}-R2, would not be due to differences in the levels of endogenous TRAF2, TRAF2 expression of the cells

was determined via Western Blotting. For this purpose whole cell lysates were prepared and subjected to SDS-PAGE and Western Blot analysis.

As seen in Figure 17, there are no apparent differences in TRAF2 levels between untransfected HeLa cells, HeLa TNFR2, HeLa TNFR2-(S/TM)_{R1}-R2 and HeLa TNFR2-(S_{Δ42}/TM)_{R2}-R2 cells. The Western Blot membrane was reprobed with antibodies against human β-actin to ensure equal loading for all samples (Figure 17, as indicated). Therefore, differences in endogenous TRAF2 levels would not account for any differences observed in TNF-mediated TRAF2 recruitment to the receptor constructs during co-IP experiments.

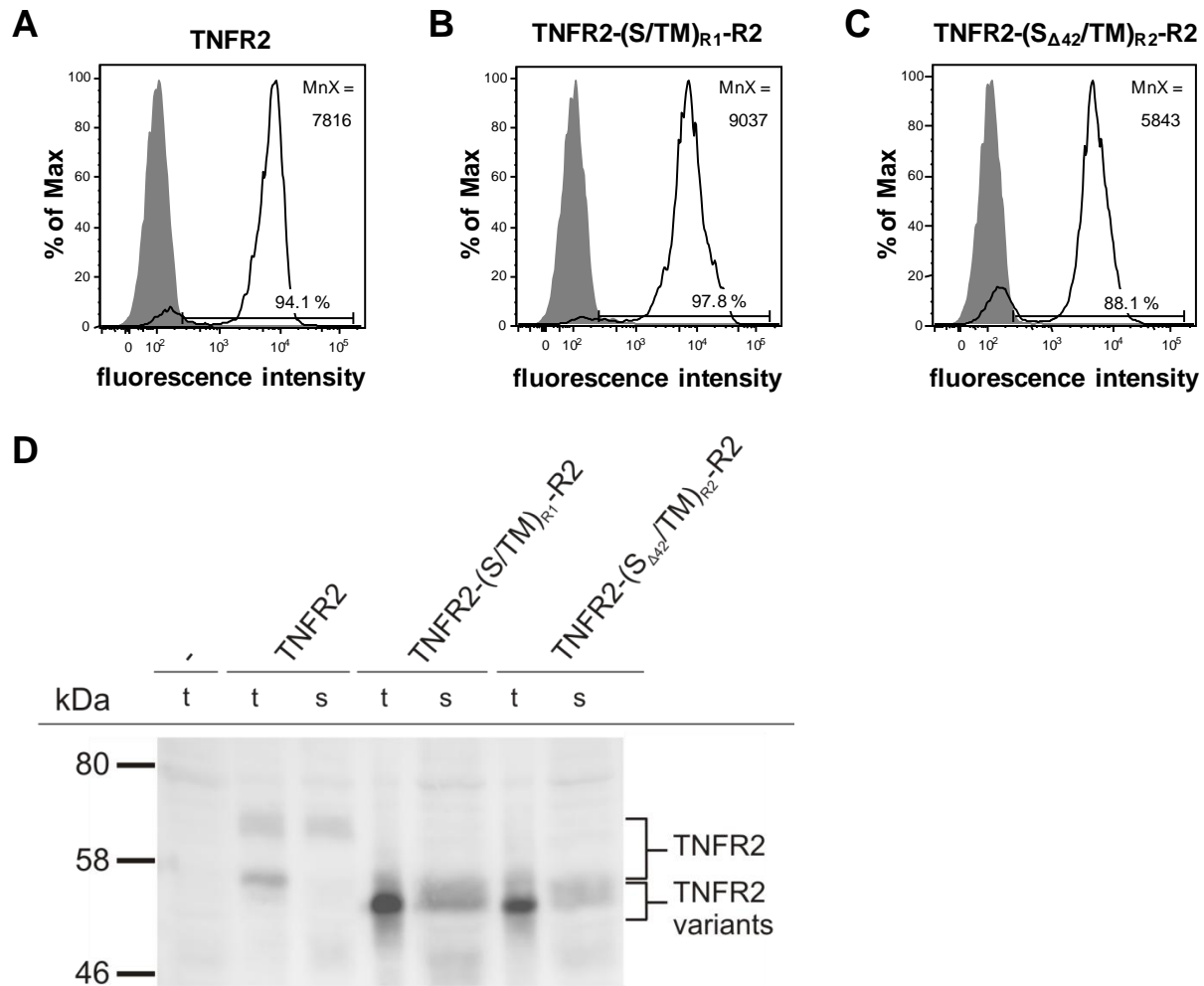


Figure 16. Characterisation of HeLa cells stably expressing TNFR2, TNFR2-(S/TM)_{R1}-R2 and TNFR2-(S_{Δ42}/TM)_{R2}-R2.

Figure 16 continued:

HeLa cells had been stably transfected with TNFR2, TNFR2-(S/TM)_{R1}-R2 and TNFR2-(S_{Δ42}/TM)_{R2}-R2, respectively. FACS analysis of **A**) TNFR2, **B**) TNFR2-(S/TM)_{R1}-R2 and **C**) TNFR2-(S_{Δ42}/TM)_{R2}-R2 is shown. Receptors were stained on the cell surface using mouse anti-human TNFR2 antibodies (clone MR2-1) and goat anti-mouse IgG-FITC antibodies (black line). Cells only incubated with goat anti-mouse IgG-FITC antibodies are depicted in grey. 94 %, 98 % and 88 % of the cells were gated positive for TNFR2, TNFR2-(S/TM)_{R1}-R2 and TNFR2-(S_{Δ42}/TM)_{R2}-R2, respectively. Data shown represent three independent experiments. **D**) Western Blot analysis of TNFR2 variants. Whole cell lysates were prepared from 6×10^4 stably transfected cells (s) and subjected to SDS-PAGE and Western Blot analysis. Untransfected HeLa cells (-) served as control. Lysates from 4×10^4 HeLa cells, which had been transiently transfected with indicated TNFR2 variants (t) served as positive control. Goat anti-human TNFR2 antibodies (1:2000) were used as primary and rabbit anti-goat-IgG-HRP (1:20000) as secondary antibodies. Acquisition was performed on a Becton Dickinson FACSCanto II flow cytometer. Data shown represent one experiment.

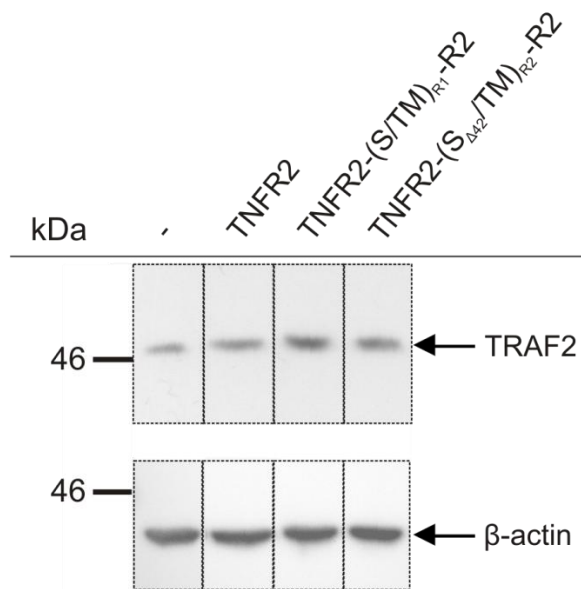


Figure 17. Endogenous TRAF2 levels in HeLa cells expressing different TNFR2 variants.

HeLa cells had been stably transfected with TNFR2, TNFR2-(S/TM)_{R1}-R2 and TNFR2-(S_{Δ42}/TM)_{R2}-R2, respectively and Western Blot analysis of endogenous TRAF2 was performed. An equivalent of 4×10^4 cells was used. Untransfected HeLa cells (-) served as control. TRAF2 was detected using mouse anti-human TRAF2 antibodies (1:2000) as primary and goat anti-mouse-IgG-HRP (1:20000) as secondary antibodies (top). Human beta-actin (bottom) served as loading control. All bands shown are from the same exposure. Data shown represent one experiment.

To investigate the potential of sTNF to recruit TRAF2 to TNFR2, TNFR2-(S/TM)_{R1}-R2 and TNFR2-(S_{Δ42}/TM)_{R2}-R2, HeLa cells stably expressing these constructs were stimulated with sTNF and CysTNF, respectively, and TRAF2 recruitment at different time points was analysed by TNFR2/TRAF2 co-IP.

When CysTNF was used, TRAF2 recruitment to TNFR2, TNFR2-(S/TM)_{R1}-R2 and TNFR2-(S_{Δ42}/TM)_{R2}-R2 could already be observed 5 min past stimulation (Figure 18 A, bottom). The TRAF2 signal persisted 10 min and 15 min after stimulation, but a trend towards a decrease in signal strength could be observed (Figure 18 A, bottom, and Figure 19).

In line with observations made by Krippner-Heidenreich *et al.* (2002), stimulation with sTNF led to a markedly reduced TRAF2 recruitment in HeLa TNFR2 cells. For HeLa TNFR2, after 5 min and 10 min (Figure 18 A, bottom) of sTNF stimulation approximately 70 % less TRAF2 were recruited compared to the amount recruited upon 5 min of stimulation with CysTNF (Figure 19). For the chosen timepoints, sTNF-mediated TRAF2 recruitment to TNFR2 was maximal at 15 min post stimulation but did not exceed 50 % of the recruitment seen after stimulation with CysTNF for 5 min (Figure 19).

In contrast, the stimulation of HeLa TNFR2-(S/TM)_{R1}-R2 and HeLa TNFR2-(S_{Δ42}/TM)_{R2}-R2 with sTNF resulted in an increased TRAF2 recruitment for all three time points when compared to sTNF-treated HeLa TNFR2 (Figure 18 A, bottom). While after 5 min only approximately 25 % of TRAF2 were recruited in HeLa TNFR2, a recruitment of approximately 44 % and 63 % could be observed for HeLa TNFR2-(S/TM)_{R1}-R2 and HeLa TNFR2-(S_{Δ42}/TM)_{R2}-R2, respectively (Figure 19). After 10 min, 56 % of TRAF2 were recruited to TNFR2-(S/TM)_{R1}-R2 and 61 % to TNFR2-(S_{Δ42}/TM)_{R2}-R2 opposed to 27 % of TRAF2 that were recruited to TNFR2 (Figure 19). When a Mann-Whitney U-test was performed, the differences between the TRAF2 recruitment to TNFR2 and TNFR2-(S_{Δ42}/TM)_{R2}-R2 upon 5 min and 10 min of sTNF stimulation were found to be statistically significant ($p = 0.0286$). The highest values for sTNF-induced TRAF2 recruitment were observed 15 min post stimulation (41 % for HeLa TNFR2, 65 % for HeLa TNFR2-(S/TM)_{R1}-R2 and 74 % for HeLa TNFR2-(S_{Δ42}/TM)_{R2}-R2; Figure 19). However, while more TRAF2 was recruited to TNFR2-(S/TM)_{R1}-R2 and TNFR2-(S_{Δ42}/TM)_{R2}-R2 than to TNFR2, these differences were not statistically significant.

As the cell surface expression of mutant TNFR2 was comparable or even lower than the one observed for wild type TNFR2 (Figure 16) and basal TRAF2 recruitment to all three TNFR2 variants was comparable (5 % for TNFR2 and TNFR2-(S/TM)_{R1}-R2 and 3 % for TNFR2-(S_{Δ42}/TM)_{R2}-R2; Figure 19), the observed differences in sTNF-mediated TRAF2 recruitment were not due to higher basal activation of the receptors but were rather determined by the different stalk regions.

To exclude the possibility that different amounts of TNF/TNFR2 complexes were precipitated, the Western Blot membranes of the co-IP experiments were reprobbed with the same polyclonal TNFR2-specific antibodies which had been used to precipitate the signalling complexes. Stronger signals were detected for HeLa TNFR2-(S/TM)_{R1}-R2 cells, while the signals obtained for HeLa TNFR2-(S_{Δ42}/TM)_{R2}-R2 were so weak that they could unfortunately not be distinguished from background (Figure 18 A, top). These results correlated with the corresponding cell surface staining of the receptors (Figure 16). As the amount of detected TNFR2, TNFR2-(S/TM)_{R1}-R2 and TNFR2-(S_{Δ42}/TM)_{R2}-R2 did not correlate with the amount of co-immunoprecipitated TRAF2 (Figure 18 A), the differences seen in TRAF2 recruitment are unlikely to be a result of differences in the pull-down of the signalling complexes.

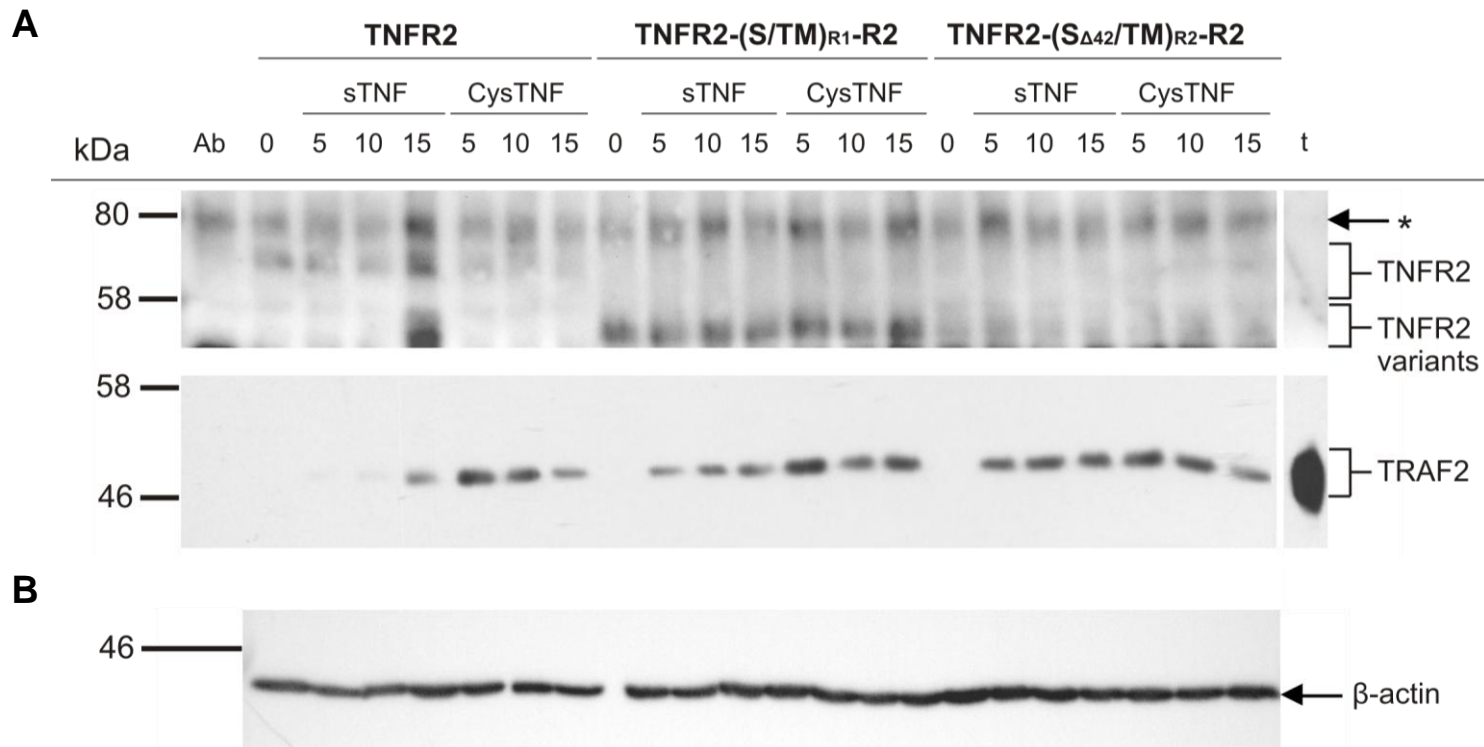


Figure 18. The TNFR2 stalk region counteracts sTNF-mediated recruitment of endogenous TRAF2 to TNFR2 in HeLa cells.

HeLa cells stably transfected with TNFR2, TNFR2-(S/TM)_{R1}-R2 and TNFR2-(S_{Δ42}/TM)_{R2}-R2, respectively, remained untreated (0) or were stimulated with 10 ng/ml sTNF or wild type CysTNF for 5, 10 and 15 min (5, 10, 15). For each treatment, TNFR signalling complexes from approximately 5 × 10⁵ HeLa cells were immunoprecipitated using 2 μg goat anti-human TNFR2 antibodies. Immunoprecipitation samples were subjected to SDS-PAGE and Western Blot analysis. **A**) TRAF2 (bottom) was detected using mouse anti-human TRAF2 antibodies (1:2000) as primary and goat anti-mouse-IgG-HRP (1:20000) as secondary antibodies. Afterwards, Western Blot membranes were reprobed with goat anti-human TNFR2 antibodies (1:2000) and rabbit anti-goat-IgG-HRP (1:20000) antibodies (top). Unspecific bands are highlighted with an asterisk. A whole cell lysate from HeLa cells transiently transfected with a human TRAF2 construct (t) served as positive control, while 2 μg goat anti-human TNFR2 antibodies (Ab) were loaded as negative control. **B**) Using mouse anti-human β-actin antibodies (1:50000) and goat anti-mouse-IgG-HRP (1:20000), immunoprecipitation supernatants were analysed for their β-actin content which served as a loading control. Data shown represent three independent experiments for TNFR2-(S/TM)_{R1}-R2 and four independent experiments for TNFR2 and TNFR2-(S_{Δ42}/TM)_{R2}-R2.

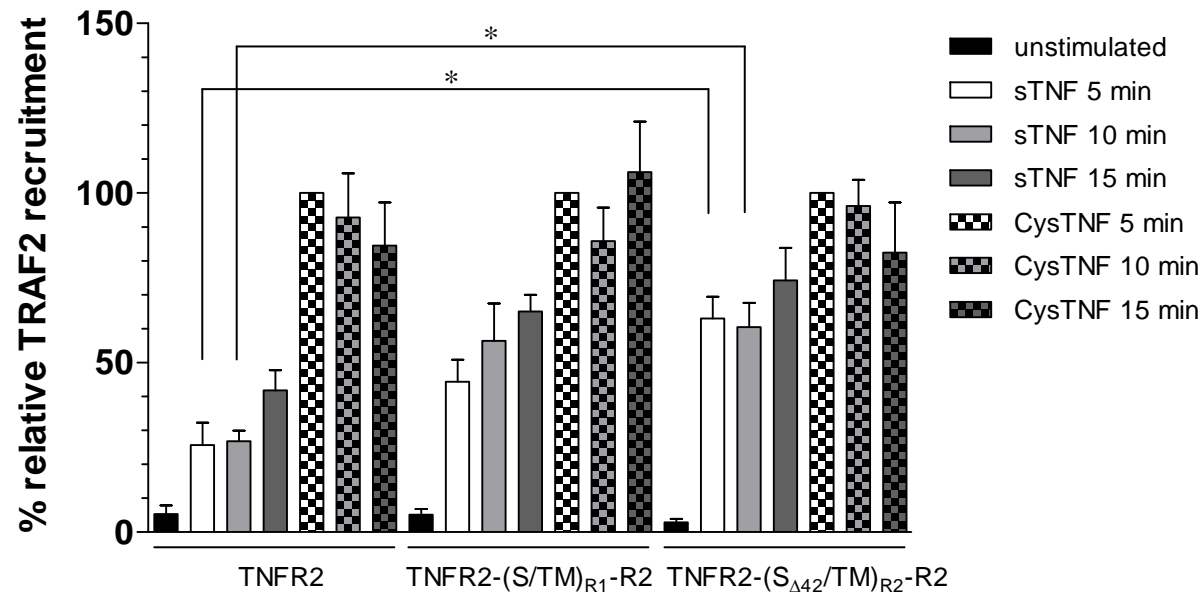


Figure 19. Quantitative analysis of TNF-mediated TRAF2 recruitment to TNFR2, TNFR2-(S/TM)_{R1}-R2 and TNFR2-(S_{Δ42}/TM)_{R2}-R2.

Band intensities of TRAF2 Western Blots from TNFR2/TRAF2 co-IP experiments depicted in Figure 18 were quantified on a Syngene G:Box using the GeneTools V4.01 analysis software. Values were corrected for background levels and normalised to endogenous β -actin. Shown is the relative TRAF2 recruitment, expressed as a percentage of the TRAF2 recruitment to the respective TNFR construct after 5 min of CysTNF stimulation. Results are expressed as mean \pm standard deviation and are representative of three (TNFR2-(S/TM)_{R1}-R2) and four (TNFR2 and TNFR2-(S_{Δ42}/TM)_{R2}-R2) independent experiments. * = $p < 0.05$

In comparison to CysTNF-mediated TRAF2 recruitment, neither TNFR2-(S/TM)_{R1}-R2 nor TNFR2-(S_{Δ42}/TM)_{R2}-R2 were fully responsive towards sTNF.

For MF TNFR2-(S/TM)_{R1}-Fas the responsiveness towards sTNF and CysTNF had been very similar (Figure 11 E). Therefore, it was somewhat surprising that TNFR2-(S/TM)_{R1}-R2 did not prove to be more potent in sTNF-mediated TRAF2 recruitment. In contrast, the partial sTNF responsiveness of TNFR2-(S_{Δ42}/TM)_{R2}-R2 reflected the partial sTNF responsiveness that had been observed for TNFR2-(S_{Δ42}/TM)_{R2}-Fas chimaeras previously very well (section 3.2).

In conclusion, a significant increase in sTNF-mediated TRAF2 recruitment could be observed for TNFR2 constructs in which the stalk region had been shortened by 42 aa residues. For TNFR2 in which the stalk and transmembrane regions had been replaced with the ones of TNFR1 also a trend towards an increased sTNF-mediated TRAF2 recruitment could be observed. However, further experiments would be required to assess whether this increase is statistically significant.

Our findings indicate that the TNFR stalk regions do not only determine sTNF responsiveness of TNFR-Fas chimaeras but also control sTNF responsiveness of wild type TNFR2. Furthermore, our data provide evidence that sTNF responsiveness of wild type TNFR2 is also inhibited by 42 aa in the TNFR2 stalk region.

3.3.2 Suitability of soluble and oligomerised TNFR2-selective TNF to study differential responsiveness of TNFR

Expression of endogenous TNFR2 is observed in only a few cell types and occurs upon cellular activation. In contrast, most cell types commonly show a basal expression of TNFR1. When these cells are expressing exogenous TNFR2, any TNF-mediated response will potentially reflect the crosstalk between TNFR1 and TNFR2. Therefore, we wanted to assess whether TNFR1 signalling was in any way contributing to the differences we had been observing for sTNF-mediated TRAF2 recruitment to TNFR2, TNFR2-(S/TM)_{R1}-R2 and TNFR2-(S_{Δ42}/TM)_{R2}-R2 (Figure 18 and Figure 19). For this purpose it was required to establish a system in which TNFR2-mediated signalling could be investigated without simultaneous activation of TNFR1.

Rauert *et al.* (2010) developed a soluble and an oligomerised TNF variant, which were TNFR2-selective due to the introduction of two point mutations (Loetscher *et al.*, 1993). Rauert *et al.* found wild type TNFR2 to be only activated upon stimulation with the oligomerised but not the soluble TNFR2-selective TNF variant. Therefore, these muteins represented ligands which were potentially suitable to compare responsiveness of TNFR2 to sTNF and membrane-bound TNF in cell lines other than MF, while avoiding potential simultaneous sTNF-mediated TNFR1 signalling. Both, the soluble (FLAG-sTNF(143N/145R)) and the oligomerised (FLAG-TNC-scTNF(143N/145R)) TNFR2-selective ligands described in Rauert *et al.* (2010) were kindly provided by Prof. Harald Wajant (Würzburg University, Germany).

To determine the suitability of FLAG-sTNF(143N/145R) and FLAG-TNC-scTNF(143N/145R) for investigating responsiveness of TNFR2 variants towards sTNF and membrane-bound TNF in a TNFR2-selective manner, we stimulated MF TNFR2-(S/TM)_{R1}-Fas and MF TNFR2-(S_{Δ42}/TM)_{R2}-Fas with these ligands. The cell lines were chosen as they both show responsiveness towards sTNF and CysTNF (Figure 11 and Figure 14). When MF TNFR2-(S/TM)_{R1}-Fas (Figure 20 A) and MF TNFR2-(S_{Δ42}/TM)_{R2}-Fas (Figure 20 B) were treated with the aforementioned ligands, the responsiveness towards CysTNF and FLAG-TNC-scTNF(143N/145R) was comparable in these cell lines (ED₅₀ = 0.5-0.7 ng/ml for FLAG-TNC-scTNF(143N/145R) and ED₅₀ = 0.9 ng/ml for wild type CysTNF). In contrast, neither MF TNFR2-(S/TM)_{R1}-Fas nor

MF TNFR2-(S_{Δ42}/TM)_{R2}-Fas were activated by the soluble variant of TNFR2-specific TNF, FLAG-sTNF(143N/145R), up to a concentration of 200 ng/ml (Figure 20 A and B).

It has been described previously that the introduction of the D143N/A145R mutations in TNF leads to a 100-fold reduced affinity to TNFR2 (Loetscher *et al.*, 1993). Furthermore, Krippner-Heidenreich *et al.* (2002) showed that the responsiveness of TNFR2-Fas towards a CysTNF variant carrying these mutations is 100-fold reduced (ED₅₀ = 30 ng/ml) compared to CysTNF (ED₅₀ = 0.2 ng/ml; Figure 11 D).

If the introduction of the D143N/A145R mutations in FLAG-sTNF(143N/145R) would similarly lead to a 100-fold reduction in activity compared to sTNF, we would, however, expect to see half-maximal responsiveness of MF TNFR2-(S/TM)_{R1}-Fas (ED₅₀ = 0.4 ng/ml for sTNF; Figure 11 E) and MF TNFR2-(S_{Δ42}/TM)_{R2}-Fas (ED₅₀ = 3 ng/ml for sTNF; Figure 14 B) at 40 ng/ml and 300 ng/ml, respectively.

To ensure that the observed lack of responsiveness to FLAG-sTNF(143N/145R) is not caused by a lack of bioactivity of the ligand, cells were pre-incubated with 1 μg/ml of the monoclonal TNFR2 antibody 80M2, which has been described to stabilise ligand binding by prolonging the half-life of the TNF-TNFR2-complex (Grell *et al.*, 1995). With the help of this antibody, the responsiveness of MF TNFR2-Fas towards a TNFR2-selective CysTNF variant can be increased up to levels comparable to wild type CysTNF (Dr. Anja Krippner-Heidenreich, personal communication). When MF TNFR2-(S_{Δ42}/TM)_{R2}-Fas were stimulated with sTNF in combination with the TNFR2 antibody 80M2 (ED₅₀ = 4 ng/ml), responsiveness was almost comparable to CysTNF (ED₅₀ = 1 ng/ml; Figure 20 C). In contrast, for FLAG-sTNF(143N/145R) in combination with the TNFR2 antibody 80M2 only very few apoptotic cells could be observed under the microscope even at concentrations of 300 ng/ml (Figure 20 C). Unfortunately, the observed effect was so marginal that it could not be depicted using crystal violet staining.

Taken together, this indicates that FLAG-sTNF(143N/145R), despite showing bioactivity to some extent, is not a suitable ligand to investigate differential sTNF responsiveness of TNFR2. Other means, such as the use of small interfering RNA (siRNA), were required to eliminate TNFR1 crosstalk (section 3.3.3).

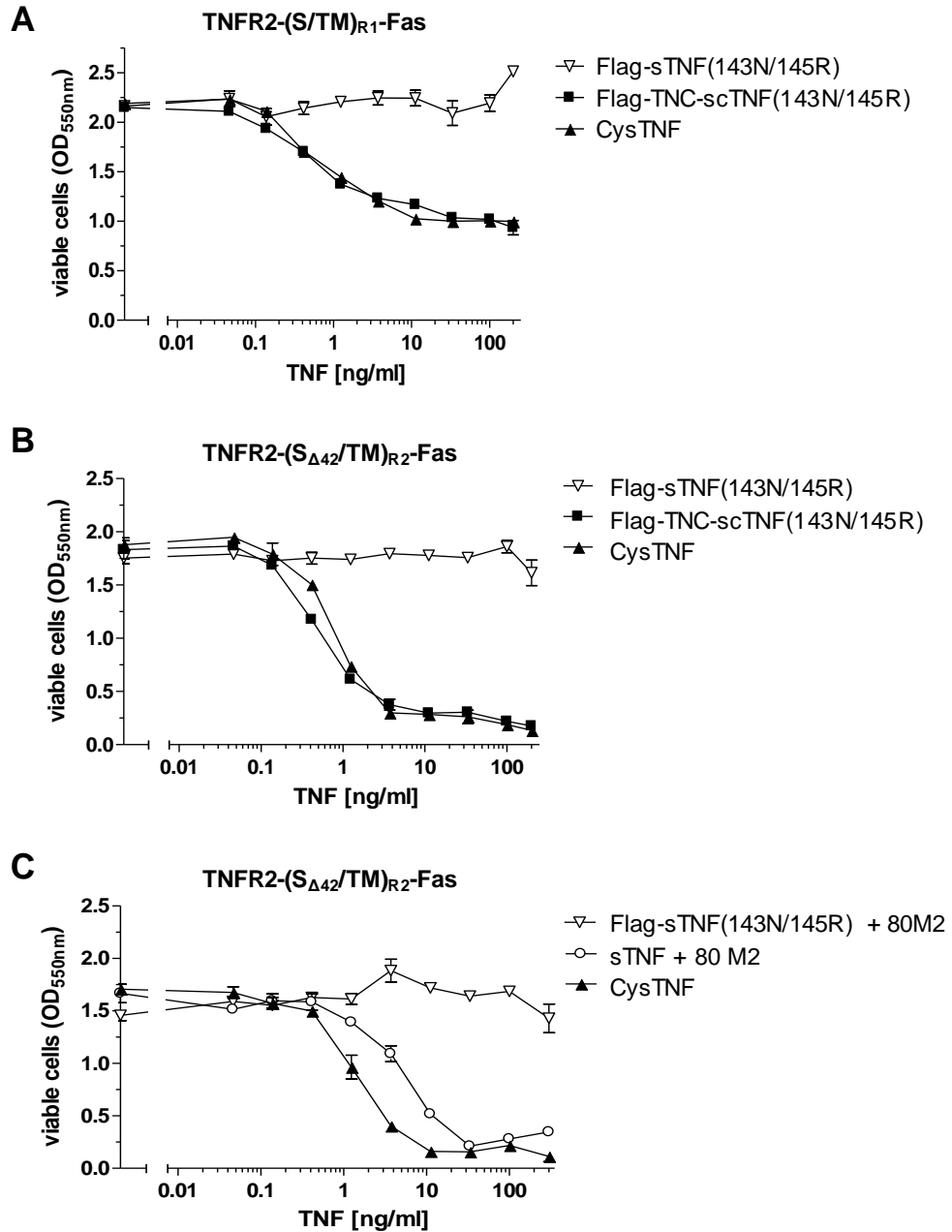


Figure 20. Evaluation of the activity of the TNFR2-selective ligands FLAG-sTNF(143N/145R) and FLAG-TNC-scTNF(143N/145R)

MF were stimulated with increasing concentrations of soluble TNFR2-selective TNF (FLAG-sTNF(143N/145R)), oligomerised TNFR2-specific TNF (FLAG-TNC-scTNF(143N/145R)), CysTNF and sTNF, respectively. Cell viability was assessed using crystal violet staining. Results are expressed as mean values of duplicates. Responsiveness of **A**) MF TNFR2-(S/TM)_{R1}-Fas and **B**) MF TNFR2-(S_{Δ42}/TM)_{R2}-Fas to 0.03-200 ng/ml of FLAG-sTNF(143N/145R), FLAG-TNC-scTNF(143N/145R) and CysTNF was determined. **C**) Shown is the responsiveness of MF TNFR2-(S_{Δ42}/TM)_{R2}-Fas to 0.09-300 ng/ml of CysTNF, FLAG-sTNF(143N/145R) and sTNF, respectively. FLAG-sTNF(143N/145R) and sTNF-treated cells had been pre-incubated with 1 μg/ml of the stabilising TNFR2 antibody 80M2 for 30 min prior to stimulation. Data shown represent A and C) one experiment and B) two independent experiments.

3.3.3 TNFR1 activation does not affect TNF-mediated TRAF2 recruitment to TNFR2

The TRAF2 experiments described in section 3.3.1 were performed with HeLa cells stably expressing TNFR2 and TNFR2 stalk mutants, respectively. These cells also expressed endogenous TNFR1, which was also stimulated by sTNF and CysTNF in these experiments. Therefore, to assess whether sTNF-mediated recruitment of TRAF2 to the receptor was affected by TNFR1 crosstalk, the co-IP experiments were repeated with HeLa cells which had been treated with TNFR1-specific siRNA (siRNA_{TNFR1}) prior to stimulation.

As a first step, the amount of siRNA and incubation time required for an efficient downregulation of TNFR1 cell surface expression had to be determined. Experiments with HeLa cells overexpressing a non-cytotoxic TNFR1 variant, which had been performed in our group previously, indicated that a treatment with 50 nM siRNA_{TNFR1} for 48 h could reduce cell surface expression of this variant by about 50 % (determined as part of the Master of Research project of Rosanna Keegan, Newcastle University, 2008). As in this PhD project HeLa cells were used which only expressed low levels of endogenous TNFR1, 50 nM siRNA_{TNFR1} as well as a lower siRNA_{TNFR1} concentration (25 nM) and two different incubation times (24 h and 48 h) were tested. Non-specific siRNA (further referred to as siRNA_{nonsense}) served as a control.

After 24 h of treatment 78 % of HeLa TNFR2 cells treated with 25 nM siRNA_{TNFR1} and 75 % of cells treated with 50 nM siRNA_{TNFR1} were gated positive for TNFR1 (Figure 21 C and D), while the corresponding percentages for the untreated cells and the cells treated with siRNA_{nonsense} were 91 % and 94 %, respectively (Figure 21 A and B). After 48 h of treatment with both, 25 nM and 50 nM siRNA_{TNFR1}, the percentage of cells gated positive for TNFR1 cell surface expression was reduced even further (36 %; Figure 21 G and H) compared to the untreated and siRNA_{nonsense} treated cells (approximately 93 %; Figure 21 F and G).

In comparison with untreated cells and cells treated with siRNA_{nonsense} (MnX = 952-1204; Figure 21 A, B, E and F), for the cells treated with 25 nM and 50 nM siRNA_{TNFR1} a decrease in MnX could be observed after 24 h (MnX = 782-810; Figure 21 C and D), which was even stronger after 48 h (MnX = 530-570; Figure 21 G and H).

In conclusion, a reduction up to 58 % in the number of TNFR1 positive cells as well as a decrease in overall TNFR1 cell surface expression could be observed when cells were treated with 50 nM siRNA_{TNFR1} for 48 h. However, as treatment with 25 nM siRNA_{TNFR1} gave similarly good results, treatment of the cells with this lower siRNA concentration was chosen for the following co-IP experiments to minimise potential off-target effects of the siRNA.

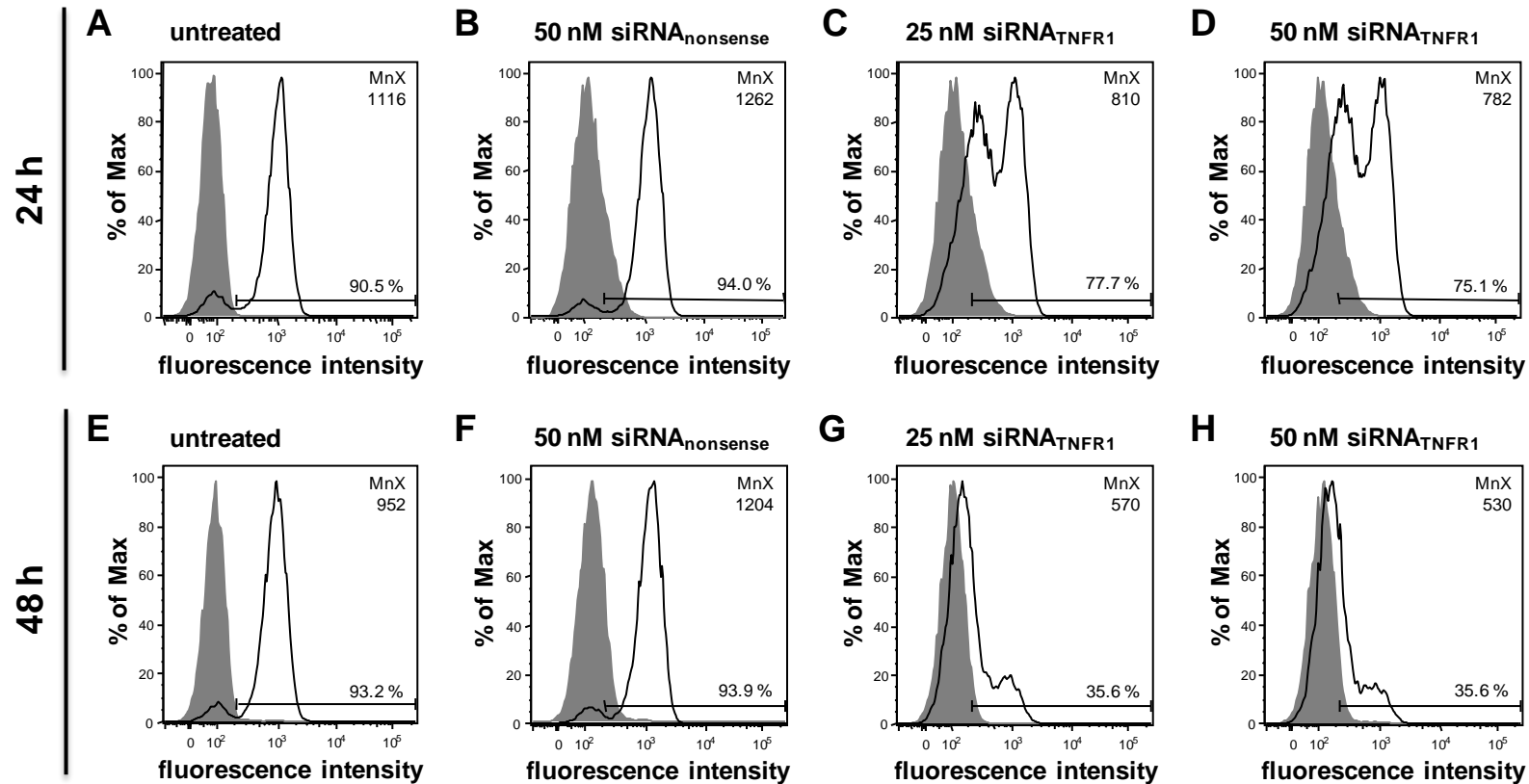


Figure 21. Optimisation for the reduction of TNFR1 cell surface expression by RNA interference.

HeLa TNFR2 cells were analysed for cell surface expression of endogenous TNFR1 after treatment with TNFR1-specific siRNA (siRNA_{TNFR1}) and non-specific siRNA (siRNA_{nonsense}). Shown are FACS analyses of HeLa TNFR2 cells which had been left untreated for **A)** 24 h and **F)** 48 h; treated with 50 nM siRNA_{nonsense} for **B)** 24 h and **F)** 48 h; treated with 25 nM siRNA_{TNFR1} for **C)** 24 h and **D)** 48 h; treated with 50 nM siRNA_{TNFR1} for **G)** 24 h and **H)** 48 h, respectively. TNFR1 was stained on the cell surface using mouse anti-human TNFR1 antibody clone H398, biotin rat anti-mouse IgG (H+L) and PE-conjugated streptavidin (black line) Cells were analysed on a Becton Dickinson FACSCanto II flow cytometer. Cells only incubated with biotin rat anti-mouse IgG (H+L) and PE-conjugated streptavidin (grey). Percentages of cells gated positive for TNFR1 and MnX are indicated. Data shown represent one experiment.

After the conditions for an efficient reduction of TNFR1 cell surface expression by RNA interference had been established, the co-IP experiments described in section 3.3.1 were repeated with HeLa TNFR2 and HeLa TNFR2-(S_{Δ42}/TM)_{R2}-R2 cells, which had both been treated with siRNA_{TNFR1}. HeLa TNFR2-(S_{Δ42}/TM)_{R2}-R2 were chosen here because they had shown a more pronounced increase in sTNF-mediated TRAF2 recruitment than HeLa TNFR2-(S/TM)_{R1}-R2 cells (Figure 18 and Figure 19). Cells treated with siRNA_{nonsense} served as negative control.

For each of these co-IP experiments FACS analysis of the cells was performed in parallel to ensure that the siRNA_{TNFR1} treatment led to reduced TNFR1 expression while the cell surface expression of the respective TNFR2 construct remained unaffected.

Cell surface expression of TNFR2 and TNFR2-(S_{Δ42}/TM)_{R2}-R2 was assessed for cells which had been left untreated, treated with siRNA_{nonsense} or treated with siRNA_{TNFR1}. The number of cells gated positive for TNFR2 and TNFR2-(S_{Δ42}/TM)_{R2}-R2, respectively, was comparable between all treatment groups (91-93 % for TNFR2, Figure 22 A, B and C; 86-88 % for TNFR2-(S_{Δ42}/TM)_{R2}-R2, Figure 22 D, E and F). Furthermore, between untreated and siRNA_{TNFR1} treated HeLa TNFR2 cells no drastic changes in TNFR2 cell surface expression could be detected (MnX = 2528-2637; Figure 22 A and C). The cell surface expression of TNFR2 was slightly reduced when these cells were treated with siRNA_{nonsense} (MnX = 1983, Figure 22 B). For TNFR2-(S_{Δ42}/TM)_{R2}-R2 the cell surface expression in untreated cells (MnX = 2921, Figure 22 D) was higher compared to the treated cells but was comparable between siRNA_{nonsense} treated and siRNA_{TNFR1} treated cells (MnX = 2229-2433; Figure 22 D and E).

In addition, the cell surface expression of endogenously expressed TNFR1 was assessed. The MnX for TNFR1 was almost identical in untreated and siRNA_{nonsense} treated HeLa TNFR2 cells (MnX = 912 versus MnX = 922; Figure 23 A and B, respectively) and HeLa TNFR2-(S_{Δ42}/TM)_{R2}-R2 cells (MnX = 1011 versus MnX = 993; Figure 23 D and E, respectively). In contrast, the TNFR1 cell surface expression was markedly reduced in siRNA_{TNFR1} treated HeLa TNFR2 cells (MnX = 430, Figure 23 C) and HeLa TNFR2-(S_{Δ42}/TM)_{R2}-R2 cells (MnX = 451, Figure 23 F).

While 97 % of untreated and 95 % of siRNA_{nonsense} treated HeLa TNFR2 cells and HeLa TNFR2-(S_{Δ42}/TM)_{R2}-R2 cells were positive for TNFR1, respectively, only 44 % of siRNA_{TNFR1} treated HeLa TNFR2 cells and 39 % of siRNA_{TNFR1} treated HeLa TNFR2-(S_{Δ42}/TM)_{R2}-R2 cells were gated positive for TNFR1 (Figure 23).

In conclusion, treatment of HeLa cells with TNFR1-specific siRNA did not alter the cell surface expression of TNFR2 and TNFR2-(S_{Δ42}/TM)_{R2}-R2 (Figure 22) but efficiently reduced TNFR1 cell surface expression by more than 50 % (Figure 23).

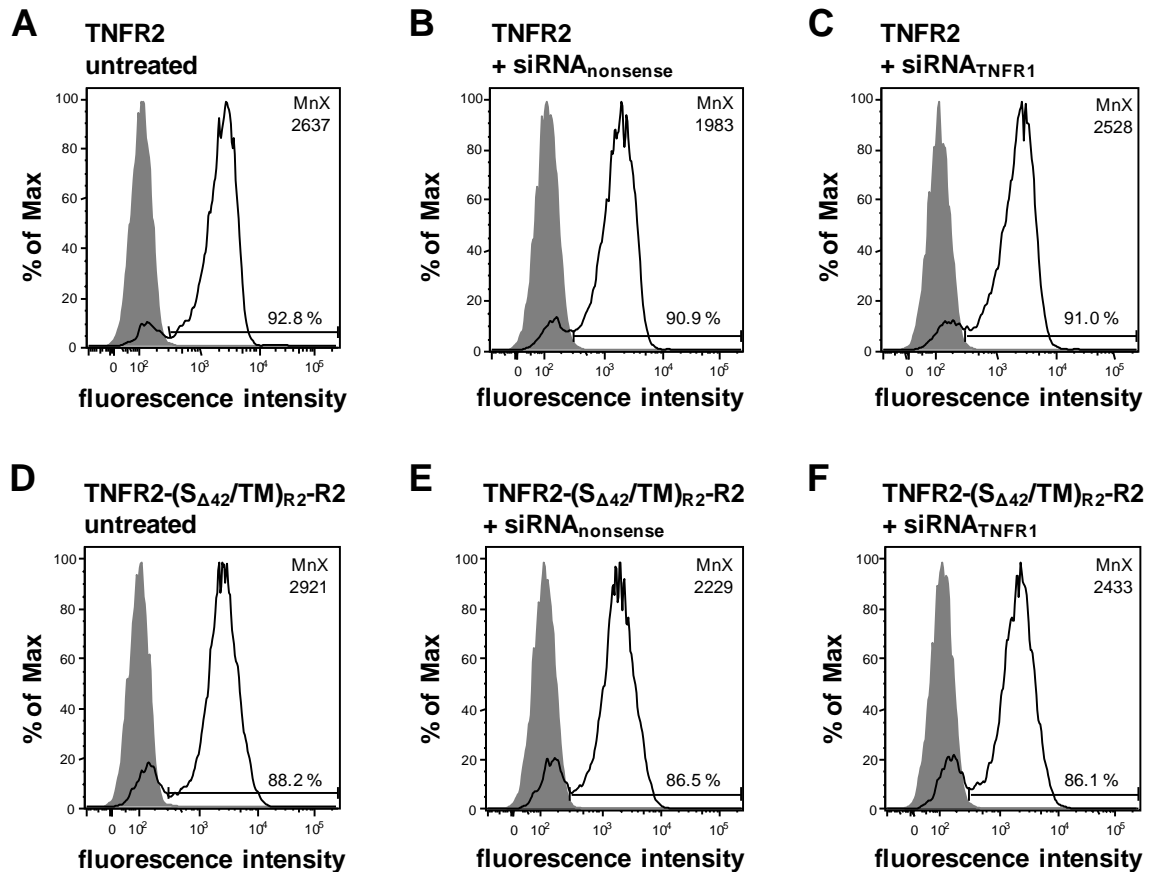


Figure 22. Reduction of TNFR1 levels by RNA interference does not alter TNFR2 cell surface expression of HeLa cells.

Cell surface expression of TNFR2 and TNFR2-(S_{Δ42}/TM)_{R2}-R2 stably expressed by HeLa cells. FACS analysis of **A)** untreated HeLa TNFR2 cells; **B)** untreated HeLa TNFR2-(S_{Δ42}/TM)_{R2}-R2 cells. FACS analysis of **C)** HeLa TNFR2 cells and **D)** HeLa TNFR2-(S_{Δ42}/TM)_{R2}-R2 cells, which had been treated with 25 nM siRNA_{nonsense} for 48 h. FACS analysis of **E)** HeLa TNFR2 cells and **F)** HeLa TNFR2-(S_{Δ42}/TM)_{R2}-R2 cells, which had been treated with 25 nM siRNA_{TNFR1} for 48 h. TNFR2 variants were stained on the cell surface using mouse anti-human TNFR2 antibody clone MR2-1 and FITC-conjugated goat anti-mouse IgG + IgM (H+L) antibody (black line). Cells only incubated with FITC-conjugated goat anti-mouse IgG + IgM (H+L) antibody (grey). Acquisition was performed on a Becton Dickinson FACSCanto II flow cytometer. Percentages of cells gated positive for TNFR2 and MnX are indicated. Data shown represent three independent experiments.

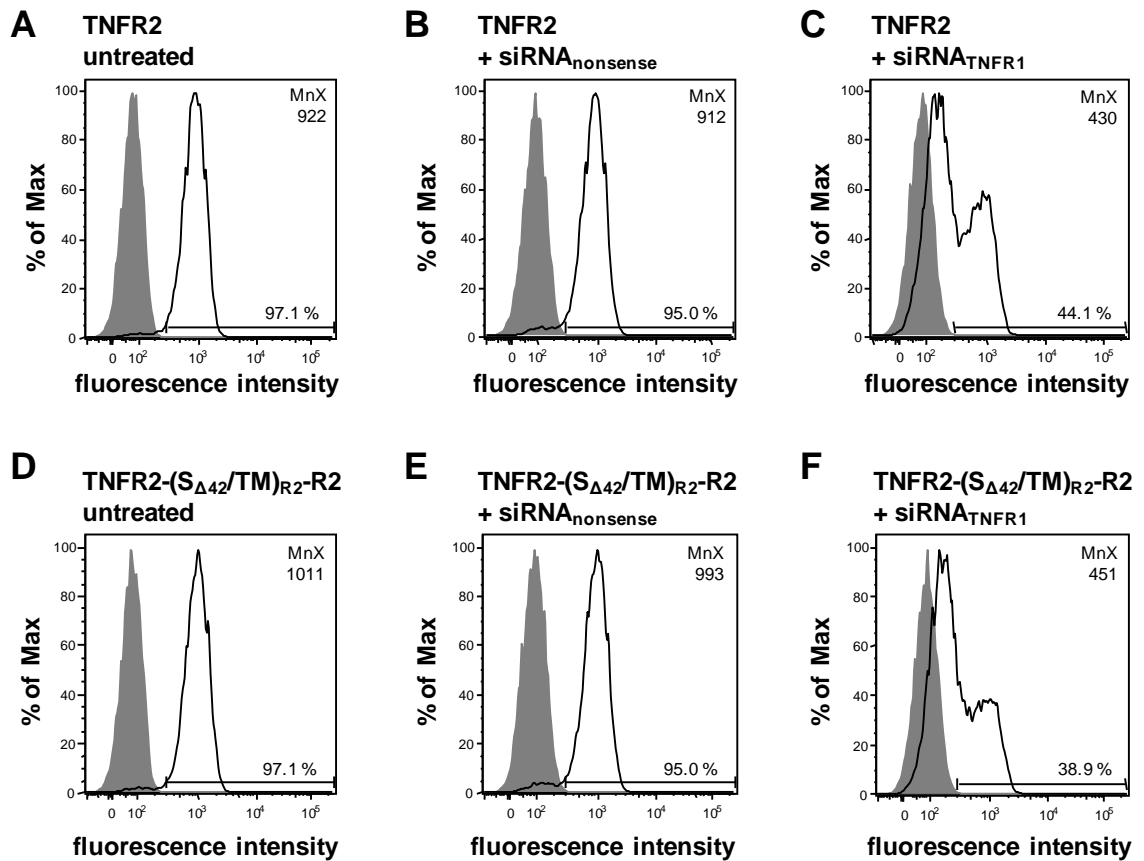


Figure 23. TNFR1 cell surface expression in HeLa cells overexpressing TNFR2 constructs after treatment with TNFR1-specific siRNA.

Cell surface expression of endogenous TNFR1 in HeLa TNFR2 and HeLa TNFR2-(S_{Δ42}/TM)_{R2-R2} cells. FACS analysis of **A**) untreated HeLa TNFR2 cells; **B**) untreated HeLa TNFR2-(S_{Δ42}/TM)_{R2-R2} cells. FACS analysis of **C**) HeLa TNFR2 cells and **D**) HeLa TNFR2-(S_{Δ42}/TM)_{R2-R2} cells, which had been treated with 25 nM siRNA_{nonsense} for 48 h. FACS analysis of **E**) HeLa TNFR2 cells and **F**) HeLa TNFR2-(S_{Δ42}/TM)_{R2-R2} cells, which had been treated with 25 nM siRNA_{TNFR1} for 48 h. TNFR1 was stained on the cell surface using mouse anti-human TNFR1 antibody clone H398, biotin rat anti-mouse IgG (H+L) and PE-conjugated streptavidin (black line). Cells only incubated with biotin rat anti-mouse IgG (H+L) and PE-conjugated streptavidin (grey). Acquisition was performed on a Becton Dickinson FACSCanto II flow cytometer. Percentages of cells gated positive for TNFR1 and MnX are indicated. Data shown represent three independent experiments.

TNFR2/TRAF2 co-IP were then performed with cells which had been treated with 25 nM siRNA_{nonsense} and siRNA_{TNFR1} for 48 h, respectively. Similar to the experiments in section 3.3.1, the siRNA_{TNFR1} treated HeLa TNFR2 cells and HeLa R2-(S_{Δ42}/TM)_{R2}-R2 cells were stimulated with 10 ng/ml sTNF and CysTNF respectively for 5 min, 10 min and 15 min. Due to experimental limitations, however, only the 5 min and 10 min timepoints could be included for the siRNA_{nonsense} treatment group.

When siRNA_{nonsense} treated HeLa TNFR2 and HeLa R2-(S_{Δ42}/TM)_{R2}-R2 cells were stimulated with CysTNF, efficient recruitment of TRAF2 to the respective TNFR2 variants could be observed after 5 min and 10 min of stimulation (Figure 24). Stimulation with CysTNF also led to efficient TRAF2 recruitment in siRNA_{TNFR1} treated HeLa TNFR2 and HeLa R2-(S_{Δ42}/TM)_{R2}-R2 cells after 5 min, 10 min and 15 min (Figure 24). In contrast, the TRAF2 recruitment efficiency differed between HeLa TNFR2 and HeLa TNFR2-(S_{Δ42}/TM)_{R2}-R2 when cells were stimulated with sTNF. In line with findings described in section 3.3.1 (Figure 18 and Figure 19), sTNF-mediated TRAF2 recruitment was increased in HeLa TNFR2-(S_{Δ42}/TM)_{R2}-R2 cells compared to HeLa TNFR2 cells. Compared to CysTNF-stimulated cells, siRNA_{nonsense} and siRNA_{TNFR1} treated HeLa TNFR2 cells showed relatively weak TRAF2 recruitment upon 5 min, 10 min and 15 min sTNF stimulation (Figure 24). This difference was smaller in both siRNA_{nonsense} treated and siRNA_{TNFR1} treated HeLa TNFR2-(S_{Δ42}/TM)_{R2}-R2 cells 5 min, 10 and 15 min after stimulation, respectively (Figure 24).

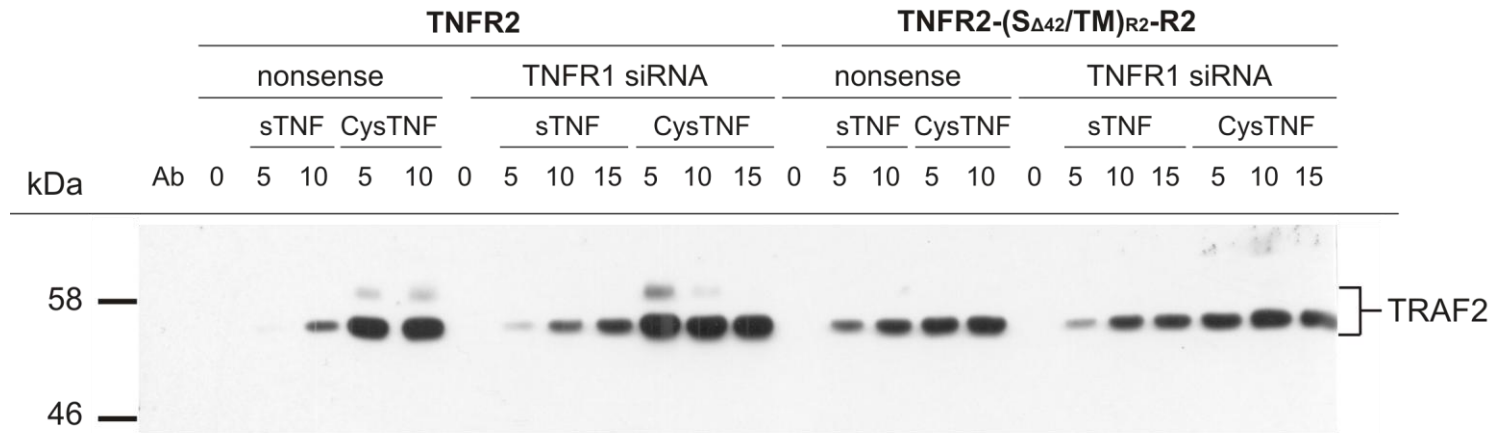


Figure 24. sTNF-mediated recruitment of TRAF2 to TNFR2 constructs is independent of TNFR1 signalling.

HeLa cells stably transfected with TNFR2 and TNFR2-(S_{Δ42}/TM)_{R2}-R2, respectively, were treated with 25 nM nonsense siRNA or 25 nM TNFR1-specific siRNA for 48 h. These cells remained untreated (0) or were stimulated as indicated with 10 ng/ml sTNF or wild type CysTNF for 5, 10 and 15 min (5, 10, 15). Lysates were prepared from these cells and equal amounts of protein were used in co-IP. For each co-IP sample an equivalent of approximately 5×10^5 HeLa cells and 2 μ g goat anti-human TNFR2 antibodies were used. Co-immunoprecipitated TRAF2 was detected using mouse anti-human TRAF2 antibodies (1:2000) as primary and goat anti-mouse-IgG-HRP (1:20000) as secondary antibodies. 2 μ g goat anti-human TNFR2 antibodies (Ab) were loaded as negative control. Data shown represent three independent experiments.

TRAF2 signal intensities were determined for the co-IP experiments depicted in using the Syngene G:Box and the GeneTools V4.01 analysis software. TRAF2 recruitment was expressed as a percentage of recruitment observed for siRNA_{nonsense} treated cells after 5 min of CysTNF stimulation.

In siRNA_{nonsense} treated HeLa TNFR2 and HeLa TNFR2-(S_{Δ42}/TM)_{R2}-R2 cells, CysTNF led to a strong TRAF2 recruitment after 5 min and 10 min of stimulation (100 % and 111 % for HeLa TNFR2, 100 % and 143 % for HeLa TNFR2-(S_{Δ42}/TM)_{R2}-R2; Figure 25). Similarly, strong TRAF2 recruitment could be observed when the corresponding siRNA_{TNFR1} treated cells were stimulated with CysTNF for 5 min, 10 min and 15 min, respectively (123 %, 130 % and 132 % for HeLa TNFR2, 127 %, 135 % and 136 % for HeLa TNFR2-(S_{Δ42}/TM)_{R2}-R2; Figure 25).

In line with observations made in section 3.3.1 (Figure 19), only relatively weak TRAF2 recruitment to the receptor could be observed in siRNA_{nonsense} treated HeLa TNFR2 cells upon stimulation with sTNF for 5 min and 10 min (11 % and 23 %, respectively; Figure 25). While the percentages for the siRNA_{TNFR1} treated HeLa TNFR2 cells after stimulation with sTNF for 5 min, 10 min and 15 min were slightly higher (18 %, 31 % and 36 %, respectively; Figure 25), they were still markedly lower than the ones observed in the corresponding CysTNF-treated samples. In contrast, sTNF-mediated TRAF2 recruitment was increased in both siRNA_{nonsense} and siRNA_{TNFR1} treated HeLa TNFR2-(S_{Δ42}/TM)_{R2}-R2 cells for all time points (46 % and 65 % for siRNA_{nonsense} treated and 51 %, 72 % and 81 % for siRNA_{TNFR1} treated cells, respectively; Figure 25) when compared with the corresponding HeLa TNFR2 samples. This indicates that the differences observed in sTNF-mediated TRAF2 recruitment of TNFR2 and TNFR2-(S_{Δ42}/TM)_{R2}-R2 are determined by the TNFR2 stalk region and are not affected by crosstalk of the receptor variants with TNFR1.

Furthermore, basal levels of TRAF2 recruitment were low in both, siRNA_{nonsense} and siRNA_{TNFR1} treated HeLa TNFR2 and HeLa TNFR2-(S_{Δ42}/TM)_{R2}-R2 cells (1-3 % for siRNA_{nonsense} and 3-5 % for siRNA_{TNFR1}; Figure 25), so that differences in basal TRAF2 recruitment could be excluded as a determining factor for the observed differences in sTNF responsiveness of these constructs.

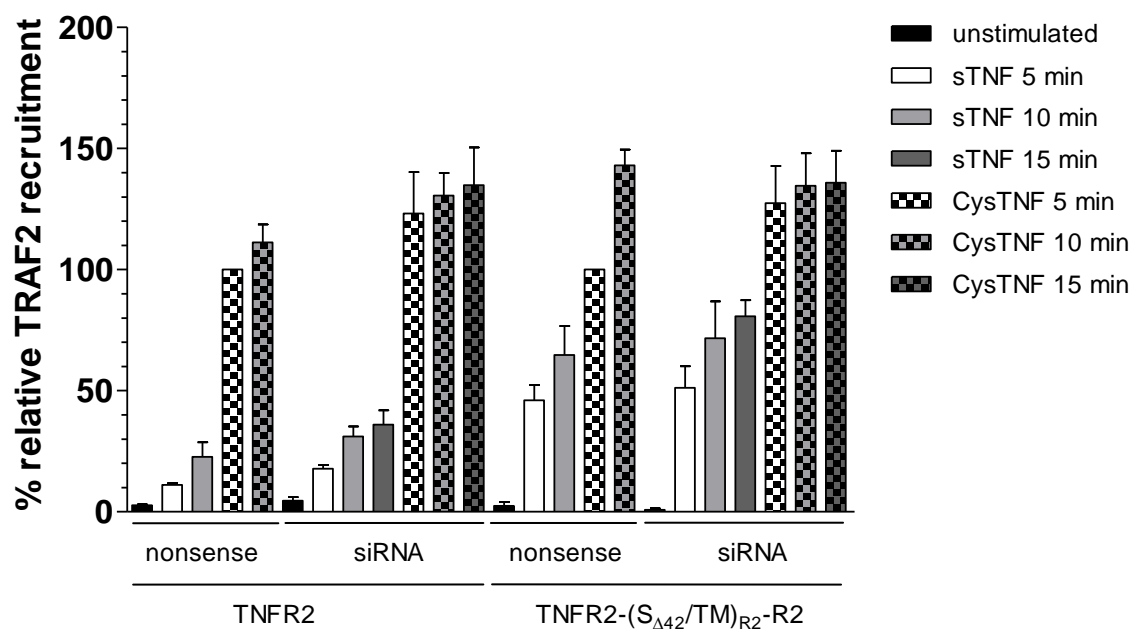


Figure 25. TNF-mediated TRAF2 recruitment to TNFR2 constructs in HeLa cells after treatment with TNFR1-specific siRNA.

Band intensities of TRAF2 Western Blots from TNFR2/TRAF2 co-IP experiments depicted in Figure 24 were quantified on a Syngene G:Box using the GeneTools V4.01 analysis software. Values were corrected for background levels. Shown is the relative TRAF2 recruitment, expressed as a percentage of the TRAF2 recruitment in nonsense RNA treated cells after 5 min of CysTNF stimulation. Results are expressed as mean \pm SD and are representative of three independent experiments.

As seen in Figure 25, all samples from siRNA_{TNFR1} treated cells showed higher percentages for TRAF2 recruitment than did the corresponding siRNA_{nonsense} samples. We, therefore, determined whether the ratios of CysTNF-mediated to sTNF-mediated TRAF2 recruitment were still comparable between the treatment groups.

In siRNA_{nonsense} treated HeLa TNFR2 cells, 5 min of CysTNF stimulation led to 9x more TRAF2 recruitment than the corresponding stimulation with sTNF, while at 10 min of stimulation CysTNF-mediated TRAF2 recruitment was 5x higher than the one for sTNF. For siRNA_{TNFR1} treated HeLa TNFR2 cells the factor was 7x at 5 min of stimulation and 4x at 10 min of stimulation. In contrast, the ratio of CysTNF-mediated to sTNF-mediated TRAF2 recruitment was approximately 2x for both siRNA_{nonsense} and siRNA_{TNFR1} treated HeLa TNFR2-(S_{Δ42}/TM)_{R2}-R2 cells for both stimulation time points (2x for 5 min and 10 min siRNA_{nonsense} treated HeLa cells, 2x for 5 min siRNA_{TNFR1} treated HeLa cells, 2.5x for 10 min siRNA_{TNFR1} treated HeLa cells).

With the exception of the 5 min timepoint for HeLa TNFR2 cells, where a slightly bigger difference in recruitment efficiency (9x versus 7x) could be detected, the ratios of CysTNF-mediated TRAF2 recruitment to sTNF-mediated TRAF2 recruitment were comparable in siRNA_{nonsense} and siRNA_{TNFR1} treated cells. An increased sTNF responsiveness in TNFR2 with a shortened stalk region could be observed which was similar to the one described in section 3.3.1. However, for statistical analysis further repeats of this experiment would be required.

Taken together, our data suggest that the differences observed in sTNF-mediated TRAF2 recruitment to TNFR2 and TNFR2-(S_{Δ42}/TM)_{R2}-R2 are determined by the stalk region and are not caused by altered crosstalk with TNFR1. In addition, these data further support the conclusions drawn in section 3.3.1 that the stalk region inhibits sTNF responsiveness of wild type TNFR2.

3.4 Preliminary experiments on the role of the TNFR2 stalk region in sTNF-mediated p65 translocation

Data from TNFR2/TRAF2 co-IP experiments support a role for the TNFR2 stalk region in the control of TNFR2 responsiveness to sTNF at the level of early receptor activation. To be able to determine whether the differences seen in the recruitment of TRAF2 would be reflected at the downstream signalling level, the TNF-induced translocation of the NF- κ B p65 subunit from the cytoplasm to the nucleus was investigated. However, due to timely limitations of this PhD project only preliminary results can be presented here.

Electrophoretic mobility shift assays (Krippner-Heidenreich *et al.*, 2002) and translocation experiments (Fischer *et al.*, 2011) had shown that upon stimulation of wild type TNFR2 the NF- κ B p65 signalling pathway is activated in MF. Therefore, we chose p65 translocation in MF stably transfected with TNFR2 and TNFR2 variants as a read-out system to investigate the role of the TNFR2 stalk region in sTNF-mediated downstream signalling. MF TNFR2 had been generated previously by Regina Pfeiffer, University of Stuttgart, Germany. The same TNFR2-(S/TM)_{R1}-R2 and TNFR2-(S _{Δ 42}/TM)_{R2}-R2 constructs, which had been used for the stable transfection of HeLa cells (section 3.3.1), were stably transfected in MF as part of this PhD project.

Cell surface expression and correct molecular weight of the transfected TNFR2, TNFR2-(S/TM)_{R1}-R2 and TNFR2-(S _{Δ 42}/TM)_{R2}-R2 variants were ensured by FACS and Western Blot analysis. All three variants were expressed on the cell surface and 91-96 % of MF could be gated positive for the receptors (MnX = 12327 for TNFR2, MnX = 10328 for TNFR2-(S/TM)_{R1}-R2 and MnX = 5500 for TNFR2-(S _{Δ 42}/TM)_{R2}-R2, respectively; Figure 26 A, B and C).

For the Western Blot analysis whole cell lysates from transiently transfected HeLa cells and stably transfected MF were used (Figure 26 D). As seen before for HeLa cells stably expressing these constructs (Figure 16), for TNFR2-(S/TM)_{R1}-R2 and TNFR2-(S _{Δ 42}/TM)_{R2}-R2 two bands could be observed in the Western Blot (Figure 26 D), of which the faster migrating bands correlated more or less with the predicted molecular weight. The slower migrating bands were approximately 50 kDa in size. Similar to the TNFR-Fas constructs analysed in results section 3.2, the faster migrating protein bands probably represent receptors which had been translated but not post-

translationally modified, whereas the slower migrating bands presumably represent the mature forms of the receptors. Importantly, the receptors from stably transfected MF co-migrated with the transiently expressed variants (Figure 26 D), excluding the possibility that, during the selection process for the stable cell lines, MF expressing receptors with larger deletions had been accumulated.

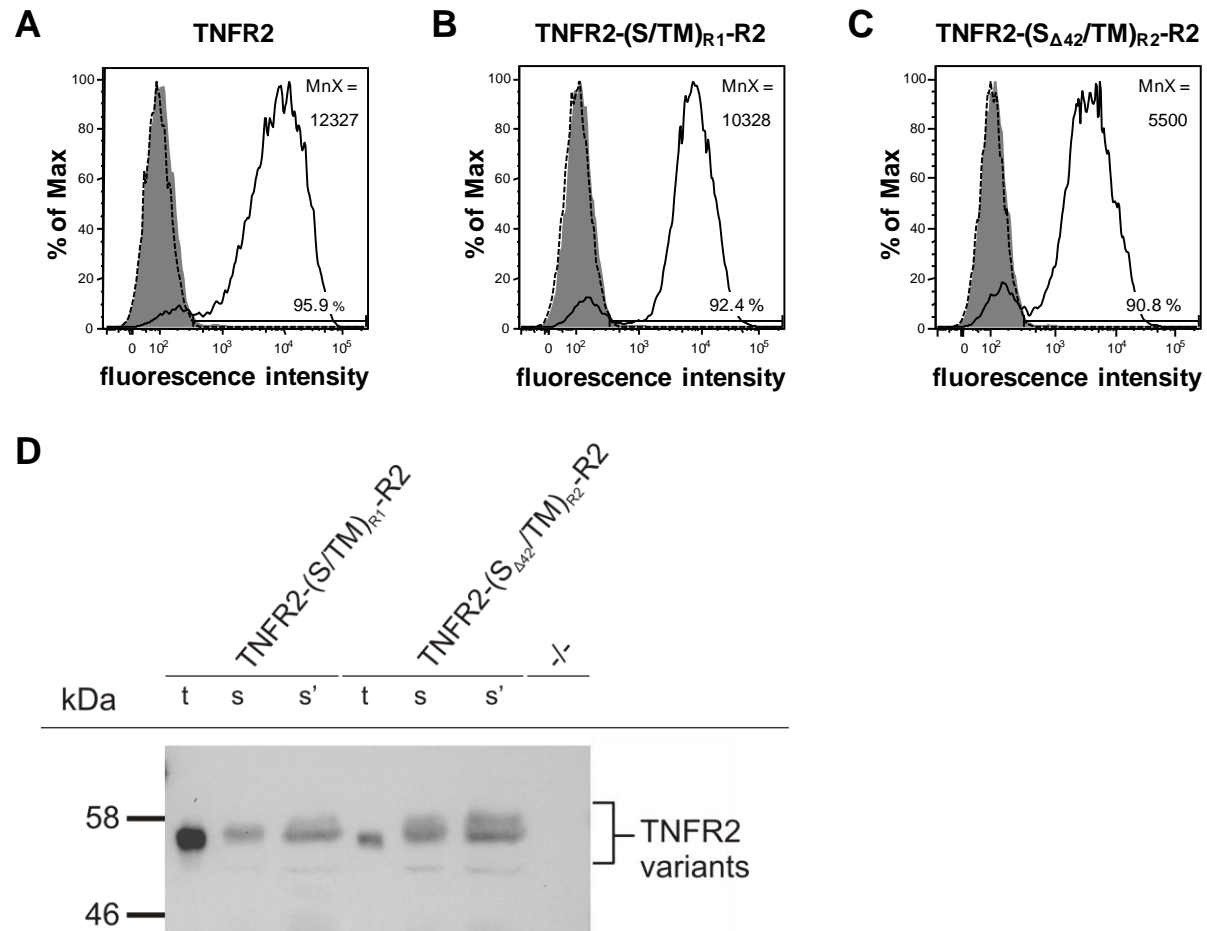


Figure 26. Characterisation of MF stably expressing TNFR2, TNFR2-(S/TM)_{R1}-R2 and TNFR2-(S_{Δ42}/TM)_{R2}-R2.

Figure 26 continued: MF had been stably transfected with TNFR2, TNFR2-(S/TM)_{R1}-R2 and TNFR2-(S_{Δ42}/TM)_{R2}-R2, respectively. FACS analysis of **A**) TNFR2, **B**) TNFR2-(S/TM)_{R1}-R2 and **C**) TNFR2-(S_{Δ42}/TM)_{R2}-R2; receptors were stained on the cell surface using mouse anti-human TNFR2 antibodies (clone MR2-1) and goat anti-mouse IgG-FITC antibodies (black line). Cells only incubated with goat anti-mouse IgG-FITC antibodies are depicted in grey. 96 %, 92 % and 91 % of the cells were gated positive for TNFR2, TNFR2-(S/TM)_{R1}-R2 and TNFR2-(S_{Δ42}/TM)_{R2}-R2, respectively. Data shown represent four independent experiments. **D**) Western Blot analysis of TNFR2 variants. Whole cell lysates were prepared from 4 x 10⁴ (s) and 6 x 10⁴ (s') stably transfected MF, respectively, and subjected to SDS-PAGE and Western Blot analysis. Untransfected MF (-/-) served as control. Lysates from 4 x 10⁴ HeLa cells, which had been transiently transfected with indicated TNFR2 variants (t) served as positive control. Goat anti-human TNFR2 antibodies (1:2000) were used as primary and rabbit anti-goat IgG-HRP (1:20000) as secondary antibodies. Acquisition was performed on a Becton Dickinson FACSCanto II flow cytometer. Data shown represent one experiment.

After characterisation of the MF TNFR2-(S/TM)_{R1-R2} and MF TNFR2-(S_{Δ42}/TM)_{R2-R2} cell lines, these cells were used for preliminary p65 translocation experiments. Cells were stimulated with 100 ng/ml sTNF and CysTNF, respectively, for 30 min and endogenous p65 was visualised via immunofluorescence. In addition, cells were stained with the DNA dye DAPI to visualise the cell nucleus (Figure 27 A, E and I and Figure 28 A, E and D).

When cells remained untreated, p65 was mostly detected in the cytoplasm of MF TNFR2-(S/TM)_{R1-R2} and MF TNFR2-(S_{Δ42}/TM)_{R2-R2} (Figure 27 C and Figure 28 C, respectively). Hardly any co-localisation with the nuclear staining could be detected (Figure 27 D and Figure 28 D). In contrast, nuclear translocation of p65 could be observed in MF TNFR2-(S/TM)_{R1-R2} and MF TNFR2-(S_{Δ42}/TM)_{R2-R2} when cells were stimulated with sTNF (Figure 27 G and Figure 28 G, respectively). Stimulation with CysTNF also led to p65 translocation from the cytoplasm to the nucleus in MF TNFR2-(S/TM)_{R1-R2} (Figure 27 K).

The stabilising anti-human TNFR2 antibody 80M2 has been described to enhance the stimulation capacities of sTNF and CysTNF (Krippner-Heidenreich *et al.*, 2002, Bryde *et al.*, 2005) and increased the responsiveness of MF TNFR2-(S_{Δ42}/TM)_{R2-R2}-Fas towards sTNF (Figure 20 C). Therefore, we included MF TNFR2-(S_{Δ42}/TM)_{R2-R2}, which had been pre-treated with 2 μg/ml of this antibody and subsequently stimulated with 100 ng/ml CysTNF, as a control for maximal stimulation of the receptor variant. p65 translocation could also be observed in these 80M2/CysTNF-treated MF TNFR2-(S_{Δ42}/TM)_{R2-R2} (Figure 28 K). The co-localisation of p65 with the nuclei after the various stimuli is shown in the corresponding overlay pictures (Figure 27 H and L and Figure 28 H and L).

A profound number of cells positive for nuclear p65 could be observed not only upon treatment with CysTNF but also when cells were stimulated with sTNF. This indicates that both sTNF and CysTNF are potent inducer of downstream signalling pathways in MF TNFR2-(S/TM)_{R1-R2} and MF TNFR2-(S_{Δ42}/TM)_{R2-R2}. However, whether the TNFR2 stalk region has an inhibitory effect on sTNF-mediated translocation of p65 similar to the one observed for sTNF-mediated TRAF2 recruitment (Figure 18 and Figure 19), still needs to be determined by comparing these cells with MF TNFR2. A quantitative analysis of sTNF- and CysTNF-mediated p65 nuclear translocation was unfortunately not possible during this PhD project.

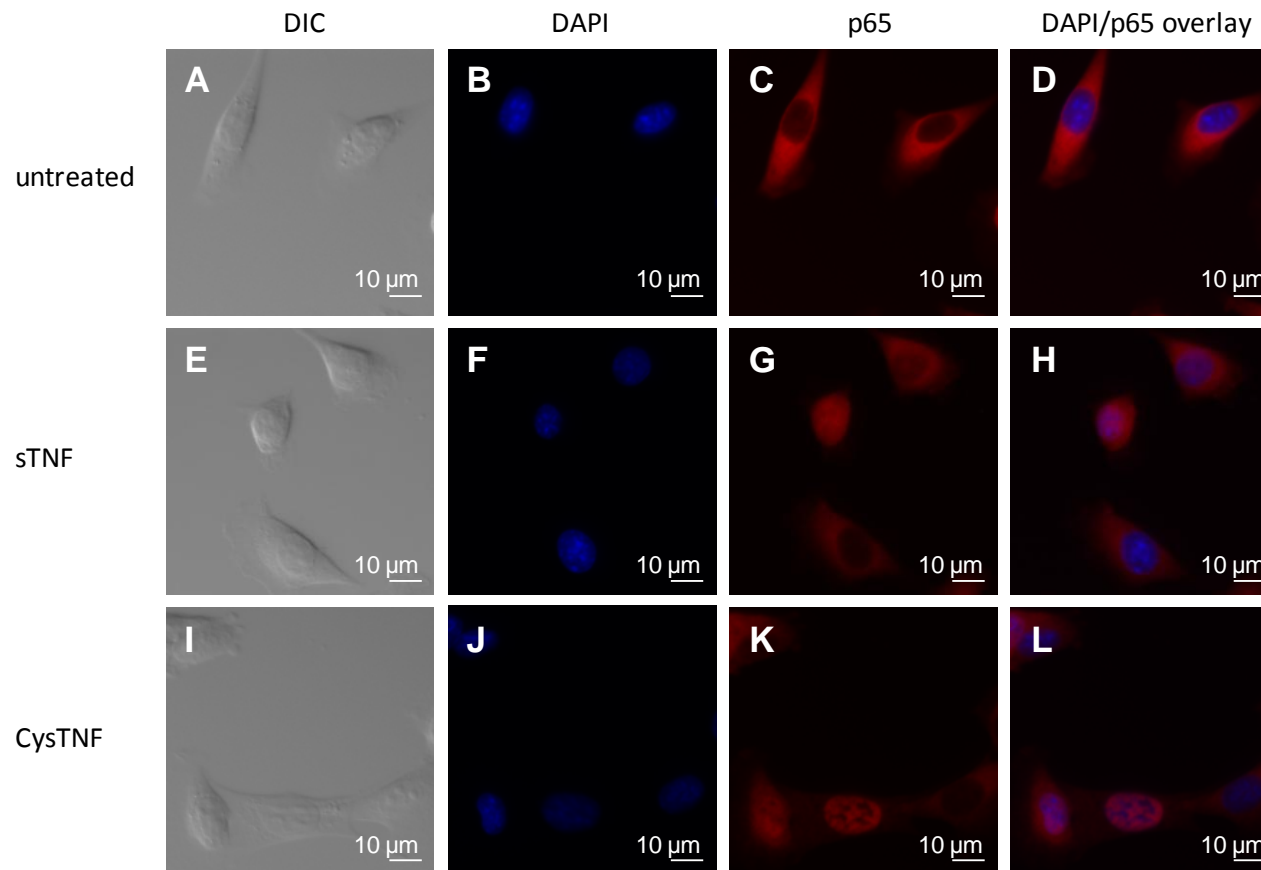


Figure 27. TNF-mediated nuclear translocation of p65 in MF TNFR2-(S/TM)_{R1}-R2 (preliminary data).

As indicated, MF TNFR2-(S/TM)_{R1}-R2 were left untreated or were stimulated with sTNF and CysTNF (100 ng/ml), respectively, for 30 min. Cell nuclei were visualised with DAPI. Additionally, cells were stained for endogenous p65 using rabbit anti-human p65 (clone C-20; 1:100) and Alexa594-conjugated goat anti-rabbit IgG (H+L) antibodies (1:100). Cells were analysed on a Zeiss Axio Imager 2 fluorescence microscope (40x magnification). Shown are **A, E and I**) Differential interference contrast (DIC) images of MF TNFR2-(S/TM)_{R1}-R2; **B, F and J**) nuclear staining with DAPI; **C, G and K**) staining for endogenous p65; **D, H and L**) overlay of DAPI and p65 images. Pink colour indicates co-localisation. Data shown represent one experiment.

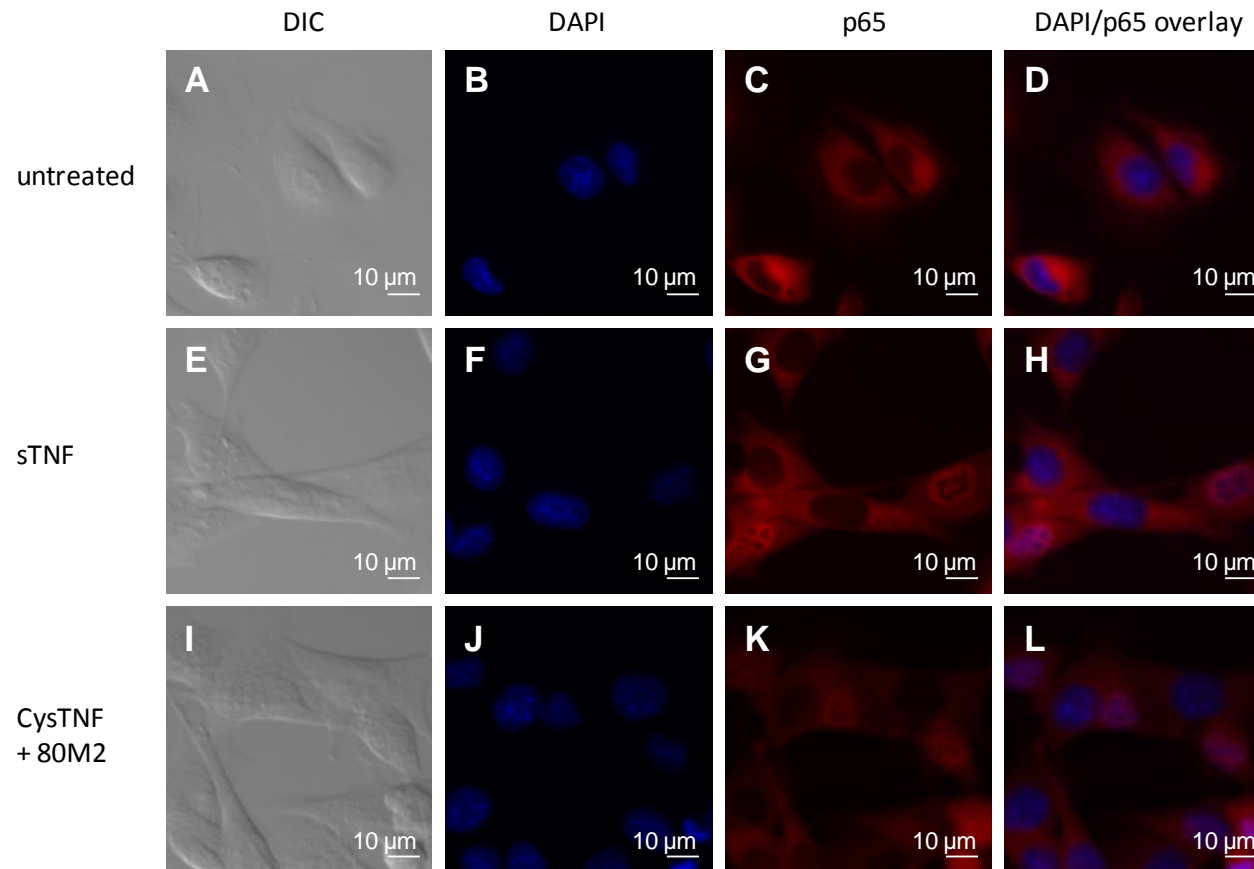


Figure 28. TNF-mediated nuclear translocation of p65 in MF TNFR2-(S_{Δ42}/TM)_{R2}-R2 (preliminary data).

MF TNFR2-(S_{Δ42}/TM)_{R2}-R2 were left untreated, stimulated with 100 ng/ml sTNF for 30 min or pre-incubated with 2 μg/ml mouse anti-human TNFR2 antibody 80M2 and then stimulated with 100 ng/ml CysTNF for 30 min (CysTNF + 80M2). Cell nuclei were visualised with DAPI and cells were stained for endogenous p65 using rabbit anti-human p65 (clone C-20; 1:100) and Alexa594-conjugated goat anti-rabbit IgG (H+L) antibodies (1:100). Cells were analysed on a Zeiss Axio Imager 2 fluorescence microscope (40x magnification). **A, E and I**) Differential interference contrast (DIC) images; **B, F and J**) nuclear staining with DAPI; **C, G and K**) staining for endogenous p65; **D, H and L**) overlay DAPI and p65 images. Pink colour indicates co-localisation. Data shown represent one experiment.

3.5 Discussion

3.5.1 The TNFR2 stalk region determines sTNF responsiveness in TNFR2-Fas chimaeras

Preliminary data by Dr Anja Krippner-Heidenreich's group obtained using the MF TNFR-Fas cell system suggested a critical role for the TNFR1 and TNFR2 stalk regions in the control of differential responsiveness to sTNF (Figure 11). The data presented here confirm that the TNFR stalk region is a major determinant for this differential responsiveness and show that 42 aa in the TNFR2 stalk region inhibit receptor responsiveness towards sTNF.

For MF stably transfected with the TNFR2-(S_{Δ42}/TM)_{R2}-Fas chimaera responsiveness towards CysTNF (ED₅₀ = 0.3 ng/ml) could be observed in 75 % of the cells (Figure 14 B). The population of CysTNF-responsive cells correlated with the TNFR2-(S_{Δ42}/TM)_{R2}-Fas positive population of the cell pool (Figure 13 A), arguing for a full CysTNF susceptibility in all receptor positive MF. In contrast, only approximately 50 % of MF TNFR2-(S_{Δ42}/TM)_{R2}-Fas were responsive towards sTNF with an ED₅₀ of 3 ng/ml (Figure 14 B). The cause of the discrepancy between the number of cells positive for TNFR2-(S_{Δ42}/TM)_{R2}-Fas cell surface expression and the number of cells responsive towards sTNF is not known to date. sTNF is not capable of inducing cytotoxicity in MF TNFR2-Fas, even at concentrations of up to 1 µg/ml (Dr Krippner-Heidenreich, personal communication). Therefore, the deletion of 42 aa in the stalk region of TNFR2-Fas chimaeras leads to a more than 100-fold increase in sTNF responsiveness compared to the parental chimaeric receptor.

However, shortening of the TNFR2 stalk region did not result in a receptor fully responsive to sTNF as MF TNFR2-(S_{Δ42}/TM)_{R2}-Fas were still 10-fold less sensitive towards sTNF when compared to CysTNF stimulated cells. This is in line with previous experiments, which showed that susceptibility towards sTNF was decreased when either the TM (Dr Anja Krippner-Heidenreich, personal communication) or CRD1 (Branschädel *et al.*, 2010) had been exchanged between TNFR1 and TNFR2. This suggests that sTNF responsiveness is controlled at a minimum of three levels: CRD1, transmembrane domain and stalk region. Therefore, full responsiveness of TNFR2-(S_{Δ42}/TM)_{R2}-Fas towards sTNF could not be expected. However, our results show that

out of the three determinants the stalk region has the strongest impact on sTNF responsiveness.

Furthermore, our data indicate that some molecular feature(s) encoded by the 42 aa, which had been deleted in the TNFR2 stalk region, inhibits responsiveness to sTNF. Post-translational modifications of the stalk region, such as glycosylation, could represent such a feature. It has been reported previously that TNFR2 is N- and O-glycosylated (Hohmann *et al.*, 1989) and specifically in the membrane proximal region of the receptor O-glycosylation has been described (Pennica *et al.*, 1993). By shortening the TNFR2 stalk region more than 10 of 12 putative O-glycosylation sites predicted by the bioinformatics programme NetOglyc (Julenius *et al.*, 2005) were deleted. This became apparent in the Western Blot analysis of TNFR2-Fas and TNFR2-(S_{Δ42}/TM)_{R2}-Fas, where both chimaeras showed two bands of which only the faster migrating one correlated with the predicted molecular mass (Figure 13). For wild type TNFR2 it has been described that N-glycosylation contributes 2-4 kDa and O-glycosylation contributes 6-10 kDa, so that in total glycosylation of the receptor adds about 10-15 kDa to its molecular mass (Hohmann *et al.*, 1989). As glycosylation takes place in the endoplasmic reticulum and/or Golgi apparatus (reviewed in Spiro, 2002), the faster migrating bands of TNFR2-Fas, therefore, presumably represent chimaeras which have been translated but not been glycosylated yet. In contrast the slower migrating bands have a molecular mass which is about 10 kDa greater and, therefore, are most likely representing the mature, glycosylated form of the receptor.

The difference in molecular mass of the mature TNFR2-Fas chimaeras and the mature TNFR2-(S_{Δ42}/TM)_{R2}-Fas chimaeras is approximately 8 kDa (Figure 13 B). 4 kDa of this difference can be attributed to the fact that TNFR2-(S_{Δ42}/TM)_{R2}-Fas is lacking the 42 amino acid residues. The remaining difference is likely to be due to the fact that O-glycosylation sites have been deleted. In contrast, N-glycosylation of the receptor constructs should not be affected by the deletion as it has been reported to take place at two asparagine residues in CRD4 (Pennica *et al.*, 1993). Indeed we could still detect two bands for TNFR2-(S_{Δ42}/TM)_{R2}-Fas constructs, of which the slower migrating one presumably represents the N-glycosylated but not O-glycosylated mature form of the chimaera. Thus, O-glycosylation of the stalk region represents a feature which potentially could influence the responsiveness of TNFR2 to sTNF.

3.5.2 The stalk region determines sTNF responsiveness of wild type TNFR2

The chimaeric TNFR-Fas system indicated that the TNFR stalk region is a major determinant for differential receptor responsiveness to sTNF. The results presented in sections 3.3.1 and 3.3.3 show that this is also the case in wild type TNFR2 and that the stalk region inhibits sTNF responsiveness at the level of TRAF2 recruitment.

Differential responsiveness to sTNF has already been described for HeLa TNFR2 cells. In these cells, only weak sTNF-mediated recruitment of TRAF2 to TNFR2 could be detected while stimulation with oligomerised TNFR2-selective CysTNF led to an efficient TRAF2 recruitment (Krippner-Heidenreich *et al.*, 2002). Using HeLa cells which stably expressed the TNFR2-(S/TM)_{R1}-R2 and TNFR2-(S_{Δ42}/TM)_{R2}-R2 variants, we could show that sTNF-mediated TRAF2 recruitment to TNFR2 is inhibited by the TNFR2 stalk region and, furthermore, that 42 aa in this region determine this inhibition (Figure 18 and Figure 19). In comparison with wild type TNFR2, sTNF-mediated TRAF2 recruitment was significantly increased for TNFR2-(S_{Δ42}/TM)_{R2}-R2.

TNFR1 overexpression leads to the self-association of the TNFR1 death domains and induces ligand-independent apoptosis (Boldin *et al.*, 1995). This overexpression-induced apoptotic effect of TNFR1 has also been observed in murine embryonic fibroblasts from wild type (Yeh *et al.*, 1998) and *tnfr1*^{-/-}/*tnfr2*^{-/-} double knockout mice (Dr Anja Krippner-Heidenreich, personal communication). Therefore, we were unfortunately not able to determine whether the TNFR2 stalk region would have a similar inhibitory effect on sTNF responsiveness in wild type TNFR1 as we had observed for TNFR2.

Upon engagement of TNFR2 TRAF2 recruitment can be observed within 3 min of stimulation (Wicovsky *et al.*, 2009) and is sustained for more than 30 min (Krippner-Heidenreich *et al.*, 2002, Wicovsky *et al.*, 2009). Furthermore, TNFR2-mediated TRAF2 translocation to detergent-insoluble cell membrane compartments and its subsequent polyubiquitination have been reported (Li *et al.*, 2002, Habelhah *et al.*, 2004, Wu *et al.*, 2005). 20-30 min after stimulation proteasomal degradation of TRAF2 is initiated (Wu *et al.*, 2005, Fischer *et al.*, 2011), which was found to be mediated by cIAP1 (Li *et al.*, 2002). In agreement with observations made by Wicovsky *et al.* (2009), we could also detect TRAF2 recruitment to TNFR2 variants as early as 5 min post stimulation with CysTNF (Figure 18). 10 min and 15 min after stimulation with

CysTNF a trend towards a decrease in TRAF2 signal strength could be observed (Figure 19) which is likely to be caused by a decreased solubility of the TNF/TNFR signalling complexes. The buffer used for the solubilisation of the signalling complexes from the cell membrane contains 1 % (v/v) Triton X-100. Whether the decreased solubility of the signalling complexes is due to their translocation to detergent-resistant membrane compartments as suggested by Li *et al.* (2002), Habelhah *et al.* (2004) and Wu *et al.* (2005) is not known to date. In addition, the formation of larger ligand/receptor clusters as described by Krippner-Heidenreich *et al.* (2002), which occurs just within 5 min of stimulation, might play a role here. Formation of these clusters might render signalling complexes inaccessible to the detergent.

Furthermore, reduced solubility of the TNF/TNFR2 signalling complexes could be the reason why the signal strength of the precipitated TNFR2 constructs did not always correlate with the one observed for the co-immunoprecipitated TRAF2. As CysTNF is a potent inducer of TNFR2 signalling and cluster formation (Krippner-Heidenreich *et al.*, 2002), this would explain the trend that less precipitation of TNFR2 constructs occurred in CysTNF stimulated samples compared to samples from sTNF stimulated and untreated cells.

In contrast, the amount of TRAF2 recruited to the TNFR2 variants was still increasing at 10 min and 15 min post stimulation with sTNF compared to the 5 min timepoint (Figure 19). This delayed recruitment could be caused by differences in the stability of the receptor/ligand complexes. With a half-life of only 1.1 min, sTNF was found to bind to TNFR2 in a relatively transient manner (Grell *et al.*, 1995). Stabilising the sTNF/TNFR2 complexes through pre-treating the cells with the TNFR2 antibody 80M2 could increase this half-life by factor 10 (Grell *et al.*, 1995). In addition, the stabilising capacity of oligomerised TNF has been described as an important component of efficient TNFR2 activation previously (Krippner-Heidenreich *et al.*, 2002, Rauert *et al.*, 2010). Therefore, the different kinetics of sTNF-mediated and CysTNF-mediated TRAF2 recruitment in the three HeLa cell lines could be explained by this difference in stabilisation potential between the two ligands.

In contrast, the differences between the sTNF-mediated TRAF2 recruitment in HeLa TNFR2 and HeLa TNFR2-(S/TM)_{R1}-R2 and HeLa TNFR2-(S_{Δ42}/TM)_{R2}-R2 are most likely not due to different sTNF affinities of the TNFR2 variants. Equilibrium binding studies with ¹²⁵I-labelled sTNF had revealed that sTNF binding affinities to TNFR2-Fas, TNFR2-(S/TM)_{R1}-Fas and TNFR2-(S_{Δ42}/TM)_{R2}-Fas were comparable in

MF (data obtained by Verena Boschert, University of Stuttgart, Germany; Dr Krippner-Heidenreich, personal communication).

In co-IP experiments Shu *et al.* (1996) found TRAF2 to be recruited to both TNFR and observed recruitment to TNFR1 within 2 min after stimulation. In cells which express both TNFR, stimulation of TNFR2 has been described to enhance TNFR1-mediated cell death in a TRAF2-dependent manner (Vandenabeele *et al.*, 1995, Weiss *et al.*, 1997, Declercq *et al.*, 1998, Chan and Lenardo, 2000) and Fotin-Mleczek *et al.* (2002) postulated this to be caused by competition of the two TNFR for TRAF2-mediated recruitment of the anti-apoptotic proteins cIAP1 and cIAP2. Furthermore, the affinity between TRAF2 and TRADD is significantly higher than the affinity between TRAF2 and a TNFR2 peptide, which indicates that TRADD acts as a stronger inducer of TRAF2 signalling (Park *et al.*, 2000, Tsao *et al.*, 2000). In addition, this suggests that activation of TNFR1 influences recruitment of TRAF2 recruited to TNFR2 and, therefore, TRAF2-dependent signalling of TNFR2.

In this project TNF-mediated TRAF2 recruitment in HeLa cells expressing endogenous TNFR1 and exogenous TNFR2 was investigated. By using TNFR1-specific siRNA, we were able to exclude the possibility that the observed differences in sTNF-induced TRAF2 recruitment to TNFR2 and TNFR2-(S_{Δ42}/TM)_{R2}-R2 resulted from altered TNFR1-TNFR2 crosstalk (Figure 24). However, in comparison to the siRNA_{nonsense} treated cells, we observed an increase in TRAF2 recruitment in siRNA_{TNFR1} treated cells after stimulation with both, sTNF and CysTNF. TNFR2 variants are approximately three times higher expressed on the cell surface of HeLa cells than TNFR1 (Figure 22 A and D and Figure 23 A and D). However, the higher affinity of the TNFR1/TRADD complexes for TRAF2 described by Park *et al.* (2000) and Tsao *et al.* (2000) suggests that after siRNA_{TNFR1}-treatment more TRAF2 would be available for recruitment to the TNFR2 variants. Therefore, the stronger TRAF2 signals observed for the siRNA_{TNFR1} treated samples would reflect the decrease in the above mentioned competition for TRAF2 between TNFR1 and TNFR2 (Vandenabeele *et al.*, 1995, Weiss *et al.*, 1997, Declercq *et al.*, 1998, Chan and Lenardo, 2000, Fotin-Mleczek *et al.*, 2002).

Recently, Fischer *et al.* (2011) demonstrated in co-IP experiments that stimulation with TNF also leads to TRAF2 recruitment to TNFR2 in MF. These experiments were performed with TNFR2-selective CysTNF in combination with the anti-human TNFR2

antibody 80M2. Therefore, it remains to be determined whether this cell system would also be suitable to investigate differential responsiveness of TNFR2 towards sTNF at the level of TRAF2 recruitment.

3.5.3 sTNF-mediated downstream signalling of TNFR2 variants

TNFR2 is a known activator of the NF- κ B signalling pathway (Rothe *et al.*, 1995). CysTNF-mediated activation of this pathway in HeLa TNFR2 cells was demonstrated by Krippner-Heidenreich *et al.* (2002) in electrophoretic mobility shift assays and TNF-mediated nuclear translocation of the NF- κ B subunit p65 has been described in primary cortical neurons (Marchetti *et al.*, 2004). Furthermore, TNFR2-selective CysTNF in combination with the anti-human TNFR2 antibody 80M2 was capable of inducing translocation of p65 from the cytoplasm to the nucleus in MF TNFR2 (Fischer *et al.*, 2011). This p65 translocation occurred in MF TNFR2 within 10 min of stimulation. However, the p65 translocation potential of sTNF in these cells is not known. Here it was shown that p65 translocates to the nucleus in MF TNFR2-(S/TM)_{R1}-R2 and MF TNFR2-(S _{Δ 42}/TM)_{R2}-R2 within 30 min of stimulation with sTNF and CysTNF (Figure 27 and Figure 28), respectively. This is in good agreement with the data obtained by Fischer *et al.* (2011). Future work will comprise quantification of cells which are positive for nuclear p65 after stimulation with sTNF and CysTNF. Comparison with MF expressing the wild type TNFR2 will then show whether the stalk region proves to be a determinant of differential responsiveness at the level of NF- κ B activation.

3.6 Conclusion

- The TNFR2 stalk region inhibits receptor responsiveness to sTNF but not membrane-bound TNF in TNFR-Fas chimaeras and wild type TNFR2.
- The TNFR2 stalk region inhibits sTNF responsiveness at the level of receptor signalling complex formation; this effect is independent of TNFR1 signalling.
- Analysis of TNF-mediated nuclear translocation of the NF- κ B p65 subunit is promising method to investigate the influence of the TNFR2 stalk region on sTNF responsiveness downstream of TNF/TNFR signalling complex formation.

CHAPTER 4

Results II: Investigations into molecular mechanisms by which the TNFR2 stalk region controls sTNF responsiveness

4.1 Introduction

Data presented in chapter 3 identified the stalk region of TNFR as a major determinant of differential responsiveness to sTNF. When the length of the TNFR2 stalk region (56 aa) was reduced to that of the TNFR1 stalk region (15 aa), the TNFR2-Fas chimera and TNFR2 showed a more than 100-fold increase in responsiveness towards sTNF (Figure 14). This suggests that sTNF responsiveness is inhibited by something which is encoded by the 42 deleted aa residues in the stalk region (Please note, that a *Bam*HI restriction site was introduced into the TNFR2 stalk region, which accounts for the substitution of an additional aa residue (Figure 29)).

A comparison of the TNFR1 and TNFR2 stalk regions reveals that these regions differ in their length (15 aa for TNFR1 as opposed to 56 aa for TNFR2), their content in proline residues (one proline in TNFR1, 12 prolines in TNFR2) and their O-glycosylation status (no O-glycosylation is present in TNFR1, TNFR2 is highly O-glycosylated (Pennica *et al.*, 1993)). When 42 aa were deleted in the TNFR2 stalk region this changed not only its length but also led to the deletion of eight of the proline residues and the deletion of more than 10 potential O-glycosylation sites (see Figure 29).

Therefore, the aims in this chapter were to:

- investigate whether the length of the TNFR stalk region determines sTNF responsiveness;
- determine whether proline residues in the TNFR2 stalk region influence receptor responsiveness towards sTNF;
- identify O-glycosylation sites in the TNFR2 stalk region and to study their role in determining sTNF responsiveness of TNFR2.

4.2 Length of the stalk region does not control TNFR2 responsiveness towards sTNF

The difference in stalk region length between TNFR1 and TNFR2 could potentially influence the responsiveness of the receptor to sTNF (Dr Anja Krippner-Heidenreich, personal communication). To determine whether the length of the stalk region does indeed affect sTNF responsiveness, artificial glycine-serine linkers of 15 aa or 56 aa in length were constructed and cloned into TNFR-Fas chimaeras as described in section 2.2.7. The aa sequences of these linkers are depicted in Figure 30.

MF stably expressing the constructs with 15 aa long linkers (TNFR1-S_{GSL15}-TM_{R1}-Fas and TNFR2-S_{GSL15}-TM_{R2}-Fas) and 56 aa long linkers (TNFR1-S_{GSL56}-TM_{R1}-Fas and TNFR2-S_{GSL56}-TM_{R2}-Fas), respectively, were characterised by Western Blot analysis. For this purpose, whole cell lysates from transiently transfected HeLa cells and stably transfected MF were analysed (Figure 31). The predicted molecular weights were as follows: 42 kDa for TNFR1-S_{GSL15}-TM_{R1}-Fas, 45 kDa for TNFR1-S_{GSL56}-TM_{R1}-Fas, 44 kDa for TNFR2-S_{GSL15}-TM_{R2}-Fas and 46 kDa for TNFR2-S_{GSL56}-TM_{R2}-Fas (determined using the ProtParam tool on the ExPaSy proteomics server)(Gasteiger *et al.*, 2005).

For all transiently transfected constructs two bands could be detected, of which the faster migrating bands correlated with the respective predicted molecular weights. The slower migrating bands of TNFR1-S_{GSL15}-TM_{R1}-Fas and TNFR2-S_{GSL15}-TM_{R2}-Fas had a molecular weight of approximately 46 kDa and the molecular weight of the slower migrating bands of TNFR1-S_{GSL56}-TM_{R1}-Fas and TNFR2-S_{GSL56}-TM_{R2}-Fas was approximately 48 kDa (Figure 31). The faster migrating protein bands presumably represent intracellular receptors which had not been post-translationally modified while the slower migrating bands probably represent the mature form of the receptor as it exists on the cell surface. For samples from stably transfected MF only one band could be detected which correlated in molecular weight with the slower migrating band of the corresponding transiently transfected HeLa cell samples (Figure 31).

In addition, the mouse anti-human Fas antibodies also recognised two proteins of approximately 55 kDa in size. As these protein bands are present in all of the MF samples regardless of the transfected construct and can also be seen for HeLa samples

after longer exposures, these bands appear to be unrelated to the exogenously expressed receptor chimaeras. The unspecific bands are highlighted Figure 31 by an asterisk.



Figure 30. Composition of artificial stalk regions for TNFR-Fas chimaeras.

Shown are the aa sequences of the stalk regions of TNFR1 and TNFR2 as well as the aa sequences for the 15 aa (TNFR1-S_{GSL15}-TM_{R1}-Fas and TNFR2-S_{GSL15}-TM_{R2}-Fas) and 56 aa (TNFR1-S_{GSL56}-TM_{R1}-Fas and TNFR2-S_{GSL56}-TM_{R2}-Fas) long artificial linkers of the indicated chimaeras. Repetitive glycine-serine motifs are shown in brackets ([GGGS]). Subscript numbers indicate the number of motif repeats.

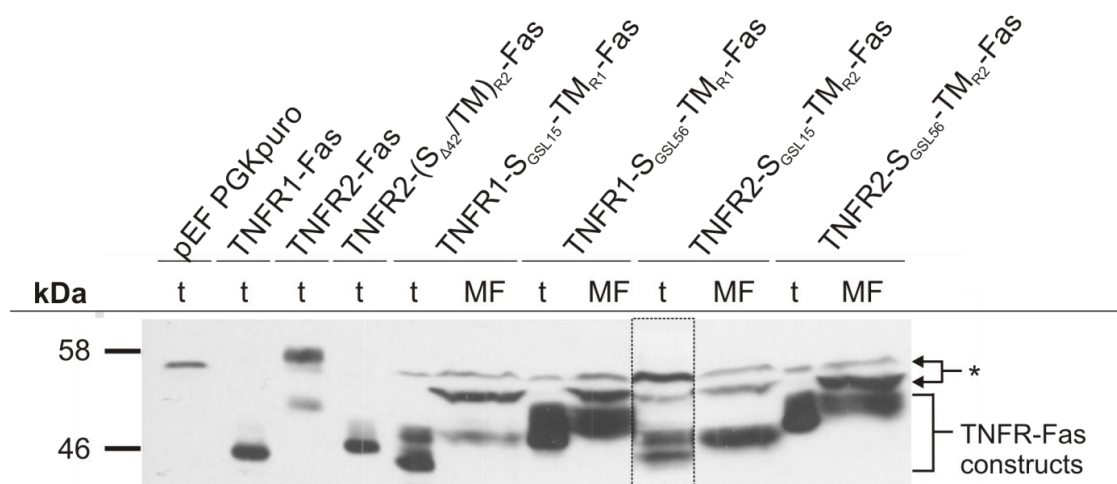


Figure 31. Western Blot analysis of TNFR-Fas chimaeras containing 15 aa and 56 aa long artificial stalk regions.

The stalk regions of TNFR1-Fas and TNFR2-Fas chimaeras were replaced with either 15 aa (TNFR1-S_{GSL15}-TM_{R1}-Fas and TNFR2-S_{GSL15}-TM_{R2}-Fas) or 56 aa (TNFR1-S_{GSL56}-TM_{R1}-Fas and TNFR2-S_{GSL56}-TM_{R2}-Fas) long artificial linkers and the resulting constructs were stably transfected into MF. Whole cell lysates were prepared from 1×10^5 cells and were subjected to SDS-PAGE and Western Blot analysis. Mouse anti-human Fas antibodies clone B10 (1:2000) were used as primary and goat anti-mouse IgG-HRP (1:20000) as secondary antibodies. Transiently transfected HeLa cells (t) served as controls. Unspecific bands are highlighted with an asterisk. Due to low construct expression, for transiently transfected TNFR2-S_{GSL15}-TM_{R2}-Fas a longer exposure time was chosen (rectangle). Data shown represent one experiment.

FACS analysis of the MF was performed to ensure that the different TNFR-Fas chimaeras were expressed on the cell surface. TNFR1-S_{GSL15}-TM_{R1}-Fas (MnX = 244, Figure 32 A), TNFR1-S_{GSL56}-TM_{R1}-Fas (MnX = 255, Figure 32 C), TNFR2-S_{GSL15}-TM_{R2}-Fas (MnX = 128, Figure 33 A) and TNFR2-S_{GSL56}-TM_{R2}-Fas (MnX = 183, Figure 33 C) were all expressed on the cell surface of MF and between 90 % and 99 % of the cells could be gated positive for the respective chimaeras (Figure 32 A and C and Figure 33 A and C).

In order to investigate whether stalk region length influences sTNF responsiveness of TNFR-Fas chimaeras, stably transfected MF were treated with increasing concentrations of the CysTNF or sTNF and cell viability was determined using crystal violet staining. For MF TNFR1-S_{GSL15}-TM_{R1}-Fas (Figure 32 B) and MF TNFR1-S_{GSL56}-TM_{R1}-Fas (Figure 32 D) full responsiveness towards both ligands with very similar ED₅₀ between 0.04 ng/ml and 0.06 ng/ml could be observed. The responsiveness correlated well with the percentages of positive cells that had been determined for these chimaeras (Figure 32 A and C) and was comparable to that of TNFR1-Fas (0.04 ng/ml; see also Figure 11 A).

Approximately 80 % of MF TNFR2-S_{GSL15}-TM_{R2}-Fas (Figure 33 B) and 90 % of MF TNFR2-S_{GSL56}-TM_{R2}-Fas (Figure 33 D) treated were responsive towards CysTNF, which correlated with the receptor cell surface stainings (Figure 33 A and C, respectively). With an ED₅₀ of 0.3-0.4 ng/ml this responsiveness towards CysTNF was comparable to that of MF TNFR2-Fas cells (ED₅₀ = 0.2 ng/ml; see also Figure 11 D). In contrast to MF TNFR2-Fas, both TNFR2-S_{GSL15}-TM_{R2}-Fas and TNFR2-S_{GSL56}-TM_{R2}-Fas were responsive towards sTNF, but with an ED₅₀ of 1.5-2.0 ng/ml this responsiveness to sTNF was approximately 5-fold reduced compared to CysTNF. Similar to MF TNFR2-(S_{Δ42}/TM)_{R2}-Fas cells described in section 3.2, only about 50 – 60 % of the cells were responsive to saturating concentrations of sTNF (Figure 33 B and D), indicating that here also a sub-population of the cells is resistant to sTNF. The cause of the partial unresponsiveness to sTNF remains elusive.

The sTNF responsiveness of TNFR1-S_{GSL15}-TM_{R1}-Fas and TNFR2-S_{GSL15}-TM_{R2}-Fas was comparable to the one observed for the corresponding chimaeras containing the shortened stalk region of TNFR2, TNFR1-(S_{Δ42}/TM)_{R2}-Fas and TNFR2-(S_{Δ42}/TM)_{R2}-Fas (Figure 11 C and Figure 14 B). This sTNF responsiveness, however, did not change when the stalk regions of TNFR1-Fas chimaeras and TNFR2-Fas chimaeras were

replaced with 56 aa long artificial linkers. Therefore, these data indicate that the length of the stalk region does not determine differential responsiveness to sTNF.

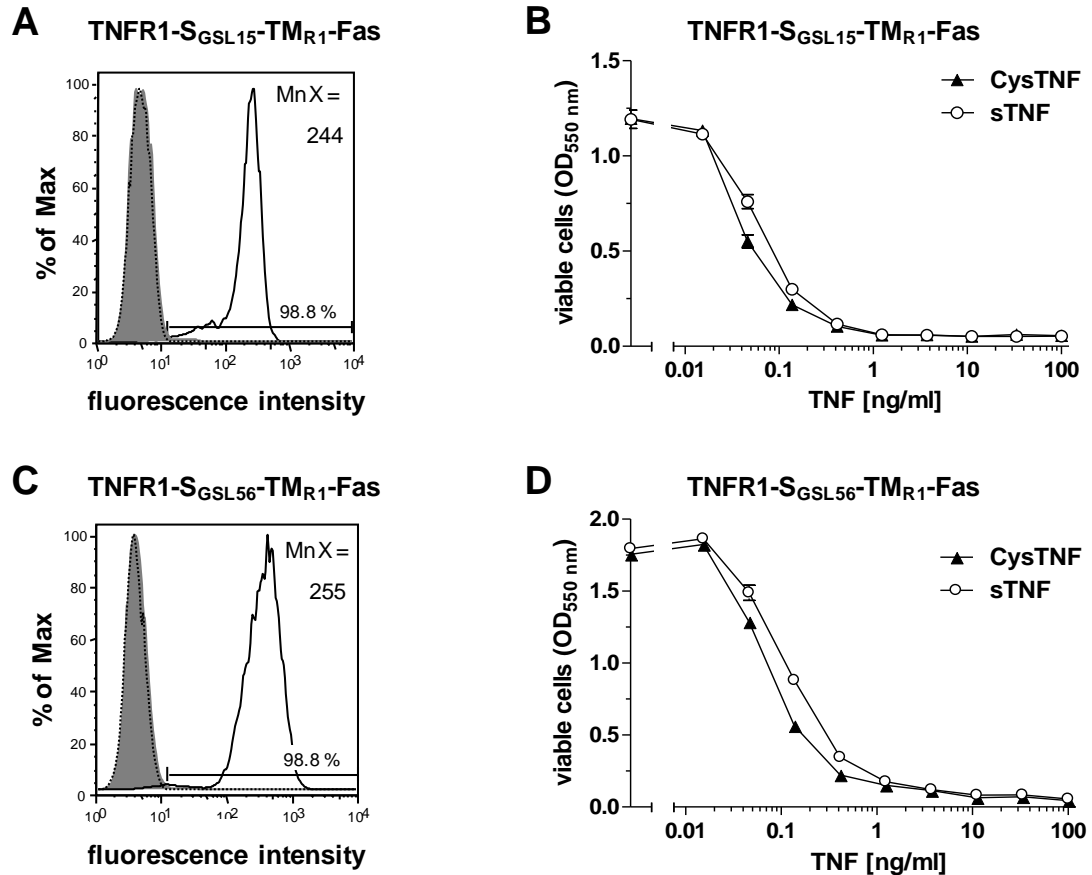


Figure 32. Characterisation of cell surface expression and TNF responsiveness of MF overexpressing TNFR1-Fas chimaeras with artificial stalk regions.

MF were stably transfected with TNFR1-Fas chimaeras containing a 15 aa long glycine/serine linker (MF TNFR1-S_{GSL15}-TM_{R1}-Fas) and a 56 aa long glycine/serine linker (MF TNFR1-S_{GSL56}-TM_{R1}-Fas), respectively. **A and C**) Histograms of MF TNFR1-S_{GSL15}-TM_{R1}-Fas and MF TNFR1-S_{GSL56}-TM_{R1}-Fas. TNFR1-Fas chimaeras were stained on the cell surface using mouse anti-human TNFR1 antibodies (H398) and goat anti-mouse IgG-FITC antibodies (black line). Unstained cells (dotted line); cells only incubated with goat anti-mouse IgG-FITC antibodies (grey). Approximately 99 % of the MF were gated positive for TNFR1-S_{GSL15}-TM_{R1}-Fas and TNFR1-S_{GSL56}-TM_{R1}-Fas, respectively. Acquisition was performed on a Becton Dickinson FACScan flow cytometer. **B and D**) MF TNFR1-S_{GSL15}-TM_{R1}-Fas and MF TNFR1-S_{GSL56}-TM_{R1}-Fas remained untreated or were stimulated with different concentrations of sTNF and CysTNF (0.015-100 ng/ml). Viable cells were stained using crystal violet after 8 h of treatment. Data shown represent three independent experiments.

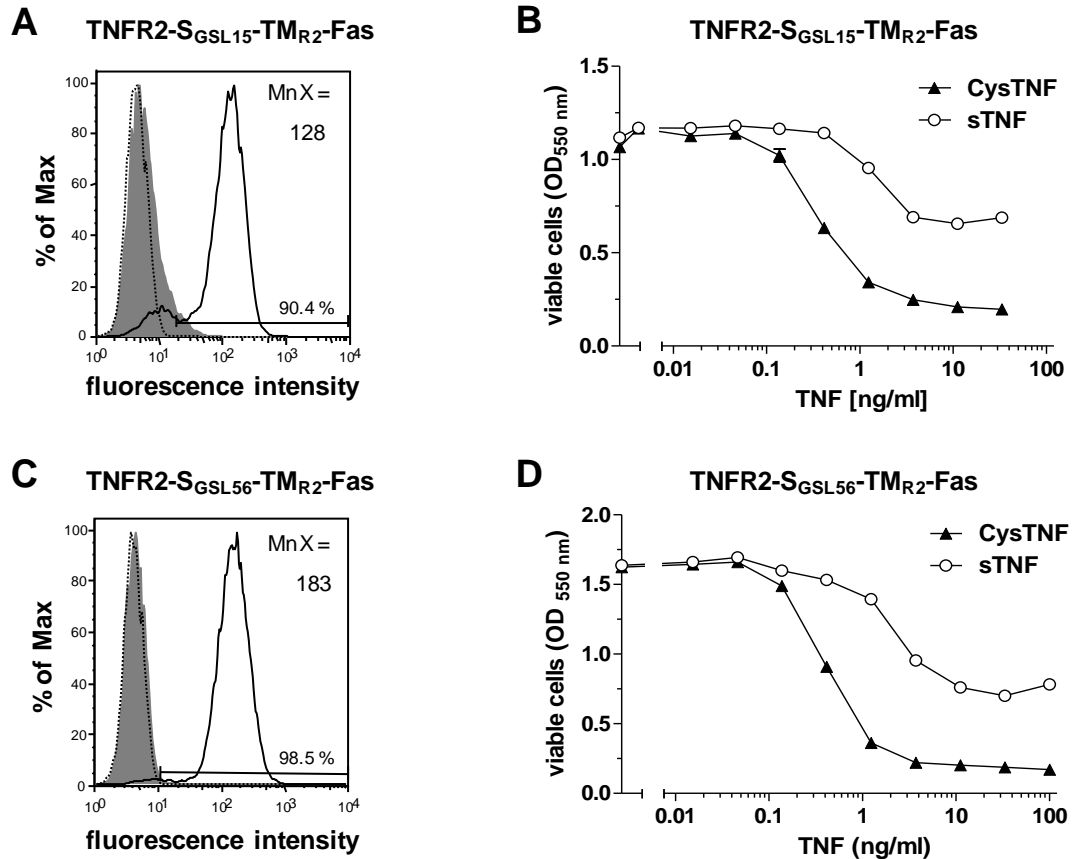


Figure 33. Characterisation of cell surface expression and TNF responsiveness of MF overexpressing TNFR2-Fas chimaeras with artificial stalk regions.

MF were stably transfected with TNFR2-Fas chimaeras containing a 15 aa long glycine/serine linker (MF TNFR2-S_{GSL15}-TM_{R2}-Fas) and a 56 aa long glycine/serine linker (MF TNFR2-S_{GSL56}-TM_{R2}-Fas), respectively. **A and C**) Histograms of MF TNFR2-S_{GSL15}-TM_{R2}-Fas and MF TNFR2-S_{GSL56}-TM_{R2}-Fas. TNFR2-Fas chimaeras were stained on the cell surface using mouse anti-human TNFR2 antibodies (MR2-1) and goat anti-mouse IgG-FITC antibodies (black line). Unstained cells (dotted line); cells only incubated with goat anti-mouse IgG-FITC antibodies (grey). 90.4 % of the MF were gated positive for TNFR2-S_{GSL15}-TM_{R2}-Fas and 98.5 % were gated positive for TNFR2-S_{GSL56}-TM_{R2}-Fas. Acquisition was performed on a Becton Dickinson FACScan flow cytometer. **B and D**) MF TNFR2-S_{GSL15}-TM_{R2}-Fas and MF TNFR2-S_{GSL56}-TM_{R2}-Fas remained untreated or were stimulated with different concentrations of sTNF and CysTNF (0.015-100 ng/ml). Viable cells were stained using crystal violet after 8 h of treatment. Data shown represent three independent experiments.

4.3 Mutagenesis of individual conserved proline residues in the TNFR2 stalk region does not alter responsiveness to sTNF

Sequence alignment of TNFR2 from different mammalian species (*homo sapiens*, *macaca mulatta*, *mus musculus*, *rattus norvegicus*, *canis familiaris* and *equus caballus*) revealed seven conserved proline residues in the TNFR2 stalk region (determined by ClustalW sequence alignment (Chenna *et al.*, 2003)). The conserved proline residues, P205, P211, P219, P231, P233, P237 and P249, are highlighted in Figure 34 A.

In proteins, prolines can adopt two distinct conformations, cis and trans. The conversion of one of these forms into the other can be catalysed by peptidyl prolyl cis-trans isomerases and has been found to function as a molecular switch during some signalling events (reviewed in Lu *et al.*, 2007, Shaw, 2007). Importantly, a member of the cyclophilin family of peptidyl prolyl cis-trans isomerases, cyclophilin B, has been found to be localised not only in the endoplasmic reticulum but also in the plasma membrane (Bukrinsky, 2002, Stumpf *et al.*, 2008), suggesting that prolyl cis-trans isomerisation could potentially play a role in plasma membrane receptor activation.

In addition, O-glycosylation of the TNFR2 stalk region has been described (Pennica *et al.*, 1993) and proline residues are found at positions -1, +1 and +3 relative to the site of O-glycosylation in the majority of proteins with mucin-type O-linked glycosylation (Wilson *et al.*, 1991, Hansen *et al.*, 1995). Therefore, proline residues in the stalk region could also play a role in determining the O-glycosylation status of the stalk region, which in turn might influence the responsiveness towards sTNF.

In order to investigate the role of conserved proline residues of the TNFR2 stalk region in determining sTNF responsiveness, these prolines were exchanged for alanines via two step site directed mutagenesis. Prolines P205, P211, P219, P237 and P249 were each exchanged separately while, for cloning reasons, prolines P231 and P233 were exchanged together. The resulting TNFR2-Fas P205A, TNFR2-Fas P211A, TNFR2-Fas P219A, TNFR2-Fas P231A/P233A, TNFR2-Fas P237A and TNFR2-Fas P249A chimaeras were stably transfected into MF. Whole cell lysates prepared from these cells were analysed via Western Blotting (Figure 34 B). Similar to TNFR2-Fas, the predicted molecular weight for these constructs was approximately 48 kDa (determined using the ProtParam tool on the ExPaSy proteomics server)(Gasteiger *et al.*, 2005).

In Western Blot analysis, for all constructs, except TNFR2-Fas P205A, three bands could be observed, of which the fastest migrating one correlated with the respective predicted molecular weight and represented the putatively not post-translationally modified form of the receptors (Figure 34 B, as indicated). The two slower migrating bands of the TNFR2-Fas variants were approximately 58 kDa - 60 kDa in size (Figure 34 B) and presumably represent the mature forms of the receptors. For the samples from MF TNFR2-Fas P205A only two bands could be observed of which the faster migrating one correlated in size with the predicted molecular weight. The slower migrating band co-migrated with the faster of the two slow migrating bands of the other constructs (Figure 34 B, compare lane 3 with lanes 4 – 8). This indicates that mutation of proline residue P205 affects post-translational modification of TNFR2-Fas. However, these findings would have to be confirmed by comparing lysates from stably and transiently transfected cells.

Using the mouse anti-human Fas antibodies clone B10, which recognises the intracellular portion of Fas, a band of approximately 90 kDa and two 55 kDa protein bands could be detected (Figure 34 B, highlighted by an asterisk). As these protein bands are present in all of the MF whole cell lysates regardless of the receptor mutant, these bands appear to be non-specific for the TNFR2-Fas variants. The 90 kDa band might represent endogenous murine Fas which is recognised by the mouse anti-human Fas antibodies.

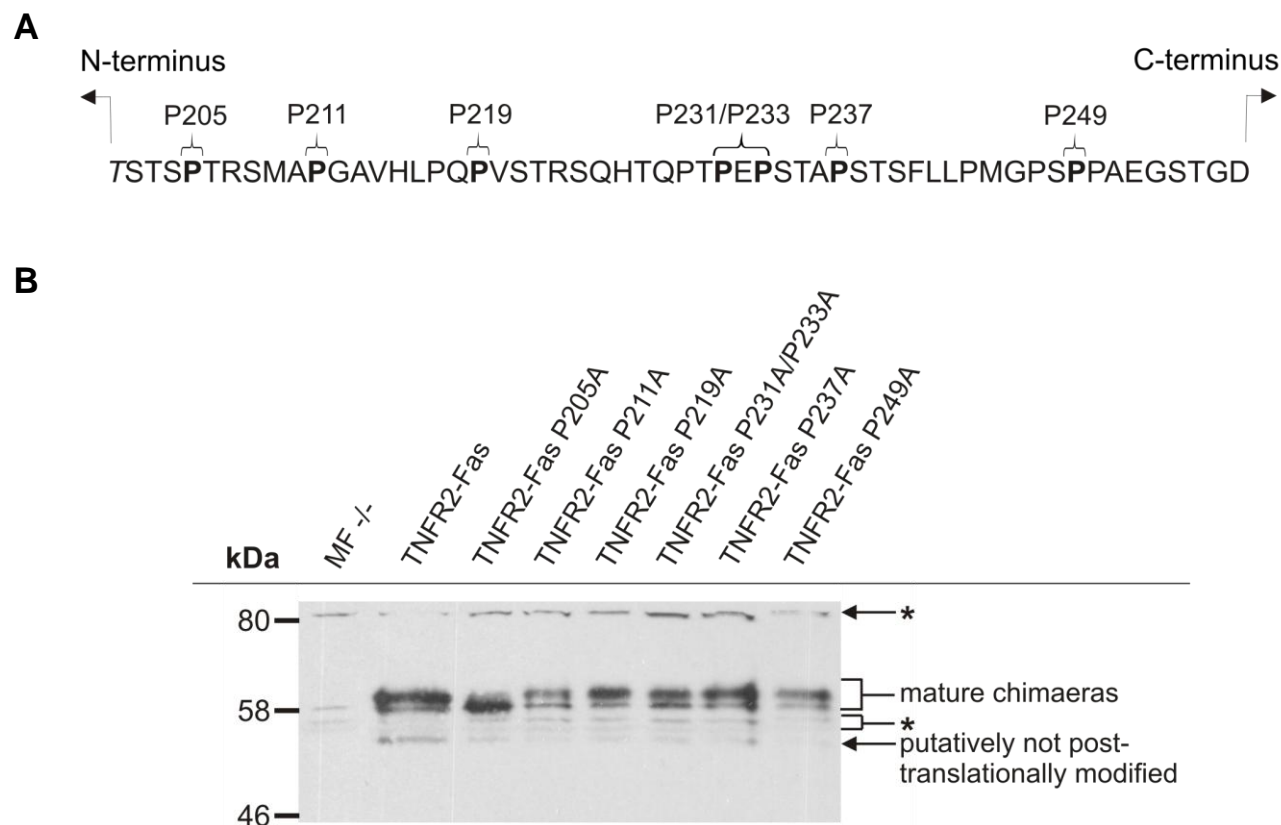


Figure 34. Western Blot analysis of TNFR2-Fas chimaeras in which conserved proline residues of the stalk region had been mutated.

A) Shown is the aa sequence of the TNFR2 stalk region (aa 202–257) and the C-terminal aa residue of CRD4 (*T*, aa 201). Conserved Proline residues are highlighted in bold letters. **B)** Analysis of conserved proline residues in the TNFR2 stalk region. MF were stably transfected with TNFR2-Fas chimaeras in which the indicated proline residues of the TNFR2 stalk region had been exchanged for alanines. Whole cell lysates from 3.3×10^4 cells were prepared and subjected to SDS-PAGE and Western Blot analysis. Mouse anti-human Fas antibodies (clone B10, 1:2000) were used as primary and goat anti-mouse IgG-HRP (1:20000) as secondary antibodies. Untransfected MF and MF TNFR2-Fas served as controls. As indicated, the slower migrating protein bands represent mature receptor chimaeras, whereas the faster migrating protein bands represent putatively not post-translationally modified chimaeric receptors. Unspecific bands are highlighted with an asterisk. Data shown represent one experiment.

Cell surface expression of the various TNFR2-Fas chimaeras, in which conserved proline residues had been exchanged for alanines, was measured by FACS analysis. All six chimaeras were expressed on the cell surface of MF. 89-93 % of the cells could be gated positive for TNFR2-Fas P205A (MnX = 46; Figure 35 A), TNFR2-Fas P211A (MnX = 50; Figure 35 C), TNFR2-Fas P219A (MnX = 115; Figure 35 E), TNFR2-Fas P231A/P233A (MnX = 94; Figure 36 A), TNFR2-Fas P237A (MnX = 122; Figure 36 C) and TNFR2-Fas P249A (MnX = 115; Figure 36 E), respectively. The cell surface expressions of the chimaeras were comparable to the ones observed for TNFR2-(S_{Δ42}/TM)_{R2}-Fas (MnX = 187; Figure 13 A) and TNFR2-S_{GSL15}-TM_{R2}-Fas (MnX = 128; Figure 33 A) or even lower.

The role of conserved prolines in the TNFR2 stalk in controlling receptor responsiveness towards sTNF was determined by stimulating MF, which stably expressed the TNFR2-Fas chimaeras in which the aforementioned prolines had been mutated to alanines, with increasing concentrations of CysTNF or sTNF. Cell viability was determined using crystal violet staining.

60-80 % of MF were responsive to CysTNF with an ED₅₀ of approximately 0.3 ng/ml. This responsiveness towards CysTNF was comparable to that seen in MF TNFR2-Fas cells (EC₅₀ = 0.2 ng/ml; see also Figure 11 D). Similar to MF TNFR2-Fas, these cells were not responsive towards sTNF, even at concentrations as high as 100 ng/ml. This suggests that single conserved proline residues do not determine responsiveness of TNFR2-Fas to sTNF. However, at this point it cannot be excluded that more than one of these conserved proline residues could be involved in controlling sTNF responsiveness. Thus, the effect of simultaneous mutation of several conserved proline residues on sTNF responsiveness remains to be determined.

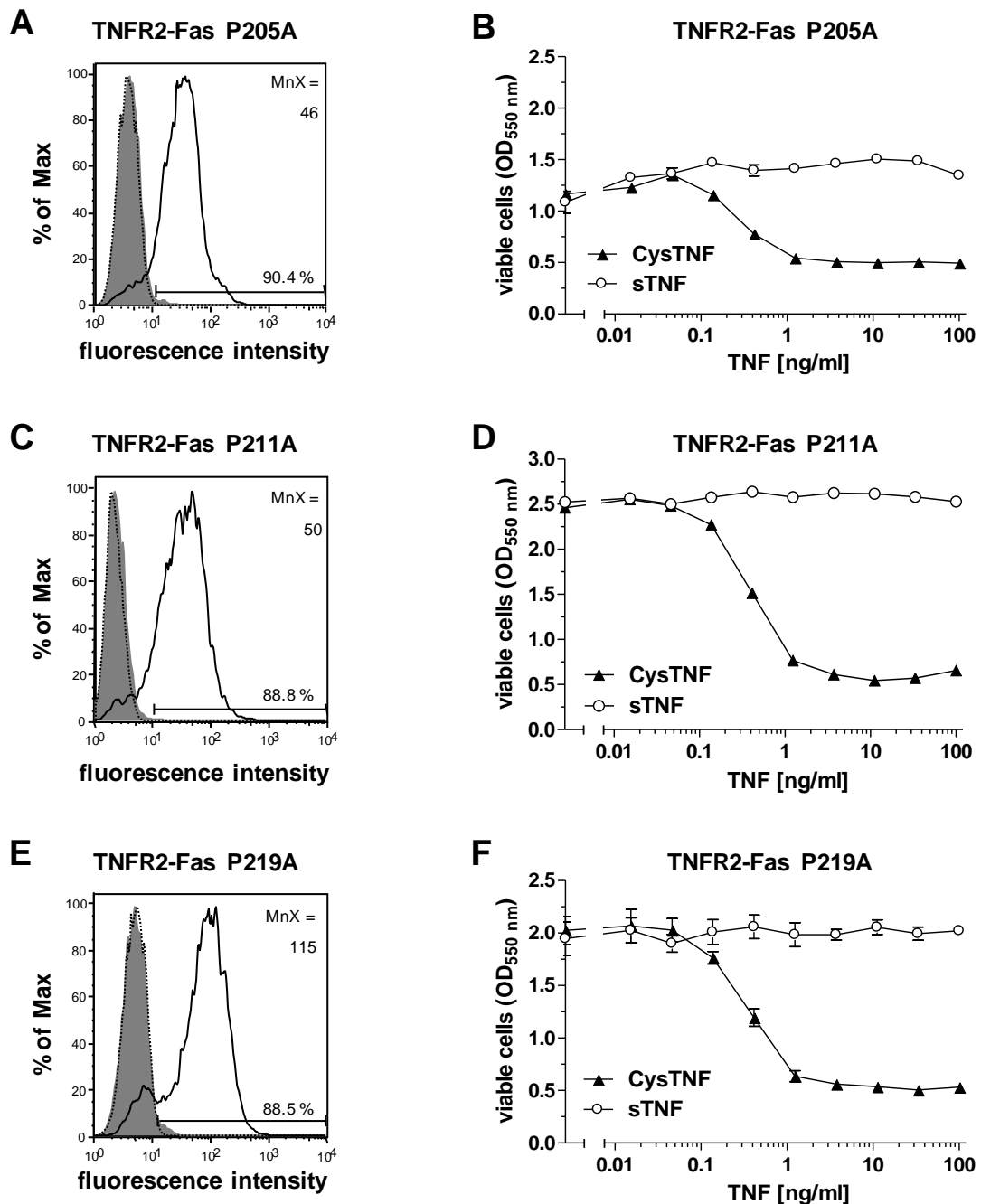


Figure 35. Replacement of the conserved proline residues P205, P211 and P219 in the TNFR2 stalk region does not alter TNF responsiveness.

MF were stably transfected with TNFR2-Fas chimaeras in which conserved proline residues (P205, P211, P219) had been exchanged for alanines via two step site directed mutagenesis. **A, C, and E**) FACS histograms. Chimaeric receptors were stained on the cell surface using mouse anti-human TNFR2 antibodies (MR2-1) and goat anti-mouse IgG-FITC antibodies (black line). Unstained cells (dotted line); cells only incubated with goat anti-mouse IgG-FITC antibodies (grey). As indicated, 89-90 % of MF were gated positive for the corresponding TNFR2-Fas chimaeras. Acquisition was performed on a Becton Dickinson FACScan flow cytometer. MnX are indicated. **B, D and F**) Cell viability assays. MF remained untreated or were stimulated with increasing concentrations of sTNF and CysTNF (0.015-100 ng/ml), respectively, and cell viability was determined using crystal violet staining. Data shown represent B and D) two and F) three independent experiments, respectively.

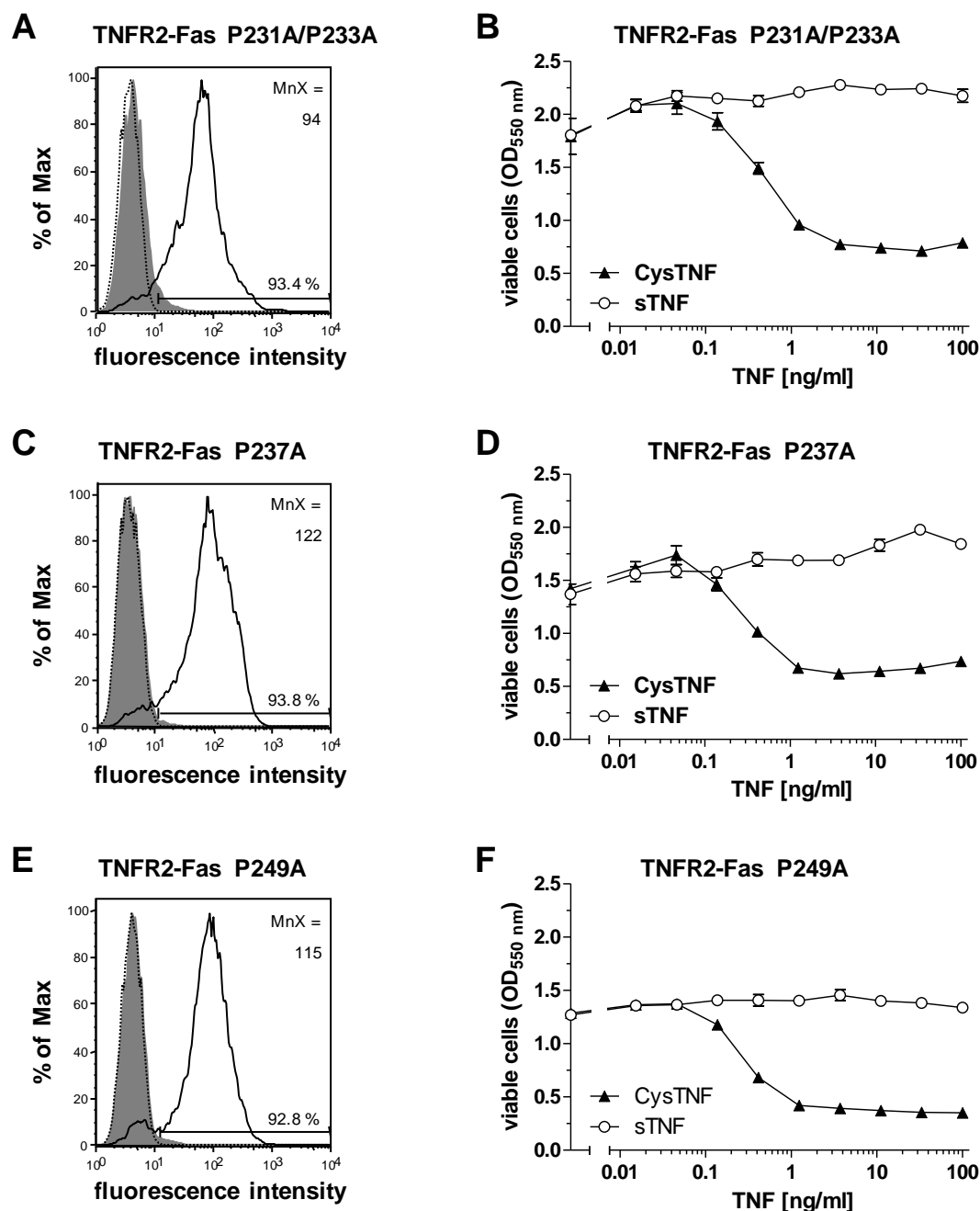


Figure 36. Replacement of the conserved proline residues P231, P233, P237 and P249 in the TNFR2 stalk region does not alter TNF responsiveness.

MF were stably transfected with TNFR2-Fas chimaeras in which conserved proline residues (P231/P233, P237 and P249) had been exchanged for alanines via two step site directed mutagenesis. **A, C, and E**) FACS histograms. Chimaeric receptors were stained on the cell surface using mouse anti-human TNFR2 antibodies (MR2-1) and goat anti-mouse IgG-FITC antibodies (black line). Unstained cells (dotted line); cells only incubated with goat anti-mouse IgG-FITC antibodies (grey). As indicated, 88.5-90.4 % of MF were gated positive for the corresponding TNFR2-Fas chimaeras. Acquisition was performed on a Becton Dickinson FACScan flow cytometer. MnX are indicated. **B, D and F**) Cell viability assays. MF remained untreated or were stimulated with increasing concentrations of sTNF and CysTNF (0.015-100 ng/ml), respectively, and cell viability was determined using crystal violet staining. Data shown represent three independent experiments.

4.4 Influence of the O-glycosylation status of the TNFR2 stalk region on responsiveness towards sTNF

In addition to its high proline residue content, the TNFR2 stalk region is also rich in serine and threonine residues, of which several could be identified as potential sites of mucin-type O-glycosylation using the bioinformatic tool NetOglyc (Julenius *et al.*, 2005) and a supported vector machine (SVM) programme (Li *et al.*, 2006)(see Figure 37 A). O-glycosylation occurs on serine or threonine residues, which are generally found in clusters with a β -turn near proline and at a distance from charged aa residues (Elhammer *et al.*, 1993).

O-glycosylation has been reported to be involved in protein trafficking, delivery and stabilisation at the cell surface (reviewed in Tian and Ten Hagen, 2009). Park and Tenner (2003), for example, described O-glycosylation of the C1qRP/CD93 receptor to be required for its stable cell surface expression.

O-glycosylation of the stalk region of TRAIL receptor 2, another member of the TNF receptor superfamily, has been found to influence the sensitivity of the receptor to its ligand and the ability of the receptor to signal for apoptosis (Wagner *et al.*, 2007). O-glycosylation has also been described in the stalk region of TNFR2 (Pennica *et al.*, 1993), but whether it plays a role in sTNF responsiveness is not known to date. Therefore, the aim was to identify sites of O-glycosylation in the TNFR2 stalk region and to investigate the role of stalk region O-glycosylation in sTNF responsiveness

4.4.1 sTNF responsiveness of TNFR2-Fas chimaeras after site-directed mutagenesis of predicted O-glycosylation sites

The role of O-glycosylation of the stalk region in TNFR2 responsiveness towards sTNF was investigated using TNFR2-Fas chimaeras with point mutations in putative O-glycosylation sites. For this purpose several expression vectors containing TNFR2-Fas chimaeras in which potential O-glycosylation sites were mutated to alanines or, in the case of T235, to an arginine had been generated previously (Dr Andrea Zappe/Dr Anja Krippner-Heidenreich, University of Stuttgart, Germany). Due to the large number of potential O-glycosylation sites, six potential O-glycosylation motifs had been defined (motifs 1-6, Figure 37 A). Expression vectors containing TNFR2-Fas chimaeras, in

which potential glycosylation sites of the following motifs and/or motif combinations were mutated, had been created: motif 1 (TNFR2-Fas mot. 1), motif 1 and 2 (TNFR2-Fas mot. 1/2), motifs 1, 2 and 3 (TNFR2-Fas mot. 1/2/3), motifs 1 and 4 (TNFR2-Fas mot. 1/4) and motifs 1 and 5 (TNFR2-Fas mot. 1/5).

As a quick and easy screening method for the effect of the mutation of potential O-glycosylation sites the resulting chimaeras were transiently transfected into HeLa cells as described in section 2.4.1 and whole cell lysates were prepared and receptors were analysed for their migration properties by Western Blotting (Figure 37 B). The plain expression vector pEF-PGK/puroA and the stalk region deletion mutant TNFR2-(S_{Δ42}/TM)_{R2}-Fas served as negative controls, while the TNFR2-Fas chimaera served as positive control. All chimaeric receptors mutated in the potential O-glycosylation motifs (Figure 37 B, lanes 4 - 8) showed an intermediate phenotype for their molecular weight, migrating between the fully glycosylated and the putatively non-glycosylated forms of TNFR2-Fas (Figure 37 B, lane 2). Again, as mentioned in section 3.2, the faster migrating protein band might represent receptors which had been translated but not undergone any post-translational modifications yet.

As TNFR2-Fas motif 1 and motifs 1/4 represent receptor mutants with minimal mutations but greatest mobility, residues mutated in motif 1 and motif 4 are most likely to be sites of O-glycosylation. Furthermore, the Western Blot analysis revealed decreased molecular weights for chimaeras, in which motifs 1, 2 and 3 and motifs 1 and 5, respectively, had been mutated, suggesting that these motifs are likely to be also O-glycosylated in TNFR2-Fas.

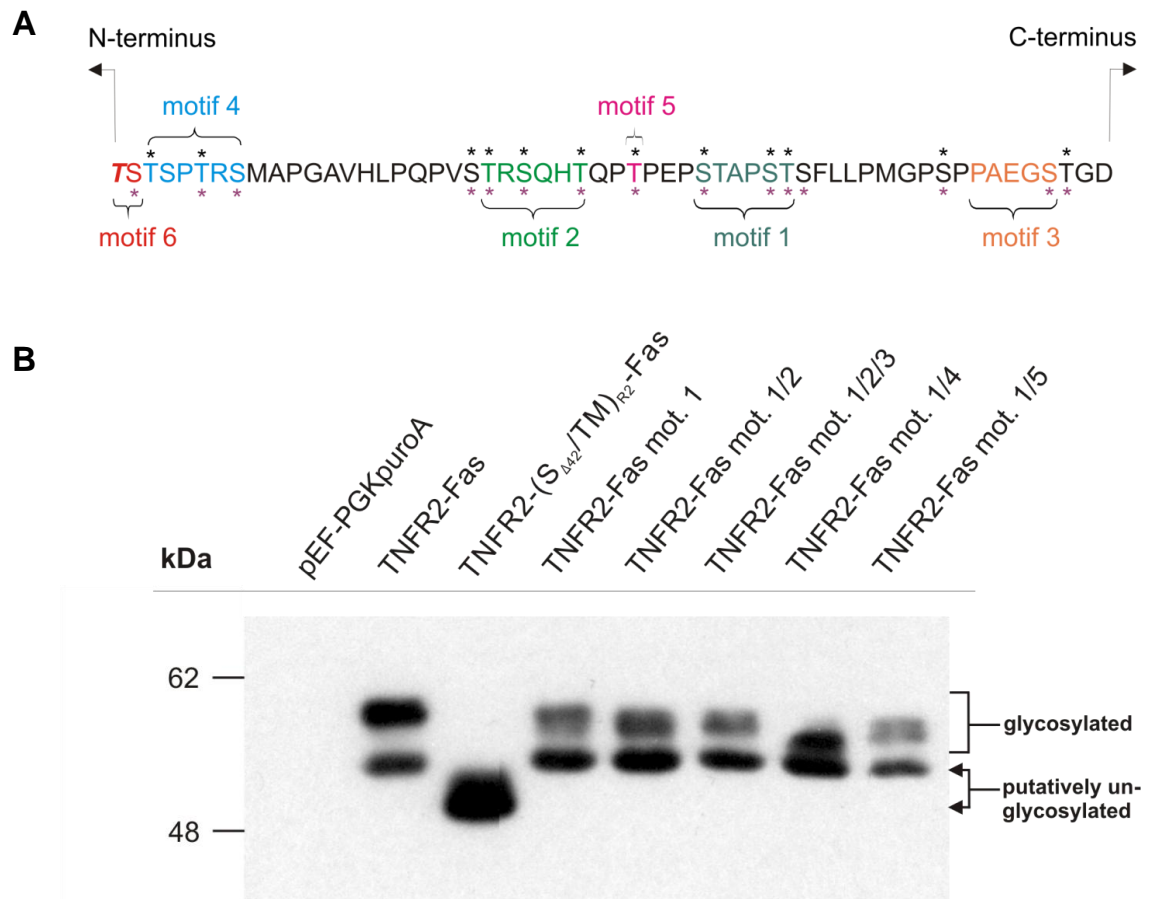


Figure 37. Characterisation of putative O-glycosylation sites within the TNFR2 stalk region.

A) Shown is the aa sequence of the TNFR2 stalk region (aa 202–257) and the C-terminal aa of CRD4 (**T**, aa 201). Putative O-glycosylation sites are marked with black stars (predicted by NetOGlyc) and/or purple stars (predicted by SVM programme). **B)** Analysis of putative O-glycosylation motifs in the TNFR2 stalk region. HeLa cells were transiently transfected with TNFR2-Fas chimaeras in which serine and threonine residues of indicated potential O-glycosylation clusters (motifs 1-5) in the TNFR2 stalk region had been mutated to alanines. In motif 1 T235 had been exchanged for an arginine. Whole cell lysates were prepared from these cells and an equivalent of 3.3×10^4 cells was used for SDS-PAGE and Western Blot analysis. Mouse anti-human Fas antibodies (clone B10, 1:2000) were used as primary and goat anti-mouse IgG-HRP (1:20000) as secondary antibodies. HeLa cells transiently transfected with TNFR2-(S_{Δ42}/TM)_{R2}-Fas, TNFR2-Fas or the plain expression vector (pEF-PGKpuroA) served as controls. As indicated, the slower migrating protein bands represent fully and partially glycosylated receptor chimaeras, respectively, whereas the faster migrating protein bands represent putatively un-O-glycosylated chimaeric receptors. Data shown are representative of three independent experiments.

MF stably transfected with chimaeras, in which the serine and threonine residues of motifs 1, 2 and 3 (MF TNFR2-Fas mot. 1/2/3) were exchanged for alanines, had been generated by Dr Andrea Zappe. In addition, MF stably transfected with chimaeras, in which all serine and threonine residues of motifs 1 and 5 (MF TNFR2-Fas mot. 1/5) were exchanged for alanines, have been generated as part of this PhD project. Both, TNFR2-Fas mot. 1/2/3 (MnX = 18; Figure 38 A) and TNFR2-Fas mot. 1/5 (MnX = 90; Figure 38 C) were expressed on the cell surface and were fully responsive to CysTNF with an $ED_{50} = 0.15$ ng/ml for TNFR2-Fas mot. 1/2/3 (Figure 38 B) and an $ED_{50} = 0.09$ ng/ml for TNFR2-Fas mot. 1/5 (Figure 38 D). However, no responsiveness towards sTNF could be observed for either construct (Figure 38 B and D, respectively), indicating that these motifs are involved in determining O-glycosylation but not sTNF responsiveness of TNFR2.

Despite high intracellular protein expression of the TNFR2-Fas mot. 1/4 chimaera, cell surface expression of this construct could be detected neither for transiently transfected HeLa cells nor for stably transfected MF (data not shown). Therefore, an analysis of the sTNF responsiveness of the TNFR2-Fas mot. 1/4 variant was not possible.

Taken together, these experiments did not reveal single O-glycosylation motifs inhibiting sTNF responsiveness of TNFR2. However, further combinations of mutated O-glycosylation motifs have yet to be tested.

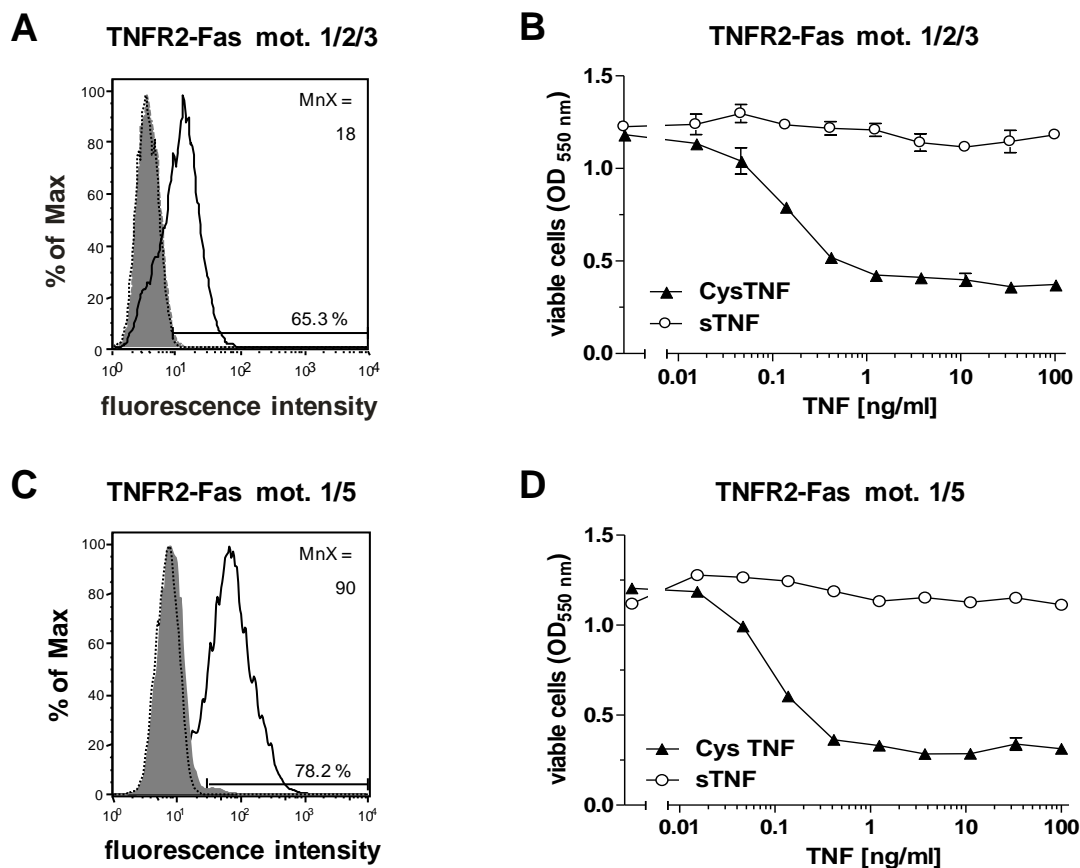


Figure 38. Characterisation of cell surface expression and TNF responsiveness of MF TNFR2-Fas with reduced O-glycosylation.

A and C) FACS Histograms of MF stably transfected with TNFR2-Fas mot. 1/2/3 (MF TNFR2-Fas mot. 1/2/3) and TNFR2-Fas mot. 1/5 (MF TNFR2-Fas mot. 1/5) expression constructs. TNFR2-Fas chimaeras were stained on the cell surface using mouse anti-human TNFR2 antibodies (MR2-1) and goat anti-mouse IgG-FITC antibodies (black line). Unstained cells (dotted line); cells only incubated with goat anti-mouse IgG-FITC antibodies (grey). 65 % of the MF were gated positive for TNFR2-Fas mot. 1/2/3 and 91 % were gated positive for TNFR2-Fas mot. 1/5. Acquisition was performed on a Becton Dickinson FACScan flow cytometer. **B and D)** MF TNFR2-Fas mot. 1/2/3 and MF TNFR2-Fas mot. 1/5 remained untreated or were stimulated with different concentrations of sTNF and CysTNF (0.015-100 ng/ml), respectively, and cell viability was determined using crystal violet staining. Data shown represent three independent experiments.

4.4.2 sTNF responsiveness of TNFR-Fas chimaeras upon inhibition of core 1/core 2 O-glycosylation

The mutation of putative O-glycosylation sites in the TNFR2 stalk region did not reveal a role for TNFR2 stalk region O-glycosylation in the control of receptor responsiveness towards sTNF so far. However, we were not able to analyse all putative O-glycosylation sites yet and Western Blot analysis data suggest that the tested O-glycosylation mutants are not fully un-O-glycosylated (Figure 37 B). Therefore, to complement our data, we used an O-glycosylation inhibitor to shed light onto the potential role of mucin-type O-glycosylation in sTNF responsiveness.

Mucin-type O-glycosylation is initiated by the addition of a GalNAc residue to the hydroxyl group of a serine or threonine residue of the protein substrate. The formation of core 1 and core 2 O-glycosylation, two of the early steps during the O-glycosylation of most proteins with mucin-type O-glycosylation, is then dependent on the addition of another GalNAc residue by β -1,3-N-galactosyltransferase (reviewed in Tian and Ten Hagen, 2009). Benzyl- α -GalNAc is a structural analog of GalNAc (see Figure 9) and, therefore, can function as a competitive inhibitor for β -1,3-galactosyltransferase-dependent core 1 and core 2 O-glycosylation (Kuan *et al.*, 1989).

To address the question whether overall core 1/core 2 O-glycosylation affects the responsiveness of TNFR towards sTNF, MF stably transfected with TNFR1-Fas and TNFR2-Fas were cultivated in the presence of 3.5 mM Benzyl- α -GalNAc for three days and four days, respectively. MF TNFR2-S_{GSL56}-TM_{R2}-Fas were cultivated in the presence 3.5 mM Benzyl- α -GalNAc for four days and served as negative control. Western Blot analysis and cell viability assays were performed on days 4 and 5. Cells incubated with 0.55 % (v/v) DMSO served as solvent control (see also section 2.11).

For the Benzyl- α -GalNAc treated cells Western Blot analysis revealed a much stronger decrease in molecular weight for TNFR2-Fas than for TNFR1-Fas in comparison to the corresponding solvent controls on both, day 4 and day 5 (Figure 39). No comparable decrease in molecular weight could be observed after Benzyl- α -GalNAc treatment of MF TNFR2-S_{GSL56}-TM_{R2}-Fas, in which the stalk region had been replaced by a 56 amino acid long artificial linker. These data indicate that the Benzyl- α -GalNAc treatment did not only lead to an overall reduction in O-glycosylation, but also that it is indeed the stalk region of the parental TNFR2-Fas chimaera which is O-glycosylated.

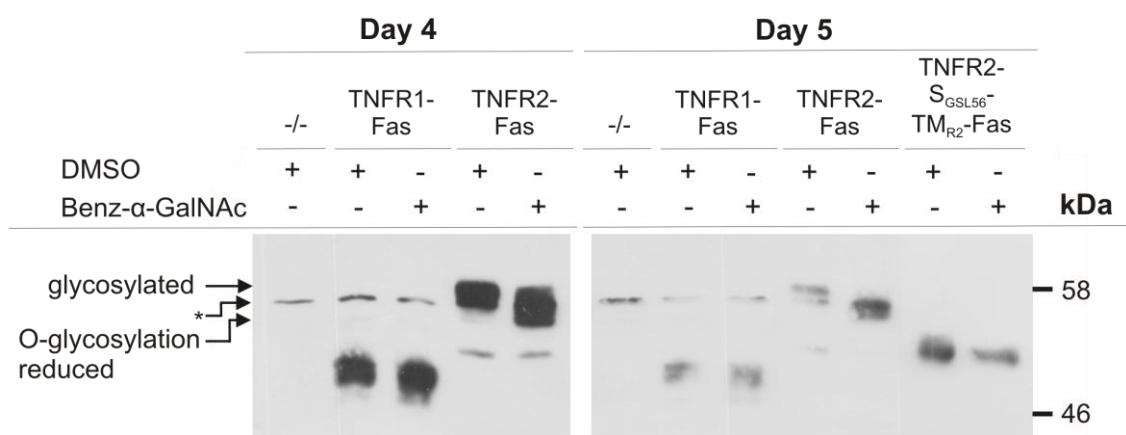


Figure 39. O-glycosylation in the TNFR2-Fas stalk region can be inhibited by Benzyl-2-acetamido-2-deoxy- α -D-galactopyranoside.

MF stably transfected with TNFR2-Fas, TNFR1-Fas and TNFR2-S_{GSL56}-TM_{R2}-Fas were cultivated in the presence of 0.55 % (v/v) DMSO or 3.5 mM Benzyl-2-acetamido-2-deoxy- α -D-galactopyranoside (Benzyl- α -GalNAc) for 3 days and 4 days, respectively. Cells were re-seeded and whole cell lysates were prepared on days 4 and 5. An equivalent of approximately 3.3×10^4 cells was used for SDS-PAGE and Western Blot analysis. Mouse anti-human Fas antibodies (clone B10, 1:2000) were used as primary and goat anti-mouse IgG-HRP (1:20000) as secondary antibodies. Untransfected MF $-/-$ served as negative control. As indicated, the faster migrating protein bands represent receptor chimaeras with reduced O-glycosylation, whereas the slower migrating protein bands represent chimaeric receptors in which O-glycosylation is not reduced. Unspecific bands are highlighted with an asterisk. Data shown represent two independent experiments.

The cell surface expression of both, TNFR1-Fas and TNFR2-Fas chimaeras remained comparable between untreated cells, solvent control and Benzyl- α -GalNAc treated cells (MnX = 104-152 for TNFR1-Fas; Figure 40 A, C and E; MnX = 213-247 for TNFR2-Fas; Figure 41 A, C and E). Responsiveness towards TNF was not affected by Benzyl- α -GalNAc treatment in MF TNFR1-Fas (Figure 40 B, D and F) and MF TNFR2-Fas (Figure 41 B, D and F). TNFR1-Fas remained responsive to both, CysTNF (ED₅₀ = 0.03-0.04 ng/ml) and sTNF (ED₅₀ = 0.04-0.08 ng/ml), while TNFR2-Fas was only responsive towards CysTNF (ED₅₀ = 0.3-0.5 ng/ml) but not sTNF. These data indicate that core 1 and core 2 dependent O-glycosylation is unlikely to be a determining factor for the differential responsiveness of TNFR2 to sTNF.

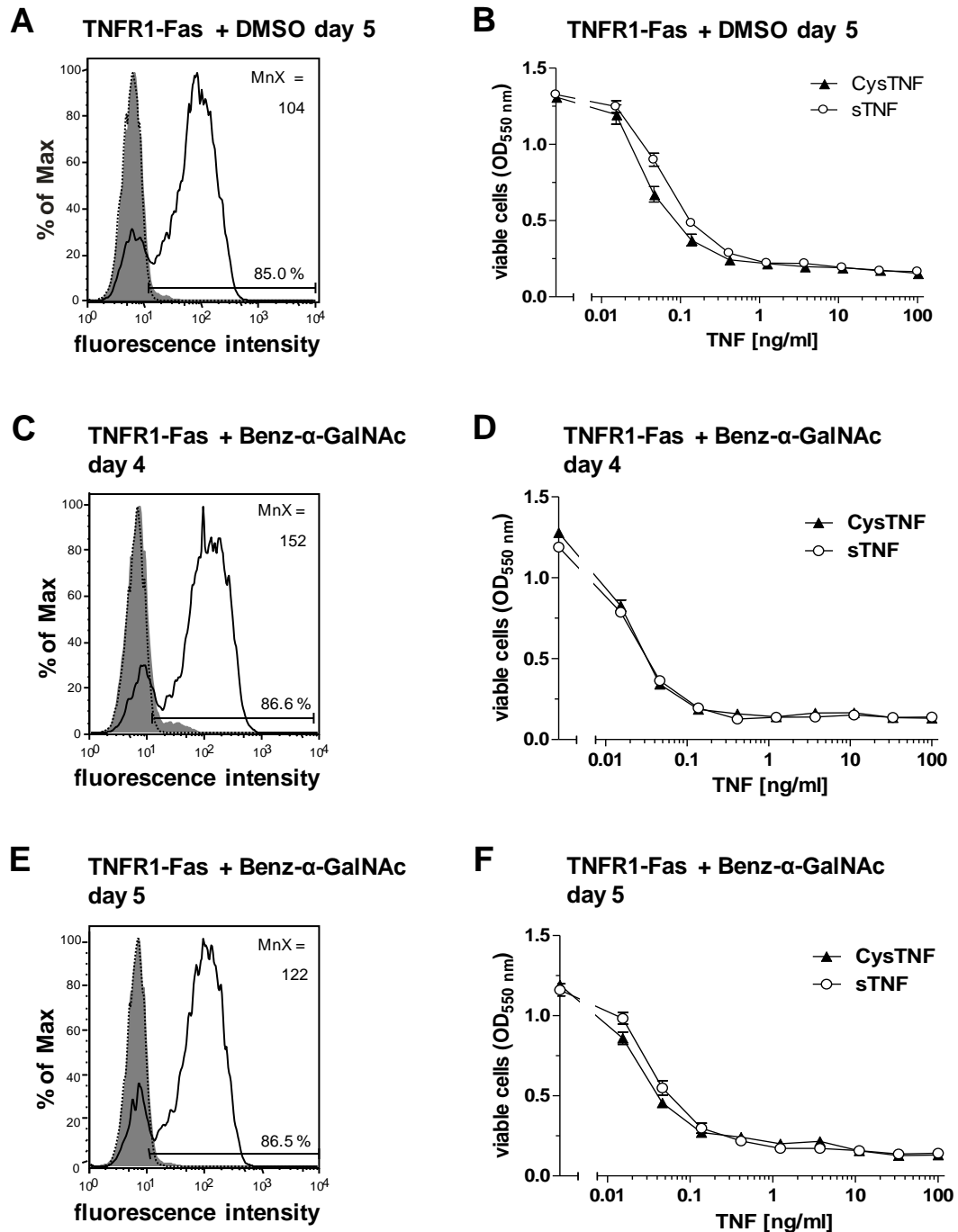


Figure 40. Inhibition of core 1/2 O-glycosylation does not alter sTNF responsiveness in MF TNFR1-Fas.

MF stably transfected with TNFR1-Fas were cultivated in the presence of 0.55 % (v/v) DMSO for 5 days (A and B) or in the presence of 3.5 mM Benzyl-2-acetamido-2-deoxy- α -D-galactopyranoside (Benzyl- α -GalNAc) for 4 days (C and D) and 5 days (E and F), respectively. **A, C and E**) FACS Histogram. TNFR1-Fas chimaeras were stained on the cell surface using mouse anti-human TNFR1 antibodies (H398) and goat anti-mouse IgG-FITC antibodies (black line). Unstained cells (dotted line); cells only incubated with goat anti-mouse IgG-FITC antibodies (grey). 85-86 % of the MF were gated positive for TNFR1-Fas. Acquisition was performed on a Becton Dickinson FACScan flow cytometer. **B, D and F**) Responsiveness to CysTNF and sTNF. Cells remained untreated or were stimulated with different concentrations of sTNF and CysTNF (0.015-100 ng/ml), respectively, and cell viability was determined using crystal violet staining. Data shown represent two independent experiments.

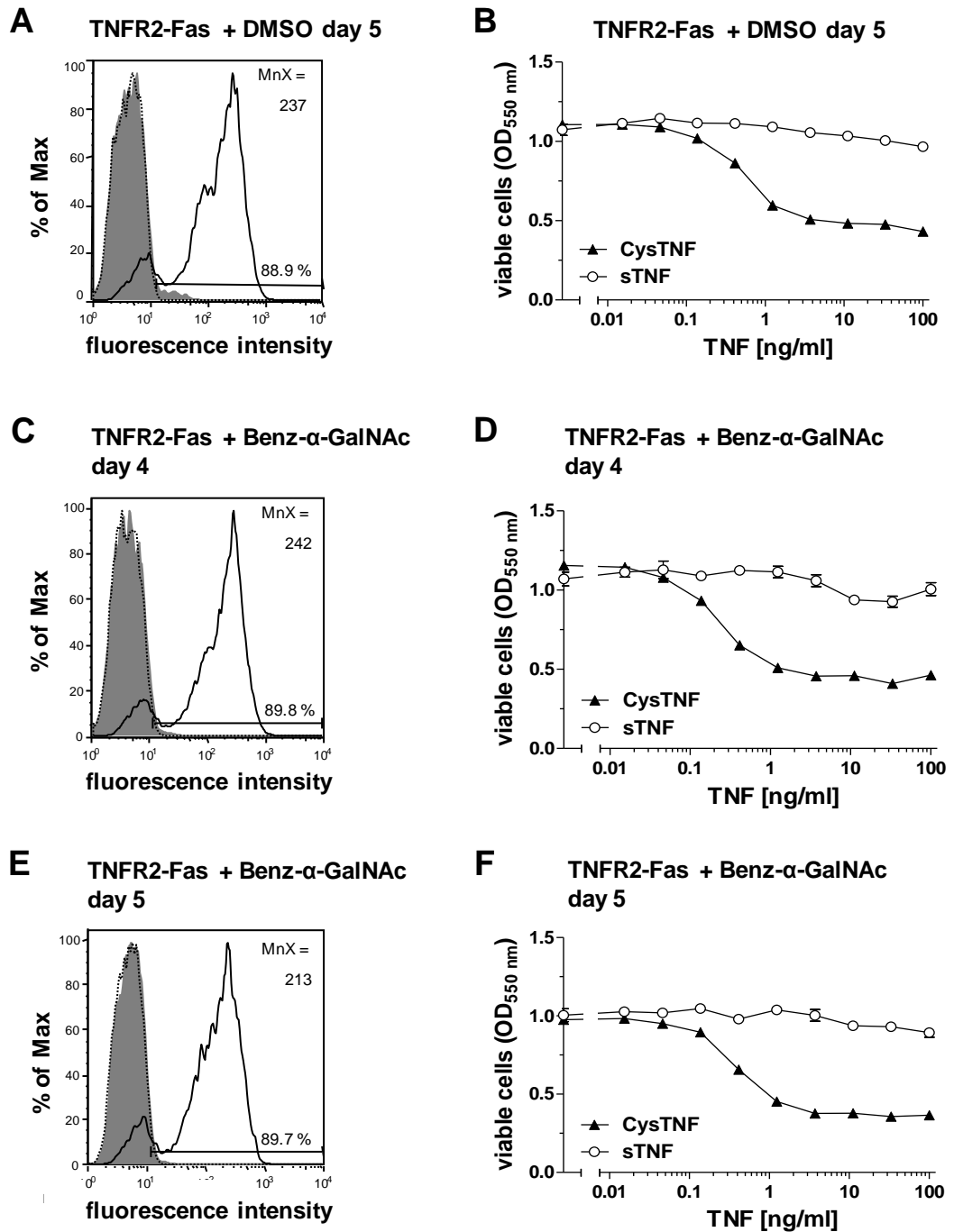


Figure 41. Inhibition of core 1/2 O-glycosylation does not alter TNF responsiveness in MF TNFR2-Fas.

MF stably transfected with TNFR2-Fas were cultivated in the presence of 0.55 % (v/v) DMSO for 5 days (A and B) or in the presence of 3.5 mM Benzyl-2-acetamido-2-deoxy- α -D-galactopyranoside (Benzyl- α -GalNAc) for 4 days (C and D) and 5 days (E and F), respectively. **A, C and E**) FACS Histogram. TNFR2-Fas chimaeras were stained on the cell surface using mouse anti-human TNFR2 antibodies (MR2-1) and goat anti-mouse IgG-FITC antibodies (black line). Unstained cells (dotted line); cells only incubated with goat anti-mouse IgG-FITC antibodies (grey). 90 % of the MF were gated positive for TNFR2-Fas. Acquisition was performed on a Becton Dickinson FACScan flow cytometer. **B, D and F**) Responsiveness to CysTNF and sTNF. Cells remained untreated or were stimulated with different concentrations of sTNF and CysTNF (0.015-100 ng/ml), respectively, and cell viability was determined using crystal violet staining. Data shown represent two independent experiments.

4.5 Effect of partial replacement of the TNFR2 stalk region on sTNF responsiveness

The data described in sections 4.2, 4.3 and 4.4, further confirmed a critical role for the TNFR2 stalk region in determining responsiveness towards sTNF. However, so far this effect could not be assigned to one specific molecular feature of this region. Therefore, to narrow down which section of the stalk region controls sTNF responsiveness, the stalk region of TNFR2-Fas chimaeras was partly replaced with artificial glycine-serine-linkers. These linkers were between 17 aa and 22 aa in length and were overlapping by five to nine aa residues (see Table 11). Four different TNFR2-Fas chimaeras were generated, in which the following aa residues were substituted: aa 202-219 in TNFR2-(S_{Exaa202-219}/TM)_{R2}-Fas, aa 215-232 in TNFR2-(S_{Exaa215-232}/TM)_{R2}-Fas, aa 228-249 in TNFR2-(S_{Exaa228-249}/TM)_{R2}-Fas and aa 241-257 in TNFR2-(S_{Exaa241-257}/TM)_{R2}-Fas. These constructs were generated as described in section 2.2.8 and stably transfected into MF.

The correct molecular weight of the constructs was confirmed via Western Blot analysis using whole cell lysates from transiently transfected HeLa cells and stably transfected MF (Figure 42). For the HeLa cell lysates two protein bands could be observed for all partial stalk replacement mutants. Again, the faster migrating protein bands presumably represented receptors which had not been post-translationally modified while the slower migrating bands most likely represented the mature forms of the constructs (Figure 42).

For the stably transfected MF only the presumably post-translationally modified band could be observed which co-migrated with the slower migrating band of the corresponding transiently transfected HeLa cell samples (Figure 41). Unspecific bands, which were also recognised by the mouse anti-human Fas antibodies, are highlighted by an asterisk (Figure 41).

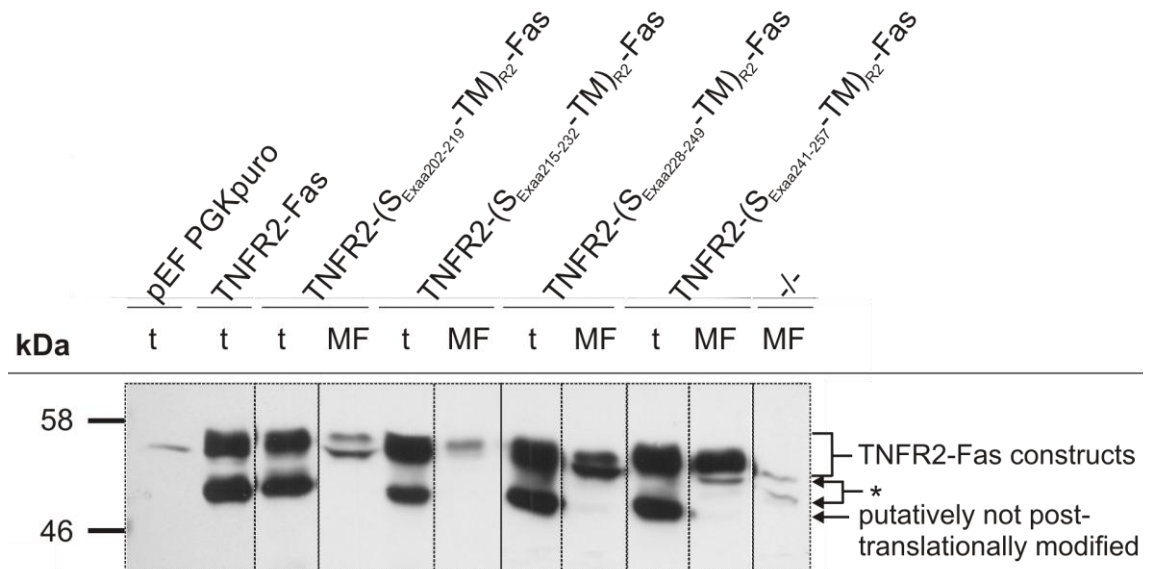


Figure 42. Western Blot analysis of TNFR2-Fas chimaeras with partially substituted stalk regions.

The receptor constructs TNFR2-(S_{Exaa202-219}/TM)_{R2}-Fas, TNFR2-(S_{Exaa215-232}/TM)_{R2}-Fas, TNFR2-(S_{Exaa228-249}/TM)_{R2}-Fas and TNFR2-(S_{Exaa241-257}/TM)_{R2}-Fas were transiently transfected into HeLa cells or stably transfected into MF. Whole cell lysates were prepared from these cells. For HeLa cells an equivalent of approximately 2.5×10^4 cells and for MF an equivalent of approximately 5×10^4 cells were used for SDS-PAGE and Western Blot analysis. Mouse anti-human Fas antibodies (clone B10, 1:2000) were used as primary and goat anti-mouse IgG-HRP (1:20000) as secondary antibodies. TNFR2-(S_{Δ42}/TM)_{R2}-Fas, TNFR2-Fas and the plain expression vector (pEF-PGKpuro) served as controls. As indicated, the slower migrating protein bands represent the mature receptor chimaeras, whereas the faster migrating protein bands represent putatively not post-translationally modified chimaeric receptors. Shown are re-arranged Western Blot data from the same exposure. Data shown represent one experiment.

As a next step, cell surface expression of the chimaeras was confirmed by FACS analysis. All four TNFR2-Fas chimaeras, in which the stalk region had been partly substituted with glycine and serine residues, were expressed on the cell surface of stably transfected MF (Figure 43 A and C). 76 % of the cells showed cell surface expression of TNFR2-(S_{Exaa202-219}/TM)_{R2}-Fas (Figure 43 A) and 91 % of the cells were gated positive for TNFR2-(S_{Exaa215-232}/TM)_{R2}-Fas (Figure 43 C). 92 % of the cells were gated positive for TNFR2-(S_{Exaa228-249}/TM)_{R2}-Fas (Figure 43 E) and 77 % of the cells were gated positive for TNFR2-(S_{Exaa241-257}/TM)_{R2}-Fas (Figure 43 G). With the exception of the data for TNFR2-(S_{Exaa202-219}/TM)_{R2}-Fas, which were acquired on a FACScan flow cytometer, acquisition of the flow cytometric data was performed on a Becton Dickinson FACSCanto II flow cytometer. A comparison of data acquired on these two flow cytometers showed that MnX were approximately 10-fold higher when the Becton Dickinson FACSCanto II flow cytometer was used as opposed to the FACScan flow cytometer (data not shown). Therefore, the MnX of TNFR2-(S_{Exaa202-219}/TM)_{R2}-Fas and TNFR2-(S_{Exaa215-232}/TM)_{R2}-Fas were comparable (MnX = 1504 for TNFR2-(S_{Exaa202-219}/TM)_{R2}-Fas and MnX = 137 TNFR2-(S_{Exaa215-232}/TM)_{R2}-Fas; Figure 43 A and C), while with MnX of 3096 and 11609, respectively, MF TNFR2-(S_{Exaa228-249}/TM)_{R2}-Fas and MF TNFR2-(S_{Exaa241-257}/TM)_{R2}-Fas showed both higher cell surface expression of the respective chimaeras (Figure 43 E and G).

MF stably expressing these partial stalk replacement variants were treated with increasing concentrations of CysTNF or sTNF and cell viability was determined using crystal violet staining. Approximately 50 % of MF TNFR2-(S_{Exaa202-219}/TM)_{R2}-Fas treated were responsive to CysTNF while about 70 % of MF TNFR2-(S_{Exaa215-232}/TM)_{R2}-Fas and MF TNFR2-(S_{Exaa228-249}/TM)_{R2}-Fas showed responsiveness towards this ligand at high concentrations. For MF TNFR2-(S_{Exaa241-257}/TM)_{R2}-Fas only about 45 % of the treated cells were responsive to 100 ng/ml CysTNF. With ED₅₀ values between 0.1 ng/ml and 0.3 ng/ml, the responsiveness towards CysTNF was comparable to that seen in MF TNFR2-Fas cells (ED₅₀ = 0.2 ng/ml; see also Figure 11 D). Importantly, similar to the parental TNFR2-Fas chimaera, neither of these receptor chimaera variants was responsive towards sTNF, indicating that potentially more than one molecular feature in the TNFR2 stalk region controls responsiveness towards sTNF.

In conclusion, we were not able to narrow down which part of the TNFR2 stalk region encodes the inhibitory capacity this region has on receptor responsiveness towards sTNF.

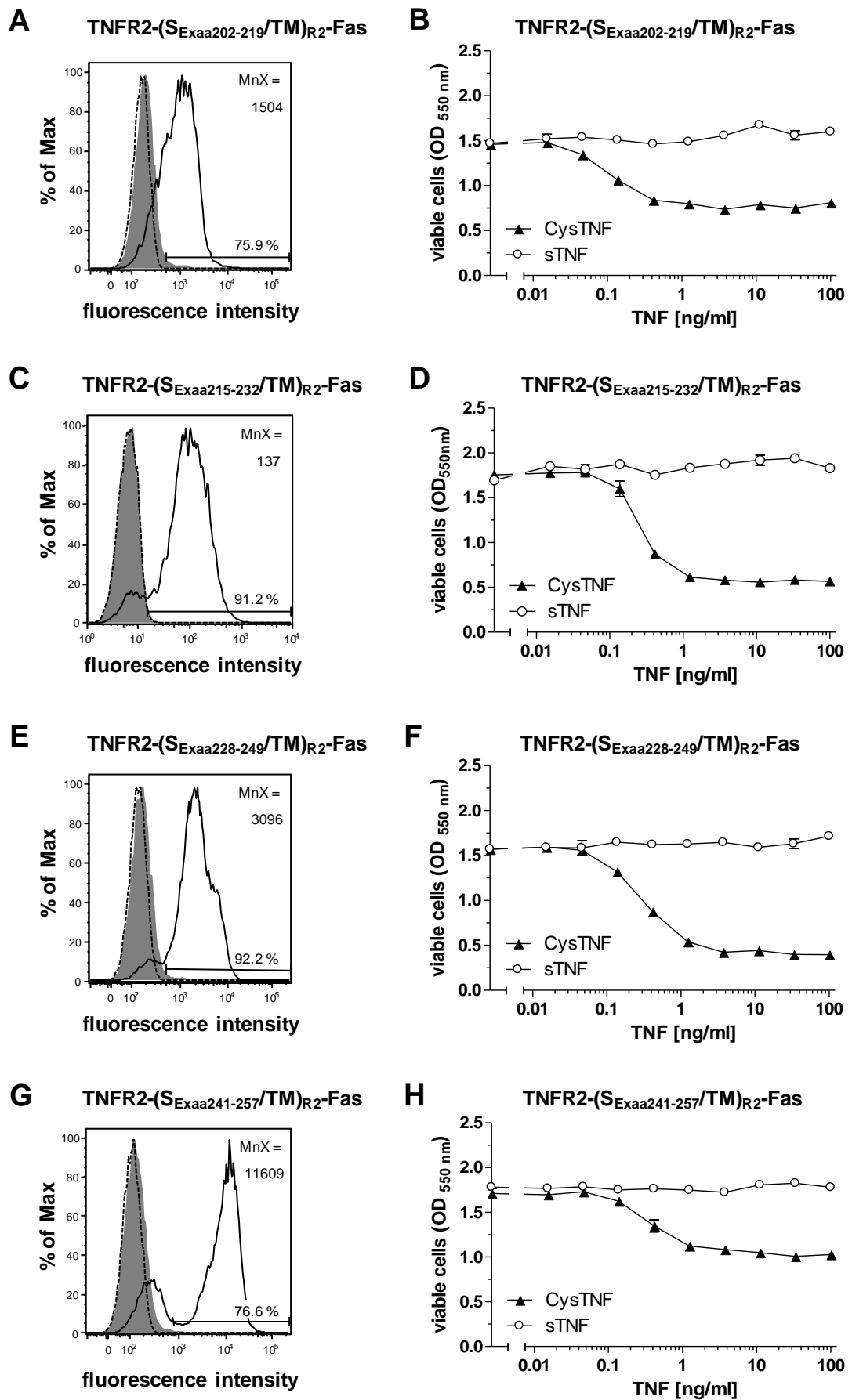


Figure 43. Partial replacement of the TNFR2 stalk region does not alter TNF responsiveness.

MF were stably transfected with expression constructs encoding for TNFR2-(S_{Exaa202-219}/TM)_{R2}-Fas, TNFR2-(S_{Exaa215-232}/TM)_{R2}-Fas TNFR2-(S_{Exaa228-249}/TM)_{R2}-Fas and TNFR2-(S_{Exaa241-257}/TM)_{R2}-Fas chimaeras. **A, C, E and G**) FACS histograms of MF stably transfected with indicated TNFR2-Fas variants. Cell surface expression of the chimaeric receptors was verified using mouse anti-human TNFR2 antibodies (MR2-1) and goat anti-mouse-IgG-FITC antibodies (black line). Unstained cells (dotted line); cells only incubated with goat anti-mouse IgG-FITC antibodies (grey). As indicated, between 76 % and 91 % of MF were gated positive for the respective chimaeras. Acquisition was performed on a Becton Dickinson FACSCanto II (C) or a Becton Dickinson FACScan (A, E and G) flow cytometer. **B, D, F and H**) MF stably transfected with indicated TNFR2-Fas chimaeras remained untreated or were stimulated with different concentrations of sTNF and CysTNF (0.015-100 ng/ml) and cell viability was determined using crystal violet staining. Data shown represent three independent experiments.

4.6 Discussion

As described below, for the stalk regions of cell surface receptors various different functions, such as the control of cell surface expression and stabilisation, involvement in ligand binding and/or activation of the receptors have been reported. These functions have often been linked to special features of these stalk regions such as the O-glycosylation status and length or certain conformations these regions adopt.

The length of the stalk region of the α -subunit of the Fc-epsilon receptor (Fc ϵ R) I, for example, was described to be important for the receptor stability on the cell surface (Kubota *et al.*, 2006), while the flexibility of the Fc ϵ RII stalk region was suggested to control receptor orientation and high affinity binding to its ligand, immunoglobulin E (Kilmon *et al.*, 2004). An involvement in ligand binding has also been reported for the stalk regions of the CD8 beta-chain (CD8 β)(Moody *et al.*, 2001, Moody *et al.*, 2003, Rettig *et al.*, 2009) and the murine Ly49 receptors (Ito *et al.*, 2009, Back *et al.*, 2009), with O-glycosylation and conformation of the stalk region being of importance, respectively. Interestingly, a potential role for the stalk region in signal transduction has already been suggested for another TNFR superfamily member, TRAILR2 (Wagner *et al.*, 2007). Preliminary data of our group together with data presented here showed that the stalk regions of TNFR1 and TNFR2 control sTNF-mediated signalling initiation. In contrast to the TRAILR2 stalk region, the stalk region of TNFR2 was found to prevent sTNF-mediated but not CysTNF-mediated signal transduction (see chapter 3). Therefore, the aim of this chapter was to investigate the role of different stalk region features, including length, proline-richness and O-glycosylation, in the control of sTNF responsiveness of TNFR2.

4.6.1 Stalk region length does not determine responsiveness towards sTNF

Relatively little is known about the influence of stalk region length on receptor functions. Kubota *et al.* (2006) found that elongation of the stalk region led to an increased half-life of the α -subunit of Fc ϵ RI (Fc ϵ RI α) on the cell surface. This effect was independent of the aa sequence of the Fc ϵ RI α stalk region and, therefore, it was proposed that the stalk region length was the determining factor for this increased half-life.

In this PhD project, the stalk regions of TNFR1-Fas and TNFR2-Fas were replaced with 15 aa and 56 aa long artificial linkers, respectively. While the receptor numbers on the cell surface were not determined experimentally, the comparable cell surface expression of the TNFR-Fas chimaeras with 15 aa artificial stalk regions and the corresponding constructs with a 56 aa artificial stalk region suggests that stalk region length does not determine the overall TNFR stability on the cell surface.

No differences in sTNF responsiveness between chimaeras with short and long artificial stalk regions could be observed for both, TNFR1-Fas and TNFR2-Fas (see Figure 32 and Figure 33). In contrast to the parental TNFR2-Fas chimaera, however, TNFR2-Fas chimaeras in which the stalk regions had been replaced with 15 aa and 56 aa long artificial linkers, respectively, did show an increased responsiveness to sTNF. The sTNF responsiveness of TNFR1-Fas and TNFR2-Fas chimaeras containing artificial 56 aa linkers (Figure 32 D and Figure 33 D, respectively) also differed markedly from the one of TNFR2-Fas and TNFR1-(S/TM)_{R2}-Fas (Figure 11), which both contain the wild type TNFR2 stalk region. While the artificial 56 aa stalk regions and the wild type TNFR2 stalk region have the same length their aa composition is different. Therefore, while our data further support an inhibitory role for the TNFR2 stalk region in receptor responsiveness to sTNF, they also suggest that this is not controlled by stalk region length. Instead sTNF responsiveness appears rather to be encoded by an intrinsic motif or feature of this region.

4.6.2 The influence of conserved proline residues in the TNFR2 stalk region on sTNF responsiveness

In contrast to the TNFR1 stalk region, the TNFR2 stalk region is rich in proline residues, of which seven are well conserved between species (Figure 34 A). Due to their bulky side chain and incapability to act as hydrogen-bond donors, proline residues function in proteins as helix- and β -sheet breakers, respectively, and proline-rich sequences are often found in extended structures and flexible regions (reviewed in Williamson, 1994). Furthermore, cis-trans isomerisation of proline residues has been found to function as a molecular switch during some signalling events of, for example, the interleukin-2-inducible T-cell kinase pathway (Brazin *et al.*, 2002, Mallis *et al.*, 2002) and the NF- κ B pathway (Ryo *et al.*, 2003, Jiang *et al.*, 2008). For one of the enzymes catalysing cis-trans isomerisation, namely the peptidyl prolyl cis-trans

isomerase cyclophilin B, localisation at the plasma membrane has been reported, suggesting a potential role of this enzyme during the initiation of signal transduction events (Bukrinsky, 2002, Stumpf *et al.*, 2008).

To investigate whether single conserved proline residues in the TNFR2 stalk region could potentially act as molecular switches in TNFR2 signalling initiation site-directed mutagenesis of the seven conserved proline residues in this region was performed. No difference in sTNF responsiveness could be observed between parental TNFR2-Fas chimaeras and chimaeras in which proline residues had been mutated (Figure 11, Figure 35 and Figure 36). Therefore, in contrast to cis-trans isomerisation events occurring during NF- κ B signalling (Ryo *et al.*, 2003) or histone methylation (Nelson *et al.*, 2006), a single proline acting as a molecular switch controlling sTNF responsiveness of TNFR2 could not be identified.

However, it is possible that a combination of several proline residues in the TNFR2 stalk region could determine sTNF responsiveness of this receptor. In several proteins proline-rich sequences have been reported to adopt folds which can confer both, flexibility and stability (reviewed in Williamson, 1994). A prominent example of such a secondary structure is the left handed collagen helix, in which proline residues and their hydroxylated form, hydroxyproline, occur as part of a regular pattern (reviewed in Bhattacharjee and Bansal, 2005). The TNFR2 stalk region does not display an equally even distribution of proline residues, but it is conceivable that with their abundance in the stalk region these aa residues could contribute to stalk region conformation and orientation to a large extent while also providing a certain degree of flexibility.

In addition, proline residues are found at positions -1, +1 and +3 relative to the site of O-glycosylation in the majority of proteins with mucin-type O-linked glycosylation (Wilson *et al.*, 1991, Hansen *et al.*, 1995). Thus, the proline residues in the TNFR2 stalk region will be involved in defining sites of O-glycosylation. Indeed for the TNFR2-Fas P205A chimaera a decreased molecular weight compared to the parental receptor chimaera could be observed, which indicates that P205 might be defining such an O-glycosylation site (Figure 34). However, this would have to be further confirmed by comparing lysates from stably and transiently transfected cells.

4.6.3 O-glycosylation of the TNFR2 stalk region does not determine responsiveness to sTNF

The stalk region of TNFR2 has been described to be O-glycosylated (Pennica *et al.*, 1993) and several potential sites of O-glycosylation were predicted by the bioinformatics tool NetOglyc (Julenius *et al.*, 2005) and a supported vector machine (SVM) programme (Li *et al.*, 2006)(see Figure 37 A). O-glycosylation of the stalk region of the TNFR superfamily member TRAILR2 has been reported to play a role in the sensitivity of the receptor to its ligand and its ability to signal for apoptosis (Wagner *et al.*, 2007). To address whether O-glycosylation in the stalk region also affects sTNF-mediated activation of TNFR2 the responsiveness of TNFR2-Fas chimaeras, in which either O-glycosylation sites had been mutated or O-glycosylation had been reduced using the inhibitor Benzyl- α -Gal-NAc, were analysed as part of this PhD project.

Five predicted O-glycosylation motifs in the TNFR2 stalk region were analysed for their effect on sTNF responsiveness. Mutation of motif 1 in combination with motif 4 identified these two motifs as major O-glycosylation sites, but also motifs 2, 3 and 5 appeared to be involved in stalk region O-glycosylation (Figure 37 B). However, for none of the analysed variants an increase in sTNF responsiveness could be observed, indicating that O-glycosylation of the serine and threonine residues of motifs 1, 2, 3 and 5 does not inhibit responsiveness of TNFR2-Fas chimaeras towards sTNF (Figure 38 B and D). Unfortunately, it was not possible to determine whether O-glycosylation of motif 4 controls sTNF responsiveness of TNFR2-Fas. Despite its high intracellular protein expression (Figure 37 B), the TNFR2-Fas mot. 1/4 chimaera was not expressed on the cell surface. This suggests that O-glycosylation of motif 4, possibly in combination with O-glycosylation of motif 1, could be essential for exporting TNFR2-Fas chimaeras from the endoplasmic reticulum and localising them at cell surface. For example, site-specific O-glycosylation of the membrane-proximal part of the extracellular portion of the neurotrophin receptor has already been reported to be required for apical sorting of this receptor (Breuza *et al.*, 2002).

In conclusion, O-glycosylation of motifs 1, 2, 3 and 5 does not appear to critically control sTNF responsiveness of TNFR2-Fas, while the role of O-glycosylation of motif 4 in determining sTNF responsiveness remains elusive.

Experiments with Benzyl- α -Gal-NAc, a substrate for β -1,3-N-galactosyltransferase (Brockhausen *et al.*, 1983) and competitive inhibitor for core 1 and core 2 mucin-type O-glycosylation (Kuan *et al.*, 1989) underlined our findings from the O-glycosylation mutants. The data obtained using this inhibitor highlight that it is rather unlikely that O-glycosylation of the TNFR2 stalk region is a determinant critical for receptor responsiveness towards sTNF. While O-glycosylation was reduced by the Benzyl- α -Gal-NAc treatment, no effect on the responsiveness of TNFR-Fas chimaeras towards sTNF could be detected when compared with solvent control (Figure 40 B, D and F and Figure 41 B, D and F). Importantly, comparison of Benzyl- α -Gal-NAc-treated TNFR2-Fas and TNFR2-S_{GSL56}-TM_{R2}-Fas, in which the stalk region is replaced by a 56 aa long artificial linker, indicates that the decrease in molecular weight of TNFR2-Fas chimaeras is indeed caused by reduced O-glycosylation in the TNFR2 stalk region (Figure 39).

With a concentration of 3.5 mM, Benzyl- α -Gal-NAc was added at a concentration which was above the one that had been used to fully inhibit O-glycosylation in a human colonic adenocarcinoma cell line (2 mM; Kuan *et al.*, 1989), but just below the 4 mM used by Wagner *et al.* (2007) to inhibit O-glycosylation of TRAILR2 in HEK 293 cells. As a substrate which is competing for β 1,3-N-galactosyltransferase, Benzyl- α -Gal-NAc leads to the accumulation of aryl-glycans in the cell, affects the sialylation of N-linked glycans (Zanetta *et al.*, 2000) and has even been described to cause apoptosis and growth inhibition (Patsos *et al.*, 2009). Therefore, Benzyl- α -Gal-NAc was used at a sensible concentration sufficient to inhibit core 1 and core 2 O-glycosylation efficiently while not being so high as to cause problems with cell growth and viability (Figure 39, Figure 40 and Figure 41).

Taken together, our data indicate that the TNFR2 stalk region carries core 1 and/or core 2 mucin-type O-glycosylation but this type of glycosylation does not control sTNF responsiveness of the TNFR.

As mentioned above, core 1 and core 2 O-glycosylation represent the most common forms of mucin-type O-glycosylation. In addition, six more types of mucin-type O-glycosylation structures (core 3-8) have been described in mammals. However, while β -1,3-N-galactosyltransferase is expressed in all cell types throughout all developmental stages (Tian and Ten Hagen, 2009), core 3 and core 4 structures have only been observed in secreted mucins and occurrence of core 5-8 mucins is very restricted (Brockhausen *et al.*, 2009). Therefore, while we cannot entirely exclude the possibility

that alternative O-glycosylation affects sTNF responsiveness in other cell types or tissues, it is, however, very unlikely to play a role in our TNFR-Fas cellular system. A full analysis of the O-glycosylation types in the TNFR2 stalk region by mass spectrometry would allow a more selective inhibition of stalk region O-glycosylation for example through the use of glycosyltransferase-specific siRNA. However, this was not possible due to timely limitations of this project and remains as future work.

4.6.4 Partial replacement of the TNFR2 stalk region suggests a more complex regulation of sTNF responsiveness by the stalk region

Data obtained using MF stably transfected with TNFR-Fas chimaeras, in which the stalk regions had been replaced with 15 aa and 56 aa long artificial linkers, suggested that sTNF responsiveness is rather determined by the aa composition than the length of the stalk region (section 4.2). To further investigate which part of the TNFR2 stalk region in particular controls responsiveness towards sTNF we exchanged this region partly with artificial linkers of 17-22 aa in length and determined sTNF responsiveness of the resulting TNFR2-Fas chimaeras. While all four partial exchange mutants were expressed on the cell surface, for none an effect of the partial stalk region replacement on the responsiveness to the soluble ligand could be observed (Figure 43). This suggests that either the region as a whole or more than one feature within this region determine responsiveness towards sTNF. Therefore, control of sTNF responsiveness by the TNFR2 stalk region appears to be determined through a more complex mechanism which remains yet to be elucidated.

4.7 Conclusion

- Single conserved proline residues in the TNFR2 stalk region do not control sTNF responsiveness of TNFR2-Fas chimaeras. However, the role of combinations of these conserved proline residues in sTNF responsiveness remains yet to be determined.
- O-glycosylation of the TNFR2 stalk region is most likely no critical determinant for the differential responsiveness of TNFR2 as mutation of putative O-glycosylation sites and inhibition of core 1 and core 2 mucin-type O-glycosylation do not alter responsiveness of TNFR2-Fas towards sTNF.
- The length of the TNFR2 stalk region does not determine receptor responsiveness to sTNF. However, the aa composition of the TNFR2 stalk region appears to play an important role in differential responsiveness of TNFR.
- Partial replacement of the TNFR2 stalk region suggests that a more complex mechanism is underlying sTNF responsiveness and that either the region as a whole or more than one feature encoded by this region control differential responsiveness.

CHAPTER 5

Results III: Influence of the TNF receptor stalk regions on ligand-independent receptor homodimerisation and formation of larger receptor clusters

5.1 Introduction

Formation of receptor clusters has been postulated to enhance signal transduction of transmembrane receptors in various ways, for example by increasing their sensitivity and specificity and enhancing response simultaneity, respectively (reviewed in Duke and Graham, 2009). Formation of such receptor clusters has already been observed for Fas (Algeciras-Schimmich *et al.*, 2002, Siegel *et al.*, 2004). These clusters were described as “signaling protein oligomeric transduction structures” (SPOTS) and were found to be formed as an early event during Fas signalling (Siegel *et al.*, 2004). The extracellular region of Fas has been reported to be sufficient for cluster formation induced by membrane-bound FasL (Henkler *et al.*, 2005). In contrast, Fas cluster formation upon stimulation with soluble FasL was found to be dependent on interactions of the intracellular portion of Fas and required localisation to cholesterol-rich plasma membrane microdomains. Based on crystallographic data, Scott *et al.* (2009) recently proposed that FasL binding stabilises the signalling-competent form of Fas. Furthermore, it results in linkage of the Fas DD, leading to rapid processive Fas cluster formation and binding of FADD, which in turn further promotes receptor cluster and DISC formation. In addition, electron microscopy data suggest that the minimal cluster-forming Fas/FADD complexes show a hexameric arrangement (Scott *et al.*, 2009).

Similarly, ligand-induced cluster formation of TNFR1, which had already been proposed by Naismith *et al.* (1995), could be demonstrated in confocal microscopy experiments by Schneider-Brachert *et al.* (2004). In line with these findings, Krippner-Heidenreich *et al.* (2002) observed that efficient TNF-mediated recruitment of FADD and TRAF2 to TNFR1-Fas chimaeras coincided with the formation of large receptor clusters. The exact composition of these receptor clusters and the mechanism by which they are formed are largely unknown. However, the so-called pre-ligand binding

assembly domains (PLAD) of the receptors and the localisation of the TNFR in microdomains of the plasma membrane have already been described as possible determinants for the formation of these receptor clusters (see below).

Ligand-independent homotypic dimerisation and/or trimerisation of TNFR1, TNFR2 (Chan *et al.*, 2000) and Fas (Papoff *et al.*, 1996, Papoff *et al.*, 1999, Siegel *et al.*, 2000) via their PLAD in CRD1 have been described previously. CRD1 has been proposed to be required for high affinity ligand binding of the receptor by mediating homotypic receptor oligomerisation (Chan *et al.*, 2000) and/or conformationally stabilising CRD2, which is directly involved in TNF binding (Branschädel *et al.*, 2010). Moreover, CRD1 was found to be, to some extent, a potential determining co-factor for conferring sTNF responsiveness to TNFR1 (Branschädel *et al.*, 2010).

Furthermore, upon stimulation with sTNF simultaneous receptor activation and receptor cluster formation can be observed for TNFR1-Fas (Krippner-Heidenreich *et al.*, 2002). In contrast, TNFR2-Fas receptor cluster formation can only be detected in MF when cells are incubated with the stabilising monoclonal mouse anti-human TNFR2 antibody Mab 80M2 prior to sTNF stimulation (Krippner-Heidenreich *et al.*, 2002). Therefore, the inability of TNFR2-Fas to form sTNF-induced receptor clusters correlates with its lacking responsiveness to sTNF. Currently, it is not known how cluster formation of TNFR2 is controlled. Fluorescence correlation spectroscopy data suggest that, in contrast to TNFR1-Fas, TNFR2-Fas chimaeras do not localise in cholesterol-rich microdomains of the plasma membrane in the absence of the ligand (Gerken *et al.*, 2010). Branschädel *et al.* (2010) found the homotypic interactions of the TNFR2 PLAD to be weaker than those seen for TNFR1. The latter accounted to some extent for the reduced sTNF responsiveness of TNFR2-Fas. However, this region is not exclusively controlling differential sTNF responsiveness as exchange of CRD1 of TNFR1 with the one of TNFR2 did not render TNFR1-Fas completely un-responsive to sTNF (Branschädel *et al.*, 2010).

As described in sections 3.2 and 3.3.1, the TNFR2 stalk region has a strong inhibitory effect on the responsiveness of TNFR2 towards sTNF. Preliminary data from chemical protein crosslinking experiments indicated a potential role for the TM and/or stalk regions of TNFR1 and TNFR2 in ligand-independent homotypic pre-assembly of the receptors (Dr Anja Krippner-Heidenreich, personal communication). Therefore, here the influence of the stalk region on ligand-independent receptor-receptor interactions was

further investigated by using stalk region deletion mutants. In addition, the influence of the stalk region on the potential of TNFR2 to form larger receptor clusters was determined as part of this PhD project.

Therefore, the aims in this chapter were to:

- determine whether TNFR2 stalk region affects ligand independent interactions of TNFR-Fas chimaeras;
- investigate whether the TNFR2 stalk region controls receptor cluster formation in TNFR-Fas chimaeras and TNFR2 variants;

5.2 The stalk region of TNF receptor type 2 counteracts ligand-independent receptor homo-dimerisation

TNFR1 and TNFR2 have been reported to self-associate prior to ligand binding via their PLAD, which are located in CRD1 (Chan *et al.*, 2000, Branschädel *et al.*, 2010). This is in line with the parallel crystal structure of the extracellular domain of TNFR1, which shows contacts between the CRD1 of two receptor chains (Naismith *et al.*, 1996a). Recent data obtained in our group linked these homotypic receptor-receptor interactions for the first time to sTNF responsiveness of TNFR (Branschädel *et al.*, 2010). In addition, preliminary protein crosslinking data from MF TNFR1-(S/TM)_{R2}-Fas and MF TNFR2-(S/TM)_{R1}-Fas indicated that the TNFR stalk regions are also potential determinants controlling receptor self-association (Dr Anja Krippner-Heidenreich, personal communication). Therefore, my aim was to investigate the role of the TNFR2 stalk region in ligand-independent TNFR pre-assembly.

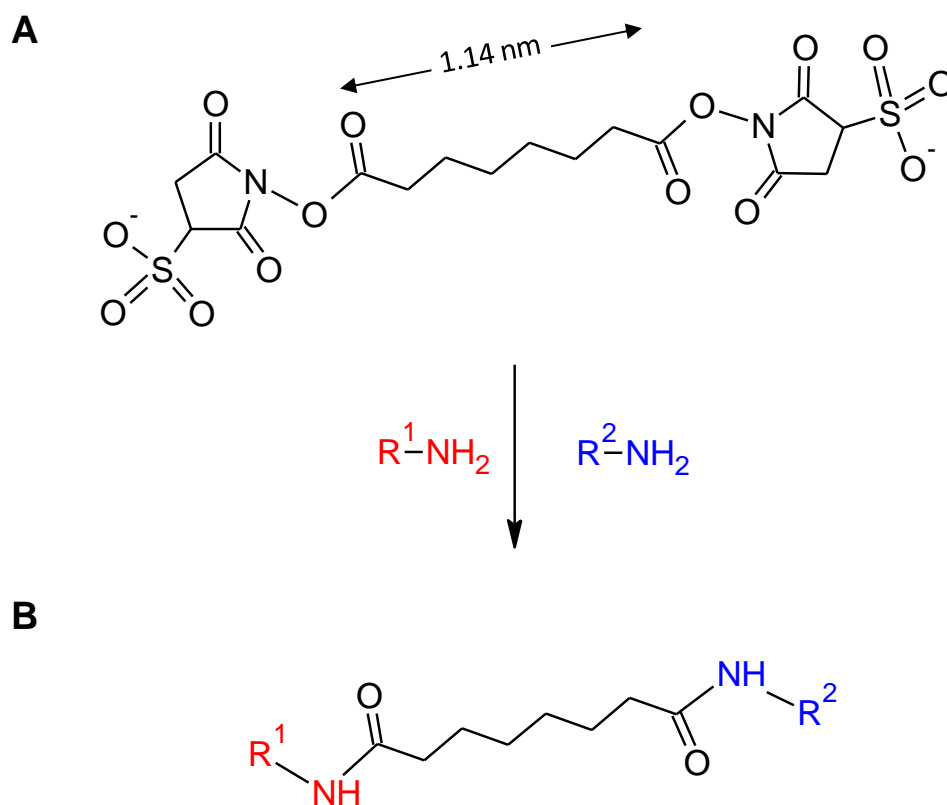


Figure 44. Schematic representation of chemical crosslinking of primary amino groups with bis-(sulfosuccinimidyl)-suberate.

The membrane-impermeable chemical crosslinker bis-(sulfosuccinimidyl)-suberate (BS³) can react with primary amino groups of proteins and peptides, i.e. lysine and arginine residues and N-terminal amino groups. **A**) The two reactive N-hydroxysulfosuccinimide ester groups of BS³ are linked by a 1.14 nm spacer and react with the amino groups of proteins (-NH₂) of proteins R¹ and R², thereby **B**) covalently linking the two proteins. Chemical structures were adopted from the Thermo Scientific/Pierce Crosslinking Technical Handbook (Thermo Scientific/Pierce, Loughborough, UK) and drawn using the ACD/Labs Software version 12.0 (Advanced Chemistry Development Inc., Toronto, Canada).

To address this question the homo-bifunctional membrane-impermeable NH_2 -reactive crosslinker bis-(sulfosuccinimidyl)-suberate (BS^3), which allows detection of weak and transient protein-protein interactions on the cell surface, was used. The chemical structure of BS^3 and a schematic representation of the crosslinking reaction are depicted in Figure 44. Chemical protein crosslinking experiments with 33-500 μM BS^3 were performed using MF stably transfected with TNFR-Fas chimaeras as described in section 2.10.

To ensure that differences between the chimaeric receptors in crosslinking experiments were not due to differences in cell surface expression, FACS analysis was performed in parallel to the crosslinking experiments. The results of these analyses were used to correct protein loading for Western Blotting for receptor cell surface expression and percentage of positive cells. Generally, minimal adjustments had to be made as the more than 90 % of the cells could be gated positive for cell surface expression of the chimaeras and MnX were also comparable (MnX = 285 for TNFR2-Fas and MnX = 298 for TNFR2-($\text{S}_{\Delta 42}/\text{TM}$) $_{\text{R}2}$ -Fas; Figure 45 A and B and MnX = 303 for TNFR1-Fas and MnX = 290 for TNFR1-($\text{S}_{\Delta 42}/\text{TM}$) $_{\text{R}2}$ -Fas; Figure 46 A and B).

Only a relatively weak signal could be detected for crosslinked oligomers of TNFR2-Fas at a BS^3 concentration of 66 μM (Figure 45 C). In contrast, a strong signal for crosslinked TNFR2-($\text{S}_{\Delta 42}/\text{TM}$) $_{\text{R}2}$ -Fas could already be observed at 33 μM BS^3 (Figure 45 C), suggesting that the full length TNFR2 stalk region decreases ligand-independent receptor-receptor interactions of TNFR2-Fas. In agreement with previous analyses (Branschädel *et al.*, 2010, Boschert *et al.*, 2010), the molecular size of the bands indicates that the TNFR1-Fas and TNFR2-Fas variants exist as homodimers in the plasma membrane. It is likely that the homodimers detected in chemical protein crosslinking experiments originate from PLAD-PLAD interactions of the chimaeras. However, it is currently unknown how the TNFR stalk regions could affect such interactions. It is likely that this also applies to wild type TNFR2 but verification would be required.

In contrast to TNFR2-Fas and in line with observations made by Branschädel *et al.* (2010), for the parental TNFR1-Fas chimaeras strong receptor-receptor interactions could already be observed at a BS^3 concentration of 33 μM . These interactions are markedly reduced when the TNFR1 stalk and TM regions are replaced with the ones of TNFR2 (Dr Anja Krippner-Heidenreich, personal communication). While deletion of the 42 aa in the TNFR2 stalk region of TNFR2-Fas enhances receptor-receptor

interactions, deletion of these aa apparently cannot restore ligand-independent receptor pre-assembly of TNFR1-(S/TM)_{R2}-Fas, as crosslinked species of TNFR1-(S_{Δ42}/TM)_{R2}-Fas chimaeras could only be detected at higher BS³ concentrations (125 μM; Figure 46 C).

Taken together, the data presented here suggest that 42 aa in the TNFR2 stalk region counteract receptor homodimerisation of TNFR2-Fas in the absence of a ligand. However, in the case of TNFR1-Fas, parameters such as the TM region and/or adjacent intracellular sequences appear to mask the potential effects of the stalk region in ligand-independent pre-assembly.

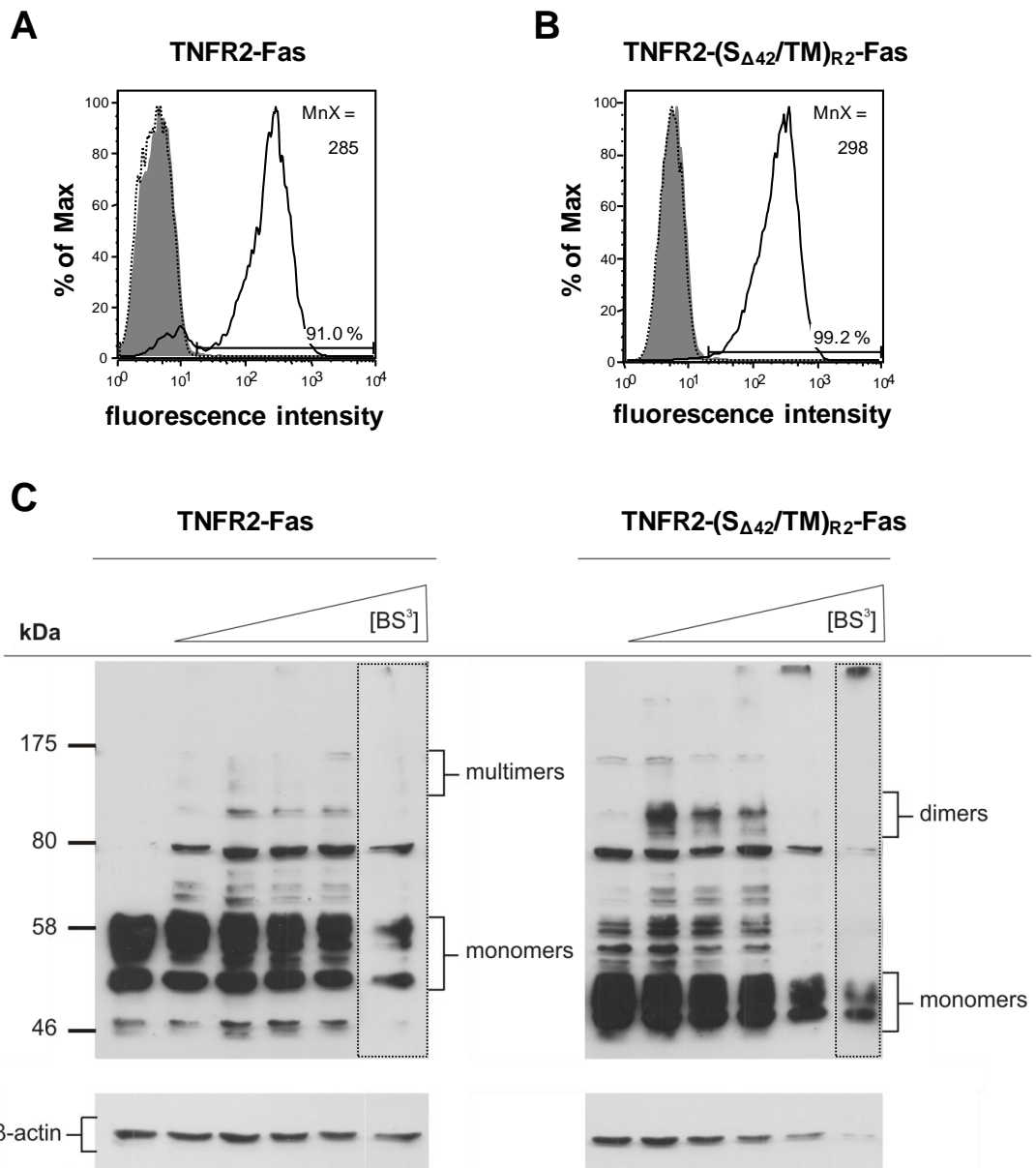


Figure 45. Shortening of the TNFR2 stalk region increases ligand-independent receptor-receptor interactions in TNFR2-Fas chimaeras.

MF were stably transfected with TNFR2-Fas and TNFR2-(S_{Δ42}/TM)_{R2}-Fas expression constructs, respectively. **A and B**) FACS analysis; chimaeric receptors were stained on the cell surface using mouse anti-human TNFR2 antibodies clone MR2-1 and goat anti-mouse IgG-FITC antibodies (black line). Unstained cells (dotted line); cells only incubated with goat anti-mouse IgG-FITC antibodies (grey). 91 % and 99 % of the cells were gated positive for TNFR2-Fas and TNFR2-(S_{Δ42}/TM)_{R2}-Fas, respectively. MnX were as indicated. **C**) Chemical protein-crosslinking and Western Blot analysis; cells were incubated with PBS or increasing amounts (33 μM, 66 μM, 125 μM, 250 μM and 500 μM) of the chemical crosslinker bis(Sulfosuccinimidyl)-suberate (BS³). Cells were harvested and membrane proteins were extracted using 1 % (v/v) TritonX-100. Membrane extracts from approximately 1 x 10⁵ cells were subjected to SDS-PAGE and Western Blot analysis. Protein concentrations were corrected for cell surface expression of the receptor chimaeras and percentages of positive cells. Mouse anti-human Fas antibodies (clone B10, 1:2000) were used as primary and goat anti-mouse IgG-HRP (1:20000) as secondary antibodies. As indicated, the faster migrating protein bands represent monomers of the receptor chimaeras, whereas the slower migrating protein bands represent dimers and multimers of chimaeric receptors, respectively (Branschädel *et al.*, 2010, Boschert *et al.*, 2010). β-actin levels served as loading control. All bands shown are from the same exposure. Data shown represent three independent experiments.

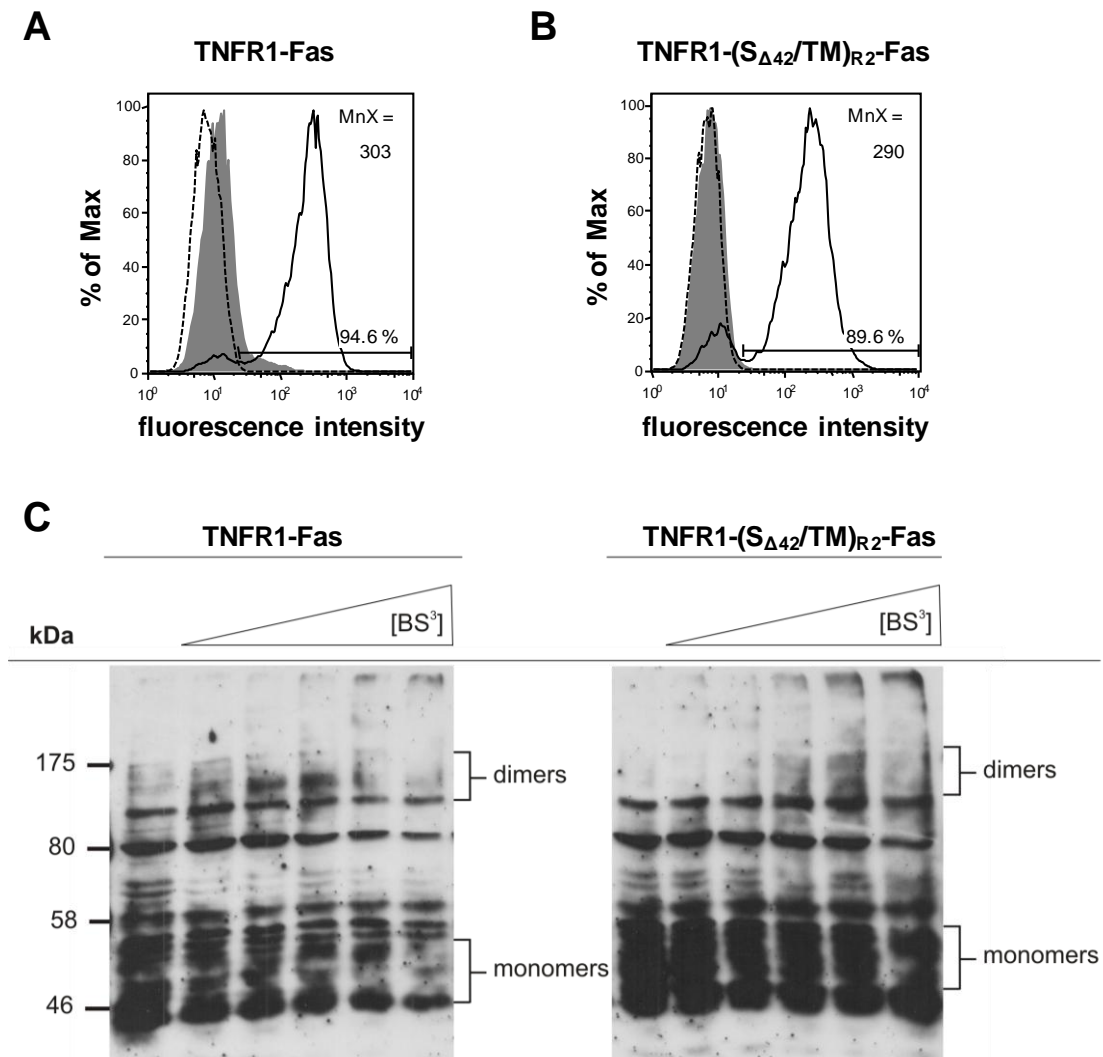


Figure 46. Ligand-independent receptor-receptor interactions of TNFR1-Fas chimaeras containing the TM and shortened stalk region of TNFR2.

MF were stably transfected with TNFR1-Fas and TNFR1-(S_{Δ42}/TM)_{R2}-Fas expression constructs, respectively. **A and B**) FACS analysis; chimaeric receptors were stained on the cell surface using mouse anti-human TNFR1 antibodies clone H398 and goat anti-mouse IgG-FITC antibodies (black line). Unstained cells (dotted line); cells only incubated with goat anti-mouse IgG-FITC antibodies (grey). 95 % and 90 % of the cells were gated positive for TNFR1-Fas and TNFR1-(S_{Δ42}/TM)_{R2}-Fas, respectively. MnX were as indicated. **C**) Chemical protein-crosslinking and Western Blot analysis; cells were incubated with PBS or increasing amounts (33 μM, 66 μM, 125 μM, 250 μM and 500 μM) of the chemical crosslinker bis(Sulfosuccinimidyl)-suberate (BS³). Cells were harvested and membrane proteins were extracted using 1 % (v/v) TritonX-100. Membrane extracts from approximately 1 x 10⁵ cells were subjected to SDS-PAGE and Western Blot analysis. Protein concentrations were corrected for cell surface expression of the receptor chimaeras and percentages of positive cells. Mouse anti-human Fas antibodies (clone B10, 1:2000) were used as primary and goat anti-mouse IgG-HRP (1:20000) as secondary antibodies. As indicated, the faster migrating protein bands represent monomers of the receptor chimaeras, whereas the slower migrating protein bands represent dimers of chimaeric receptors, respectively (Branschädel *et al.*, 2010, Boschert *et al.*, 2010). β-actin levels served as loading control. Data shown represent three independent experiments.

5.3 The stalk region of TNFR2 abrogates efficient cluster formation of TNFR2-Fas and wild type TNFR2

As shown in section 5.2, the TNFR2 stalk region has an inhibitory effect on ligand-independent receptor-receptor interactions. This could potentially also extend to the inhibition of the formation of larger receptor clusters, which has previously been proposed to be a potential prerequisite for efficient activation of TNFR1 and TNFR2 (Krippner-Heidenreich *et al.*, 2002).

To investigate whether the TNFR2 stalk region influences the ability of TNFR to form receptor clusters, we used the doxycycline-inducible HEK 293 FlpIN T-Rex cell system. HEK 293 Flp-IN T-Rex cells, which overexpress TNFR1-Fas, TNFR2-Fas and TNFR2-(S/TM)_{R1}-Fas upon induction with doxycycline have been generated and characterised in our group previously (Branschädel *et al.*, 2010). HEK 293 Flp-IN T-Rex cells inducibly overexpressing TNFR2-(S_{Δ42}/TM)_{R2}-Fas, TNFR2, TNFR2-(S/TM)_{R1}-R2 and TNFR2-(S_{Δ42}/TM)_{R2}-R2, respectively, have been generated as part of this PhD project.

For the HEK 293 FlpIN T-Rex cell system induction with 0.1-1.0 µg/ml of tetracycline or doxyxycline for 24 h has been suggested (Invitrogen). Therefore, HEK 293 FlpIN T-Rex TNFR2 cells were induced with increasing concentrations of doxycycline (0.5- 2.5 ng/ml) for 18 h and TNFR2 expression was determined by FACS analysis and Western Blotting (Figure 47). A dose-dependent induction of overall and cell surface TNFR2 expression could be observed. While uninduced cells showed only low TNFR2 expression (MnX = 1266; Figure 47 A, black) a marked increase could be observed for induction with 0.5 ng/ml (MnX = 5964; Figure 47 A, blue), 1 ng/ml (MnX = 7654; Figure 47 A, green) and 1.5 ng/ml (MnX = 9752; Figure 47 A, orange) of doxycycline. At 2 ng/ml and 2.5 ng/ml doxycycline TNFR2 cell surface expression was comparable (MnX = 11080 and MnX = 11307, respectively; Figure 47 A, red and margenta), suggesting that maximal induction of TNFR2 expression was reached at these concentrations. Higher doxycycline concentrations of up to 5 ng/ml increased cell surface expression of TNFR2 only marginally (data not shown). Therefore, a saturating doxycycline concentration of 6 ng/ml was chosen for the induction of HEK 293 FlpIN T-Rex cells in the following experiments.

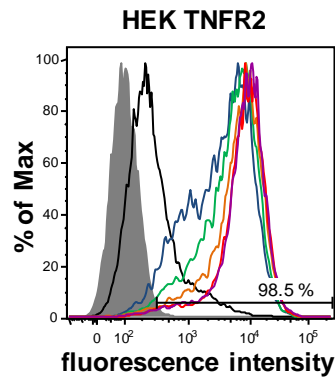
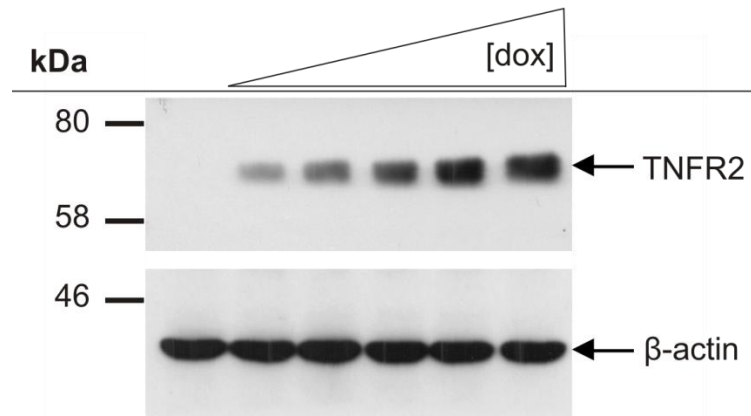
A**B**

Figure 47. Dose-dependent doxycycline-induced expression of TNFR2 in HEK 293 FlpIN T-Rex cells.

Doxycycline-inducible HEK 293 FlpIN T-Rex cells expressing TNFR2 (HEK TNFR2) were left untreated or were induced with increasing concentrations of doxycycline ([dox]; 0.5 ng/ml, 1 ng/ml, 1.5 ng/ml, 2 ng/ml and 2.5 ng/ml) for 18 h. **A**) FACS analysis. TNFR2 was stained on the cell surface using mouse anti-human TNFR2 antibodies (MR2-1) and goat anti-mouse IgG-FITC antibodies. Cells only incubated with goat anti-mouse IgG-FITC antibodies (grey); uninduced cells (black), cells induced with 0.5 ng/ml (blue), 1 ng/ml (green), 1.5 ng/ml (orange), 2 ng/ml (red) and 2.5 ng/ml (magenta) of doxycycline, respectively. Acquisition was performed on a FACSCanto II flow cytometer. Percentages indicate cells positive for TNFR2 cell surface expression at the highest doxycycline concentration. **B**) Western Blot analysis. Whole cell lysates were prepared from an equivalent of 5×10^4 cells and were subjected to SDS-PAGE and Western Blot analysis. Polyclonal goat anti-human TNFR2 antibodies (1:2000) were used as primary and rabbit anti-goat IgG-HRP (1:20000) as secondary antibodies. β -actin levels served as loading control. Data shown represent one experiment.

5.3.1 The TNFR2 stalk region inhibits formation of larger TNFR2-Fas clusters

Preliminary data obtained from HEK 293 Flp-IN T-Rex cells overexpressing TNFR-Fas chimaeras suggested a potential role for the TNFR stalk regions in controlling receptor cluster formation. To investigate whether the 42 aa in the TNFR2 stalk region, which have been shown have an inhibitory effect on ligand-independent receptor-receptor interactions and sTNF responsiveness (sections 3.2 and 3.3.1), also affect the potential of TNFR2-Fas to form larger receptor clusters, inducible HEK 293 Flp-IN T-Rex TNFR2-(S_{Δ42}/TM)_{R2}-Fas cells were generated and analysed by confocal microscopy.

As a first characterisation step, cell surface expression of TNFR2-(S_{Δ42}/TM)_{R2}-Fas on the HEK 293 FlpIN T-Rex cells was determined for various induction times using FACS analysis. While only low cell surface expression could be detected for un-induced cells (MnX = 965; Figure 48 A), TNFR2-(S_{Δ42}/TM)_{R2}-Fas was expressed at comparably high levels 9 h, 12 h, 18 h and 24 h after induction (MnX = 15380 – 16538; Figure 48 B – E). Similar results were obtained when overall TNFR2-(S_{Δ42}/TM)_{R2}-Fas expression was analysed by Western Blotting (Figure 48 F). Furthermore, TNFR2-(S_{Δ42}/TM)_{R2}-Fas expressed by HEK 293 Flp-IN T-Rex cells upon induction with doxycycline co-migrated with the TNFR2-(S_{Δ42}/TM)_{R2}-Fas chimaera transiently expressed in HeLa cells. This indicates that TNFR2-(S_{Δ42}/TM)_{R2}-Fas is expressed as the full length protein in HEK cells.

As TNFR2-(S_{Δ42}/TM)_{R2}-Fas was expressed at high levels after 12 h and 18 h of induction, respectively, for experimental set-up reasons an induction time of 18 h was chosen for the following experiments.

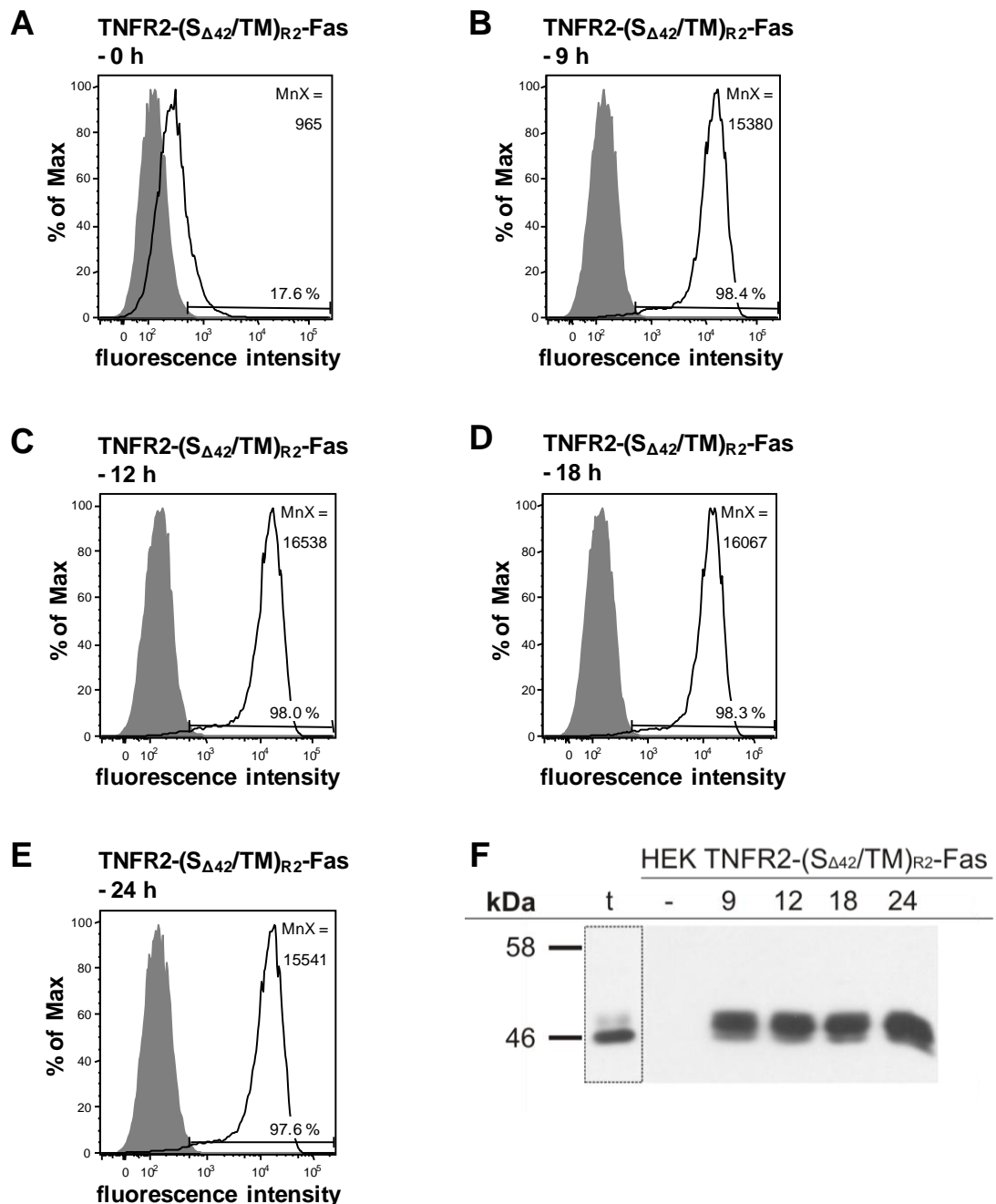


Figure 48. Kinetics of doxycycline induced expression of TNFR2-(S Δ 42/TM)_{R2}-Fas in HEK 293 Flp-IN T-Rex cells.

HEK 293 FlpIN T-Rex TNFR2-(S Δ 42/TM)_{R2}-Fas cells were left untreated (-) or were induced with 6 ng/ml doxycycline for 9 h, 12 h, 18 h and 24 h, respectively. Shown are FACS analyses of **A**) uninduced cells and **B, C, D and E**) cells which had been induced with doxycycline for the indicated times. TNFR2-(S Δ 42/TM)_{R2}-Fas was stained on the cell surface using mouse anti-human TNFR2 (MR2-1) and goat anti-mouse IgG-FITC antibodies (black line). Cells only incubated with goat anti-mouse IgG-FITC antibodies (grey). Acquisition was performed on a FACSCanto II flow cytometer. Percentages indicate cells gated positive for TNFR2-(S Δ 42/TM)_{R2}-Fas and MnX are indicated. **F**) Western Blot analysis. Whole cell lysates were prepared from 5×10^4 of uninduced cells and cells, which had been induced for the indicated times, respectively, and subjected to SDS-PAGE and Western Blot analysis. Polyclonal goat anti-human TNFR2 antibodies (1:2000) were used as primary and rabbit anti-goat-IgG-HRP (1:20000) as secondary antibodies. HeLa cells transiently transfected with the expression vector pEF-PGK/puro polyA TNFR2-(S Δ 42/TM)_{R2}-Fas (t) served as positive control. Data shown represent two independent experiments.

To investigate the role of the TNFR2 stalk region in receptor cluster formation, HEK 293 FlpIN T-Rex cells expressing the parental chimaeras TNFR1-Fas and TNFR2-Fas, the stalk/TM exchange mutant TNFR2-(S/TM)_{R1}-Fas and the stalk region deletion mutant TNFR2-(S_{Δ42}/TM)_{R2}-Fas, respectively, were induced with 6 ng/ml doxycycline for 18 h. Cells were then stained with AlexaFluor546-labelled sTNF on ice for 5 min, fixed with formaldehyde and analysed via confocal microscopy.

For TNFR1-Fas a clear tendency towards formation of few but large receptor clusters could be observed (Figure 49 A – D). In contrast, for TNFR2-Fas mainly homogenous distribution on the cell surface with only occasional, relatively weak cluster formation could be detected (Figure 49 E – H). This difference in cluster formation was not due to higher cell surface expression, as FACS analysis revealed higher relative expression levels for TNFR2-Fas than for TNFR1-Fas (MnX = 8911 for TNFR1-Fas and MnX = 18873 for TNFR2-Fas; Dr Anja-Krippner-Heidenreich, personal communication). When the stalk and TM regions of TNFR2 were exchanged for the ones of TNFR1, a strong increase in number and size of TNFR2-Fas clusters could be observed (TNFR2-(S/TM)_{R1}-Fas; Figure 49 I – L). Similar results were obtained when the TNFR2 stalk region was shortened by 42 aa (TNFR2-(S_{Δ42}/TM)_{R2}-Fas; Figure 49 M – P). This increase in receptor cluster formation of TNFR2-(S/TM)_{R1}-Fas and TNFR2-(S_{Δ42}/TM)_{R2}-Fas was again not caused by a stronger cell surface expression of these chimaeras as the relative expression levels of these chimaeras were comparable to parental TNFR2-Fas (MnX = 17305 for TNFR2-(S/TM)_{R1}-Fas (Dr Anja-Krippner-Heidenreich, personal communication) and MnX = 16067 for TNFR2-(S_{Δ42}/TM)_{R2}-Fas (Figure 48)).

The analysis of cluster formation described above was performed on cells which had been fixed after the incubation with AlexaFluor546-labelled sTNF. Despite working at low temperatures, the short incubation with TNF and the subsequent incubation at room temperature during the fixing of the cells may have sufficed to induce ligand-mediated receptor clusters. Therefore, HEK 293 FlpIN T-Rex cells overexpressing TNFR2-Fas and TNFR2-(S_{Δ42}/TM)_{R2}-Fas, respectively, were fixed and then stained with a phycoerythrin-conjugated mouse anti-human TNFR2 antibody (clone # 22235) to determine whether the observed cluster formation was ligand-independent. While for TNFR2-Fas similar results were obtained with labelled TNF and antibody (Figure 49 I – L and Figure 50 A), a clear yet less pronounced cluster formation was observed for antibody staining of TNFR2-(S_{Δ42}/TM)_{R2}-Fas in comparison to cells which had been stained with AlexaFluor546-labelled sTNF (Figure 49 M – P and Figure 50 B). This

suggests that the TNFR2-(S_{Δ42}/TM)_{R2}-Fas cluster formation described above is only partly ligand-independent. However, our data indicate that 42 aa in the TNFR2 stalk region have an inhibitory effect on TNFR2-Fas receptor cluster formation and that this is the case in both, the absence and the presence of the ligand.

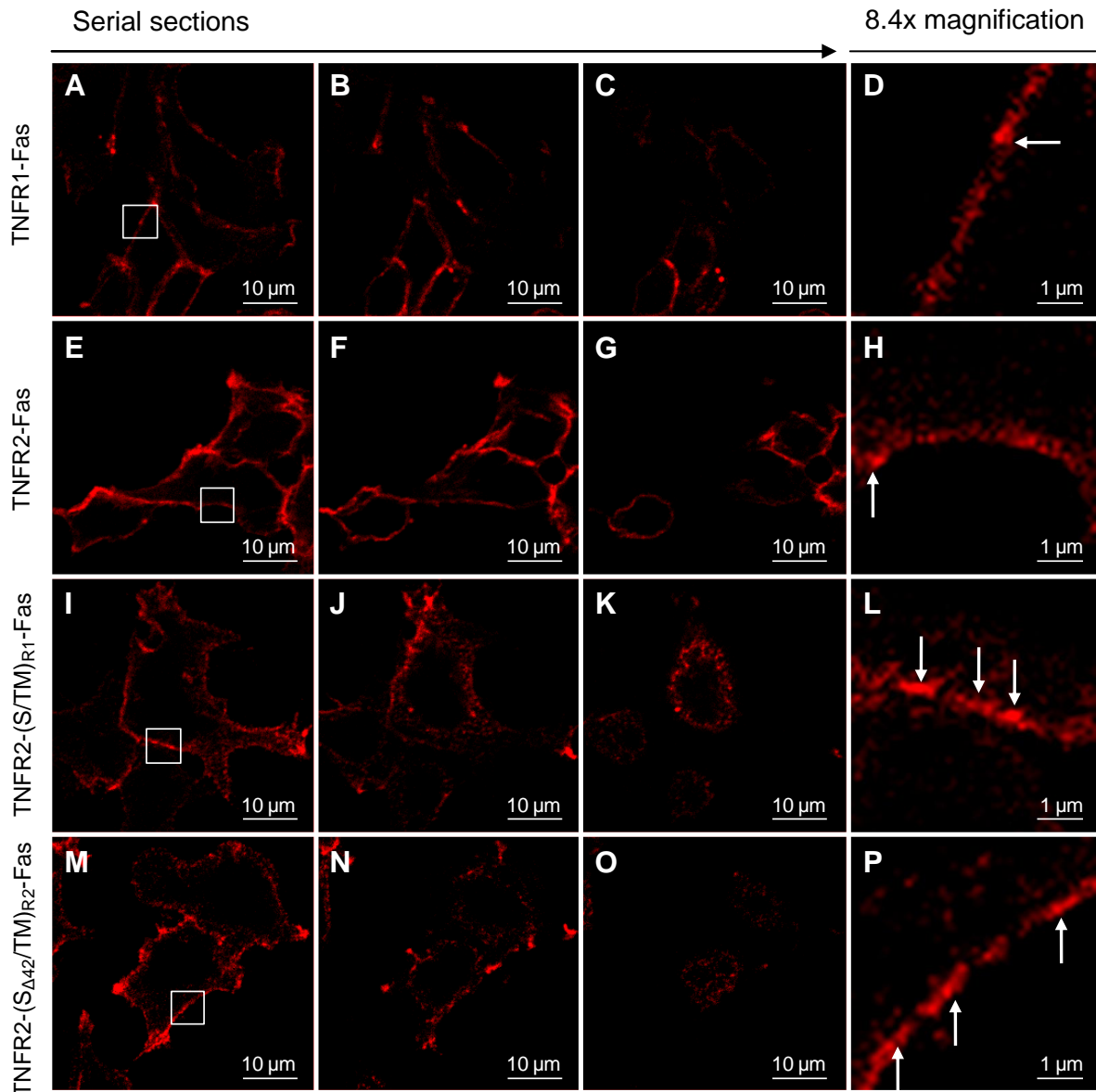


Figure 49. Control of receptor cluster formation by the TNFR2 stalk region in TNFR2-Fas chimaeras.

HEK 293 FlpIN T-Rex cells were induced with 6 ng/ml doxycycline for 18 h. Cells were then stained with Alexa546-labelled sTNF on ice for 5 min and fixed with formaldehyde. Images were acquired as z-series on an Andor Revolution XD confocal microscope. Shown are serial sections of HEK 293 FlpIN T-Rex cells overexpressing **A, B and C**) TNFR1-Fas; **E, F and G**) TNFR2-Fas; **I, J and K**) TNFR2-(S/TM)_{R1}-Fas and **M, N and O**) TNFR2-(S_{Δ42}/TM)_{R2}-Fas, respectively. The thickness of each single section was 0.37 μm and the distance between the sections was 1.48 μm. **D, H, L and P**) 8.4x magnification of the selected area in A, E, I and M, respectively (white box). Larger receptor clusters are highlighted with white arrows. Data shown represent three independent experiments.

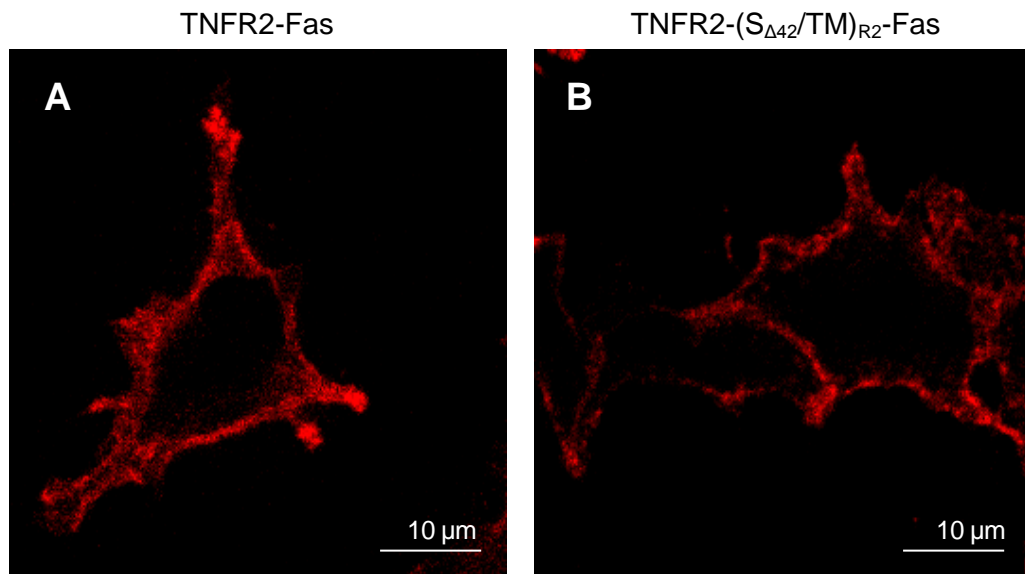


Figure 50. Ligand-independent receptor cluster formation of TNFR2-Fas and TNFR2-(S_{Δ42}/TM)_{R2}-Fas chimaeras.

HEK 293 FlpIN T-Rex cells were induced with 6 ng/ml doxycycline for 18 h. Cells were then fixed with formaldehyde and stained with phycoerythrin-conjugated mouse anti-human TNFR2 antibodies (clone # 22235; 1:75; R&D). Images (0.37 μm sections) were acquired on an Andor Revolution XD confocal microscope. Shown are **A**) HEK 293 FlpIN T-Rex TNFR2-Fas and **B**) HEK 293 FlpIN T-Rex TNFR2-(S_{Δ42}/TM)_{R2}-Fas cells. Data shown represent three independent experiments.

5.3.2 Cluster formation of wild type TNFR2 is abrogated by the TNFR2 stalk region

Overexpression of TNFR-Fas chimaeras in an inducible HEK cell system had revealed an inhibitory role for the TNFR2 stalk in TNFR cluster formation (section 5.3.1). To address, whether these results also translate to the cluster formation of wild type TNFR2, confocal microscopy experiments were repeated with HEK 293 FlpIN T-Rex cells expressing TNFR2, TNFR2-(S/TM)_{R1}-R2 and TNFR2-(S_{Δ42}/TM)_{R2}-R2, respectively.

The inducible HEK 293 FlpIN T-Rex cell lines for TNFR2, TNFR2-(S/TM)_{R1}-R2 and TNFR2-(S_{Δ42}/TM)_{R2}-R2 were generated as part of this PhD project. Overall expression and cell surface expression of the TNFR2 variants were determined by Western Blot and FACS analysis of HEK 293 FlpIN T-Rex cell lines which remained uninduced or were induced with 6 ng/ml doxycycline for 9 h, 12 h, 18 h and 24 h.

For uninduced cells no expression of the TNFR2 variants could be detected in Western Blot analyses (Figure 51). Furthermore, only low cell surface expression was detectable for all three variants (MnX = 672- 920; Figure 52 A, Figure 53 A and Figure 54 A, respectively). Upon induction, comparably high expression of TNFR2 and TNFR2-(S_{Δ42}/TM)_{R2}-R2 could be determined for all induction time points in both Western Blot (Figure 51) and FACS analysis (MnX = 11847-12755 for TNFR2 and MnX = 9967-11127 for TNFR2-(S_{Δ42}/TM)_{R2}-R2; Figure 52 B – E and Figure 54 B – E). In contrast, overall expression and cell surface expression of TNFR2-(S/TM)_{R1}-R2 was higher than the one observed for wild type TNFR2 at all induction time points (MnX = 15833- 21911; Figure 51 and Figure 52 B – E). For experimental set-up reasons, again the 18 h time-point was chosen for analysis of receptor cluster formation.

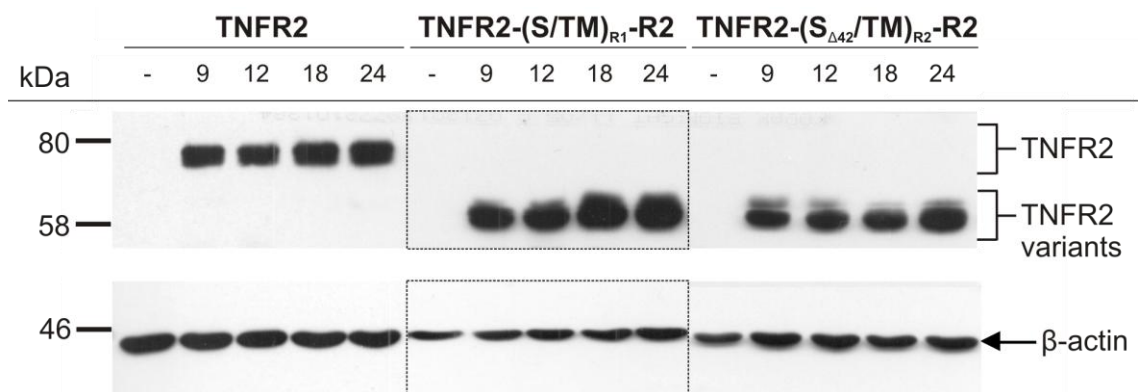


Figure 51. Time-course of doxycycline-induced expression of TNFR2 and variants thereof. Doxycycline-inducible HEK 293 FlpIN T-Rex cells expressing TNFR2, TNFR2-(S/TM)_{R1}-R2 and TNFR2-(S_{Δ42}/TM)_{R2}-R2, respectively, were induced with 6 ng/ml doxycycline for the 9 h (9), 12 h (12), 18 h (18) and 24 h (24) or were left untreated (-). Whole cell lysates were prepared and an equivalent of 3.3×10^4 cells was used for SDS-PAGE and Western Blot analysis. Polyclonal goat anti-human TNFR2 antibodies (1:2000; R&D) were used as primary and rabbit anti-goat IgG-HRP (1:20000) as secondary antibodies. β -actin levels served as loading control. Data shown represent two independent experiments.

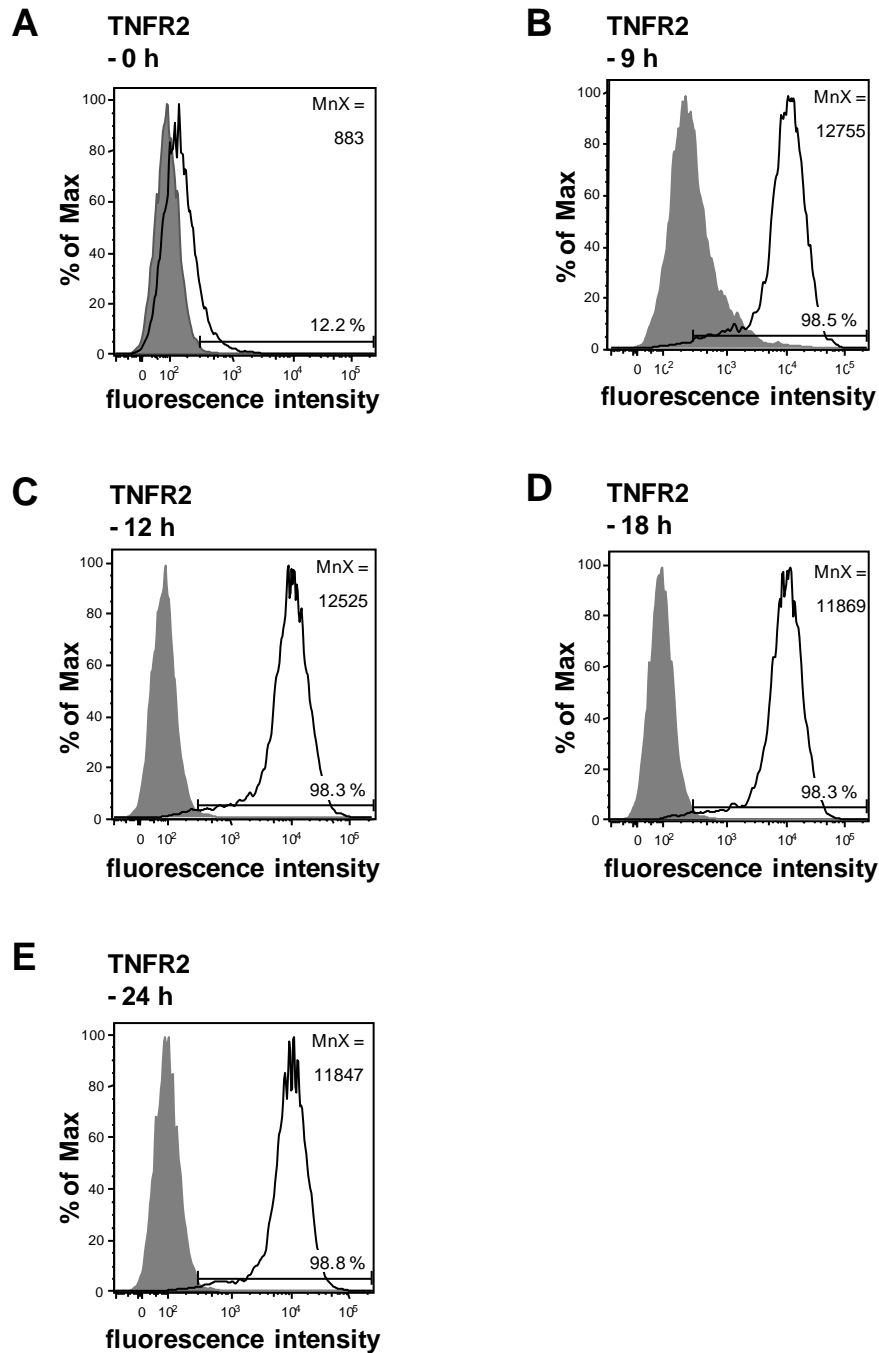


Figure 52. Cell surface expression of TNFR2 in HEK 293 Flp-IN T-Rex cells upon induction with doxycycline.

Doxycycline-inducible HEK 293 Flp-IN T-Rex TNFR2 cells were induced with 6 ng/ml doxycycline for the 9 h, 12 h, 18 h and 24 h or were left untreated (0 h). Shown are FACS analyses of **A**) uninduced HEK 293 Flp-IN T-Rex TNFR2 cells and **B, C, D, E**) HEK 293 Flp-IN T-Rex TNFR2 cells after induction with 6 ng/ml doxycycline for 9 h, 12 h, 18 h and 24 h. TNFR2 was stained on the cell surface using mouse anti-human TNFR2 antibodies (MR2-1) and goat anti-mouse IgG-FITC antibodies (black line). Cells only incubated with goat anti-mouse IgG-FITC antibodies (grey). Acquisition was performed on a FACSCanto II flow cytometer. Percentages indicate cells gated positive for TNFR2 cell surface expression. MnX are indicated. Data shown represent two independent experiments.

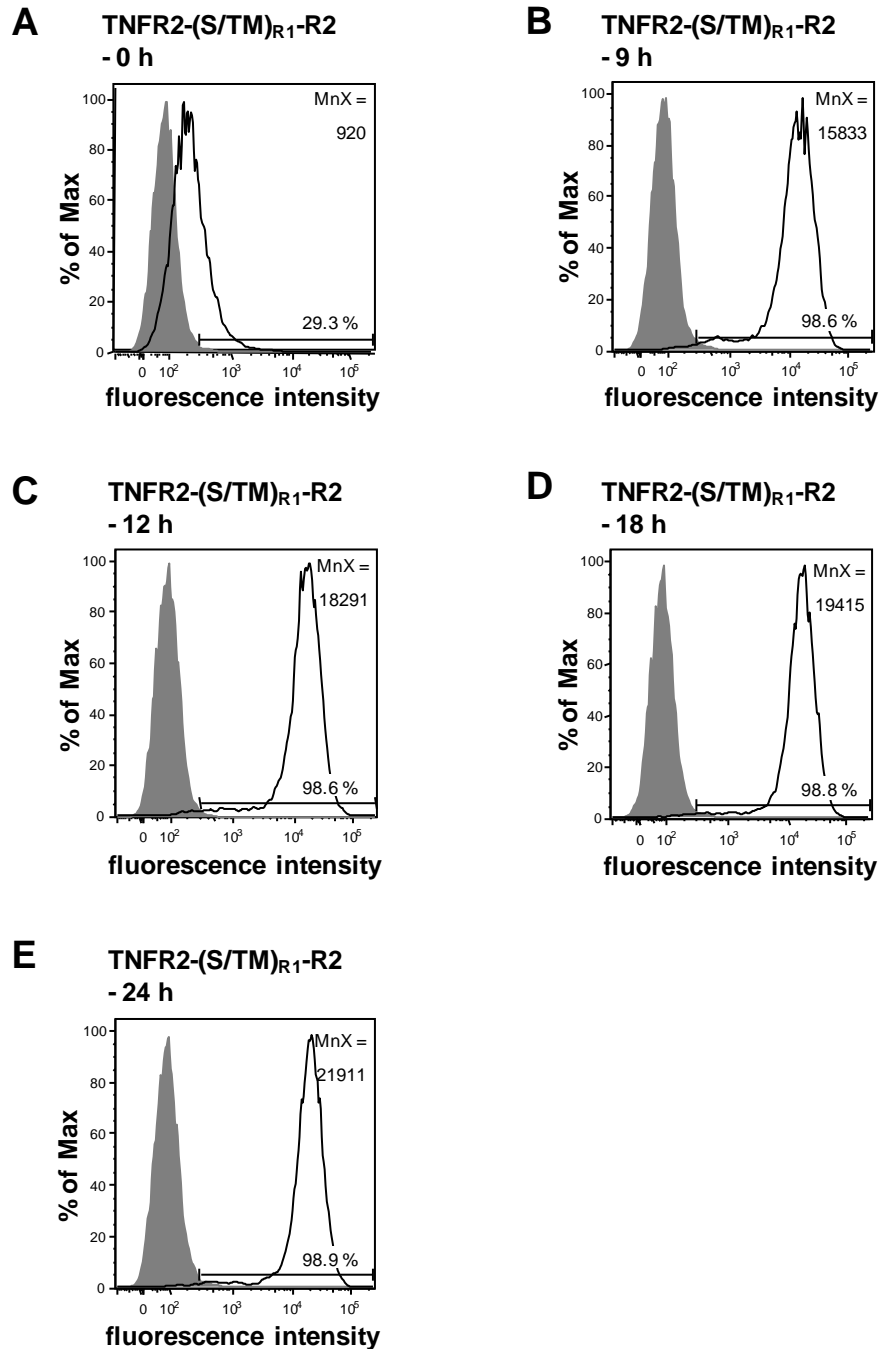


Figure 53. Cell surface expression of TNFR2-(S/TM)_{R1-R2} in HEK 293 Flp-IN T-Rex cells upon induction with doxycycline.

Doxycycline-inducible HEK 293 Flp-IN T-Rex TNFR2-(S/TM)_{R1-R2} cells were induced with 6 ng/ml doxycycline for the 9 h, 12 h, 18 h and 24 h or were left untreated (0 h). Shown are FACS analyses of **A**) uninduced HEK 293 Flp-IN T-Rex TNFR2-(S/TM)_{R1-R2} cells and **B, C, D, E**) HEK 293 Flp-IN T-Rex TNFR2-(S/TM)_{R1-R2} cells after induction with 6 ng/ml doxycycline for 9 h, 12 h, 18 h and 24 h. TNFR2-(S/TM)_{R1-R2} was stained on the cell surface using mouse anti-human TNFR2 antibodies (MR2-1) and goat anti-mouse IgG-FITC antibodies (black line). Cells only incubated with goat anti-mouse IgG-FITC antibodies (grey). Acquisition was performed on a FACSCanto II flow cytometer. Percentages indicate cells gated positive for TNFR2-(S/TM)_{R1-R2} cell surface expression. MnX are indicated. Data shown represent two independent experiments.

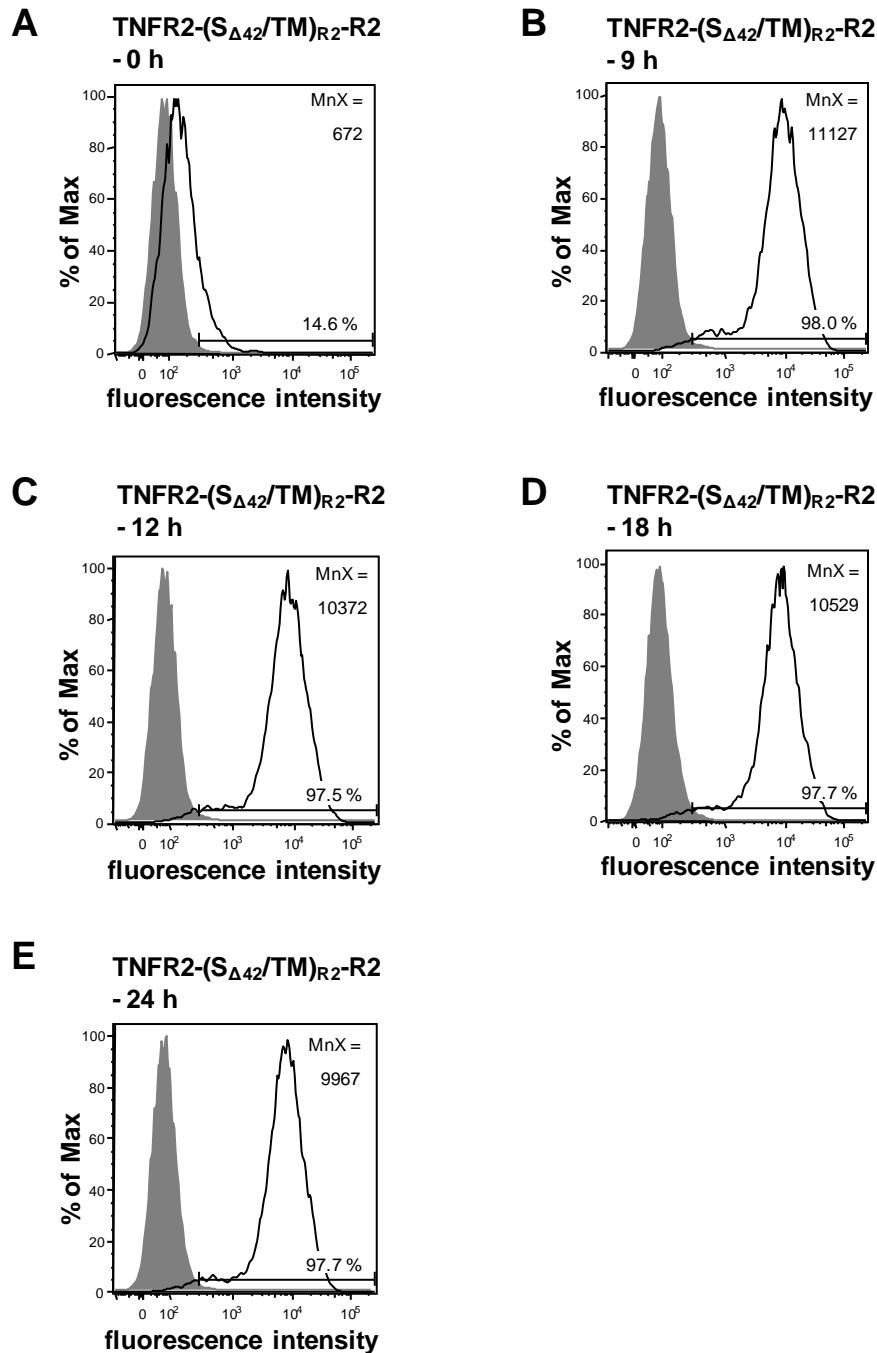


Figure 54. Cell surface expression of TNFR2-(S_{Δ42}/TM)_{R2}-R2 in HEK 293 Flp-IN T-Rex cells upon induction with doxycycline.

Doxycycline-inducible HEK 293 FlpIN T-Rex cells expressing TNFR2-(S_{Δ42}/TM)_{R2}-R2 were induced with 6 ng/ml doxycycline for 9 h, 12 h, 18 h and 24 h or were left untreated (0 h). Shown are FACS analyses of **A**) uninduced HEK 293 Flp-IN T-Rex TNFR2-(S_{Δ42}/TM)_{R2}-R2 cells and **B, C, D, E**) HEK 293 Flp-IN T-Rex TNFR2-(S_{Δ42}/TM)_{R2}-R2 cells after induction with 6 ng/ml doxycycline for 9 h, 12 h, 18 h and 24 h. TNFR2-(S_{Δ42}/TM)_{R2}-R2 was stained on the cell surface using mouse anti-human TNFR2 antibodies (MR2-1) and goat anti-mouse IgG-FITC antibodies (black line). Cells only incubated with goat anti-mouse IgG-FITC antibodies (grey). Acquisition was performed on a FACSCanto II flow cytometer. Percentages indicate cells gated positive for TNFR2-(S_{Δ42}/TM)_{R2}-R2 cell surface expression. MnX are indicated. Data shown represent two independent experiments.

To investigate the role of the TNFR2 stalk region in receptor cluster formation of wild type TNFR2, confocal microscopy studies of TNFR2 and variants thereof were performed. HEK 293 FlpIN T-Rex cell lines were induced with 6 ng/ml doxycycline for 18 h, stained with AlexaFluor546-labelled sTNF on ice and fixed with formaldehyde.

Similar to TNFR2-Fas, an overall homogenous distribution with only very few and rather small clusters could be detected for overexpressed wild type TNFR2 (Figure 55 A – D). In contrast, formation of more and larger receptor clusters was discovered for the two TNFR2 variants, TNFR2-(S/TM)_{R1}-R2 and TNFR2-(S_{Δ42}/TM)_{R2}-R2 (Figure 55 E – L). The differences in the cluster formation potential of TNFR2 and TNFR2-(S_{Δ42}/TM)_{R2}-R2 were not due to differences in cell surface expression as similar relative expression levels were seen at 18 h of induction for these two variants (MnX = 11869 for TNFR2 and MnX = 10529 for TNFR2-(S_{Δ42}/TM)_{R2}-R2; Figure 52 D and Figure 54 D). While a higher cell surface expression was determined for TNFR2-(S/TM)_{R1}-R2 at 18 h of induction (MnX = 19415; Figure 53 D), it is relatively unlikely that this accounted for the observed receptor cluster formation as, despite lower cell surface expression, a similarly pronounced cluster formation of TNFR2-(S/TM)_{R1}-R2 was detected at 6 h of induction (MnX < 15000; data not shown).

By staining the respective receptor variants with phycoerythrin-conjugated mouse anti-human TNFR2 antibodies (clone # 22235) it was assessed whether the cluster formation observed for sTNF stained cells was occurring in a ligand-independent fashion. Similar to the results obtained with labelled sTNF, the antibody staining revealed homogenous distribution and no cluster formation for wild type TNFR2 (compare Figure 55 A – D and Figure 56 A). For TNFR2-(S/TM)_{R1}-R2 and TNFR2-(S_{Δ42}/TM)_{R2}-R2, however, where pronounced receptor clusters had been seen for AlexaFluor546-labelled sTNF stained cells (Figure 55 E – L), little or no pronounced cluster formation was observed when cells were stained with the TNFR2 antibody (Figure 56 B and C). In line with results obtained from the TNFR2-Fas and TNFR2-(S_{Δ42}/TM)_{R2}-Fas chimaeras (Figure 49 and Figure 50), this indicates that the cluster formation observed for TNFR2 variants is not (entirely) ligand-independent and indeed controlled by the TNFR2 stalk region.

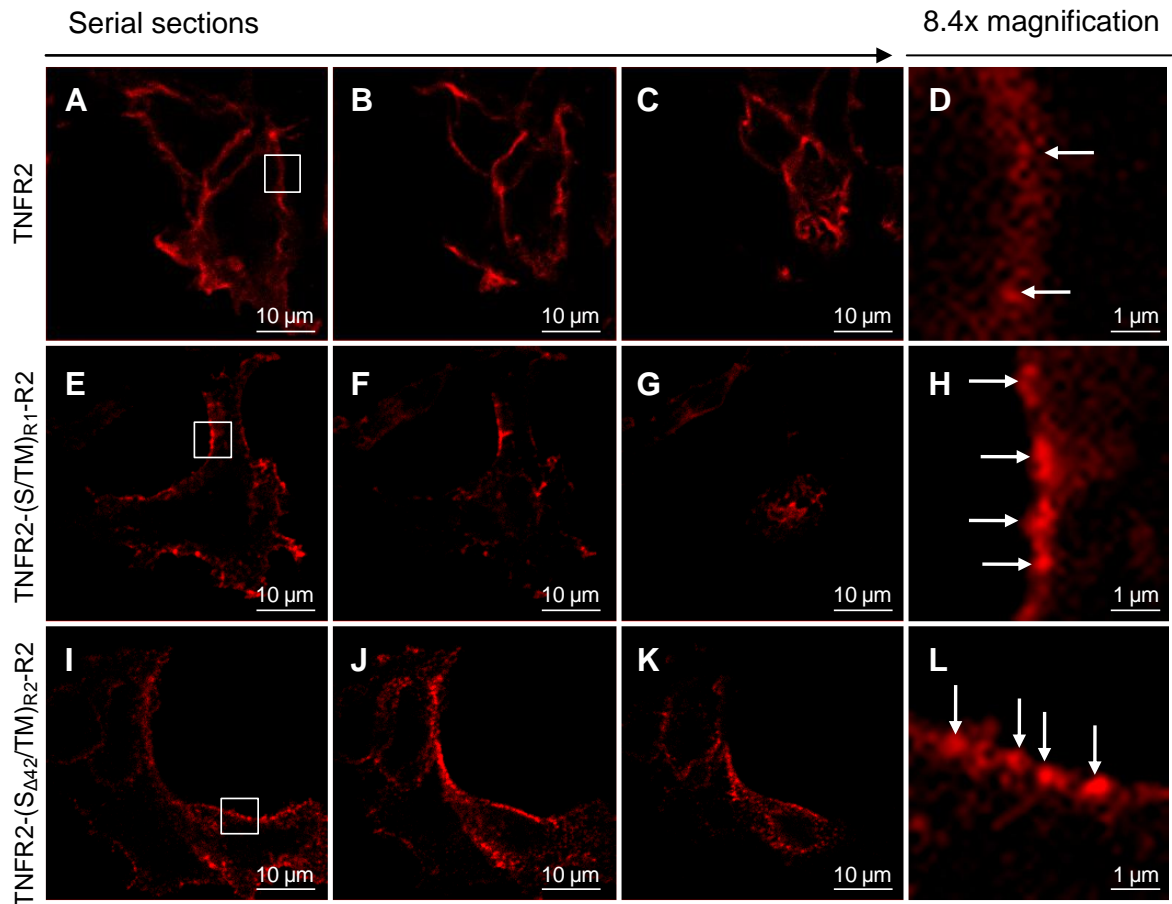


Figure 55. The stalk region prevents cluster formation of wild type TNFR2.

HEK 293 FlpIN T-Rex cells were induced with 6 ng/ml doxycycline for 18 h. Cells were then stained with Alexa546-labelled TNF on ice and fixed with formaldehyde. Images were acquired as z-series on an Andor Revolution XD confocal microscope. Shown are serial sections of induced HEK 293 FlpIN T-Rex cells expressing **A, B and C**) TNFR2, **E, F and G**) TNFR2-(S/TM)_{R1}-R2 and **I, J and K**) TNFR2-(S_{Δ42}/TM)_{R2}-R2, respectively. The thickness of each single section was 0.37 μm and the distance between the sections was 1.48 μm. **D, H and L**) 8.4x magnification of the selected area (white box) in A, E and I, respectively. Larger receptor clusters are highlighted with white arrows. Data shown represent three independent experiments.

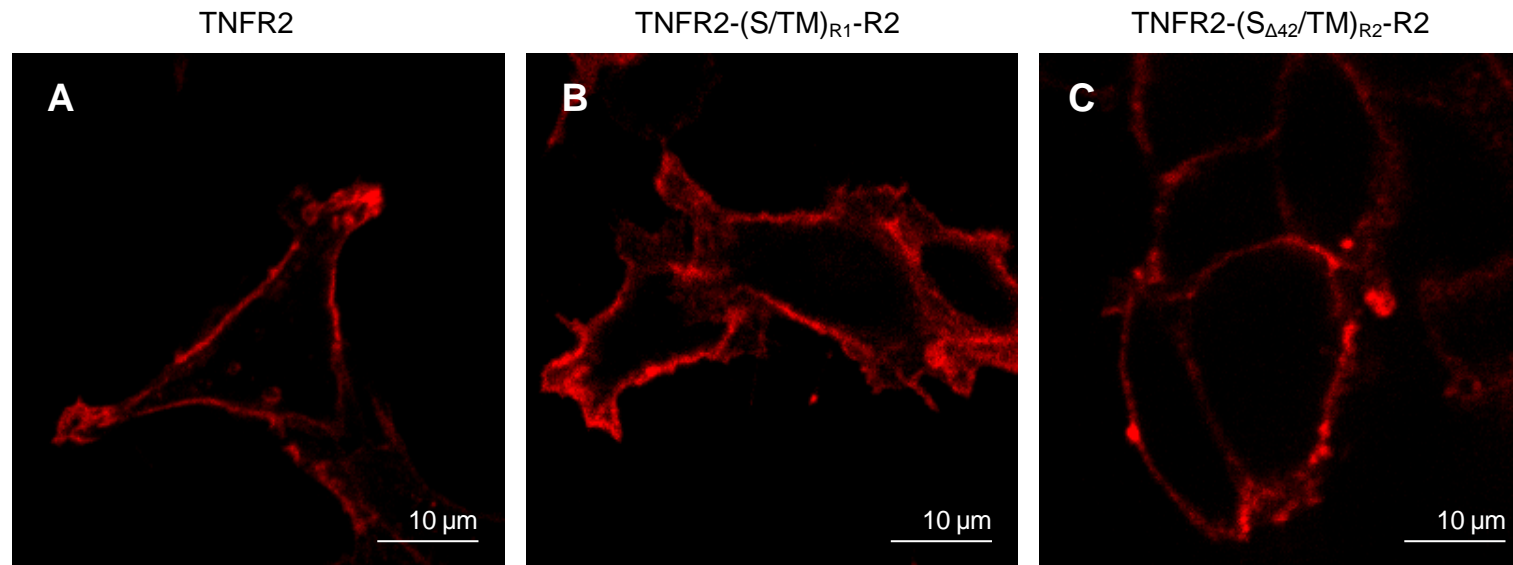


Figure 56. Ligand-independent receptor cluster formation of wild type TNFR2 and variants thereof.

HEK 293 FlpIN T-Rex cells were induced with 6 ng/ml doxycycline for 18 h. Cells were then fixed with formaldehyde and stained with the phycoerythrin-conjugated mouse anti-human TNFR2 antibody clone # 22235 (1:75; R&D). Images (0.37 μ m sections) were acquired on an Andor Revolution XD confocal microscope. Shown are **A**) HEK 293 FlpIN T-Rex TNFR2 **B**) HEK 293 FlpIN T-Rex TNFR2-(S/TM)_{R1}-R2 and **C**) HEK 293 FlpIN T-Rex TNFR2-(S_{Δ42}/TM)_{R2}-R2 cells. Data shown represent three independent experiments.

5.4 Discussion

PLAD-mediated ligand-independent receptor-receptor interactions of TNFR1 and TNFR2, respectively, have been described previously (Chan *et al.*, 2000) and CRD1 exchange mutants linked sTNF responsiveness of the receptors to their capacity to form homotypic receptor dimers (Branschädel *et al.*, 2010). Furthermore, responsiveness to sTNF has been observed to correlate with sTNF-mediated formation of larger receptor clusters (Krippner-Heidenreich *et al.*, 2002). As shown in sections 3.2 and 3.3, the TNFR2 stalk region inhibits sTNF responsiveness (Figure 14 and Figure 18). Data presented in this chapter demonstrate that the TNFR2 stalk region prevents ligand-independent homotypic dimerisation of TNFR2-Fas chimaeras and inhibits formation of larger receptor clusters of TNFR2-Fas chimaeras and wildtype TNFR2.

5.4.1 Control of TNFR2-Fas homo-dimerisation by the TNFR2 stalk region

Pilot data obtained in our group disclosed strong homotypic receptor interactions for TNFR1-Fas chimaeras whereas these interactions are only weak for TNFR2-Fas (Boschert *et al.*, 2010). This is only partly mediated by CRD1 of the receptors as exchange of this region between TNFR1-Fas and TNFR2-Fas did not abrogate sTNF responsiveness of TNFR1-Fas completely (Branschädel *et al.*, 2010). Preliminary data showed that the strong homotypic interactions of TNFR1-Fas could be abrogated by the introduction of the stalk and TM regions of TNFR2 (TNFR1-(S/TM)_{R2}-Fas). Furthermore, the relatively weak homotypic interactions of TNFR2-Fas chimaeras could be enhanced by replacing stalk and TM regions with the ones of TNFR1 (TNFR2-(S/TM)_{R1}-Fas; Dr Anja Krippner-Heidenreich, personal communication). All these data point to a critical role of the TM and/or stalk region in homotypic receptor dimerisation.

As sTNF responsiveness was found to be strongly regulated by the stalk region of the TNFR, protein crosslinking experiments were performed as part of this PhD project to investigate the influence of the TNFR2 stalk region on ligand-independent receptor-receptor interactions of TNFR-Fas chimaeras. Deletion of 42 aa residues in the TNFR2 stalk region increased the homotypic receptor interactions of TNFR2-Fas, indicating that this region inhibits ligand-independent receptor pre-assembly of the parental TNFR2-Fas chimaera. In contrast, no such increase could be observed when the same 42 aa residues were deleted in the stalk region of TNFR1-(S/TM)_{R2}-Fas, which

suggests that the control of ligand-independent receptor-receptor interactions of TNFR1-Fas differs from the ones seen for TNFR2-Fas.

For the parental TNFR2-Fas and TNFR1-Fas chimaeras as well as their respective stalk deletion mutants a strong decrease in signal strength of the monomeric and dimeric/multimeric forms could be observed at high BS³ concentrations (250 μM and 500 μM; Figure 45 C and Figure 46 C). At the same time high molecular weight bands appeared in these samples, which presumably represent receptor species which had not only been crosslinked with one another but had, due to the high BS³ concentrations, also been crosslinked unspecifically with other plasma membrane components. Furthermore, the decrease in signal intensity observed for β-actin, which is an intracellular protein, indicates that at these high concentrations BS³ is either no longer membrane-impermeable or, alternatively, cannot not be quenched efficiently enough to completely abrogate the crosslinking reaction (Figure 45 C, bottom). Therefore, crosslinking occurring at 250 μM and 500 μM BS³ cannot be regarded as specific and no assumptions about homotypic receptor-receptor interactions can be made for these samples.

While samples which did not contain the crosslinking reagent only showed bands for the respective monomers, in lysates from BS³-treated cells also protein bands of higher molecular weight could be detected, which corresponded in their molecular weight to dimeric receptors (TNFR1-Fas, TNFR1-(S_{Δ42}/TM)_{R2}-Fas and TNFR2-(S_{Δ42}/TM)_{R2}-Fas; Figure 45 C as indicated). The observation of dimeric TNFR-Fas chimaeras is in good agreement with crystallographic data obtained by Naismith *et al.* (1995, 1996a, 1996b) who depicted wild type TNFR1 to exist as dimers in the absence of the ligand. Furthermore, according to Mukai *et al.* (2010) wild type TNFR2 occurs as receptor dimers in the presence of TNF. In contrast to TNFR1-Fas, TNFR1-(S_{Δ42}/TM)_{R2}-Fas and TNFR2-(S_{Δ42}/TM)_{R2}-Fas, the molecular weight of crosslinked TNFR2-Fas cannot definitely be assigned to a TNFR2-Fas dimer but could, due to the limited resolution of 10 % SDS-PAGE gels, also represent receptor trimers. The occurrence of TNFR2 as trimers has already been proposed by Chan *et al.* (2000). However, previous protein crosslinking experiments with MF TNFR2-Fas rather suggest that in the absence of ligand this chimaera exists as a dimer in the plasma membrane (Boschert *et al.*, 2010).

Regardless of whether these chimaeras exist as dimers or trimers, it becomes apparent that the homotypic interactions of TNFR2-Fas are relatively weak with only

low signal strength for the crosslinked receptors at 64 μM BS³. Importantly, an increase in homotypic interactions of TNFR2-Fas could be observed when 42 aa residues were deleted in the TNFR2 stalk region (Figure 45 C), highlighting the inhibitory effect of the TNFR2 stalk region on ligand-independent homotypic receptor-receptor interactions.

Unexpectedly, shortening of the stalk region by the same 42 aa could not restore the receptor-receptor interactions of TNFR1-(S/TM)_{R2}-Fas chimaeras to match the ones observed for parental TNFR1-Fas (Figure 46 C). While crosslinked species of TNFR1-Fas could readily be observed at a BS³ concentration of 33 μM , only a weak signal could be observed for crosslinked TNFR1-(S _{Δ 42}/TM)_{R2}-Fas dimers at 125 μM BS³. Preliminary protein crosslinking data generated by Gerlinde Holeiter (Stuttgart University, Germany), showed that the exchange of the TNFR1 TM region with that of TNFR2 already leads to a decrease in homotypic receptor-receptor interactions of TNFR1-Fas. Therefore, data presented here (Figure 46 C) together with data by Gerlinde Holeiter suggest that ligand-independent receptor-receptor interactions of TNFR1-Fas are probably rather controlled by the TM region and/or the adjacent intracellular aa residues than the TNFR stalk region. Whether this could be associated with different requirements of TNFR1 and TNFR2 regarding their plasma membrane localisation is discussed in chapter 6.

Importantly, the differences in signal strength for the crosslinked TNFR-Fas chimaeras are most probably not caused by a lack of crosslinkable aa residues. BS³ interacts with the primary amino groups of arginines, lysines and the protein N-terminus (Figure 44). Based on the published crystal structures of the soluble TNFR, one or more covalent linkages by BS³ are possible for TNFR1-Fas and TNFR2-Fas in both, parallel and antiparallel arrangement of the receptor dimers (Prof. Richard Lewis, Newcastle University, personal communication). Moreover, the two arginine residues amongst the deleted 42 aa residues in the TNFR2 stalk region do not appear to qualify as sites for potential BS³-mediated crosslinking as suggested by the increase in signal strength for crosslinked TNFR2-(S _{Δ 42}/TM)_{R2}-Fas compared to TNFR2-Fas.

In conclusion, the data presented here together with previously obtained preliminary data demonstrate that for TNFR2-Fas the strength of ligand-independent homotypic receptor-receptor interactions is determined by its stalk region and correlates with the

potential of the TNFR-Fas chimaeras to be activated by sTNF. This suggests that the lack of receptor pre-assembly could prevent TNFR2 responsiveness to sTNF. However, in case of TNFR1-Fas efficient receptor activation by sTNF seems to be regulated by an additional mechanism (or mechanisms) as sTNF responsiveness of TNFR1-(S_{Δ42}/TM)_{R2}-Fas does show no such correlation with the strength of ligand-independent receptor pre-assembly. Therefore, the mechanism(s) underlying efficient sTNF-mediated activation of TNFR1-(S_{Δ42}/TM)_{R2}-Fas despite chimaera's lower degree of ligand-independent pre-assembly remains yet to be determined.

MF are deficient for murine TNFR1 and TNFR2 but do express endogenous murine TNF. Comparison of murine and human TNF showed that the murine ligand is capable of binding both human TNFR almost equally well as the human version of TNF (reviewed in Lucas *et al.*, 2005). Therefore, there is the possibility that the differences in receptor homodimerisation between the parental chimaeras and the stalk region deletion mutants TNFR1-(S_{Δ42}/TM)_{R2}-Fas and TNFR2-(S_{Δ42}/TM)_{R2}-Fas could be caused by altered interactions of the receptors with endogenous murine TNF. However, binding studies with iodinated human sTNF had revealed that ligand-binding affinities for the parental chimaeras and the corresponding stalk region deletion mutants were comparable (Dr Anja Krippner-Heidenreich, personal communication). Based on the data from the binding study, rather similar results should be expected in the crosslinking experiments for both, parental and mutant chimaeras if murine TNF played a role as crosslinking mediator here. As this is not the case, it is, therefore, relatively unlikely that the differences in homotypic receptor interactions can be attributed to altered TNFR-Fas interactions with endogenous murine TNF.

5.4.2 Inhibition of TNFR2 and TNFR2-Fas cluster formation by the TNFR2 stalk region

As mentioned above, ligand-independent TNFR-Fas pre-assembly overall correlates with the potential of the chimaeras to respond to sTNF. In addition, the ability of TNFR to form large receptor clusters upon stimulation with sTNF has been found to correlate with receptor responsiveness towards sTNF (Krippner-Heidenreich *et al.*, 2002). Data presented here, which were obtained using an inducible cell system, revealed an

inhibitory role for the TNFR2 stalk region in the formation of larger clusters of both TNFR2-Fas chimaeras and wild type TNFR2.

As a first approach to detect receptor clusters, TNFR-Fas chimaeras and TNFR2 variants were stained on the cell surface using Alexa546-labelled sTNF. Based on the crystal structure published by Mukai *et al.* (2010), a diameter of approximately 8.5 nm was determined for a TNF trimer in complex the extracellular domains of three TNFR2 molecules. This is also consistent with the crystal structure for the LT α /TNFR1 complex, which has been described previously (Banner *et al.*, 1993). Consequently, one of the trimeric TNF/TNFR complexes presumably occupies a cell surface area of roughly 57 nm². As determined from the confocal microscopy images, receptor cluster sizes for TNFR-Fas chimaeras and wild type TNFR2 variants ranged from approximately 1 x 10⁴ nm² – 8 x 10⁴ nm² and, therefore, comprise a maximum of 200-1400 ligand/receptor complexes consisting of trimeric TNF and three receptors.

For TNFR1-Fas, TNFR2-Fas and wild-type TNFR2 fewer and smaller receptor clusters could be observed (200-500 trimeric TNF/TNFR complexes/cluster; Figure 49 A – H and Figure 55 A – D). An increase in number and size of the receptor clusters was seen when stalk and TM regions of TNFR1 were introduced into TNFR2-Fas and wild-type TNFR2, respectively (900 – 1400 TNF/TNFR complexes/cluster; Figure 49 I – L and Figure 55 E – H). Similarly, deletion of 42 aa residues in the TNFR2 stalk region lead to an increase in receptor cluster number and size of both TNFR2-Fas and wild-type TNFR2 (300 – 1400 TNF/TNFR complexes/cluster; Figure 49 M – P and Figure 55 I – L).

We cannot exclude that for the TNFR1-(S Δ ₄₂/TM)_{R2}-R2 variant its higher cell surface expression (MnX = 19415; Figure 53 D) compared to wild-type TNFR2 (MnX = 11869; Figure 52 D) causes increased receptor aggregation on the cell surface. However, despite equal or even lower cell surface expression compared to the parental receptors, enhanced cluster formation could be observed for TNFR1-(S Δ ₄₂/TM)_{R2}-Fas and TNFR2-(S Δ ₄₂/TM)_{R2}-Fas compared to TNFR2-Fas and TNFR2-(S Δ ₄₂/TM)_{R2}-R2 compared to wild type TNFR2. This suggests that indeed the TNFR2 stalk region controls TNFR2 cluster formation and that this is independent of receptor cell surface expression.

In addition to the staining with Alexa546-labelled sTNF, receptor cluster formation has also been investigated using a PE-labelled TNFR2-specific antibody. Again, for

TNFR2-Fas and wild type TNFR2 only weak cluster formation could be observed when fixed cells were stained with this antibody (Figure 50 A and Figure 56 A). In contrast, for both stalk deletion mutants, TNFR2-(S_{Δ42}/TM)_{R2}-Fas and TNFR2-(S_{Δ42}/TM)_{R2}-R2, more distinct receptor clusters could be observed. However, the observed clusters were less pronounced than the ones seen in the staining with sTNF. As the sTNF staining was performed on live cells and followed by a fixing step at room temperature this might have been sufficient to allow the ligand to promote formation of receptor clusters. Therefore, the size of signalling competent receptor clusters is probably smaller than estimated above and the formation of larger receptor clusters appears to be not (entirely) ligand-independent but requires the presence of sTNF.

This also seems to be the case for the TNFR2-(S/TM)_{R1}-R2 variant, which clearly shows larger receptor clusters in sTNF stained samples (Figure 55 E – H) but no obvious aggregation of the receptors when cells were stained with the antibody (Figure 56 B). For the corresponding TNFR2-(S/TM)_{R1}-Fas chimaera also enhanced cluster formation could be detected on sTNF-stained cells (Figure 49 I – L). However, to what extent this cluster formation occurs ligand-independently remains yet to be determined.

It has been shown previously that the formation of signalling competent TNFR-Fas complexes can be measured by the level of apoptosis HEK cells undergo upon overexpression of the chimaeras (Branschädel *et al.*, 2010). Experiments recently performed by Dr Anja Krippner-Heidenreich showed that the cluster size of the TNFR-Fas chimaeras investigated in this PhD project correlated with the potential of the respective receptor to signal for apoptosis (Dr Anja Krippner-Heidenreich, personal communication). While efficient induction of apoptosis could be observed for TNFR1-Fas, TNFR2-(S/TM)_{R1}-Fas and TNFR2-(S_{Δ42}/TM)_{R2}-Fas, hardly any apoptotic response was seen for TNFR2-Fas. Therefore, the TNFR2 stalk region counteracts the formation of larger receptor clusters, which is in turn apparently required for efficient receptor activation.

Taken together, our data show that by deleting 42 aa residues in the TNFR2 stalk region TNFR2-Fas chimaeras and wild type TNFR2 can be converted into receptors which form larger aggregates upon incubation with sTNF similar to the ones observed for TNFR1 and TNFR1-Fas (Krippner-Heidenreich *et al.*, 2002, Schneider-Brachert *et al.*, 2004).

5.5 Conclusion

- The TNFR2 stalk region prevents ligand-independent, most likely PLAD-PLAD-mediated homotypic receptor dimerisation of TNFR2-Fas chimaeras.
- Ligand-independent homotypic receptor interactions of TNFR1 are not entirely controlled by the stalk region but rather may be determined by the TM region and/or the adjacent membrane-proximal intracellular aa residues and CRD1.
- 42 aa residues in the TNFR2 stalk region inhibit formation of larger receptor clusters of TNFR2-Fas chimaeras and wildtype TNFR2. Deletion of these 42 aa facilitates the formation of larger sTNF-induced clusters of both, TNFR2-Fas and wildtype TNFR2.

CHAPTER 6

General Discussion

The aim of this thesis has been to investigate the role of the stalk region in differential TNFR responsiveness to sTNF at the level of signalling complex formation and cluster formation and to identify the component(s) in this region controlling sTNF responsiveness.

6.1 General perspective

TNF is a pro-inflammatory cytokine which plays an important role in the regulation of the immune system and, consequently, in the pathogenesis of various autoimmune diseases (reviewed in Bradley, 2008, Faustman and Davis, 2010). It exists either as a transmembrane homotrimer or, upon protease-mediated cleavage, as its soluble form sTNF (Black *et al.*, 1997). The soluble and membrane-bound forms of TNF appear to play different roles in immunity and data from mouse models indicate that it is rather sTNF than membrane-bound TNF which plays a role in the development of autoimmune diseases such as RA and MS (Steed *et al.*, 2003, Alexopoulou *et al.*, 2006). In good agreement with these observations, neutralisation of TNF proves to be a successful therapy for RA (Bradley, 2008) and neutralisation of sTNF in particular can ameliorate disease symptoms in experimental arthritis (Steed *et al.*, 2003).

In addition to the different roles for the two forms of TNF, divergent biological functions have also been described for the two TNFR with, for example, TNFR1 being critically involved in host defence and sepsis (Pfeffer *et al.*, 1993, Rothe *et al.*, 1993, Castanos-Velez *et al.*, 1998, Fujita *et al.*, 2008) and TNFR2 playing an important role in the modulation of immune tolerance (Valencia *et al.*, 2006, Ban *et al.*, 2008, Chen *et al.*, 2008, Nagar *et al.*, 2010). In addition, data from animal models of RA have implied a pro-inflammatory role for TNFR1 and a rather suppressive function for TNFR2 (Mori *et al.*, 1996, Tada *et al.*, 2001b).

Both forms of TNF can bind to TNFR1 and TNFR2 with high affinity, but, while the membrane-bound variant can fully activate both receptors, sTNF is only capable of

activating TNFR1 efficiently (Grell *et al.*, 1995, Grell *et al.*, 1998b). This differential responsiveness of TNFR2 towards the soluble and the membrane-bound ligand is a characteristic which can also be observed for various other members of the TNFR superfamily. For the soluble form of FasL, for example, a strong reduction in its proapoptotic activity compared to membrane-bound FasL has been described (Suda *et al.*, 1997, Schneider *et al.*, 1998), which was found to be associated with increased autoimmunity and enhanced anti-apoptotic, pro-inflammatory signalling (O'Reilly *et al.*, 2009). Differences in receptor activation potential between the soluble and membrane-bound forms of TRAIL (Wajant *et al.*, 2001), APRIL (Bossen *et al.*, 2008), OX40 ligand (Müller *et al.*, 2008) and TWEAK (Roos *et al.*, 2010) have also been described.

Ligand trimer stabilisation and/or oligomerisation have been reported to be important parameters for the efficient activation of some of the TNFR superfamily members including TNFR2 (Krippner-Heidenreich *et al.*, 2002, Bryde *et al.*, 2005, Müller *et al.*, 2008, Wyzgol *et al.*, 2009, Rauert *et al.*, 2010). In addition, responsiveness towards sTNF correlates with the ability of the TNFR1 and TNFR2 to form larger sTNF-mediated receptor clusters (Krippner-Heidenreich *et al.*, 2002, Schneider-Brachert *et al.*, 2004, Branschädel *et al.*, 2010). While stimulation with sTNF leads to the formation of large TNFR1 clusters, the formation of similar TNFR2 clusters requires additional stabilisation (Krippner-Heidenreich *et al.*, 2002, Schneider-Brachert *et al.*, 2004).

A domain which mediates homotypic receptor-receptor interaction in the absence of the ligand is the PLAD, which is located in CRD1. As already described for Fas (Papoff *et al.*, 1996, Papoff *et al.*, 1999, Siegel *et al.*, 2000), this domain mediates ligand-independent homotypic interactions of TNFR1 and TNFR2, respectively, (Chan *et al.*, 2000) and CRD1, which mediates these interactions, was found to be a potential co-factor for conferring sTNF responsiveness to TNFR1 (Branschädel *et al.*, 2010). However, CRD1 exchange mutants revealed that this domain is not the sole determinant for sTNF responsiveness of the TNFR.

In an attempt to locate the receptor region(s) responsible for controlling TNFR responsiveness towards sTNF, different regions were exchanged between TNFR1-Fas and TNFR2-Fas. When receptor chimaeras, in which only the TM region had been exchanged, were analysed, only a minor role for the TM regions in differential responsiveness towards sTNF could be observed (Dr Anja Krippner-Heidenreich, personal communication). However, preliminary data from MF transfected with TNFR-

Fas chimaeras in which both, stalk and TM regions had been exchanged between receptors (TNFR1-(S/TM)_{R2}-Fas and TNFR2-(S/TM)_{R1}-Fas) indicated that the stalk regions, potentially together with the TM regions, are involved in determining differential responsiveness to sTNF (Figure 11 B and E).

Furthermore, ligand-independent homotypic receptor-receptor interactions and formation of receptor clusters of these chimaeras correlated with the observed sTNF responsiveness. Chimaeras containing the TM and stalk regions of TNFR2 (TNFR2-Fas and TNFR1-(S/TM)_{R2}-Fas) showed weak ligand-independent homotypic interactions and no formation of larger receptor clusters. In contrast, for the corresponding chimaeras with TNFR1 stalk and TM regions (TNFR1-Fas and TNFR2-(S/TM)_{R1}-Fas) stronger homotypic interactions and formation of larger receptor clusters could be observed (Dr Anja Krippner-Heidenreich, personal communication). Taken together, these data suggest that the TNFR stalk regions, potentially together with the TM regions, determine responsiveness towards sTNF and that this may be controlled at the level of ligand-independent receptor pre-assembly and cluster formation. Therefore, it was the aim of this PhD project to establish the role of the TNFR stalk regions in sTNF responsiveness as well as ligand-independent pre-assembly and cluster formation of the TNFR and to investigate the underlying molecular mechanism(s).

6.2 The TNFR stalk region and its prominent molecular features in the control of receptor responsiveness to sTNF

Preliminary data obtained from the TNFR1-(S_{Δ42}/TM)_{R2}-Fas chimaera, which contains a version of the TNFR2 stalk region of the same length as the TNFR1 stalk region, had suggested that it is the stalk regions of TNFR1 and TNFR2 in particular which play a role in differential responsiveness towards sTNF (Figure 11 C). The data obtained during this PhD project demonstrate that the TNFR stalk region is indeed a major determinant for this differential responsiveness and show that 42 aa in the TNFR2 stalk region inhibit receptor responsiveness towards sTNF. This was found to be the case for both, TNFR-Fas chimaeras as well as wild type TNFR2 (sections 3.2 and 3.3).

The sTNF responsiveness of TNFR2-Fas can be increased more than 100-fold by the deletion of 42 aa in the TNFR2 stalk region (section 3.2). However, this chimaera is still 10-fold less responsive towards sTNF compared to CysTNF. This finding is in

agreement with data, which showed that susceptibility towards sTNF was decreased when either the TM regions (Dr Anja Krippner-Heidenreich, personal communication) or CRD1 (Branschädel *et al.*, 2010) had been exchanged between TNFR1 and TNFR2. Together these data indicate that sTNF responsiveness is controlled by at least three different regions of the receptor: the N-terminal CRD1, the TM region and the stalk region.

Similar results were obtained for wild type TNFR2 when either the stalk and TM regions of TNFR2 were exchanged for the ones of TNFR1 (TNFR1-(S/TM)_{R2}-R2) or the TNFR2 stalk region was shortened by 42 aa (TNFR2-(S_{Δ42}/TM)_{R2}-R2). A significant increase in sTNF responsiveness at the level of TRAF2 recruitment to the TNFR2 signalling complex could be observed compared to the wild type receptor (Figure 18 and Figure 19) and this was independent of TNFR1 signalling (Figure 24 and Figure 25). Moreover, very recently it could be shown that the enhanced sTNF-mediated TRAF2 recruitment to TNFR2-(S_{Δ42}/TM)_{R2}-R2 is reflected by an increased activation of NF-κB signalling (Dr Anja Krippner-Heidenreich, personal communication). This indicates that the 42 aa residues in the TNFR2 stalk region also affect sTNF-mediated downstream signalling and that results obtained from the TNFR-Fas cellular system can be directly translated into the wild type TNFR2 system.

6.2.1 The role of stalk region O-glycosylation in sTNF responsiveness of TNFR2

The stalk regions of the two TNFR differ in their aa composition and, with 15 aa for TNFR1 and 56 aa for TNFR2, also in their length. When 42 aa residues were deleted in the TNFR2 stalk region to match its length to the one of the TNFR1 stalk region, this also abolished predicted O-glycosylation sites as well as eight proline residues.

For TNFR1 and TNFR2 post-translational modifications have been reported. Both receptors have been described to be N-glycosylated (Hohmann *et al.*, 1989) and the membrane proximal region of TNFR2 was also found to be O-glycosylated (Pennica *et al.*, 1993). When the TNFR2 stalk region was shortened by 42 aa, more than 10 putative O-glycosylation sites were deleted (Figure 29). Three lines of evidence support O-glycosylation of the stalk region of wild type TNFR2 and TNFR2-Fas variants investigated in this thesis. Firstly, in Western Blot analysis a decreased molecular weight could be observed for stalk deletion mutants of both wild-type TNFR2 and TNFR2-Fas (Figure 13, Figure 16 and Figure 26) and this decrease was greater than the

calculated sum of molecular weights of the single deleted aa residues. Secondly, full replacement of the TNFR2 stalk region with a 56 aa long artificial linker (TNFR2-S_{GSL56}-TM_{R2}-Fas) resulted in a chimaera which again showed reduced molecular weight compared to TNFR2-Fas (Figure 31). Thirdly, in contrast to parental TNFR2-Fas, the molecular weight of TNFR2-S_{GSL56}-TM_{R2}-Fas also remained unaltered when cells were treated with the O-glycosylation inhibitor Benzyl- α -GalNAc (Figure 39). Therefore, TNFR2-Fas and TNFR2 appear to be O-glycosylated when stably expressed in MF and this O-glycosylation seems to be located in the stalk region. This is in agreement with data, which have been published for wild type TNFR2 previously (Pennica *et al.*, 1993).

As mentioned above, TNFR2 has also been reported to be N-glycosylated. N-glycosylation of any of the TNFR2-Fas and TNFR2 variants should, however, not be affected by TNFR2 stalk region deletion or replacement as it has been reported to occur not in this region but at two asparagine residues in CRD4 (Pennica *et al.*, 1993). In line with this, two bands could be detected for the stalk deletion mutants TNFR2-(S _{Δ 42/TM)_{R2}-Fas and TNFR2-(S _{Δ 42/TM)_{R2}-R2 as well as the stalk replacement mutants TNFR2-S_{GSL15}-TM_{R2}-Fas and TNFR2-S_{GSL56}-TM_{R2}-Fas in Western Blot analyses (Figure 13, Figure 16 and Figure 31). Whether these receptor variants are indeed N-glycosylated similarly to wild type TNFR2 remains, however, yet to be confirmed.}}

Differential responsiveness to soluble and membrane-bound ligand has also been described for two other members of the TNFR-related superfamily, TRAILR1 and TRAILR2 (Wajant *et al.*, 2001). While TRAILR1 can be activated by both, the soluble and the membrane-bound form of TRAIL, TRAILR2 activation requires membrane-bound TRAIL. Similar to TNFR1 and TNFR2, the stalk regions of the two TRAILR differ in their length (10 aa for TRAILR1, 32 aa for TRAILR2) and their predicted O-glycosylation sites. Interestingly, O-glycosylation of the stalk region of TRAILR2 has been found to influence the receptor sensitivity towards TRAIL and the ability of the receptor to signal for apoptosis (Wagner *et al.*, 2007). In contrast to TRAILR2, in which the stalk region has an activating function in the induction of apoptosis, the stalk region of TNFR2 seems to play rather a inhibitory role in signalling initiation. This inhibitory role of the TNFR2 stalk region, however, remained unaltered when putative O-glycosylation sites were mutated or, alternatively, TNFR2-Fas chimaeras were treated with the core 1/core 2 O-glycosylation inhibitor Benzyl- α -GalNAc. Therefore, this type of O-glycosylation apparently plays no role in receptor responsiveness towards sTNF under the given experimental conditions.

While O-glycosylation of the stalk region might not be a prerequisite for TNFR2 responsiveness to sTNF it might exert other functions. Involvement of O-glycosylation has been reported in trafficking, delivery and cell surface stabilisation of proteins (reviewed in Tian and Ten Hagen, 2009) and site-specific O-glycosylation of the membrane-proximal part of the extracellular portion of the neurotrophin receptor, for example, was proposed to be essential for apical sorting of this receptor (Breuza *et al.*, 2002). One of the TNFR2-Fas chimaeras with mutated O-glycosylation sites, TNFR2-Fas mot. 1/4 (Figure 37), was not expressed at the cell surface despite its high intracellular expression, suggesting that motif 4 may be required for the export of TNFR2-Fas chimaeras from the endoplasmic reticulum and/or plasma membrane localisation. However, neither the partial stalk exchange mutant TNFR2-(S_{Exaa202-219}/TM)_{R2}-Fas nor the full stalk exchange mutants TNFR2-S_{GSL15}-TM_{R2}-Fas and TNFR2-S_{GSL56}-TM_{R2}-Fas contain O-glycosylation motif 4 but are both expressed on the cell surface at high levels. Hence, the role of motif 4 O-glycosylation remains elusive and there is the possibility that specifically its mutation in combination with motif 1 leads to a misfolding of the chimaera which in turn inhibits its membrane localisation. Alternatively, the effect of motif 4 could be dependent on other sequences which are not present in the full and partial stalk exchange mutants, for which no such inhibitory effect on membrane localisation could be observed (Figure 33 and Figure 43).

The O-glycosylation status of the stalk region does apparently not affect the ligand binding affinity of the receptor. In contrast to the CD8 β receptor, in which O-glycosylation/sialylation of the stalk region was proposed to influence its ligand binding affinity (Moody *et al.*, 2001, Moody *et al.*, 2003), binding studies indicated that sTNF binds with comparably high affinity to TNFR-Fas chimaeras with wild type and shortened TNFR2 stalk regions, respectively (Dr Anja Krippner-Heidenreich, personal communication).

6.2.2 Control of sTNF responsiveness by proline residues in the TNFR2 stalk region

In addition to the O-glycosylation of the TNFR2 stalk region we also investigated the role of stalk region length and conserved proline residues in this region. Our data show that neither the length nor single conserved proline residues of the stalk region control TNFR2-Fas responsiveness towards sTNF (sections 4.2 and 4.3).

While our data indicate that it is unlikely that a single proline residue in the TNFR2 stalk region is acting as a molecular switch controlling sTNF responsiveness, there is the possibility that a combination of several proline residues in this region could determine sTNF responsiveness. This, however, has not been further investigated in this PhD project. In proteins, proline-rich sequences are often found in extended structures and flexible regions and can confer both, flexibility and stability (reviewed in Williamson, 1994). The left handed collagen helix is a prominent example of such a secondary structure (reviewed in Bhattacharjee and Bansal, 2005). In comparison to collagen, the proline residues in the TNFR2 stalk region are less abundant and do not occur in an equally regular pattern, but they may still determine stalk region conformation and orientation while also providing a certain degree of flexibility and/or rigidity.

In this context, it is worth noting that, by introducing artificial linkers into TNFR-Fas chimaeras, the wild type TNFR2 stalk region was replaced with an aa sequence which is postulated to be very flexible and predicted to adopt no distinct secondary structure but a random coil fold (Evers *et al.*, 2006). This replacement of the wild type TNFR2 stalk region with artificial 56 aa stalk regions turned TNFR2-Fas into a receptor which was responsive towards sTNF. Therefore, one might speculate that the rigidity of wild type TNFR2 stalk region, which is potentially determined by its proline-richness, inhibits responsiveness towards sTNF and can only be overcome when either the ligand exists in an oligomerised state such as described by Bryde *et al.* (2005) and Rauert *et al.* (2010) or additional stabilisation is provided by e.g. the mouse anti-human TNFR2 antibody 80M2 (Grell *et al.*, 1995, Krippner-Heidenreich *et al.*, 2002). If the rigidity of the stalk region as a whole was counteracting sTNF responsiveness of TNFR2, partial replacement of this region with flexible linkers might not be sufficient to overcome this inhibition. This could explain why the sTNF responsiveness of TNFR2-Fas chimaeras, in which the stalk region had been only partly exchanged with

artificial linkers, did not differ from the one seen for the parental chimaera (Figure 11 and Figure 43).

6.3 Inhibition of ligand-independent TNFR interactions and cluster formation by the TNFR2 stalk region

Receptor cluster formation is thought to enhance signal transduction of transmembrane receptors by, for example, increasing their sensitivity and specificity and enhancing response simultaneity, respectively (reviewed in Duke and Graham, 2009). Formation of ligand-induced clusters of TNFR1 has been demonstrated previously (Schneider-Brachert *et al.*, 2004) and Krippner-Heidenreich *et al.* (2002) observed that TNF-mediated activation of TNFR1-Fas chimaeras also coincided with the formation large receptor clusters. The TNFR PLAD and the localisation of the TNFR in plasma membrane microdomains have already been described as two possible determinants for the formation of these receptor clusters. CRD1, which contains the PLAD, has been proposed to be required for high affinity ligand binding of TNFR1 (Chan *et al.*, 2000). The homotypic interactions of the TNFR2 PLAD are weaker than the ones seen for TNFR1 and a correlation of the strength of PLAD/PLAD-mediated interactions with sTNF responsiveness of TNFR1-Fas has been described recently (Branschädel *et al.*, 2010). However, these weaker PLAD/PLAD interactions only account to some extent for the reduced sTNF responsiveness of TNFR1-Fas as the exchange of the TNFR1 PLAD with the one of TNFR2 did not render TNFR1-Fas fully unresponsive to sTNF (Branschädel *et al.*, 2010).

6.3.1 The TNFR2 stalk region abrogates ligand-independent TNFR interactions

Preliminary data from chemical protein crosslinking experiments indicated a potential role for the stalk regions of TNFR1 and TNFR2 in ligand-independent homotypic pre-assembly of the receptors (Dr Anja Krippner-Heidenreich, personal communication). In this PhD project an inhibitory role for the TNFR2 stalk region in the control of homotypic interactions of TNFR2-Fas could be confirmed. An increase in homotypic interactions of TNFR2-Fas could be observed when 42 aa residues were deleted in the TNFR2 stalk region (Figure 45 C). In contrast, shortening of the TNFR2 stalk region by 42 aa could not restore the homotypic receptor-receptor interactions of TNFR1-

(S/TM)_{R2}-Fas chimaeras to the same level as seen for the parental TNFR1-Fas chimaera (Figure 46 C). As mentioned in section 5.4.1, protein crosslinking data by Gerlinde Holeiter indicated that the exchange of the TNFR1 TM region with the one of TNFR2 already leads to a decrease in homotypic receptor-receptor interactions of TNFR1-Fas. Together with the data presented here (Figure 46 C) this suggests that ligand-independent receptor-receptor interactions of TNFR1-Fas are rather controlled by the TM region and/or the adjacent intracellular aa residues, which were exchanged together with the TM region, than by the stalk region.

Interestingly, for TNFR1 the aa sequence YQRW (aa 236-239), which comprises four aa of the proposed TM region and two membrane-proximal intracellular aa of TNFR1, has been described to be essential for TNFR1 internalisation (Schneider-Brachert *et al.*, 2004, Schütze *et al.*, 2008). Data on whether these aa residues are required for localisation of TNFR1 to cholesterol-rich membrane microdomains are conflicting (Schneider-Brachert *et al.*, 2004, D'Alessio *et al.*, 2010), but some of these aa are part of a potential cholesterol binding motif. The aa consensus sequence L/V-X₍₁₋₅₎-Y-X₍₁₋₅₎-R/K, where X is any aa, has previously been described for cholesterol binding proteins (Li and Papadopoulos, 1998). In the case of TNFR1 a potential cholesterol binding motif is represented by the aa sequence LMYRYQR (aa 232 – 238). Variations of this potential cholesterol binding motif are maintained in the TNFR1-Fas and TNFR2-(S/TM)_{R1}-Fas chimaeras with the aa sequence LMYRYLK and in the TNFR2 variant TNFR2-(S/TM)_{R1}-R2 with the aa sequence LMYRKKK. In contrast, wild type TNFR2 and (chimaeric) variants thereof, which include the TNFR2 TM region and the 14 membrane-proximal intracellular aa residues, do not contain such a potential cholesterol binding motif. The presence of this motif may be required for the localisation of TNFR1 to cholesterol-rich plasma membrane compartments, which would be in agreement with data describing different localisation of the two TNFR in the plasma membrane (Ranzinger *et al.*, 2009, Gerken *et al.*, 2010). It is conceivable that this different membrane localisation could be a determining factor for homotypic interactions of the TNFR-Fas chimaeras (see also following section).

6.3.2 The TNFR2 stalk region counteracts TNFR2 cluster formation

While receptor activation and cluster formation of TNFR1-Fas chimaeras occur simultaneously upon stimulation with sTNF, sTNF-mediated cluster formation of TNFR2 (Dr Anja Krippner-Heidenreich personal communication) and TNFR2-Fas (Krippner-Heidenreich *et al.*, 2002) only occurs in the presence of the stabilising mouse anti-human TNFR2 antibody 80M2. Therefore, the ability of TNFR2 and TNFR2-Fas to form sTNF-induced receptor clusters correlates with their responsiveness to sTNF.

The role of formation of receptor clusters is not quite clear to date as recent evidence emerged that the formation of larger receptor clusters might be dispensable for efficient TNFR1-Fas activation (Ranzinger *et al.*, 2009). Studies with nanoscale arranged TNF rather suggest that a confinement of TNFR1-Fas to membrane microdomains of approximately 200 nm in diameter is required for apoptosis induction (Ranzinger *et al.*, 2009). While this apoptosis induction appears to be largely cholesterol independent (Ranzinger *et al.*, 2009), cholesterol depletion increases the diffusion constant of TNFR1-Fas on the MF cell surface (Gerken *et al.*, 2010), indicating that TNFR1-Fas chimaeras are localised in cholesterol-rich membrane domains. Moreover, co-IP of caveolin-1 with a peptide encoding the TM region and part of the intracellular domain of TNFR1 has been described, suggesting a potential localisation of TNFR1 in caveolae, a subtype of cholesterol-rich membrane compartments (D'Alessio *et al.*, 2010). Therefore, this localisation may facilitate aggregation of the receptors by promoting interactions with lipids or certain proteins in these microdomains.

An important role for receptor localisation in cholesterol- and sphingolipid-rich plasma membrane microdomains has already been described for signalling of the TNFR superfamily member Fas (Eramo *et al.*, 2004). Fas localisation to cholesterol-rich plasma membrane microdomains has been proposed to be required for cluster formation of this receptor in response to soluble FasL (Henkler *et al.*, 2005). Formation of larger Fas receptor clusters requires the presence of the ligand, which was suggested to stabilise the signalling-competent form of Fas (Scott *et al.*, 2009). Furthermore, it has been speculated that TRAILR1 and TRAILR2 activation may function accordingly and FADD interactions may also stabilise receptor multimerisation of these receptors (Scott *et al.*, 2009).

What controls cluster formation of TNFR2 is also not understood to date. TNFR2 contains a membrane-proximal intracellular aa sequence similar to the lysine-

rich membrane-proximal intracellular sequence of Fas, which is required for constitutive localisation of Fas to cholesterol-rich membrane microdomains (Rossin *et al.*, 2010). Based on this sequence homology between TNFR2 and Fas a potential interaction of TNFR2 with the actin-binding protein ezrin has been proposed, which would link TNFR2 localisation and internalisation to the actin cytoskeleton (Fischer *et al.*, 2011). However, recent evidence emerged that the membrane-proximal lysine residues are not essential for Fas interaction with ezrin but rather palmitoylation of a membrane-proximal intracellular cysteine residue of Fas is required (Chakrabandhu *et al.*, 2007, Rossin *et al.*, 2010). Fas and TRAILR1 are both palmitoylated. However, this receptor modification appears to be not absolutely crucial for localisation in cholesterol-rich microdomains as TRAILR2 and TNFR1, which are not palmitoylated, still localise in these microdomains (Rossin *et al.*, 2009). It is conceivable that the presence of the aforementioned cholesterol binding motif may already be sufficient for this localisation of TNFR1.

In contrast, TNFR2 has not been reported to localise in such cholesterol-rich microdomains and in fluorescence correlation spectroscopy studies with TNFR-EGFP fusion proteins cholesterol depletion with methyl- β -cyclodextrin altered the diffusion of TNFR1 but not TNFR2 in the plasma membrane (Gerken *et al.*, 2010). In addition, methyl- β -cyclodextrin pre-treatment did not affect the apoptosis kinetics in MF TNFR2-Fas stimulated with sTNF in combination with the stabilising anti-human TNFR2 antibody 80M2 (Krippner-Heidenreich *et al.*, 2002).

By replacing the TM and four adjacent intracellular aa residues of TNFR2 and TNFR2-Fas with the ones of TNFR1 a potential cholesterol binding motif was introduced into the respective receptors (see above). Whether these receptors show a microdomain localisation which differs from the parental TNFR2-Fas chimaera and wild type TNFR2, respectively, remains yet to be determined. However, data from the stalk region deletion mutants TNFR2-(S _{Δ 42}/TM)_{R2}-Fas and TNFR2-(S _{Δ 42}/TM)_{R2}-R2 indicate that TNFR2 cluster formation is rather controlled by the stalk than the TM region (Figure 49 M - P and Figure 55 I - L). The exact mechanism of how the stalk region interferes with cluster formation remains elusive and whether the TNFR2 stalk region plays a role in controlling the localisation of TNFR2 into e.g. cholesterol-rich microdomains is yet to be determined.

In addition, TNFR2 contains two more features which could potentially affect its tendency to form receptor clusters: N-glycosylation in CRD4 at N149 and N171

(Pennica *et al.*, 1993) and a GXXXG (X represents any amino acid) motif in the TM region.

N-glycosylation of cell surface receptors has already been described to play a role in dimerisation and microdomain localisation of epidermal growth factor receptor (EGFR) and T-cell receptor (TCR; reviewed in Dennis *et al.*, 2009). Galectins, which belong to the sugar-binding lectins, have been found to counteract the dimerisation of epidermal growth factor receptor 1 (ErbB-1) and the multimerisation and the plasma membrane microdomain localisation of TCR. N-glycosylation is less efficient in the proximity of disulfide bonds, the TM region and at the termini of proteins (reviewed in Dennis *et al.*, 2009). The TNFR2 stalk region could theoretically adopt a bent secondary structure which would provide additional space for the N-linked oligosaccharide chains in CRD4. When 42 aa in the stalk region of TNFR2-Fas and wild type TNFR2 were deleted, we could observe an increase in the number and size of receptor clusters. It is conceivable that due to the shorter stalk region and the resulting closer proximity to the plasma membrane there would be less space for full-sized N-glycosylation of CRD4 and, therefore, less potential interaction with inhibitory lectins as described above. Moreover, full replacement of the TNFR2 stalk region with artificial linkers can render TNFR2-Fas chimaeras responsive towards sTNF, suggesting that a certain rigidity of the stalk region as previously discussed (section 6.2.2) may be required. Whether N-glycosylation could play a role in TNFR2 cluster formation and activation by sTNF remains yet to be determined.

Furthermore, receptor-receptor interactions and receptor oligomerisation of TNFR2 may also be influenced to some extent by a GXXXG motif in the TM region. Transmembrane helix-helix association by GXXXG motifs has been described to be involved in the dimerisation of several cell surface receptors including ErbB-1 and ErbB-2 (Bennasroune *et al.*, 2004) and neuropilin-1 (Roth *et al.*, 2008). A GXXXG motif would be represented by the aa sequence GLIVG (aa 263 – 267) in the TM region of TNFR2. This motif by itself, however, appears to be not sufficient to mediate strong homotypic receptor-receptor interactions as only weak bands could be observed for TNFR1-TM_{R2}-Fas (data not shown) and TNFR1-(S_{Δ42}/TM)_{R2}-Fas (Figure 46 C) in crosslinking experiments. This may be due to the fact that with 30 aa residues the predicted TM region of TNFR2 is relatively long and, as determined by *in silico* modelling experiments on artificial lipid bi-layers, is likely to span the plasma membrane not in a 90 ° angle but rather in a tilted angle (Prof. Peter Scheurich, University of Stuttgart, Germany, personal communication). Therefore, the GXXXG

motif could alter receptor conformation and/or orientation in the plasma membrane and thereby affect receptor pre-assembly and ability to form clusters.

The crystal structures of TNFR1 show that the receptor can exist as either parallel or anti-parallel dimers (Naismith *et al.*, 1995, Naismith *et al.*, 1996b, Naismith *et al.*, 1996a), of which only the parallel ones have been proposed to be able to bind TNF as in the anti-parallel dimers the TNF binding site is occluded (Naismith *et al.*, 1996a). Recently published crystallographic data of TNFR2 in complex with TNF showed that the secondary structure of this receptor is very similar to the one seen for TNFR1 (Mukai *et al.*, 2010), indicating that TNFR2 may form parallel and anti-parallel dimers similar to the ones seen for TNFR1. Therefore, orientation of the TNFR as anti-parallel dimers could represent a state in which the receptors would be maintained inactive.

The crystal structure published by Mukai *et al.* (2010) showed that in the TNF/TNFR2 complex TNF interaction with TNFR2 still occurred although the receptors were arranged as anti-parallel dimers. However, it has been suggested that this TNFR2 arrangement could represent an artefact from the crystallisation process (Mukai *et al.*, 2010). Moreover, if TNFR2 existed in such anti-parallel dimers, four aa residue pairs should be available to allow three covalent linkages of the receptor pair by the crosslinking reagent BS³ (K120 and K120, K120 and R99, R77 and R158, R99 and R158; Prof. Richard Lewis, Newcastle University, personal communication). However, protein crosslinking data presented in this PhD thesis (Figure 45) together with data by Boschert *et al.* (2010) showed only weak homotypic interactions of TNFR2-Fas chimaeras. Therefore, it is very unlikely that TNFR2 exists as such an anti-parallel dimer in the plasma membrane.

In contrast, TNFR2 could exist in a more upright position in the membrane, in which receptor dimer formation via the GXXXG motif is potentially supported by the loosely associated TNFR2 PLAD. In such a scenario, the rigid, bent TNFR2 stalk region together with the tilted TM region would ensure that the cytoplasmic parts of the dimeric receptors stay spatially separated and, therefore, in an inactive state. In this conformation, TNFR2 dimers would be able to bind sTNF but no signalling initiation would occur. This would be in agreement with previously published data, which showed that already TNFR2 dimers can bind sTNF with high affinity (Boschert *et al.*, 2010). Binding of membrane-bound TNF, however, could potentially cause conformational rearrangements of the TNFR2 dimer so that the effects of TM and stalk region could be overcome, larger receptor/ligand clusters could be formed and the

receptors would become activated. Through the deletion of the 42 aa residues in the TNFR2 stalk region the inhibitory effect of this region would be abrogated and sTNF would already be capable to induce the conformational changes in TNFR2 required for signalling initiation. Interestingly, TRAILR2, which has also been reported to be unresponsive to the soluble form of its ligand (Wajant *et al.*, 2001), also carries such a GXXXG motif in its TM region. Hence, further investigations into the mechanisms underlying the sTNF responsiveness of TNFR2 may also provide new insights into signalling mechanisms of this receptor.

As the TNFR2 stalk region was found to be a major determinant for receptor responsiveness to sTNF and both, sTNF and TNFR2 have been identified to be critically involved in autoimmune diseases, targeting of this region may represent an interesting new therapeutic approach in the treatment of such diseases. It has been shown previously that the stalk region of TNFR2 is accessible to polyclonal antibodies, which showed a mild agonistic effect (Bigda *et al.*, 1994). However, the effect of antibodies against the stalk region in combination with sTNF remains to be determined as part of future research.

6.4 Future work

While I could establish a role for the TNFR2 stalk region in receptor responsiveness towards sTNF, ligand-independent homotypic receptor-receptor interactions and receptor multimerisation/cluster formation, the work in this thesis has also raised a number of questions about the underlying mechanism(s). Further work will be required to address these questions and, in addition, to confirm some of the conclusions drawn here.

- Site directed mutagenesis of further predicted O-glycosylation sites and combinations of conserved proline residues in the TNFR2 stalk region, respectively, will be performed to elucidate their role in determining responsiveness to sTNF.
- Based on computational analysis of the published crystal structures of the parallel and anti-parallel dimers, aa residues which do not affect the overall receptor structure but are potentially involved in mediating receptor-

receptor interactions will be determined for the two TNFR. Site directed mutagenesis of these aa residues and subsequent crosslinking experiments with crosslinkers of different length will provide insights about conformational receptor arrangements and their role in TNFR responsiveness towards sTNF.

- While it could be demonstrated that the TNFR stalk region is an important determinant for differential sTNF responsiveness, it remains unknown whether the adjacent CRD4 could also play a role here. Especially the N-glycosylation described in CRD4 may represent a feature which determines TNFR2 cluster formation. Therefore, the role of this post-translational modification will be further investigated by mutational abrogation of the N-glycosylation sites in this region and subsequent analysis in the TNFR-Fas cell system.
- The role of receptor membrane localisation in homotypic ligand-independent receptor-receptor interactions and cluster formation will be determined. Protein crosslinking experiments and confocal microscopy experiments will be repeated with methyl- β -cyclodextrin-treated cells. This will shed light onto the role of the TNFR stalk regions in determining receptor localisation to cholesterol-rich plasma membrane microdomains and the consequences for ligand-independent receptor pre-assembly and cluster formation of TNFR1 and TNFR2. Isolation and biochemical characterisation of detergent-resistant membrane microdomains will elucidate to which cholesterol-rich membrane compartments the TNFR locate in particular.
- Live cell imaging at 37 °C will elucidate the role of the stalk region in sTNF-mediated cluster formation of TNFR2 under more physiological conditions. Furthermore, by using green fluorescent protein-coupled versions of TRAF2 and NF- κ B it will also be possible to investigate whether the observed cluster formation correlates with signalling initiation.
- The expression of TNFR2 is strongly regulated and mainly restricted to cells of the immune system, neuronal tissues, cardiac myocytes, mesenchymal stem cells and endothelial cells (reviewed in Faustman and Davis, 2010). As TNFR2 has been described to be involved in the proliferation of thymocytes (Grell *et al.*, 1998a), modulation of this TNFR2-mediated proliferation will be investigated to establish the role of the TNFR stalk region in receptor

responsiveness towards sTNF in a more physiological context. For this purpose, thymocytes will be isolated from *tnfr1^{-/-}* and *tnfr1^{-/-}/tnfr2^{-/-}* mice and transfected with lentiviral expression vectors for wild type TNFR2 and stalk mutants thereof. Analysis of these cells will elucidate whether the data obtained from the cellular model systems described in this PhD thesis also apply to more physiologically relevant cell types. Furthermore, this approach will provide a cellular system in which reagents affecting stalk region function can be ultimately tested for their suitability as new TNFR-selective therapeutics.

6.5 Summary

In this PhD thesis the TNFR2 stalk region could be established as an important determinant of TNFR2 responsiveness towards sTNF. Pilot data had already discovered a role for CRD1 in differential responsiveness of TNFR (Branschädel *et al.*, 2010) and preliminary data also suggested an involvement of the TNFR TM and/or stalk regions (Dr Anja Krippner-Heidenreich, personal communication). In this PhD project it could be demonstrated for the first time that the stalk region is the main determinant of differential sTNF responsiveness of TNFR1 and TNFR2 and that 42 aa residues in the TNFR2 stalk region inhibit responsiveness towards sTNF. Furthermore, data from various point and exchange mutants highlighted the complexity of the mechanism underlying the inhibitory effect of the TNFR2 stalk region on responsiveness towards sTNF. In addition, the data presented in this thesis show that the TNFR2 stalk region controls homotypic ligand-independent receptor-receptor interactions and receptor cluster formation, which both correlate with sTNF responsiveness of the receptor. Whether the TNFR stalk regions control these receptor interactions and cluster formation by affecting intrinsic structural arrangements, facilitating interactions with other proteins or by determining receptor localisation in the plasma membrane requires further investigation.

The findings in this thesis highlight the potential of the TNFR stalk region to serve as a potential target for future therapeutic agents for the treatment of sTNF-mediated auto-immune diseases and provide, furthermore, insight into signalling mechanisms which may also be valid for other members of the TNF/TNFR superfamilies.

References

- Aggarwal, B. B. (2003) 'Signalling pathways of the TNF superfamily: a double-edged sword', *Nat Rev Immunol*, 3, (9), pp. 745-56.
- Aggarwal, B. B., Kohr, W. J., Hass, P. E., Moffat, B., Spencer, S. A., Henzel, W. J., Bringman, T. S., Nedwin, G. E., Goeddel, D. V. and Harkins, R. N. (1985) 'Human tumor necrosis factor. Production, purification, and characterization', *J Biol Chem*, 260, (4), pp. 2345-54.
- Akassoglou, K., Bauer, J., Kassiotis, G., Pasparakis, M., Lassmann, H., Kollias, G. and Probert, L. (1998) 'Oligodendrocyte apoptosis and primary demyelination induced by local TNF/p55TNF receptor signaling in the central nervous system of transgenic mice: models for multiple sclerosis with primary oligodendroglipathy', *Am J Pathol*, 153, (3), pp. 801-13.
- Akassoglou, K., Douni, E., Bauer, J., Lassmann, H., Kollias, G. and Probert, L. (2003) 'Exclusive tumor necrosis factor (TNF) signaling by the p75TNF receptor triggers inflammatory ischemia in the CNS of transgenic mice', *Proc Natl Acad Sci U S A*, 100, (2), pp. 709-14.
- Alexopoulou, L., Kranidioti, K., Xanthoulea, S., Denis, M., Kotanidou, A., Douni, E., Blackshear, P. J., Kontoyiannis, D. L. and Kollias, G. (2006) 'Transmembrane TNF protects mutant mice against intracellular bacterial infections, chronic inflammation and autoimmunity', *Eur J Immunol*, 36, (10), pp. 2768-80.
- Algeciras-Schimmich, A., Pietras, E. M., Barnhart, B. C., Legembre, P., Vijayan, S., Holbeck, S. L. and Peter, M. E. (2003) 'Two CD95 tumor classes with different sensitivities to antitumor drugs', *Proc Natl Acad Sci U S A*, 100, (20), pp. 11445-50.
- Algeciras-Schimmich, A., Shen, L., Barnhart, B. C., Murmann, A. E., Burkhardt, J. K. and Peter, M. E. (2002) 'Molecular ordering of the initial signaling events of CD95', *Mol Cell Biol*, 22, (1), pp. 207-20.
- Alkalay, I., Yaron, A., Hatzubai, A., Orian, A., Ciechanover, A. and Ben-Neriah, Y. (1995) 'Stimulation-dependent I kappa B alpha phosphorylation marks the NF-kappa B inhibitor for degradation via the ubiquitin-proteasome pathway', *Proc Natl Acad Sci U S A*, 92, (23), pp. 10599-603.
- Aspalter, R. M., Eibl, M. M. and Wolf, H. M. (2003) 'Regulation of TCR-mediated T cell activation by TNF-RII', *J Leukoc Biol*, 74, (4), pp. 572-82.

- Back, J., Malchiodi, E. L., Cho, S., Scarpellino, L., Schneider, P., Kerzic, M. C., Mariuzza, R. A. and Held, W. (2009) 'Distinct conformations of Ly49 natural killer cell receptors mediate MHC class I recognition in trans and cis', *Immunity*, 31, (4), pp. 598-608.
- Ban, L., Zhang, J., Wang, L., Kuhnreber, W., Burger, D. and Faustman, D. L. (2008) 'Selective death of autoreactive T cells in human diabetes by TNF or TNF receptor 2 agonism', *Proc Natl Acad Sci U S A*, 105, (36), pp. 13644-9.
- Banner, D. W., D'Arcy, A., Janes, W., Gentz, R., Schoenfeld, H. J., Broger, C., Loetscher, H. and Lesslauer, W. (1993) 'Crystal structure of the soluble human 55 kd TNF receptor-human TNF beta complex: implications for TNF receptor activation', *Cell*, 73, (3), pp. 431-45.
- Basak, S. and Hoffmann, A. (2008) 'Crosstalk via the NF-kappaB signaling system', *Cytokine Growth Factor Rev*, 19, (3-4), pp. 187-97.
- Bennasroune, A., Fickova, M., Gardin, A., Dirrig-Grosch, S., Aunis, D., Cremel, G. and Hubert, P. (2004) 'Transmembrane peptides as inhibitors of ErbB receptor signaling', *Mol Biol Cell*, 15, (7), pp. 3464-74.
- Bertrand, M. J., Milutinovic, S., Dickson, K. M., Ho, W. C., Boudreault, A., Durkin, J., Gillard, J. W., Jaquith, J. B., Morris, S. J. and Barker, P. A. (2008) 'cIAP1 and cIAP2 facilitate cancer cell survival by functioning as E3 ligases that promote RIP1 ubiquitination', *Mol Cell*, 30, (6), pp. 689-700.
- Beutler, B., Milsark, I. W. and Cerami, A. C. (1985) 'Passive immunization against cachectin/tumor necrosis factor protects mice from lethal effect of endotoxin', *Science*, 229, (4716), pp. 869-71.
- Bhattacharjee, A. and Bansal, M. (2005) 'Collagen structure: the Madras triple helix and the current scenario', *IUBMB Life*, 57, (3), pp. 161-72.
- Bigda, J., Beletsky, I., Brakebusch, C., Varfolomeev, Y., Engelmann, H., Holtmann, H. and Wallach, D. (1994) 'Dual role of the p75 tumor necrosis factor (TNF) receptor in TNF cytotoxicity', *J Exp Med*, 180, (2), pp. 445-60.
- Birnboim, H. C. and Doly, J. (1979) 'A rapid alkaline extraction procedure for screening recombinant plasmid DNA', *Nucleic Acids Res*, 7, (6), pp. 1513-23.
- Black, R. A., Rauch, C. T., Kozlosky, C. J., Peschon, J. J., Slack, J. L., Wolfson, M. F., Castner, B. J., Stocking, K. L., Reddy, P., Srinivasan, S., Nelson, N., Boiani, N., Schooley, K. A., Gerhart, M., Davis, R., Fitzner, J. N., Johnson, R. S., Paxton, R. J., March, C. J. and Cerretti, D. P. (1997) 'A metalloproteinase disintegrin

- that releases tumour-necrosis factor-alpha from cells', *Nature*, 385, (6618), pp. 729-33.
- Blüml, S., Binder, N. B., Niederreiter, B., Polzer, K., Hayer, S., Tauber, S., Schett, G., Scheinecker, C., Kollias, G., Selzer, E., Bilban, M., Smolen, J. S., Superti-Furga, G. and Redlich, K. (2010) 'Antiinflammatory effects of tumor necrosis factor on hematopoietic cells in a murine model of erosive arthritis', *Arthritis Rheum*, 62, (6), pp. 1608-19.
- Bodmer, J. L., Schneider, P. and Tschopp, J. (2002) 'The molecular architecture of the TNF superfamily', *Trends Biochem Sci*, 27, (1), pp. 19-26.
- Boldin, M. P., Goncharov, T. M., Goltsev, Y. V. and Wallach, D. (1996) 'Involvement of MACH, a novel MORT1/FADD-interacting protease, in Fas/APO-1- and TNF receptor-induced cell death', *Cell*, 85, (6), pp. 803-15.
- Boldin, M. P., Mett, I. L., Varfolomeev, E. E., Chumakov, I., Shemer-Avni, Y., Camonis, J. H. and Wallach, D. (1995) 'Self-association of the "death domains" of the p55 tumor necrosis factor (TNF) receptor and Fas/APO1 prompts signaling for TNF and Fas/APO1 effects', *J Biol Chem*, 270, (1), pp. 387-91.
- Boschert, V., Krippner-Heidenreich, A., Branschadel, M., Tepperink, J., Aird, A. and Scheurich, P. (2010) 'Single chain TNF derivatives with individually mutated receptor binding sites reveal differential stoichiometry of ligand receptor complex formation for TNFR1 and TNFR2', *Cell Signal*, 22, (7), pp. 1088-96.
- Bossen, C., Cachero, T. G., Tardivel, A., Ingold, K., Willen, L., Dobles, M., Scott, M. L., Maquelin, A., Belnoue, E., Siegrist, C. A., Chevrier, S., Acha-Orbea, H., Leung, H., Mackay, F., Tschopp, J. and Schneider, P. (2008) 'TACI, unlike BAFF-R, is solely activated by oligomeric BAFF and APRIL to support survival of activated B cells and plasmablasts', *Blood*, 111, (3), pp. 1004-12.
- Bossen, C., Ingold, K., Tardivel, A., Bodmer, J. L., Gaide, O., Hertig, S., Ambrose, C., Tschopp, J. and Schneider, P. (2006) 'Interactions of tumor necrosis factor (TNF) and TNF receptor family members in the mouse and human', *J Biol Chem*, 281, (20), pp. 13964-71.
- Botchkina, G. I., Meistrell, M. E., 3rd, Botchkina, I. L. and Tracey, K. J. (1997) 'Expression of TNF and TNF receptors (p55 and p75) in the rat brain after focal cerebral ischemia', *Mol Med*, 3, (11), pp. 765-81.
- Bradley, J. R. (2008) 'TNF-mediated inflammatory disease', *J Pathol*, 214, (2), pp. 149-60.

- Brancho, D., Tanaka, N., Jaeschke, A., Ventura, J. J., Kelkar, N., Tanaka, Y., Kyuuma, M., Takeshita, T., Flavell, R. A. and Davis, R. J. (2003) 'Mechanism of p38 MAP kinase activation in vivo', *Genes Dev*, 17, (16), pp. 1969-78.
- Branschädel, M., Aird, A., Zappe, A., Tietz, C., Krippner-Heidenreich, A. and Scheurich, P. (2010) 'Dual function of cysteine rich domain (CRD) 1 of TNF receptor type 1: conformational stabilization of CRD2 and control of receptor responsiveness', *Cell Signal*, 22, (3), pp. 404-14.
- Brazin, K. N., Mallis, R. J., Fulton, D. B. and Andreotti, A. H. (2002) 'Regulation of the tyrosine kinase Itk by the peptidyl-prolyl isomerase cyclophilin A', *Proc Natl Acad Sci U S A*, 99, (4), pp. 1899-904.
- Breuza, L., Garcia, M., Delgrossi, M. H. and Le Bivic, A. (2002) 'Role of the membrane-proximal O-glycosylation site in sorting of the human receptor for neurotrophins to the apical membrane of MDCK cells', *Exp Cell Res*, 273, (2), pp. 178-86.
- Brockhaus, M., Schoenfeld, H. J., Schlaeger, E. J., Hunziker, W., Lesslauer, W. and Loetscher, H. (1990) 'Identification of two types of tumor necrosis factor receptors on human cell lines by monoclonal antibodies', *Proc Natl Acad Sci U S A*, 87, (8), pp. 3127-31.
- Brockhausen, I., Rachaman, E. S., Matta, K. L. and Schachter, H. (1983) 'The separation by liquid chromatography (under elevated pressure) of phenyl, benzyl, and O-nitrophenyl glycosides of oligosaccharides. Analysis of substrates and products for four N-acetyl-D-glucosaminyl-transferases involved in mucin synthesis', *Carbohydr Res*, 120, pp. 3-16.
- Brockhausen, I., Schachter, H. and Stanley, P. (eds.) (2009) *O-GalNAc Glycans*. Cold Spring Harbor Laboratory Press.
- Bruce, A. J., Boling, W., Kindy, M. S., Peschon, J., Kraemer, P. J., Carpenter, M. K., Holtsberg, F. W. and Mattson, M. P. (1996) 'Altered neuronal and microglial responses to excitotoxic and ischemic brain injury in mice lacking TNF receptors', *Nat Med*, 2, (7), pp. 788-94.
- Bryde, S., Grunwald, I., Hammer, A., Krippner-Heidenreich, A., Schiestel, T., Brunner, H., Tovar, G. E., Pfizenmaier, K. and Scheurich, P. (2005) 'Tumor necrosis factor (TNF)-functionalized nanostructured particles for the stimulation of membrane TNF-specific cell responses', *Bioconj Chem*, 16, (6), pp. 1459-67.
- Bukrinsky, M. I. (2002) 'Cyclophilins: unexpected messengers in intercellular communications', *Trends Immunol*, 23, (7), pp. 323-5.

- Camirero, A., Comabella, M. and Montalban, X. (2011) 'Tumor necrosis factor alpha (TNF-alpha), anti-TNF-alpha and demyelination revisited: An ongoing story', *J Neuroimmunol*.
- Carpentier, I., Coornaert, B. and Beyaert, R. (2004) 'Function and regulation of tumor necrosis factor type 2', *Curr Med Chem*, 11, (16), pp. 2205-12.
- Carpentier, I., Coornaert, B. and Beyaert, R. (2008) 'Smurf2 is a TRAF2 binding protein that triggers TNF-R2 ubiquitination and TNF-R2-induced JNK activation', *Biochem Biophys Res Commun*, 374, (4), pp. 752-7.
- Carswell, E. A., Old, L. J., Kassel, R. L., Green, S., Fiore, N. and Williamson, B. (1975) 'An endotoxin-induced serum factor that causes necrosis of tumors', *Proc Natl Acad Sci U S A*, 72, (9), pp. 3666-70.
- Castanos-Velez, E., Maerlan, S., Osorio, L. M., Aberg, F., Biberfeld, P., Orn, A. and Rottenberg, M. E. (1998) 'Trypanosoma cruzi infection in tumor necrosis factor receptor p55-deficient mice', *Infect Immun*, 66, (6), pp. 2960-8.
- Chakrabandhu, K., Herincs, Z., Huault, S., Dost, B., Peng, L., Conchonaud, F., Marguet, D., He, H. T. and Hueber, A. O. (2007) 'Palmitoylation is required for efficient Fas cell death signaling', *EMBO J*, 26, (1), pp. 209-20.
- Chan, F. K., Chun, H. J., Zheng, L., Siegel, R. M., Bui, K. L. and Lenardo, M. J. (2000) 'A domain in TNF receptors that mediates ligand-independent receptor assembly and signaling', *Science*, 288, (5475), pp. 2351-4.
- Chan, F. K. and Lenardo, M. J. (2000) 'A crucial role for p80 TNF-R2 in amplifying p60 TNF-R1 apoptosis signals in T lymphocytes', *Eur J Immunol*, 30, (2), pp. 652-60.
- Chan, F. K., Siegel, R. M., Zacharias, D., Swofford, R., Holmes, K. L., Tsien, R. Y. and Lenardo, M. J. (2001) 'Fluorescence resonance energy transfer analysis of cell surface receptor interactions and signaling using spectral variants of the green fluorescent protein', *Cytometry*, 44, (4), pp. 361-8.
- Chang, D. W., Xing, Z., Capacio, V. L., Peter, M. E. and Yang, X. (2003) 'Interdimer processing mechanism of procaspase-8 activation', *EMBO J*, 22, (16), pp. 4132-42.
- Chen, X., Hamano, R., Subleski, J. J., Hurwitz, A. A., Howard, O. M. and Oppenheim, J. J. (2010) 'Expression of costimulatory TNFR2 induces resistance of CD4⁺FoxP3⁻ conventional T cells to suppression by CD4⁺FoxP3⁺ regulatory T cells', *J Immunol*, 185, (1), pp. 174-82.

- Chen, X. and Oppenheim, J. J. (2010) 'TNF-alpha: an activator of CD4+FoxP3+TNFR2+ regulatory T cells', *Curr Dir Autoimmun*, 11, pp. 119-34.
- Chen, X. and Oppenheim, J. J. (2011) 'The phenotypic and functional consequences of tumour necrosis factor receptor type 2 expression on CD4(+) FoxP3(+) regulatory T cells', *Immunology*, 133, (4), pp. 426-33.
- Chen, X., Subleski, J. J., Kopf, H., Howard, O. M., Mannel, D. N. and Oppenheim, J. J. (2008) 'Cutting edge: expression of TNFR2 defines a maximally suppressive subset of mouse CD4+CD25+FoxP3+ T regulatory cells: applicability to tumor-infiltrating T regulatory cells', *J Immunol*, 180, (10), pp. 6467-71.
- Chenna, R., Sugawara, H., Koike, T., Lopez, R., Gibson, T. J., Higgins, D. G. and Thompson, J. D. (2003) 'Multiple sequence alignment with the Clustal series of programs', *Nucleic Acids Res*, 31, (13), pp. 3497-500.
- Chesnoy, S. and Huang, L. (2000) 'Structure and function of lipid-DNA complexes for gene delivery', *Annu Rev Biophys Biomol Struct*, 29, pp. 27-47.
- Choi, Y. E., Butterworth, M., Malladi, S., Duckett, C. S., Cohen, G. M. and Bratton, S. B. (2009) 'The E3 ubiquitin ligase cIAP1 binds and ubiquitinates caspase-3 and -7 via unique mechanisms at distinct steps in their processing', *J Biol Chem*, 284, (19), pp. 12772-82.
- Clay, H., Volkman, H. E. and Ramakrishnan, L. (2008) 'Tumor necrosis factor signaling mediates resistance to mycobacteria by inhibiting bacterial growth and macrophage death', *Immunity*, 29, (2), pp. 283-94.
- Crowe, P. D., VanArsdale, T. L., Walter, B. N., Ware, C. F., Hession, C., Ehrenfels, B., Browning, J. L., Din, W. S., Goodwin, R. G. and Smith, C. A. (1994) 'A lymphotoxin-beta-specific receptor', *Science*, 264, (5159), pp. 707-10.
- D'Alessio, A., Kluger, M. S., Li, J. H., Al-Lamki, R., Bradley, J. R. and Pober, J. S. (2010) 'Targeting of tumor necrosis factor receptor 1 to low density plasma membrane domains in human endothelial cells', *J Biol Chem*, 285, (31), pp. 23868-79.
- Declercq, W., Denecker, G., Fiers, W. and Vandenabeele, P. (1998) 'Cooperation of both TNF receptors in inducing apoptosis: involvement of the TNF receptor-associated factor binding domain of the TNF receptor 75', *J Immunol*, 161, (1), pp. 390-9.
- Declercq, W., Vandenabeele, P. and Fiers, W. (1995) 'Dimerization of chimeric erythropoietin/75 kDa tumour necrosis factor (TNF) receptors transduces TNF

- signals: necessity for the 75 kDa-TNF receptor transmembrane domain', *Cytokine*, 7, (7), pp. 701-9.
- Deng, G. M., Liu, L. and Tsokos, G. C. (2010) 'Targeted tumor necrosis factor receptor I preligand assembly domain improves skin lesions in MRL/lpr mice', *Arthritis Rheum*, 62, (8), pp. 2424-31.
- Deng, G. M., Zheng, L., Chan, F. K. and Lenardo, M. (2005) 'Amelioration of inflammatory arthritis by targeting the pre-ligand assembly domain of tumor necrosis factor receptors', *Nat Med*, 11, (10), pp. 1066-72.
- Deng, Y., Ren, X., Yang, L., Lin, Y. and Wu, X. (2003) 'A JNK-dependent pathway is required for TNFalpha-induced apoptosis', *Cell*, 115, (1), pp. 61-70.
- Dennis, J. W., Nabi, I. R. and Demetriou, M. (2009) 'Metabolism, cell surface organization, and disease', *Cell*, 139, (7), pp. 1229-41.
- Derijard, B., Raingeaud, J., Barrett, T., Wu, I. H., Han, J., Ulevitch, R. J. and Davis, R. J. (1995) 'Independent human MAP-kinase signal transduction pathways defined by MEK and MKK isoforms', *Science*, 267, (5198), pp. 682-5.
- Devin, A., Cook, A., Lin, Y., Rodriguez, Y., Kelliher, M. and Liu, Z. (2000) 'The distinct roles of TRAF2 and RIP in IKK activation by TNF-R1: TRAF2 recruits IKK to TNF-R1 while RIP mediates IKK activation', *Immunity*, 12, (4), pp. 419-29.
- Dhanasekaran, D. N. and Reddy, E. P. (2008) 'JNK signaling in apoptosis', *Oncogene*, 27, (48), pp. 6245-51.
- Duke, T. and Graham, I. (2009) 'Equilibrium mechanisms of receptor clustering', *Prog Biophys Mol Biol*, 100, (1-3), pp. 18-24.
- Eckelman, B. P., Salvesen, G. S. and Scott, F. L. (2006) 'Human inhibitor of apoptosis proteins: why XIAP is the black sheep of the family', *EMBO Rep*, 7, (10), pp. 988-94.
- Ehlers, S., Kutsch, S., Ehlers, E. M., Benini, J. and Pfeffer, K. (2000) 'Lethal granuloma disintegration in mycobacteria-infected TNFRp55^{-/-} mice is dependent on T cells and IL-12', *J Immunol*, 165, (1), pp. 483-92.
- Elhammer, A. P., Poorman, R. A., Brown, E., Maggiora, L. L., Hoogerheide, J. G. and Kezdy, F. J. (1993) 'The specificity of UDP-GalNAc:polypeptide N-acetylgalactosaminyltransferase as inferred from a database of in vivo substrates and from the in vitro glycosylation of proteins and peptides', *J Biol Chem*, 268, (14), pp. 10029-38.

- Elliott, M. J., Maini, R. N., Feldmann, M., Kalden, J. R., Antoni, C., Smolen, J. S., Leeb, B., Breedveld, F. C., Macfarlane, J. D., Bijl, H. and et al. (1994) 'Randomised double-blind comparison of chimeric monoclonal antibody to tumour necrosis factor alpha (cA2) versus placebo in rheumatoid arthritis', *Lancet*, 344, (8930), pp. 1105-10.
- Elliott, M. J., Maini, R. N., Feldmann, M., Long-Fox, A., Charles, P., Katsikis, P., Brennan, F. M., Walker, J., Bijl, H., Ghayeb, J. and et al. (1993) 'Treatment of rheumatoid arthritis with chimeric monoclonal antibodies to tumor necrosis factor alpha', *Arthritis Rheum*, 36, (12), pp. 1681-90.
- Eramo, A., Sargiacomo, M., Ricci-Vitiani, L., Todaro, M., Stassi, G., Messina, C. G., Parolini, I., Lotti, F., Sette, G., Peschle, C. and De Maria, R. (2004) 'CD95 death-inducing signaling complex formation and internalization occur in lipid rafts of type I and type II cells', *Eur J Immunol*, 34, (7), pp. 1930-40.
- Evers, T. H., van Dongen, E. M., Faesen, A. C., Meijer, E. W. and Merckx, M. (2006) 'Quantitative understanding of the energy transfer between fluorescent proteins connected via flexible peptide linkers', *Biochemistry*, 45, (44), pp. 13183-92.
- Fan, Y., Yu, Y., Shi, Y., Sun, W., Xie, M., Ge, N., Mao, R., Chang, A., Xu, G., Schneider, M. D., Zhang, H., Fu, S., Qin, J. and Yang, J. (2010) 'Lysine 63-linked polyubiquitination of TAK1 at lysine 158 is required for tumor necrosis factor alpha- and interleukin-1beta-induced IKK/NF-kappaB and JNK/AP-1 activation', *J Biol Chem*, 285, (8), pp. 5347-60.
- Faustman, D. and Davis, M. (2010) 'TNF receptor 2 pathway: drug target for autoimmune diseases', *Nat Rev Drug Discov*, 9, (6), pp. 482-93.
- Feldmann, M. (2008) 'Many cytokines are very useful therapeutic targets in disease', *J Clin Invest*, 118, (11), pp. 3533-6.
- Fischer, R., Maier, O., Naumer, M., Krippner-Heidenreich, A., Scheurich, P. and Pfizenmaier, K. (2011) 'Ligand-induced internalization of TNF receptor 2 mediated by a di-leucin motif is dispensable for activation of the NFkappaB pathway', *Cell Signal*, 23, (1), pp. 161-70.
- Fontaine, V., Mohand-Said, S., Hanoteau, N., Fuchs, C., Pfizenmaier, K. and Eisel, U. (2002) 'Neurodegenerative and neuroprotective effects of tumor Necrosis factor (TNF) in retinal ischemia: opposite roles of TNF receptor 1 and TNF receptor 2', *J Neurosci*, 22, (7), pp. RC216.
- Foster, J. R. (2001) 'The functions of cytokines and their uses in toxicology', *Int J Exp Pathol*, 82, (3), pp. 171-92.

- Fotin-Mleczeck, M., Henkler, F., Samel, D., Reichwein, M., Hausser, A., Parmryd, I., Scheurich, P., Schmid, J. A. and Wajant, H. (2002) 'Apoptotic crosstalk of TNF receptors: TNF-R2-induces depletion of TRAF2 and IAP proteins and accelerates TNF-R1-dependent activation of caspase-8', *J Cell Sci*, 115, (Pt 13), pp. 2757-70.
- Fu, Z. Q., Harrison, R. W., Reed, C., Wu, J., Xue, Y. N., Chen, M. J. and Weber, I. T. (1995) 'Model complexes of tumor necrosis factor-alpha with receptors R1 and R2', *Protein Eng*, 8, (12), pp. 1233-41.
- Fujita, M., Ikegame, S., Harada, E., Ouchi, H., Inoshima, I., Watanabe, K., Yoshida, S. and Nakanishi, Y. (2008) 'TNF receptor 1 and 2 contribute in different ways to resistance to Legionella pneumophila-induced mortality in mice', *Cytokine*, 44, (2), pp. 298-303.
- Gasteiger, E., Hoogland, C., Gattiker, A., Duvaud, S., Wilkins, M. R., Appel, R. D. and Bairoch, A. (2005) 'Protein Identification and Analysis Tools on the ExPASy Server', *The Proteomics Protocols Handbook*, Humana Press, pp. 571-607.
- Gerken, M., Krippner-Heidenreich, A., Steinert, S., Willi, S., Neugart, F., Zappe, A., Wrachtrup, J., Tietz, C. and Scheurich, P. (2010) 'Fluorescence correlation spectroscopy reveals topological segregation of the two tumor necrosis factor membrane receptors', *Biochim Biophys Acta*, 1798, (6), pp. 1081-9.
- Grech, A. P., Gardam, S., Chan, T., Quinn, R., Gonzales, R., Basten, A. and Brink, R. (2005) 'Tumor necrosis factor receptor 2 (TNFR2) signaling is negatively regulated by a novel, carboxyl-terminal TNFR-associated factor 2 (TRAF2)-binding site', *J Biol Chem*, 280, (36), pp. 31572-81.
- Grell, M., Becke, F. M., Wajant, H., Mannel, D. N. and Scheurich, P. (1998a) 'TNF receptor type 2 mediates thymocyte proliferation independently of TNF receptor type 1', *Eur J Immunol*, 28, (1), pp. 257-63.
- Grell, M., Douni, E., Wajant, H., Lohden, M., Clauss, M., Maxeiner, B., Georgopoulos, S., Lesslauer, W., Kollias, G., Pfizenmaier, K. and Scheurich, P. (1995) 'The transmembrane form of tumor necrosis factor is the prime activating ligand of the 80 kDa tumor necrosis factor receptor', *Cell*, 83, (5), pp. 793-802.
- Grell, M., Wajant, H., Zimmermann, G. and Scheurich, P. (1998b) 'The type 1 receptor (CD120a) is the high-affinity receptor for soluble tumor necrosis factor', *Proc Natl Acad Sci U S A*, 95, (2), pp. 570-5.
- Grell, M., Zimmermann, G., Gottfried, E., Chen, C. M., Grunwald, U., Huang, D. C., Wu Lee, Y. H., Durkop, H., Engelmann, H., Scheurich, P., Wajant, H. and

- Strasser, A. (1999) 'Induction of cell death by tumour necrosis factor (TNF) receptor 2, CD40 and CD30: a role for TNF-R1 activation by endogenous membrane-anchored TNF', *EMBO J*, 18, (11), pp. 3034-43.
- Haas, T. L., Emmerich, C. H., Gerlach, B., Schmukle, A. C., Cordier, S. M., Rieser, E., Feltham, R., Vince, J., Warnken, U., Wenger, T., Koschny, R., Komander, D., Silke, J. and Walczak, H. (2009) 'Recruitment of the linear ubiquitin chain assembly complex stabilizes the TNF-R1 signaling complex and is required for TNF-mediated gene induction', *Mol Cell*, 36, (5), pp. 831-44.
- Habelhah, H., Takahashi, S., Cho, S. G., Kadoya, T., Watanabe, T. and Ronai, Z. (2004) 'Ubiquitination and translocation of TRAF2 is required for activation of JNK but not of p38 or NF-kappaB', *EMBO J*, 23, (2), pp. 322-32.
- Hansen, J. E., Lund, O., Engelbrecht, J., Bohr, H. and Nielsen, J. O. (1995) 'Prediction of O-glycosylation of mammalian proteins: specificity patterns of UDP-GalNAc:polypeptide N-acetylgalactosaminyltransferase', *Biochem J*, 308 (Pt 3), pp. 801-13.
- Hashimoto, T., Schlessinger, D. and Cui, C. Y. (2008) 'Troy binding to lymphotoxin-alpha activates NF kappa B mediated transcription', *Cell Cycle*, 7, (1), pp. 106-11.
- Heldmann, U., Thored, P., Claasen, J. H., Arvidsson, A., Kokaia, Z. and Lindvall, O. (2005) 'TNF-alpha antibody infusion impairs survival of stroke-generated neuroblasts in adult rat brain', *Exp Neurol*, 196, (1), pp. 204-8.
- Henkler, F., Behrle, E., Dennehy, K. M., Wicovsky, A., Peters, N., Warnke, C., Pfizenmaier, K. and Wajant, H. (2005) 'The extracellular domains of FasL and Fas are sufficient for the formation of supramolecular FasL-Fas clusters of high stability', *J Cell Biol*, 168, (7), pp. 1087-98.
- Herman, C. and Chernajovsky, Y. (1998) 'Mutation of proline 211 reduces shedding of the human p75 TNF receptor', *J Immunol*, 160, (5), pp. 2478-87.
- Hoffmann, A., Natoli, G. and Ghosh, G. (2006) 'Transcriptional regulation via the NF-kappaB signaling module', *Oncogene*, 25, (51), pp. 6706-16.
- Hofman, F. M., Hinton, D. R., Johnson, K. and Merrill, J. E. (1989) 'Tumor necrosis factor identified in multiple sclerosis brain', *J Exp Med*, 170, (2), pp. 607-12.
- Hohmann, H. P., Remy, R., Brockhaus, M. and van Loon, A. P. (1989) 'Two different cell types have different major receptors for human tumor necrosis factor (TNF alpha)', *J Biol Chem*, 264, (25), pp. 14927-34.

- Horiuchi, T., Mitoma, H., Harashima, S., Tsukamoto, H. and Shimoda, T. (2010) 'Transmembrane TNF-alpha: structure, function and interaction with anti-TNF agents', *Rheumatology (Oxford)*, 49, (7), pp. 1215-28.
- Hsu, H., Huang, J., Shu, H. B., Baichwal, V. and Goeddel, D. V. (1996a) 'TNF-dependent recruitment of the protein kinase RIP to the TNF receptor-1 signaling complex', *Immunity*, 4, (4), pp. 387-96.
- Hsu, H., Shu, H. B., Pan, M. G. and Goeddel, D. V. (1996b) 'TRADD-TRAF2 and TRADD-FADD interactions define two distinct TNF receptor 1 signal transduction pathways', *Cell*, 84, (2), pp. 299-308.
- Huang, D. C., Cory, S. and Strasser, A. (1997) 'Bcl-2, Bcl-XL and adenovirus protein E1B19kD are functionally equivalent in their ability to inhibit cell death', *Oncogene*, 14, (4), pp. 405-14.
- Ito, D., Iizuka, Y. M., Katepalli, M. P. and Iizuka, K. (2009) 'Essential role of the Ly49A stalk region for immunological synapse formation and signaling', *Proc Natl Acad Sci U S A*, 106, (27), pp. 11264-9.
- Jiang, W., Cazacu, S., Xiang, C., Zenklusen, J. C., Fine, H. A., Berens, M., Armstrong, B., Brodie, C. and Mikkelsen, T. (2008) 'FK506 binding protein mediates glioma cell growth and sensitivity to rapamycin treatment by regulating NF-kappaB signaling pathway', *Neoplasia*, 10, (3), pp. 235-43.
- Jin, Z. and El-Deiry, W. S. (2006) 'Distinct signaling pathways in TRAIL- versus tumor necrosis factor-induced apoptosis', *Mol Cell Biol*, 26, (21), pp. 8136-48.
- Julenius, K., Molgaard, A., Gupta, R. and Brunak, S. (2005) 'Prediction, conservation analysis, and structural characterization of mammalian mucin-type O-glycosylation sites', *Glycobiology*, 15, (2), pp. 153-64.
- Kalb, A., Bluethmann, H., Moore, M. W. and Lesslauer, W. (1996) 'Tumor necrosis factor receptors (Tnfr) in mouse fibroblasts deficient in Tnfr1 or Tnfr2 are signaling competent and activate the mitogen-activated protein kinase pathway with differential kinetics', *J Biol Chem*, 271, (45), pp. 28097-104.
- Kilmon, M. A., Shelburne, A. E., Chan-Li, Y., Holmes, K. L. and Conrad, D. H. (2004) 'CD23 trimers are preassociated on the cell surface even in the absence of its ligand, IgE', *J Immunol*, 172, (2), pp. 1065-73.
- Kim, E. Y., Priatel, J. J., Teh, S. J. and Teh, H. S. (2006) 'TNF receptor type 2 (p75) functions as a costimulator for antigen-driven T cell responses in vivo', *J Immunol*, 176, (2), pp. 1026-35.

- Kim, E. Y. and Teh, H. S. (2001) 'TNF type 2 receptor (p75) lowers the threshold of T cell activation', *J Immunol*, 167, (12), pp. 6812-20.
- Kischkel, F. C., Hellbardt, S., Behrmann, I., Germer, M., Pawlita, M., Krammer, P. H. and Peter, M. E. (1995) 'Cytotoxicity-dependent APO-1 (Fas/CD95)-associated proteins form a death-inducing signaling complex (DISC) with the receptor', *EMBO J*, 14, (22), pp. 5579-88.
- Körner, H., Cook, M., Riminton, D. S., Lemckert, F. A., Hoek, R. M., Ledermann, B., Kontgen, F., Fazekas de St Groth, B. and Sedgwick, J. D. (1997) 'Distinct roles for lymphotoxin-alpha and tumor necrosis factor in organogenesis and spatial organization of lymphoid tissue', *Eur J Immunol*, 27, (10), pp. 2600-9.
- Kreuz, S., Siegmund, D., Scheurich, P. and Wajant, H. (2001) 'NF-kappaB inducers upregulate cFLIP, a cycloheximide-sensitive inhibitor of death receptor signaling', *Mol Cell Biol*, 21, (12), pp. 3964-73.
- Krippner-Heidenreich, A., Tubing, F., Bryde, S., Willi, S., Zimmermann, G. and Scheurich, P. (2002) 'Control of receptor-induced signaling complex formation by the kinetics of ligand/receptor interaction', *J Biol Chem*, 277, (46), pp. 44155-63.
- Kuan, S. F., Byrd, J. C., Basbaum, C. and Kim, Y. S. (1989) 'Inhibition of mucin glycosylation by aryl-N-acetyl-alpha-galactosaminides in human colon cancer cells', *J Biol Chem*, 264, (32), pp. 19271-7.
- Kubota, T., Mukai, K., Minegishi, Y. and Karasuyama, H. (2006) 'Different stabilities of the structurally related receptors for IgE and IgG on the cell surface are determined by length of the stalk region in their alpha-chains', *J Immunol*, 176, (11), pp. 7008-14.
- Lei, K. and Davis, R. J. (2003) 'JNK phosphorylation of Bim-related members of the Bcl2 family induces Bax-dependent apoptosis', *Proc Natl Acad Sci U S A*, 100, (5), pp. 2432-7.
- Letai, A., Bassik, M. C., Walensky, L. D., Sorcinelli, M. D., Weiler, S. and Korsmeyer, S. J. (2002) 'Distinct BH3 domains either sensitize or activate mitochondrial apoptosis, serving as prototype cancer therapeutics', *Cancer Cell*, 2, (3), pp. 183-92.
- Li, H. and Papadopoulos, V. (1998) 'Peripheral-type benzodiazepine receptor function in cholesterol transport. Identification of a putative cholesterol recognition/interaction amino acid sequence and consensus pattern', *Endocrinology*, 139, (12), pp. 4991-7.

- Li, H., Zhu, H., Xu, C. J. and Yuan, J. (1998) 'Cleavage of BID by caspase 8 mediates the mitochondrial damage in the Fas pathway of apoptosis', *Cell*, 94, (4), pp. 491-501.
- Li, S., Liu, B., Zeng, R., Cai, Y. and Li, Y. (2006) 'Predicting O-glycosylation sites in mammalian proteins by using SVMs', *Comput Biol Chem*, 30, (3), pp. 203-8.
- Li, X., Yang, Y. and Ashwell, J. D. (2002) 'TNF-RII and c-IAP1 mediate ubiquitination and degradation of TRAF2', *Nature*, 416, (6878), pp. 345-7.
- Locksley, R. M., Killeen, N. and Lenardo, M. J. (2001) 'The TNF and TNF receptor superfamilies: integrating mammalian biology', *Cell*, 104, (4), pp. 487-501.
- Loetscher, H., Stueber, D., Banner, D., Mackay, F. and Lesslauer, W. (1993) 'Human tumor necrosis factor alpha (TNF alpha) mutants with exclusive specificity for the 55-kDa or 75-kDa TNF receptors', *J Biol Chem*, 268, (35), pp. 26350-7.
- Lu, K. P., Finn, G., Lee, T. H. and Nicholson, L. K. (2007) 'Prolyl cis-trans isomerization as a molecular timer', *Nat Chem Biol*, 3, (10), pp. 619-29.
- Lucas, R., Kresse, M., Latta, M. and Wendel, A. (2005) 'Tumor necrosis factor: how to make a killer molecule tumor-specific?', *Curr Cancer Drug Targets*, 5, (6), pp. 381-92.
- Mallis, R. J., Brazin, K. N., Fulton, D. B. and Andreotti, A. H. (2002) 'Structural characterization of a proline-driven conformational switch within the Itk SH2 domain', *Nat Struct Biol*, 9, (12), pp. 900-5.
- Marchetti, L., Klein, M., Schlett, K., Pfizenmaier, K. and Eisel, U. L. (2004) 'Tumor necrosis factor (TNF)-mediated neuroprotection against glutamate-induced excitotoxicity is enhanced by N-methyl-D-aspartate receptor activation. Essential role of a TNF receptor 2-mediated phosphatidylinositol 3-kinase-dependent NF-kappa B pathway', *J Biol Chem*, 279, (31), pp. 32869-81.
- Marino, M. W., Dunn, A., Grail, D., Inglese, M., Noguchi, Y., Richards, E., Jungbluth, A., Wada, H., Moore, M., Williamson, B., Basu, S. and Old, L. J. (1997) 'Characterization of tumor necrosis factor-deficient mice', *Proc Natl Acad Sci U S A*, 94, (15), pp. 8093-8.
- Martin, R., McFarland, H. F. and McFarlin, D. E. (1992) 'Immunological aspects of demyelinating diseases', *Annu Rev Immunol*, 10, pp. 153-87.
- Mauri, D. N., Ebner, R., Montgomery, R. I., Kochel, K. D., Cheung, T. C., Yu, G. L., Ruben, S., Murphy, M., Eisenberg, R. J., Cohen, G. H., Spear, P. G. and Ware, C. F. (1998) 'LIGHT, a new member of the TNF superfamily, and lymphotoxin alpha are ligands for herpesvirus entry mediator', *Immunity*, 8, (1), pp. 21-30.

- Mercurio, F., Zhu, H., Murray, B. W., Shevchenko, A., Bennett, B. L., Li, J., Young, D. B., Barbosa, M., Mann, M., Manning, A. and Rao, A. (1997) 'IKK-1 and IKK-2: cytokine-activated I κ B kinases essential for NF- κ B activation', *Science*, 278, (5339), pp. 860-6.
- Meusch, U., Rossol, M., Baerwald, C., Hauschildt, S. and Wagner, U. (2009) 'Outside-to-inside signaling through transmembrane tumor necrosis factor reverses pathologic interleukin-1 β production and deficient apoptosis of rheumatoid arthritis monocytes', *Arthritis Rheum*, 60, (9), pp. 2612-21.
- Micheau, O., Lens, S., Gaide, O., Alevizopoulos, K. and Tschopp, J. (2001) 'NF- κ B signals induce the expression of c-FLIP', *Mol Cell Biol*, 21, (16), pp. 5299-305.
- Micheau, O. and Tschopp, J. (2003) 'Induction of TNF receptor I-mediated apoptosis via two sequential signaling complexes', *Cell*, 114, (2), pp. 181-90.
- Mitoma, H., Horiuchi, T., Hatta, N., Tsukamoto, H., Harashima, S., Kikuchi, Y., Otsuka, J., Okamura, S., Fujita, S. and Harada, M. (2005) 'Infliximab induces potent anti-inflammatory responses by outside-to-inside signals through transmembrane TNF- α ', *Gastroenterology*, 128, (2), pp. 376-92.
- Miyara, M. and Sakaguchi, S. (2011) 'Human FoxP3(+)CD4(+) regulatory T cells: their knowns and unknowns', *Immunol Cell Biol*, 89, (3), pp. 346-51.
- Moody, A. M., Chui, D., Reche, P. A., Priatel, J. J., Marth, J. D. and Reinherz, E. L. (2001) 'Developmentally regulated glycosylation of the CD8 α beta coreceptor stalk modulates ligand binding', *Cell*, 107, (4), pp. 501-12.
- Moody, A. M., North, S. J., Reinhold, B., Van Dyken, S. J., Rogers, M. E., Panico, M., Dell, A., Morris, H. R., Marth, J. D. and Reinherz, E. L. (2003) 'Sialic acid capping of CD8 β core 1-O-glycans controls thymocyte-major histocompatibility complex class I interaction', *J Biol Chem*, 278, (9), pp. 7240-6.
- Mori, L., Iselin, S., De Libero, G. and Lesslauer, W. (1996) 'Attenuation of collagen-induced arthritis in 55-kDa TNF receptor type 1 (TNFR1)-IgG1-treated and TNFR1-deficient mice', *J Immunol*, 157, (7), pp. 3178-82.
- Moriguchi, T., Toyoshima, F., Masuyama, N., Hanafusa, H., Gotoh, Y. and Nishida, E. (1997) 'A novel SAPK/JNK kinase, MKK7, stimulated by TNF α and cellular stresses', *EMBO J*, 16, (23), pp. 7045-53.
- Mukai, Y., Nakamura, T., Yoshikawa, M., Yoshioka, Y., Tsunoda, S., Nakagawa, S., Yamagata, Y. and Tsutsumi, Y. (2010) 'Solution of the structure of the TNF-TNFR2 complex', *Sci Signal*, 3, (148), pp. ra83.

- Mukai, Y., Nakamura, T., Yoshioka, Y., Tsunoda, S., Kamada, H., Nakagawa, S., Yamagata, Y. and Tsutsumi, Y. (2009) 'Crystallization and preliminary X-ray analysis of the tumour necrosis factor alpha-tumour necrosis factor receptor type 2 complex', *Acta Crystallogr Sect F Struct Biol Cryst Commun*, 65, (Pt 3), pp. 295-8.
- Müller, N., Wyzgol, A., Munkel, S., Pfizenmaier, K. and Wajant, H. (2008) 'Activity of soluble OX40 ligand is enhanced by oligomerization and cell surface immobilization', *FEBS J*, 275, (9), pp. 2296-304.
- Musicki, K., Briscoe, H., Tran, S., Britton, W. J. and Saunders, B. M. (2006) 'Differential requirements for soluble and transmembrane tumor necrosis factor in the immunological control of primary and secondary *Listeria monocytogenes* infection', *Infect Immun*, 74, (6), pp. 3180-9.
- Muzio, M., Chinnaiyan, A. M., Kischkel, F. C., O'Rourke, K., Shevchenko, A., Ni, J., Scaffidi, C., Bretz, J. D., Zhang, M., Gentz, R., Mann, M., Krammer, P. H., Peter, M. E. and Dixit, V. M. (1996) 'FLICE, a novel FADD-homologous ICE/CED-3-like protease, is recruited to the CD95 (Fas/APO-1) death-inducing signaling complex', *Cell*, 85, (6), pp. 817-27.
- Myers, E. W. and Miller, W. (1988) 'Optimal alignments in linear space', *Comput Appl Biosci*, 4, (1), pp. 11-7.
- Nagar, M., Jacob-Hirsch, J., Vernitsky, H., Berkun, Y., Ben-Horin, S., Amariglio, N., Bank, I., Kloog, Y., Rechavi, G. and Goldstein, I. (2010) 'TNF activates a NF-kappaB-regulated cellular program in human CD45RA- regulatory T cells that modulates their suppressive function', *J Immunol*, 184, (7), pp. 3570-81.
- Naismith, J. H., Brandhuber, B. J., Devine, T. Q. and Sprang, S. R. (1996a) 'Seeing double: crystal structures of the type I TNF receptor', *J Mol Recognit*, 9, (2), pp. 113-7.
- Naismith, J. H., Devine, T. Q., Brandhuber, B. J. and Sprang, S. R. (1995) 'Crystallographic evidence for dimerization of unliganded tumor necrosis factor receptor', *J Biol Chem*, 270, (22), pp. 13303-7.
- Naismith, J. H., Devine, T. Q., Kohno, T. and Sprang, S. R. (1996b) 'Structures of the extracellular domain of the type I tumor necrosis factor receptor', *Structure*, 4, (11), pp. 1251-62.
- Naismith, J. H. and Sprang, S. R. (1998) 'Modularity in the TNF-receptor family', *Trends Biochem Sci*, 23, (2), pp. 74-9.

- Nakano, H., Nakajima, A., Sakon-Komazawa, S., Piao, J. H., Xue, X. and Okumura, K. (2006) 'Reactive oxygen species mediate crosstalk between NF-kappaB and JNK', *Cell Death Differ*, 13, (5), pp. 730-7.
- Nashleanas, M., Kanaly, S. and Scott, P. (1998) 'Control of Leishmania major infection in mice lacking TNF receptors', *J Immunol*, 160, (11), pp. 5506-13.
- Nelson, C. J., Santos-Rosa, H. and Kouzarides, T. (2006) 'Proline isomerization of histone H3 regulates lysine methylation and gene expression', *Cell*, 126, (5), pp. 905-16.
- Neumann, B., Luz, A., Pfeffer, K. and Holzmann, B. (1996) 'Defective Peyer's patch organogenesis in mice lacking the 55-kD receptor for tumor necrosis factor', *J Exp Med*, 184, (1), pp. 259-64.
- Nikolaev, A., McLaughlin, T., O'Leary, D. D. and Tessier-Lavigne, M. (2009) 'APP binds DR6 to trigger axon pruning and neuron death via distinct caspases', *Nature*, 457, (7232), pp. 981-9.
- Nowak, M., Gaines, G. C., Rosenberg, J., Minter, R., Bahjat, F. R., Rectenwald, J., MacKay, S. L., Edwards, C. K., 3rd and Moldawer, L. L. (2000) 'LPS-induced liver injury in D-galactosamine-sensitized mice requires secreted TNF-alpha and the TNF-p55 receptor', *Am J Physiol Regul Integr Comp Physiol*, 278, (5), pp. R1202-9.
- O'Reilly, L. A., Tai, L., Lee, L., Kruse, E. A., Grabow, S., Fairlie, W. D., Haynes, N. M., Tarlinton, D. M., Zhang, J. G., Belz, G. T., Smyth, M. J., Bouillet, P., Robb, L. and Strasser, A. (2009) 'Membrane-bound Fas ligand only is essential for Fas-induced apoptosis', *Nature*, 461, (7264), pp. 659-63.
- Olleros, M. L., Guler, R., Corazza, N., Vesin, D., Eugster, H. P., Marchal, G., Chavarot, P., Mueller, C. and Garcia, I. (2002) 'Transmembrane TNF induces an efficient cell-mediated immunity and resistance to Mycobacterium bovis bacillus Calmette-Guerin infection in the absence of secreted TNF and lymphotoxin-alpha', *J Immunol*, 168, (7), pp. 3394-401.
- Olleros, M. L., Vesin, D., Fotio, A. L., Santiago-Raber, M. L., Tauzin, S., Szymkowski, D. E. and Garcia, I. (2010) 'Soluble TNF, but not membrane TNF, is critical in LPS-induced hepatitis', *J Hepatol*, 53, (6), pp. 1059-68.
- Ozaki, K. and Leonard, W. J. (2002) 'Cytokine and cytokine receptor pleiotropy and redundancy', *J Biol Chem*, 277, (33), pp. 29355-8.

- Pan, S., An, P., Zhang, R., He, X., Yin, G. and Min, W. (2002) 'Etk/Bmx as a tumor necrosis factor receptor type 2-specific kinase: role in endothelial cell migration and angiogenesis', *Mol Cell Biol*, 22, (21), pp. 7512-23.
- Panja, S., Aich, P., Jana, B. and Basu, T. (2008) 'How does plasmid DNA penetrate cell membranes in artificial transformation process of Escherichia coli?', *Mol Membr Biol*, 25, (5), pp. 411-22.
- Panja, S., Saha, S., Jana, B. and Basu, T. (2006) 'Role of membrane potential on artificial transformation of E. coli with plasmid DNA', *J Biotechnol*, 127, (1), pp. 14-20.
- Papa, S., Bubici, C., Zazzeroni, F., Pham, C. G., Kuntzen, C., Knabb, J. R., Dean, K. and Franzoso, G. (2006) 'The NF-kappaB-mediated control of the JNK cascade in the antagonism of programmed cell death in health and disease', *Cell Death Differ*, 13, (5), pp. 712-29.
- Papoff, G., Cascino, I., Eramo, A., Starace, G., Lynch, D. H. and Ruberti, G. (1996) 'An N-terminal domain shared by Fas/Apo-1 (CD95) soluble variants prevents cell death in vitro', *J Immunol*, 156, (12), pp. 4622-30.
- Papoff, G., Hausler, P., Eramo, A., Pagano, M. G., Di Leve, G., Signore, A. and Ruberti, G. (1999) 'Identification and characterization of a ligand-independent oligomerization domain in the extracellular region of the CD95 death receptor', *J Biol Chem*, 274, (53), pp. 38241-50.
- Park, K. M. and Bowers, W. J. (2010) 'Tumor necrosis factor-alpha mediated signaling in neuronal homeostasis and dysfunction', *Cell Signal*, 22, (7), pp. 977-83.
- Park, M. and Tenner, A. J. (2003) 'Cell surface expression of C1qRP/CD93 is stabilized by O-glycosylation', *J Cell Physiol*, 196, (3), pp. 512-22.
- Park, Y. C., Burkitt, V., Villa, A. R., Tong, L. and Wu, H. (1999) 'Structural basis for self-association and receptor recognition of human TRAF2', *Nature*, 398, (6727), pp. 533-8.
- Park, Y. C., Ye, H., Hsia, C., Segal, D., Rich, R. L., Liou, H. C., Myszka, D. G. and Wu, H. (2000) 'A novel mechanism of TRAF signaling revealed by structural and functional analyses of the TRADD-TRAF2 interaction', *Cell*, 101, (7), pp. 777-87.
- Patsos, G., Hebbe-Viton, V., Robbe-Masselot, C., Masselot, D., San Martin, R., Greenwood, R., Paraskeva, C., Klein, A., Graessmann, M., Michalski, J. C., Gallagher, T. and Corfield, A. (2009) 'O-glycan inhibitors generate aryl-glycans,

- induce apoptosis and lead to growth inhibition in colorectal cancer cell lines', *Glycobiology*, 19, (4), pp. 382-98.
- Pennica, D., Hayflick, J. S., Bringman, T. S., Palladino, M. A. and Goeddel, D. V. (1985) 'Cloning and expression in *Escherichia coli* of the cDNA for murine tumor necrosis factor', *Proc Natl Acad Sci U S A*, 82, (18), pp. 6060-4.
- Pennica, D., Lam, V. T., Mize, N. K., Weber, R. F., Lewis, M., Fendly, B. M., Lipari, M. T. and Goeddel, D. V. (1992) 'Biochemical properties of the 75-kDa tumor necrosis factor receptor. Characterization of ligand binding, internalization, and receptor phosphorylation', *J Biol Chem*, 267, (29), pp. 21172-8.
- Pennica, D., Lam, V. T., Weber, R. F., Kohr, W. J., Basa, L. J., Spellman, M. W., Ashkenazi, A., Shire, S. J. and Goeddel, D. V. (1993) 'Biochemical characterization of the extracellular domain of the 75-kilodalton tumor necrosis factor receptor', *Biochemistry*, 32, (12), pp. 3131-8.
- Perkins, N. D. (2006) 'Post-translational modifications regulating the activity and function of the nuclear factor kappa B pathway', *Oncogene*, 25, (51), pp. 6717-30.
- Pfeffer, K., Matsuyama, T., Kundig, T. M., Wakeham, A., Kishihara, K., Shahinian, A., Wiegmann, K., Ohashi, P. S., Kronke, M. and Mak, T. W. (1993) 'Mice deficient for the 55 kd tumor necrosis factor receptor are resistant to endotoxic shock, yet succumb to *L. monocytogenes* infection', *Cell*, 73, (3), pp. 457-67.
- Piguet, P. F., Grau, G. E., Vesin, C., Loetscher, H., Gentz, R. and Lesslauer, W. (1992) 'Evolution of collagen arthritis in mice is arrested by treatment with anti-tumour necrosis factor (TNF) antibody or a recombinant soluble TNF receptor', *Immunology*, 77, (4), pp. 510-4.
- Ranzinger, J., Krippner-Heidenreich, A., Haraszti, T., Bock, E., Tepperink, J., Spatz, J. P. and Scheurich, P. (2009) 'Nanoscale arrangement of apoptotic ligands reveals a demand for a minimal lateral distance for efficient death receptor activation', *Nano Lett*, 9, (12), pp. 4240-5.
- Rauert, H., Wicovsky, A., Muller, N., Siegmund, D., Spindler, V., Waschke, J., Kneitz, C. and Wajant, H. (2010) 'Membrane tumor necrosis factor (TNF) induces p100 processing via TNF receptor-2 (TNFR2)', *J Biol Chem*, 285, (10), pp. 7394-404.
- Reddy, P., Slack, J. L., Davis, R., Cerretti, D. P., Kozlosky, C. J., Blanton, R. A., Shows, D., Peschon, J. J. and Black, R. A. (2000) 'Functional analysis of the domain structure of tumor necrosis factor-alpha converting enzyme', *J Biol Chem*, 275, (19), pp. 14608-14.

- Reinhard, C., Shamoony, B., Shyamala, V. and Williams, L. T. (1997) 'Tumor necrosis factor alpha-induced activation of c-jun N-terminal kinase is mediated by TRAF2', *EMBO J*, 16, (5), pp. 1080-92.
- Riedl, S. J. and Salvesen, G. S. (2007) 'The apoptosome: signalling platform of cell death', *Nat Rev Mol Cell Biol*, 8, (5), pp. 405-13.
- Riedl, S. J. and Shi, Y. (2004) 'Molecular mechanisms of caspase regulation during apoptosis', *Nat Rev Mol Cell Biol*, 5, (11), pp. 897-907.
- Rodriguez, M. S., Wright, J., Thompson, J., Thomas, D., Baleux, F., Virelizier, J. L., Hay, R. T. and Arenzana-Seisdedos, F. (1996) 'Identification of lysine residues required for signal-induced ubiquitination and degradation of I kappa B-alpha in vivo', *Oncogene*, 12, (11), pp. 2425-35.
- Roos, C., Wicovsky, A., Muller, N., Salzmann, S., Rosenthal, T., Kalthoff, H., Trauzold, A., Seher, A., Henkler, F., Kneitz, C. and Wajant, H. (2010) 'Soluble and transmembrane TNF-like weak inducer of apoptosis differentially activate the classical and noncanonical NF-kappa B pathway', *J Immunol*, 185, (3), pp. 1593-605.
- Rossin, A., Derouet, M., Abdel-Sater, F. and Hueber, A. O. (2009) 'Palmitoylation of the TRAIL receptor DR4 confers an efficient TRAIL-induced cell death signalling', *Biochem J*, 419, (1), pp. 185-92, 2 p following 192.
- Rossin, A., Kral, R., Lounnas, N., Chakrabandhu, K., Mailfert, S., Marguet, D. and Hueber, A. O. (2010) 'Identification of a lysine-rich region of Fas as a raft nanodomain targeting signal necessary for Fas-mediated cell death', *Exp Cell Res*, 316, (9), pp. 1513-22.
- Rossol, M., Meusch, U., Pierer, M., Kaltenhauser, S., Hantzschel, H., Hauschildt, S. and Wagner, U. (2007) 'Interaction between transmembrane TNF and TNFR1/2 mediates the activation of monocytes by contact with T cells', *J Immunol*, 179, (6), pp. 4239-48.
- Roth, L., Nasarre, C., Dirrig-Grosch, S., Aunis, D., Cremel, G., Hubert, P. and Bagnard, D. (2008) 'Transmembrane domain interactions control biological functions of neuropilin-1', *Mol Biol Cell*, 19, (2), pp. 646-54.
- Rothe, J., Lesslauer, W., Lotscher, H., Lang, Y., Koebel, P., Kontgen, F., Althage, A., Zinkernagel, R., Steinmetz, M. and Bluethmann, H. (1993) 'Mice lacking the tumour necrosis factor receptor 1 are resistant to TNF-mediated toxicity but highly susceptible to infection by *Listeria monocytogenes*', *Nature*, 364, (6440), pp. 798-802.

- Rothe, M., Sarma, V., Dixit, V. M. and Goeddel, D. V. (1995) 'TRAF2-mediated activation of NF-kappa B by TNF receptor 2 and CD40', *Science*, 269, (5229), pp. 1424-7.
- Ryo, A., Suizu, F., Yoshida, Y., Perrem, K., Liou, Y. C., Wulf, G., Rottapel, R., Yamaoka, S. and Lu, K. P. (2003) 'Regulation of NF-kappaB signaling by Pin1-dependent prolyl isomerization and ubiquitin-mediated proteolysis of p65/RelA', *Mol Cell*, 12, (6), pp. 1413-26.
- Saunders, B. M., Tran, S., Ruuls, S., Sedgwick, J. D., Briscoe, H. and Britton, W. J. (2005) 'Transmembrane TNF is sufficient to initiate cell migration and granuloma formation and provide acute, but not long-term, control of Mycobacterium tuberculosis infection', *J Immunol*, 174, (8), pp. 4852-9.
- Scaffidi, C., Fulda, S., Srinivasan, A., Friesen, C., Li, F., Tomaselli, K. J., Debatin, K. M., Krammer, P. H. and Peter, M. E. (1998) 'Two CD95 (APO-1/Fas) signaling pathways', *EMBO J*, 17, (6), pp. 1675-87.
- Schall, T. J., Lewis, M., Koller, K. J., Lee, A., Rice, G. C., Wong, G. H., Gatanaga, T., Granger, G. A., Lentz, R., Raab, H. and et al. (1990) 'Molecular cloning and expression of a receptor for human tumor necrosis factor', *Cell*, 61, (2), pp. 361-70.
- Schneider-Brachert, W., Tchikov, V., Neumeyer, J., Jakob, M., Winoto-Morbach, S., Held-Feindt, J., Heinrich, M., Merkel, O., Ehrenschwender, M., Adam, D., Mentlein, R., Kabelitz, D. and Schutze, S. (2004) 'Compartmentalization of TNF receptor 1 signaling: internalized TNF receptorsomes as death signaling vesicles', *Immunity*, 21, (3), pp. 415-28.
- Schneider, P., Holler, N., Bodmer, J. L., Hahne, M., Frei, K., Fontana, A. and Tschopp, J. (1998) 'Conversion of membrane-bound Fas(CD95) ligand to its soluble form is associated with downregulation of its proapoptotic activity and loss of liver toxicity', *J Exp Med*, 187, (8), pp. 1205-13.
- Schütze, S., Tchikov, V. and Schneider-Brachert, W. (2008) 'Regulation of TNFR1 and CD95 signalling by receptor compartmentalization', *Nat Rev Mol Cell Biol*, 9, (8), pp. 655-62.
- Scott, F. L., Stec, B., Pop, C., Dobaczewska, M. K., Lee, J. J., Monosov, E., Robinson, H., Salvesen, G. S., Schwarzenbacher, R. and Riedl, S. J. (2009) 'The Fas-FADD death domain complex structure unravels signalling by receptor clustering', *Nature*, 457, (7232), pp. 1019-22.

- Sethi, G., Ahn, K. S., Xia, D., Kurie, J. M. and Aggarwal, B. B. (2007) 'Targeted deletion of MKK4 gene potentiates TNF-induced apoptosis through the down-regulation of NF-kappa B activation and NF-kappa B-regulated antiapoptotic gene products', *J Immunol*, 179, (3), pp. 1926-33.
- Sharief, M. K. and Hentges, R. (1991) 'Association between tumor necrosis factor-alpha and disease progression in patients with multiple sclerosis', *N Engl J Med*, 325, (7), pp. 467-72.
- Shaw, P. E. (2007) 'Peptidyl-prolyl cis/trans isomerases and transcription: is there a twist in the tail?', *EMBO Rep*, 8, (1), pp. 40-5.
- Shu, H. B., Takeuchi, M. and Goeddel, D. V. (1996) 'The tumor necrosis factor receptor 2 signal transducers TRAF2 and c-IAP1 are components of the tumor necrosis factor receptor 1 signaling complex', *Proc Natl Acad Sci U S A*, 93, (24), pp. 13973-8.
- Siegel, R. M., Frederiksen, J. K., Zacharias, D. A., Chan, F. K., Johnson, M., Lynch, D., Tsien, R. Y. and Lenardo, M. J. (2000) 'Fas preassociation required for apoptosis signaling and dominant inhibition by pathogenic mutations', *Science*, 288, (5475), pp. 2354-7.
- Siegel, R. M., Muppidi, J. R., Sarker, M., Lobito, A., Jen, M., Martin, D., Straus, S. E. and Lenardo, M. J. (2004) 'SPOTS: signaling protein oligomeric transduction structures are early mediators of death receptor-induced apoptosis at the plasma membrane', *J Cell Biol*, 167, (4), pp. 735-44.
- Spiro, R. G. (2002) 'Protein glycosylation: nature, distribution, enzymatic formation, and disease implications of glycopeptide bonds', *Glycobiology*, 12, (4), pp. 43R-56R.
- Steed, P. M., Tansey, M. G., Zalevsky, J., Zhukovsky, E. A., Desjarlais, J. R., Szymkowski, D. E., Abbott, C., Carmichael, D., Chan, C., Cherry, L., Cheung, P., Chirino, A. J., Chung, H. H., Doberstein, S. K., Eivazi, A., Filikov, A. V., Gao, S. X., Hubert, R. S., Hwang, M., Hyun, L., Kashi, S., Kim, A., Kim, E., Kung, J., Martinez, S. P., Muchhal, U. S., Nguyen, D. H., O'Brien, C., O'Keefe, D., Singer, K., Vafa, O., Vielmetter, J., Yoder, S. C. and Dahiyat, B. I. (2003) 'Inactivation of TNF signaling by rationally designed dominant-negative TNF variants', *Science*, 301, (5641), pp. 1895-8.
- Stehlik, C., de Martin, R., Kumabashiri, I., Schmid, J. A., Binder, B. R. and Lipp, J. (1998) 'Nuclear factor (NF)-kappaB-regulated X-chromosome-linked iap gene

- expression protects endothelial cells from tumor necrosis factor alpha-induced apoptosis', *J Exp Med*, 188, (1), pp. 211-6.
- Stumpf, T., Zhang, Q., Hirnet, D., Lewandrowski, U., Sickmann, A., Wissenbach, U., Dorr, J., Lohr, C., Deitmer, J. W. and Fecher-Trost, C. (2008) 'The human TRPV6 channel protein is associated with cyclophilin B in human placenta', *J Biol Chem*, 283, (26), pp. 18086-98.
- Suda, T., Hashimoto, H., Tanaka, M., Ochi, T. and Nagata, S. (1997) 'Membrane Fas ligand kills human peripheral blood T lymphocytes, and soluble Fas ligand blocks the killing', *J Exp Med*, 186, (12), pp. 2045-50.
- Tada, K., Okazaki, T., Sakon, S., Koburai, T., Kurosawa, K., Yamaoka, S., Hashimoto, H., Mak, T. W., Yagita, H., Okumura, K., Yeh, W. C. and Nakano, H. (2001a) 'Critical roles of TRAF2 and TRAF5 in tumor necrosis factor-induced NF-kappa B activation and protection from cell death', *J Biol Chem*, 276, (39), pp. 36530-4.
- Tada, Y., Ho, A., Koarada, S., Morito, F., Ushiyama, O., Suzuki, N., Kikuchi, Y., Ohta, A., Mak, T. W. and Nagasawa, K. (2001b) 'Collagen-induced arthritis in TNF receptor-1-deficient mice: TNF receptor-2 can modulate arthritis in the absence of TNF receptor-1', *Clin Immunol*, 99, (3), pp. 325-33.
- Tang, P., Hung, M. C. and Klostergaard, J. (1996) 'Human pro-tumor necrosis factor is a homotrimer', *Biochemistry*, 35, (25), pp. 8216-25.
- Tang, W., Lu, Y., Tian, Q. Y., Zhang, Y., Guo, F. J., Liu, G. Y., Syed, N. M., Lai, Y., Lin, E. A., Kong, L., Su, J., Yin, F., Ding, A. H., Zanin-Zhorov, A., Dustin, M. L., Tao, J., Craft, J., Yin, Z., Feng, J. Q., Abramson, S. B., Yu, X. P. and Liu, C. J. (2011) 'The Growth Factor Progranulin Binds to TNF Receptors and Is Therapeutic Against Inflammatory Arthritis in Mice', *Science*.
- Tartaglia, L. A., Ayres, T. M., Wong, G. H. and Goeddel, D. V. (1993a) 'A novel domain within the 55 kd TNF receptor signals cell death', *Cell*, 74, (5), pp. 845-53.
- Tartaglia, L. A., Goeddel, D. V., Reynolds, C., Figari, I. S., Weber, R. F., Fendly, B. M. and Palladino, M. A., Jr. (1993b) 'Stimulation of human T-cell proliferation by specific activation of the 75-kDa tumor necrosis factor receptor', *J Immunol*, 151, (9), pp. 4637-41.
- Tartaglia, L. A., Weber, R. F., Figari, I. S., Reynolds, C., Palladino, M. A., Jr. and Goeddel, D. V. (1991) 'The two different receptors for tumor necrosis factor

- mediate distinct cellular responses', *Proc Natl Acad Sci U S A*, 88, (20), pp. 9292-6.
- Theiss, A. L., Simmons, J. G., Jobin, C. and Lund, P. K. (2005) 'Tumor necrosis factor (TNF) alpha increases collagen accumulation and proliferation in intestinal myofibroblasts via TNF receptor 2', *J Biol Chem*, 280, (43), pp. 36099-109.
- Thorbecke, G. J., Shah, R., Leu, C. H., Kuruvilla, A. P., Hardison, A. M. and Palladino, M. A. (1992) 'Involvement of endogenous tumor necrosis factor alpha and transforming growth factor beta during induction of collagen type II arthritis in mice', *Proc Natl Acad Sci U S A*, 89, (16), pp. 7375-9.
- Tian, E. and Ten Hagen, K. G. (2009) 'Recent insights into the biological roles of mucin-type O-glycosylation', *Glycoconj J*, 26, (3), pp. 325-34.
- Ting, A. T., Pimentel-Muinos, F. X. and Seed, B. (1996) 'RIP mediates tumor necrosis factor receptor 1 activation of NF-kappaB but not Fas/APO-1-initiated apoptosis', *EMBO J*, 15, (22), pp. 6189-96.
- Tokunaga, F., Sakata, S., Saeki, Y., Satomi, Y., Kirisako, T., Kamei, K., Nakagawa, T., Kato, M., Murata, S., Yamaoka, S., Yamamoto, M., Akira, S., Takao, T., Tanaka, K. and Iwai, K. (2009) 'Involvement of linear polyubiquitylation of NEMO in NF-kappaB activation', *Nat Cell Biol*, 11, (2), pp. 123-32.
- Torres, D., Janot, L., Quesniaux, V. F., Grivennikov, S. I., Maillet, I., Sedgwick, J. D., Ryffel, B. and Erard, F. (2005) 'Membrane tumor necrosis factor confers partial protection to Listeria infection', *Am J Pathol*, 167, (6), pp. 1677-87.
- Tournier, C., Whitmarsh, A. J., Cavanagh, J., Barrett, T. and Davis, R. J. (1997) 'Mitogen-activated protein kinase kinase 7 is an activator of the c-Jun NH2-terminal kinase', *Proc Natl Acad Sci U S A*, 94, (14), pp. 7337-42.
- Tracey, D., Klareskog, L., Sasso, E. H., Salfeld, J. G. and Tak, P. P. (2008) 'Tumor necrosis factor antagonist mechanisms of action: a comprehensive review', *Pharmacol Ther*, 117, (2), pp. 244-79.
- Tracey, K. J., Fong, Y., Hesse, D. G., Manogue, K. R., Lee, A. T., Kuo, G. C., Lowry, S. F. and Cerami, A. (1987) 'Anti-cachectin/TNF monoclonal antibodies prevent septic shock during lethal bacteraemia', *Nature*, 330, (6149), pp. 662-4.
- Tsao, D. H., McDonagh, T., Telliez, J. B., Hsu, S., Malakian, K., Xu, G. Y. and Lin, L. L. (2000) 'Solution structure of N-TRADD and characterization of the interaction of N-TRADD and C-TRAF2, a key step in the TNFR1 signaling pathway', *Mol Cell*, 5, (6), pp. 1051-7.

- Valencia, X., Stephens, G., Goldbach-Mansky, R., Wilson, M., Shevach, E. M. and Lipsky, P. E. (2006) 'TNF downmodulates the function of human CD4+CD25hi T-regulatory cells', *Blood*, 108, (1), pp. 253-61.
- Vandenabeele, P., Declercq, W., Vanhaesebroeck, B., Grooten, J. and Fiers, W. (1995) 'Both TNF receptors are required for TNF-mediated induction of apoptosis in PC60 cells', *J Immunol*, 154, (6), pp. 2904-13.
- Varfolomeev, E., Blankenship, J. W., Wayson, S. M., Fedorova, A. V., Kayagaki, N., Garg, P., Zobel, K., Dynek, J. N., Elliott, L. O., Wallweber, H. J., Flygare, J. A., Fairbrother, W. J., Deshayes, K., Dixit, V. M. and Vucic, D. (2007) 'IAP antagonists induce autoubiquitination of c-IAPs, NF-kappaB activation, and TNFalpha-dependent apoptosis', *Cell*, 131, (4), pp. 669-81.
- Varfolomeev, E., Goncharov, T., Fedorova, A. V., Dynek, J. N., Zobel, K., Deshayes, K., Fairbrother, W. J. and Vucic, D. (2008) 'c-IAP1 and c-IAP2 are critical mediators of tumor necrosis factor alpha (TNFalpha)-induced NF-kappaB activation', *J Biol Chem*, 283, (36), pp. 24295-9.
- Varfolomeev, E. and Vucic, D. (2008) '(Un)expected roles of c-IAPs in apoptotic and NFkappaB signaling pathways', *Cell Cycle*, 7, (11), pp. 1511-21.
- Vercammen, D., Vandenabeele, P., Declercq, W., Van de Craen, M., Grooten, J. and Fiers, W. (1995) 'Cytotoxicity in L929 murine fibrosarcoma cells after triggering of transfected human p75 tumour necrosis factor (TNF) receptor is mediated by endogenous murine TNF', *Cytokine*, 7, (5), pp. 463-70.
- Vince, J. E., Pantaki, D., Feltham, R., Mace, P. D., Cordier, S. M., Schumke, A. C., Davidson, A. J., Callus, B. A., Wong, W. W., Gentle, I. E., Carter, H., Lee, E. F., Walczak, H., Day, C. L., Vaux, D. L. and Silke, J. (2009) 'TRAF2 must bind to cellular inhibitors of apoptosis for tumor necrosis factor (tnf) to efficiently activate nf- κ b and to prevent tnf-induced apoptosis', *J Biol Chem*, 284, (51), pp. 35906-15.
- Vince, J. E., Wong, W. W., Khan, N., Feltham, R., Chau, D., Ahmed, A. U., Benetatos, C. A., Chunduru, S. K., Condon, S. M., McKinlay, M., Brink, R., Leverkus, M., Tergaonkar, V., Schneider, P., Callus, B. A., Koentgen, F., Vaux, D. L. and Silke, J. (2007) 'IAP antagonists target cIAP1 to induce TNFalpha-dependent apoptosis', *Cell*, 131, (4), pp. 682-93.
- Wagner, K. W., Punnoose, E. A., Januario, T., Lawrence, D. A., Pitti, R. M., Lancaster, K., Lee, D., von Goetz, M., Yee, S. F., Totpal, K., Huw, L., Katta, V., Cavet, G., Hymowitz, S. G., Amler, L. and Ashkenazi, A. (2007) 'Death-receptor O-

- glycosylation controls tumor-cell sensitivity to the proapoptotic ligand Apo2L/TRAIL', *Nat Med*, 13, (9), pp. 1070-7.
- Wajant, H., Moosmayer, D., Wuest, T., Bartke, T., Gerlach, E., Schonherr, U., Peters, N., Scheurich, P. and Pfizenmaier, K. (2001) 'Differential activation of TRAIL-R1 and -2 by soluble and membrane TRAIL allows selective surface antigen-directed activation of TRAIL-R2 by a soluble TRAIL derivative', *Oncogene*, 20, (30), pp. 4101-6.
- Weiss, T., Grell, M., Hessabi, B., Bourteele, S., Muller, G., Scheurich, P. and Wajant, H. (1997) 'Enhancement of TNF receptor p60-mediated cytotoxicity by TNF receptor p80: requirement of the TNF receptor-associated factor-2 binding site', *J Immunol*, 158, (5), pp. 2398-404.
- Whitney, N. P., Eidem, T. M., Peng, H., Huang, Y. and Zheng, J. C. (2009) 'Inflammation mediates varying effects in neurogenesis: relevance to the pathogenesis of brain injury and neurodegenerative disorders', *J Neurochem*, 108, (6), pp. 1343-59.
- Wicovsky, A., Henkler, F., Salzmann, S., Scheurich, P., Kneitz, C. and Wajant, H. (2009) 'Tumor necrosis factor receptor-associated factor-1 enhances proinflammatory TNF receptor-2 signaling and modifies TNFR1-TNFR2 cooperation', *Oncogene*, 28, (15), pp. 1769-81.
- Wilbur, W. J. and Lipman, D. J. (1983) 'Rapid similarity searches of nucleic acid and protein data banks', *Proc Natl Acad Sci U S A*, 80, (3), pp. 726-30.
- Williams, R. O., Feldmann, M. and Maini, R. N. (1992) 'Anti-tumor necrosis factor ameliorates joint disease in murine collagen-induced arthritis', *Proc Natl Acad Sci U S A*, 89, (20), pp. 9784-8.
- Williamson, M. P. (1994) 'The structure and function of proline-rich regions in proteins', *Biochem J*, 297 (Pt 2), pp. 249-60.
- Willis, S. N. and Adams, J. M. (2005) 'Life in the balance: how BH3-only proteins induce apoptosis', *Curr Opin Cell Biol*, 17, (6), pp. 617-25.
- Willis, S. N., Chen, L., Dewson, G., Wei, A., Naik, E., Fletcher, J. I., Adams, J. M. and Huang, D. C. (2005) 'Proapoptotic Bak is sequestered by Mcl-1 and Bcl-xL, but not Bcl-2, until displaced by BH3-only proteins', *Genes Dev*, 19, (11), pp. 1294-305.
- Willis, S. N., Fletcher, J. I., Kaufmann, T., van Delft, M. F., Chen, L., Czabotar, P. E., Ierino, H., Lee, E. F., Fairlie, W. D., Bouillet, P., Strasser, A., Kluck, R. M., Adams, J. M. and Huang, D. C. (2007) 'Apoptosis initiated when BH3 ligands









- engage multiple Bcl-2 homologs, not Bax or Bak', *Science*, 315, (5813), pp. 856-9.
- Wilson, I. B., Gavel, Y. and von Heijne, G. (1991) 'Amino acid distributions around O-linked glycosylation sites', *Biochem J*, 275 (Pt 2), pp. 529-34.
- Woronicz, J. D., Gao, X., Cao, Z., Rothe, M. and Goeddel, D. V. (1997) 'IkappaB kinase-beta: NF-kappaB activation and complex formation with IkappaB kinase-alpha and NIK', *Science*, 278, (5339), pp. 866-9.
- Wu, C. and Ghosh, S. (2003) 'Differential phosphorylation of the signal-responsive domain of I kappa B alpha and I kappa B beta by I kappa B kinases', *J Biol Chem*, 278, (34), pp. 31980-7.
- Wu, C. J., Conze, D. B., Li, X., Ying, S. X., Hanover, J. A. and Ashwell, J. D. (2005) 'TNF-alpha induced c-IAP1/TRAF2 complex translocation to a Ubc6-containing compartment and TRAF2 ubiquitination', *EMBO J*, 24, (10), pp. 1886-98.
- Wu, Z., Wu, J., Jacinto, E. and Karin, M. (1997) 'Molecular cloning and characterization of human JNKK2, a novel Jun NH2-terminal kinase-specific kinase', *Mol Cell Biol*, 17, (12), pp. 7407-16.
- Wyzgol, A., Muller, N., Fick, A., Munkel, S., Grigoleit, G. U., Pfizenmaier, K. and Wajant, H. (2009) 'Trimer stabilization, oligomerization, and antibody-mediated cell surface immobilization improve the activity of soluble trimers of CD27L, CD40L, 41BBL, and glucocorticoid-induced TNF receptor ligand', *J Immunol*, 183, (3), pp. 1851-61.
- Yao, Z., Diener, K., Wang, X. S., Zukowski, M., Matsumoto, G., Zhou, G., Mo, R., Sasaki, T., Nishina, H., Hui, C. C., Tan, T. H., Woodgett, J. P. and Penninger, J. M. (1997) 'Activation of stress-activated protein kinases/c-Jun N-terminal protein kinases (SAPKs/JNKs) by a novel mitogen-activated protein kinase kinase', *J Biol Chem*, 272, (51), pp. 32378-83.
- Yeh, W. C., Pompa, J. L., McCurrach, M. E., Shu, H. B., Elia, A. J., Shahinian, A., Ng, M., Wakeham, A., Khoo, W., Mitchell, K., El-Deiry, W. S., Lowe, S. W., Goeddel, D. V. and Mak, T. W. (1998) 'FADD: essential for embryo development and signaling from some, but not all, inducers of apoptosis', *Science*, 279, (5358), pp. 1954-8.
- Yeh, W. C., Shahinian, A., Speiser, D., Kraunus, J., Billia, F., Wakeham, A., de la Pompa, J. L., Ferrick, D., Hum, B., Iscove, N., Ohashi, P., Rothe, M., Goeddel, D. V. and Mak, T. W. (1997) 'Early lethality, functional NF-kappaB activation,

- and increased sensitivity to TNF-induced cell death in TRAF2-deficient mice', *Immunity*, 7, (5), pp. 715-25.
- Yu, J. W. and Shi, Y. (2008) 'FLIP and the death effector domain family', *Oncogene*, 27, (48), pp. 6216-27.
- Zalevsky, J., Secher, T., Ezhevsky, S. A., Janot, L., Steed, P. M., O'Brien, C., Eivazi, A., Kung, J., Nguyen, D. H., Doberstein, S. K., Erard, F., Ryffel, B. and Szymkowski, D. E. (2007) 'Dominant-negative inhibitors of soluble TNF attenuate experimental arthritis without suppressing innate immunity to infection', *J Immunol*, 179, (3), pp. 1872-83.
- Zandi, E., Rothwarf, D. M., Delhase, M., Hayakawa, M. and Karin, M. (1997) 'The I κ B kinase complex (IKK) contains two kinase subunits, IKK α and IKK β , necessary for I κ B phosphorylation and NF- κ B activation', *Cell*, 91, (2), pp. 243-52.
- Zanetta, J. P., Gouyer, V., Maes, E., Pons, A., Hemon, B., Zweibaum, A., Delannoy, P. and Huet, G. (2000) 'Massive in vitro synthesis of tagged oligosaccharides in 1-benzyl-2-acetamido-2-deoxy- α -D-galactopyranoside treated HT-29 cells', *Glycobiology*, 10, (6), pp. 565-75.
- Zarubin, T. and Han, J. (2005) 'Activation and signaling of the p38 MAP kinase pathway', *Cell Res*, 15, (1), pp. 11-8.
- Zhao, Y., Conze, D. B., Hanover, J. A. and Ashwell, J. D. (2007) 'Tumor necrosis factor receptor 2 signaling induces selective c-IAP1-dependent ASK1 ubiquitination and terminates mitogen-activated protein kinase signaling', *J Biol Chem*, 282, (11), pp. 7777-82.
- Zheng, L., Bidere, N., Staudt, D., Cubre, A., Orenstein, J., Chan, F. K. and Lenardo, M. (2006) 'Competitive control of independent programs of tumor necrosis factor receptor-induced cell death by TRADD and RIP1', *Mol Cell Biol*, 26, (9), pp. 3505-13.
- Zhou, H., Wertz, I., O'Rourke, K., Ultsch, M., Seshagiri, S., Eby, M., Xiao, W. and Dixit, V. M. (2004) 'Bcl10 activates the NF- κ B pathway through ubiquitination of NEMO', *Nature*, 427, (6970), pp. 167-71.

Appendix

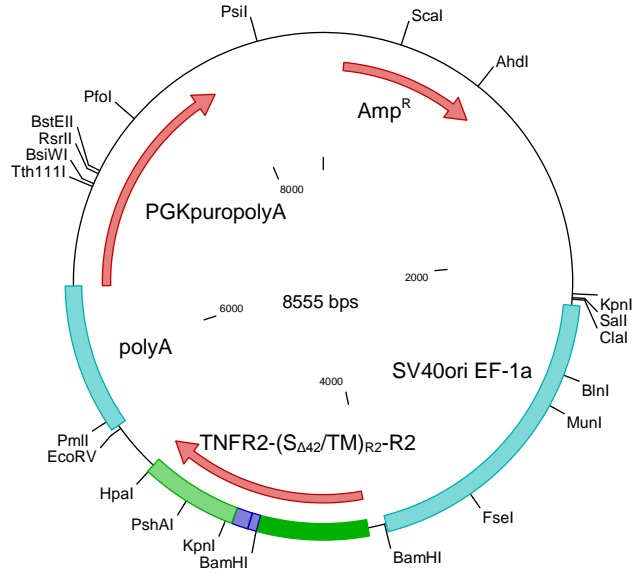
Various subcloning plasmids and expression vectors were generated during this PhD project. For these vectors plasmids maps were created using the the Clone Manager 9 software. The appropriate colour code and abbreviations for the plasmid maps are depicted in

Table 20. Colour codes and abbreviations for plasmid maps

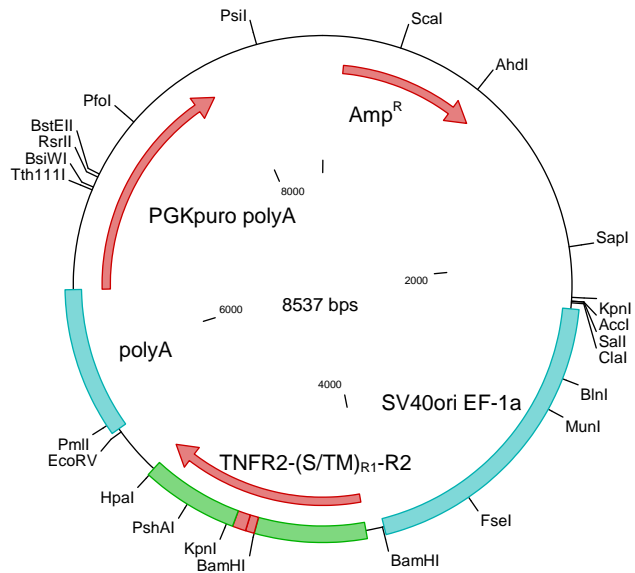
Colour code/abbreviation	Explanation
	DNA encoding indicated sequence
	Cytoplasmic portion Fas (aa 191-335)
	TNFR1 (aa 1-236)
	TNFR1 TM/stalk region
	TNFR2 (aa 1-301)
	TNFR2 TM/stalk region
	Artificial glycine/serine linker
	FRT site of recombination
Amp ^R	Ampicillin resistance gene
CMV promoter	Cytomegalovirus promoter
ColE1 ori	ColE1 origin of replication
f1 ori	f1 filamentous phage origin of replication
Hygro ^R	Hygromycin resistance gene
PGKpuropolyA	Puromycin resistance gene under the control of a phosphoglycerate kinase promoter and a poly A sequence
pUC ori	pUC origin of replication
polyA	Polyadenylation sequence
SV40ori EF-1a	Simian virus 40 origin of replication and elongation factor 1a promoter sequence
TetO2	Tetracycline operator O2

I Mammalian expression plasmids for wild-type TNFR2 variants

pEF-PGK/puro polyA TNFR2-(S_{Δ42}/TM)_{R2}-R2 (#450)



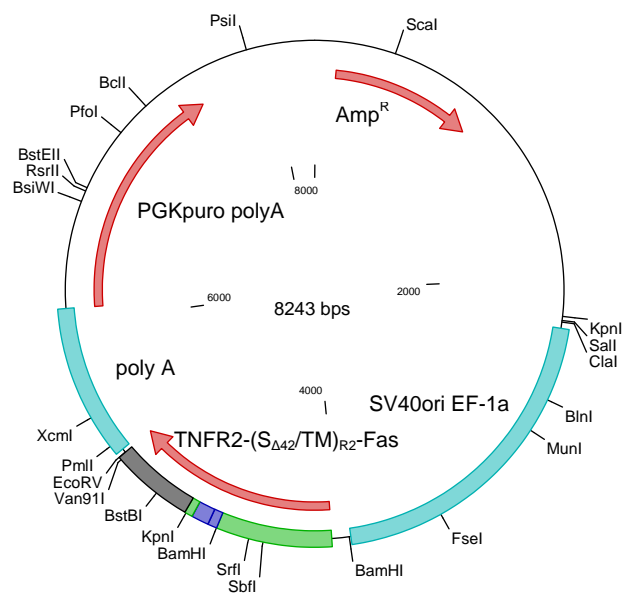
pEF-PGK/puro polyA TNFR2-(S/TM)_{R1}-R2 (#451)



II Mammalian expression plasmid for TNFR2-(S_{Δ42}/TM)_{R2}-Fas

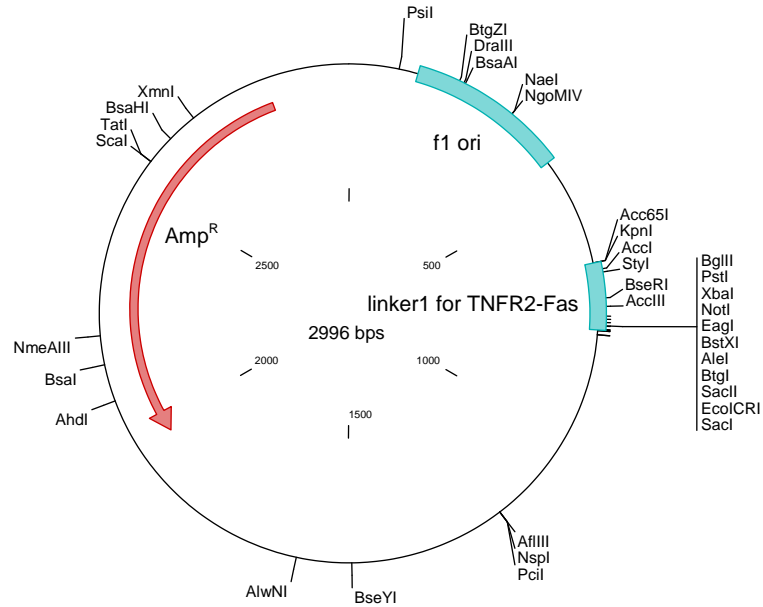
The mammalian expression plasmid pEF-PGK/puro polyA TNFR2-(S_{Δ42}/TM)_{R2}-Fas has been generated by Dr Andrea Zappe at the University of Stuttgart and has been used for stable and transient transfections of this PhD project.

pEF-PGK/puro polyA TNFR2-(S_{Δ42}/TM)_{R2}-Fas (#436)

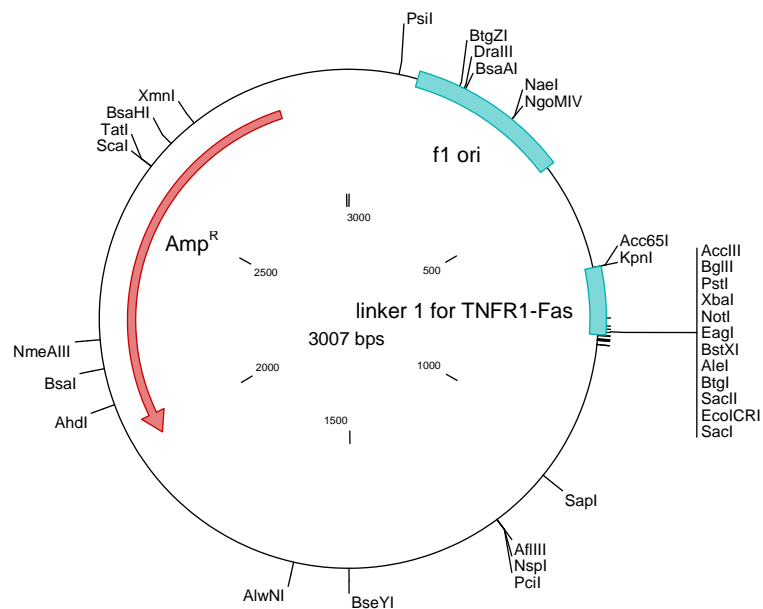


III Subcloning plasmids for the introduction of S_{GSL} into TNFR-Fas

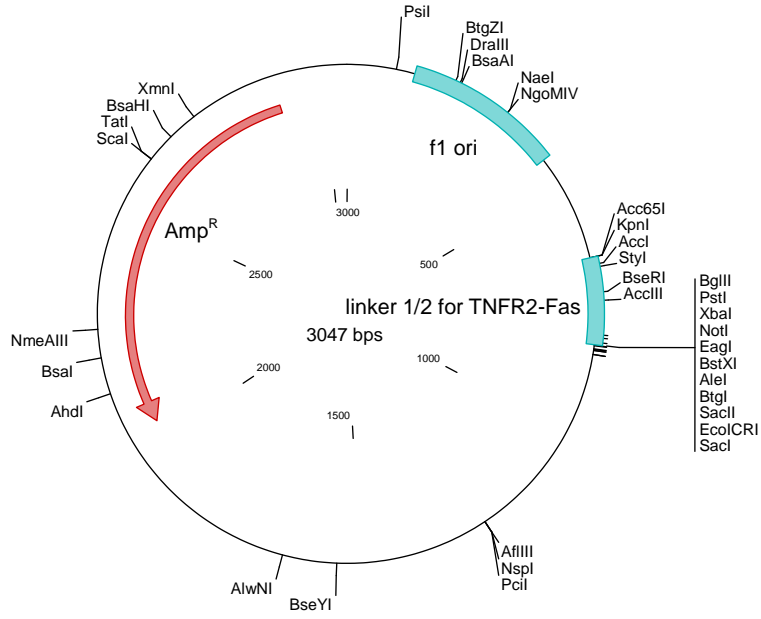
pBS SK(+) subclon. linker 1 for TNFR2-S_{GSL}-TM_{R2}-Fas (#501)



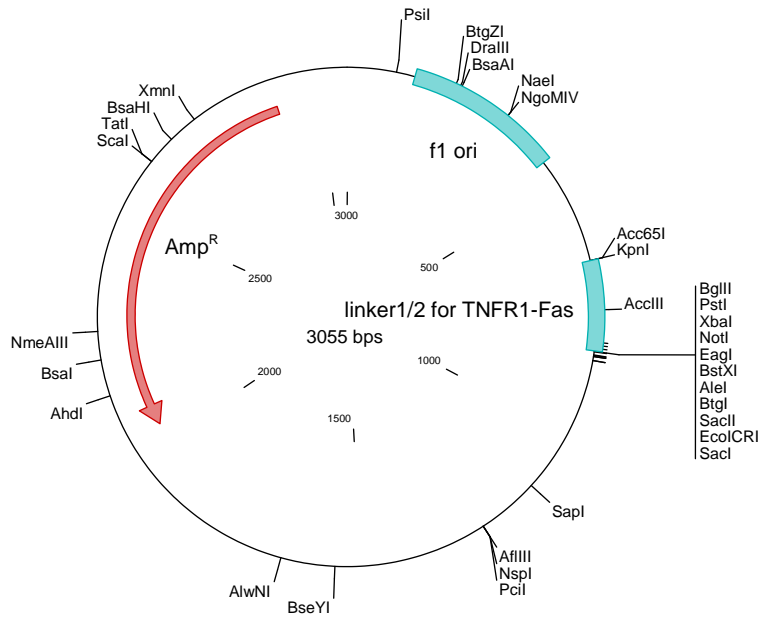
pBS SK(+) subclon. linker 1 for TNFR1-S_{GSL}-TM_{R1}-Fas (#502)



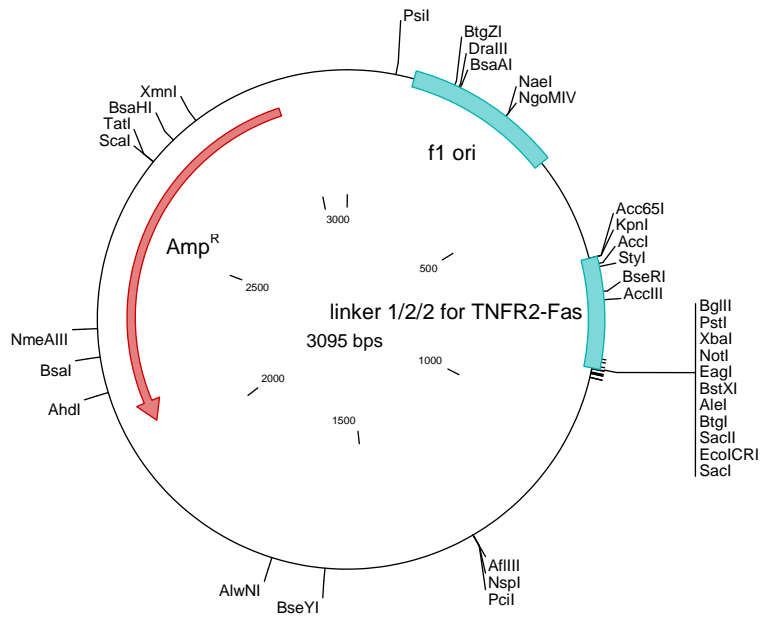
pBS SK(+) subclon. linker 1/2 for TNFR2-S_{GSL}-TM_{R2}-Fas (#507)



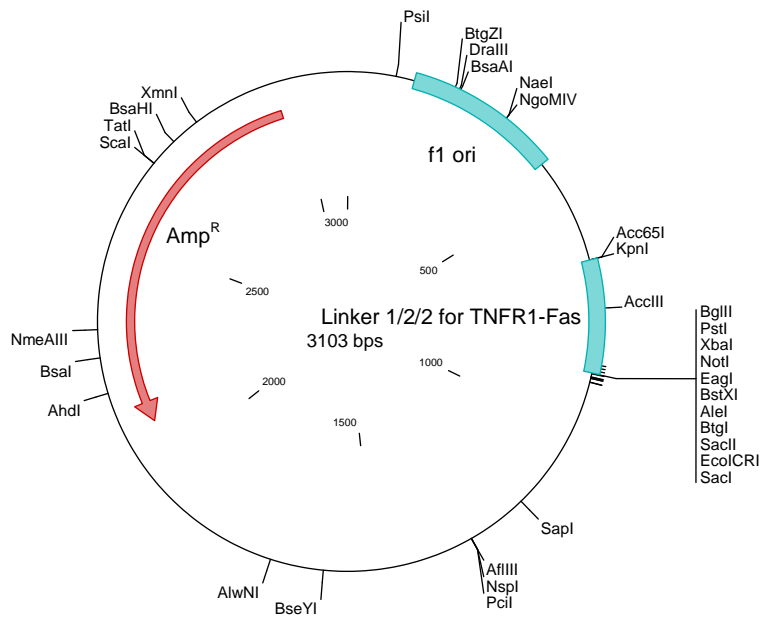
pBS SK(+) subclon. linker 1/2 for TNFR1-S_{GSL}-TM_{R1}-Fas (#508)



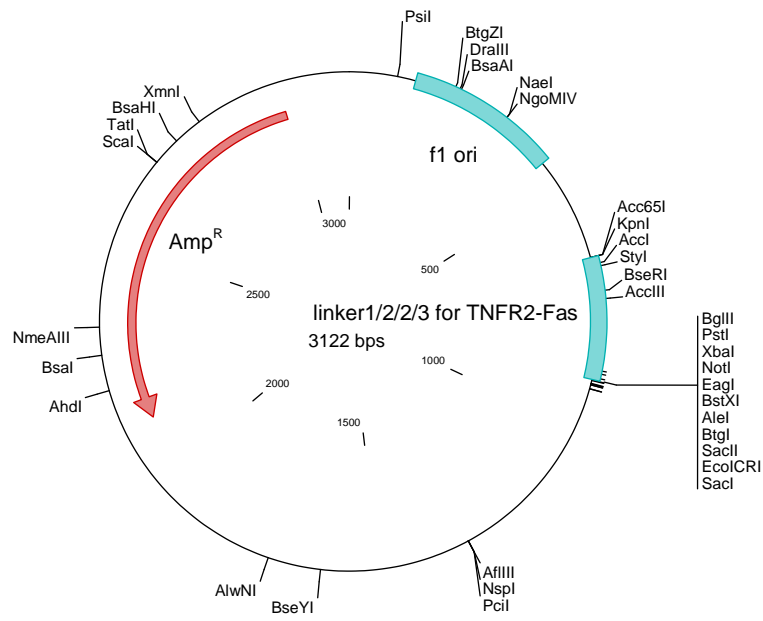
pBS SK(+) subclon. linker 1/2/2 for TNFR2-S_{GSL}-TM_{R2}-Fas (#513)



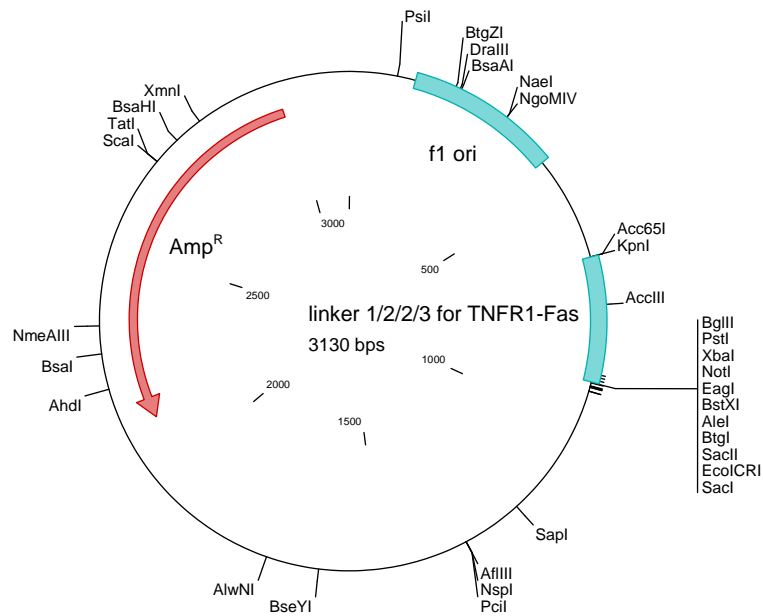
pBS SK(+) subclon. linker 1/2/2 for TNFR1-S_{GSL}-TM_{R1}-Fas (#514)



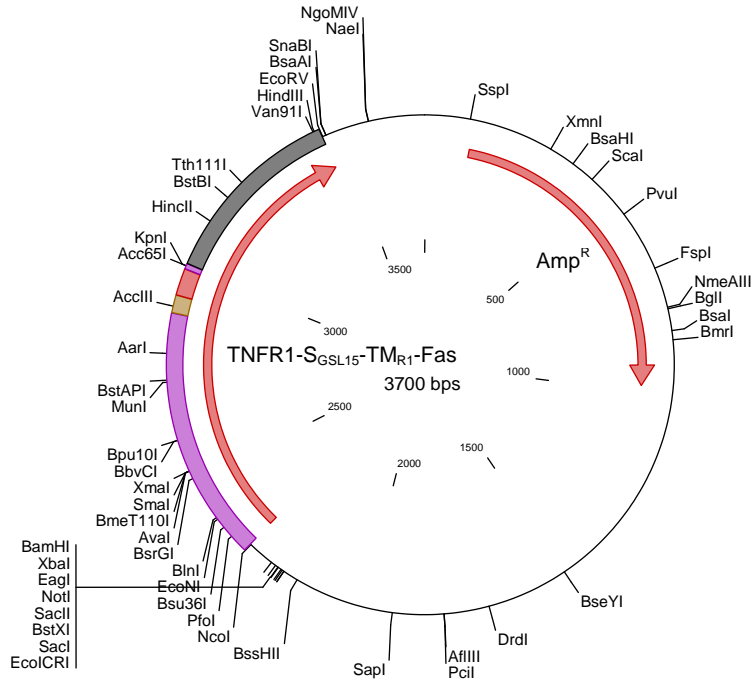
pBS SK(+) subclon. linker 1/2/2/3 for TNFR2-S_{GSL}-TM_{R2}-Fas (#519)



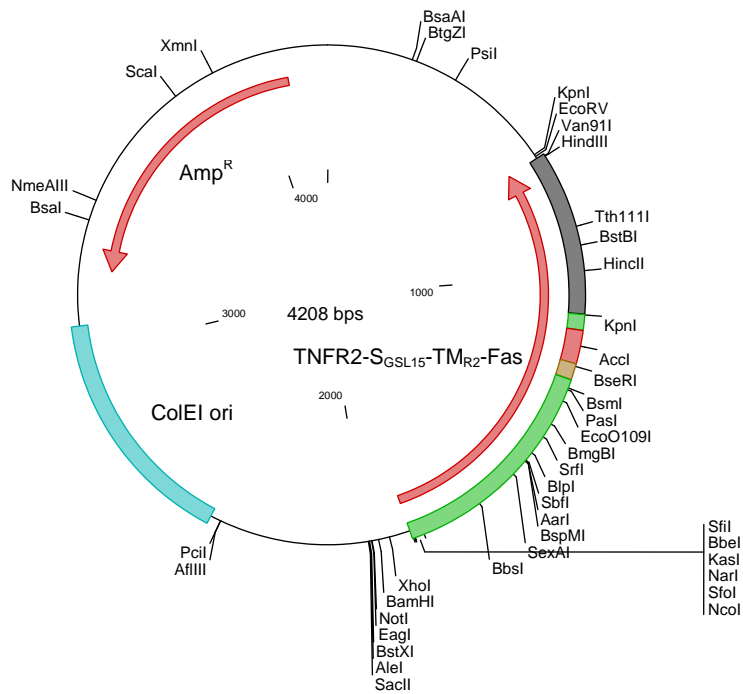
pBS SK(+) subclon. linker 1/2/2/3 for TNFR1-S_{GSL}-TM_{R1}-Fas (#520)



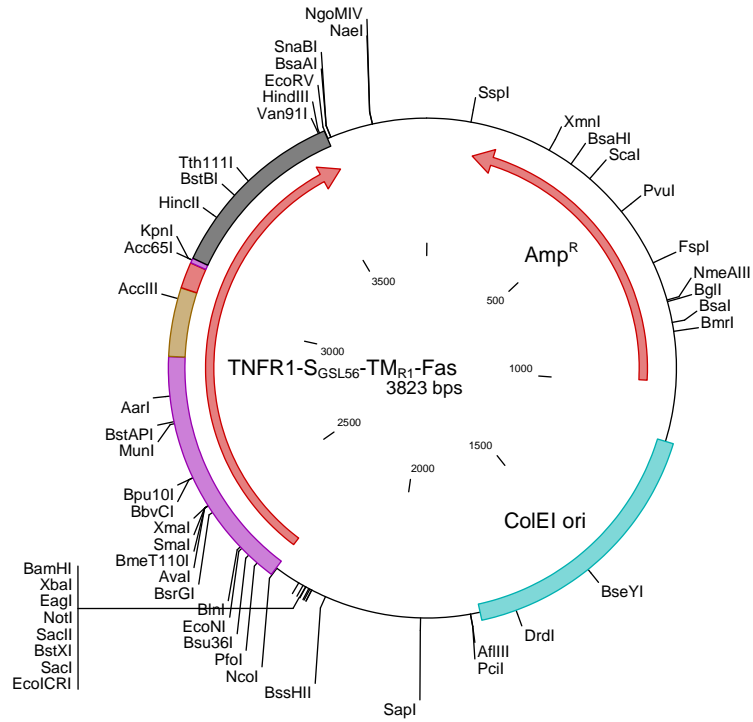
pBS SK(+)-KpnI TNFR1-S_{GSL15}-TM_{R1}-Fas (#503)



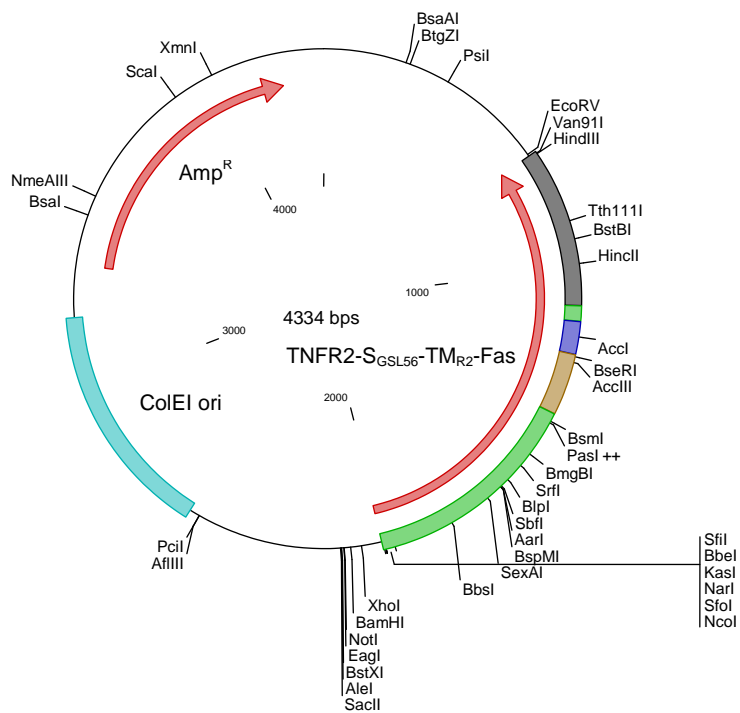
pBS SK(+)-TNFR2-S_{GSL15}-TM_{R2}-Fas (#504)



pBS SK(+)-KpnI TNFR1-S_{GSL56}-TM_{R1}-Fas (#521)

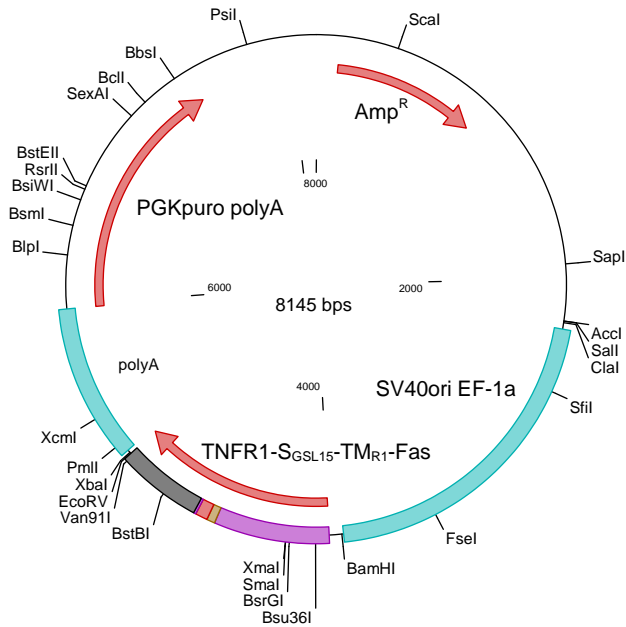


pBS SK(+)-TNFR2-S_{GSL56}-TM_{R2}-Fas (#522)

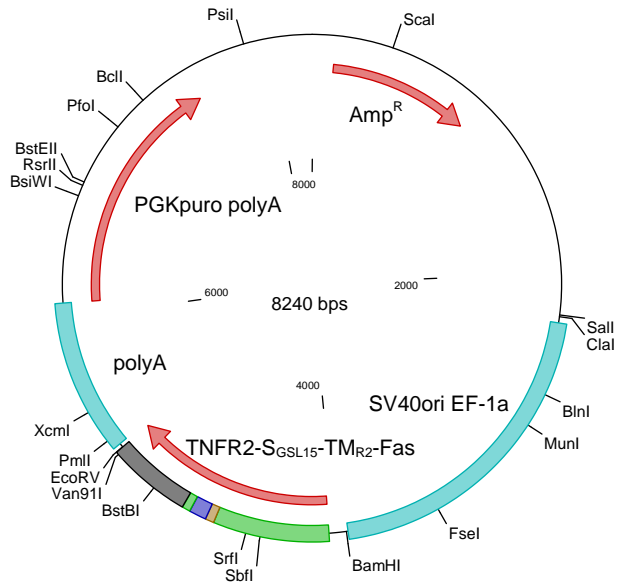


IV Mammalian expression plasmids for TNFR-S_{GSL}-TM-Fas chimaeras

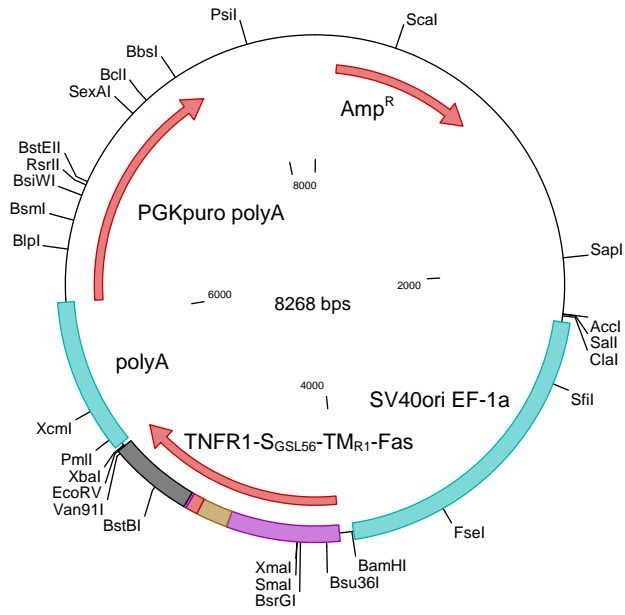
pEF-PGK/puro polyA TNFR1-S_{GSL15}-TM_{R1}-Fas (#505)



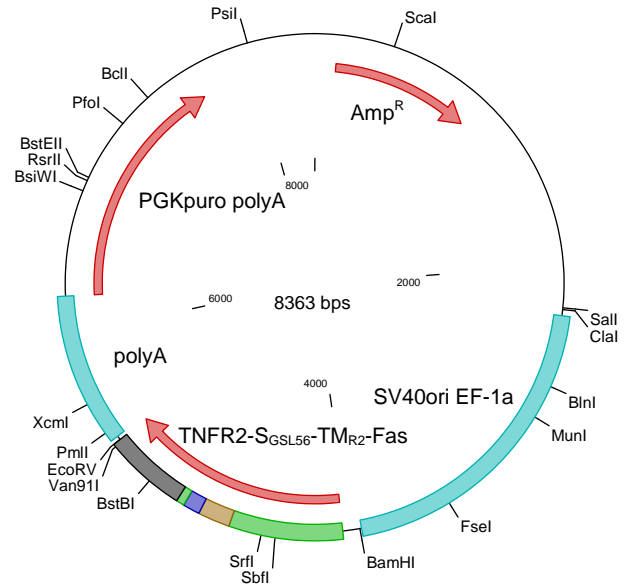
pEF-PGK/puro polyA TNFR2-S_{GSL15}-TM_{R2}-Fas (#506)



pEF-PGK/puro polyA TNFR1-S_{GSL56}-TM_{R1}-Fas (#523)

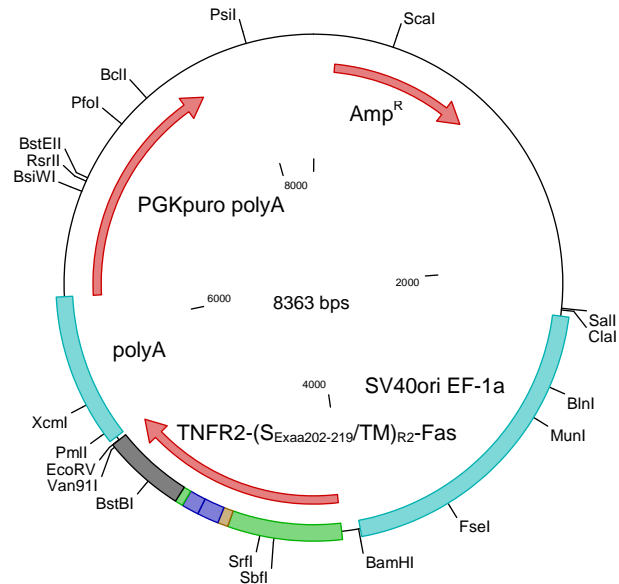


pEF-PGK/puro polyA TNFR2-S_{GSL56}-TM_{R2}-Fas (#524)

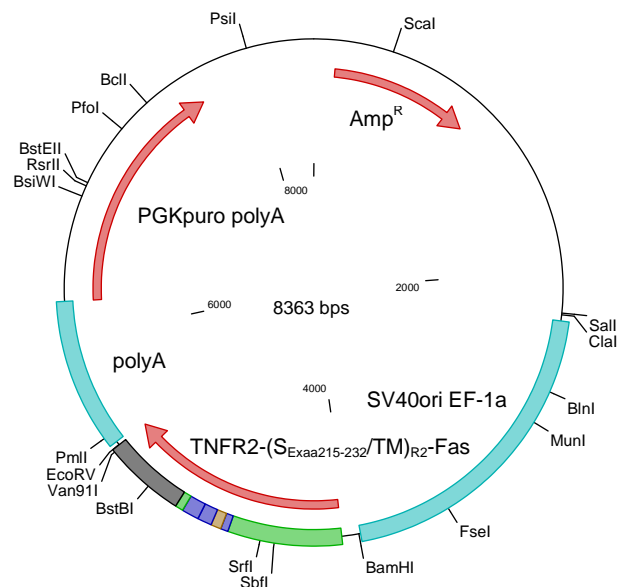


V Mammalian expression plasmids for partial stalk exchange mutants

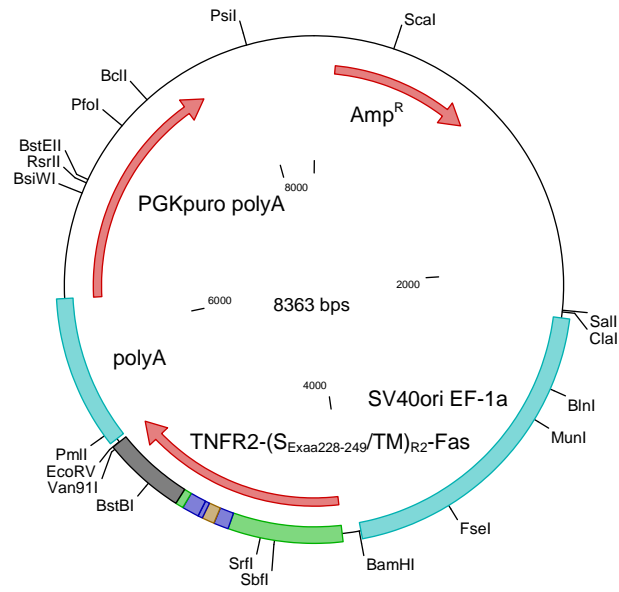
pEF-PGK/puro polyA TNFR2-(S_{Exaa202-219}/TM)_{R2}-Fas (#532)



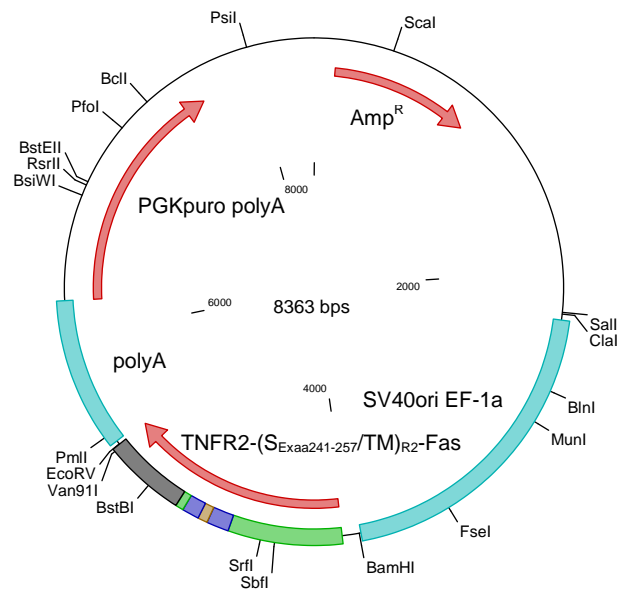
pEF-PGK/puro polyA TNFR2-(S_{Exaa215-232}/TM)_{R2}-Fas (#533)



pEF-PGK/puro polyA TNFR2-(S_{Exaa228-249}/TM)_{R2}-Fas (#534)

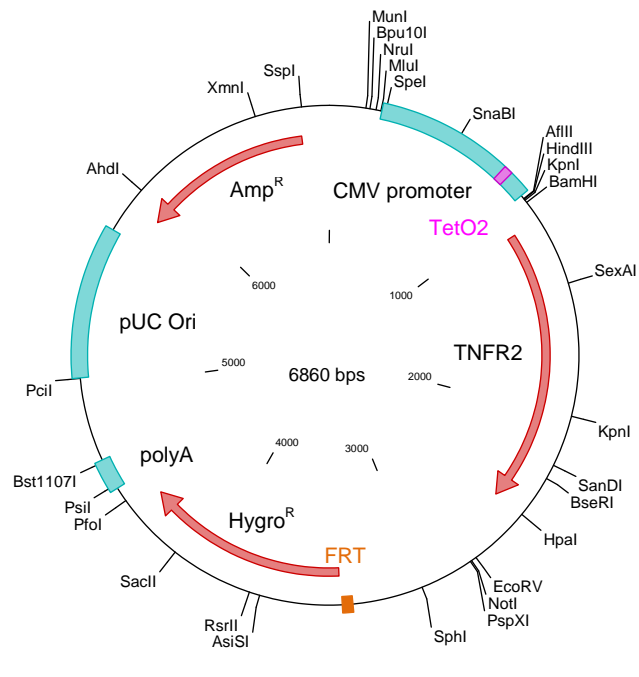


pEF-PGK/puro polyA TNFR2-(S_{Exaa241-257}/TM)_{R2}-Fas (#535)

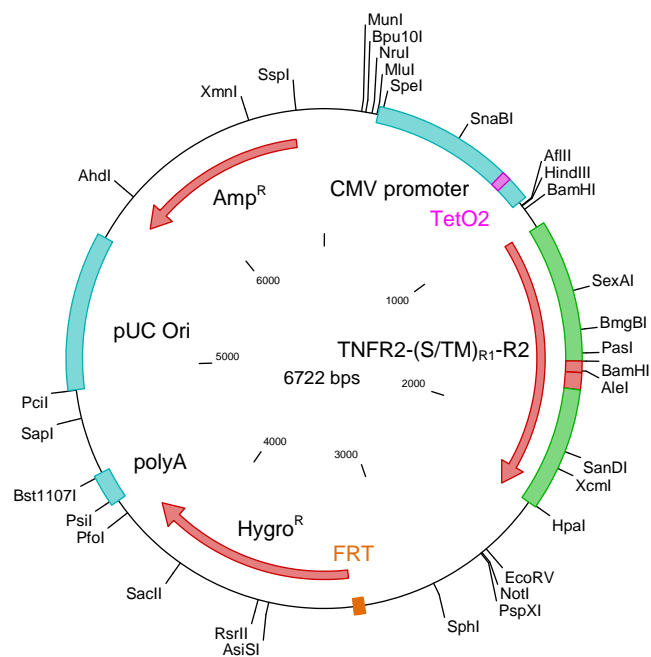


VI Plasmids for the generation of inducible HEK 293 FlpIN T-Rex cells

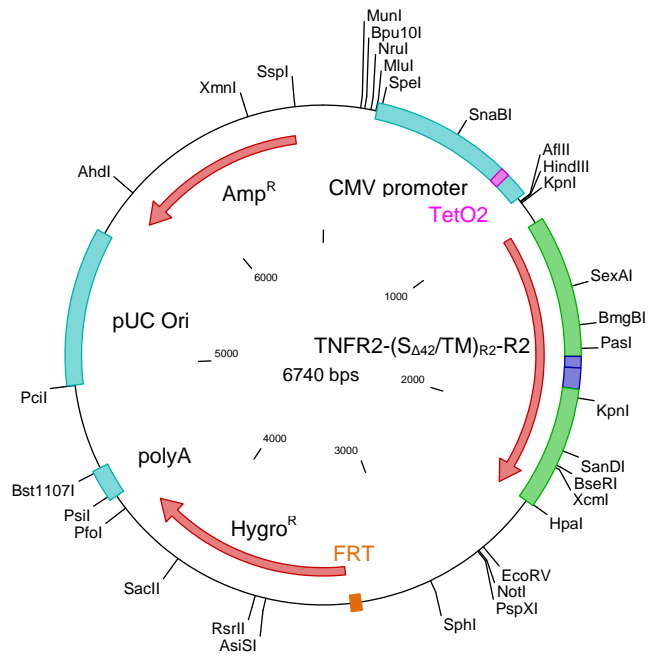
pcDNA5/FRT/TO TNFR2 (#539)



pcDNA5/FRT/TO TNFR2-(S/TM)_{R1}-R2 (#540)



pcDNA5/FRT/TO TNFR2-(S_{Δ42}/TM)_{R2}-R2 (#541)



pcDN5/FRT/TO TNFR2-(S_{Δ42}/TM)_{R2}-Fas (#546)

